Title
REV. DOSIMETRY FOR RADIOLOGICAL PROTECTION AT HIGH-ENERGY PARTICLE ACCELERATORS

Authors
Swanson, W.P.
Thomas, R.H.

Publication Date
1989-04-01

Lawrence Berkeley Laboratory
UNIVERSITY OF CALIFORNIA

OCCUPATIONAL HEALTH DIVISION

To be published as a chapter in **The Dosimetry of Ionizing Radiation,** K.R. Kase, E.B. Bjärngard, and F.H. Attix, Eds., Vol. III, Academic Press. New York City, NY

Dosimetry for Radiological Protection at High-Energy Particle Accelerators

W.P. Swanson and R.H. Thomas

April 1989

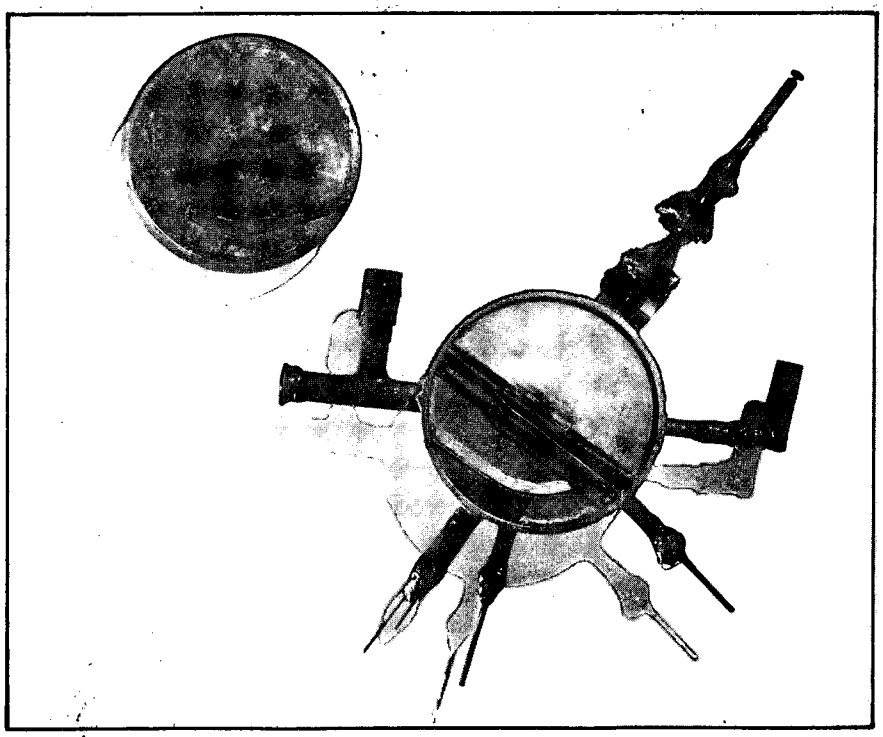

Prepared for the U.S. Department of Energy under Contract Number DE-AC03-76SF00098.

DISCLAIMER

LBL-24119 Rev.

DOSIMETRY FOR RADIOLOGICAL PROTECTION AT HIGH-ENERGY PARTICLE ACCELERATORS

A Chapter for Volume III of "The Dosimetry of Ionizing Radiation,"
Edited by K.R. Kase, E.B. Bjarngard and F.H. Attix
and to be published by Academic Press, New York

William P. Swanson
Lawrence Berkeley Laboratory
University of California
Berkeley, California

Ralph H. Thomas
Lawrence Berkeley Laboratory and School of Public Health
University of California
Berkeley, California
and
Keble College
University of Oxford

"It seems ... to be one of those simple cases
which are so extremely difficult."

from

"The Boscombe Valley Mystery"
in The Adventures of Sherlock Holmes.
Sir Arthur Conan Doyle 1859–1930

This work was done with partial support from the U.S. Department of Energy
under Contract No. DE-AC03-76SF00098

In Memoriam: William P. Swanson 1931-1988

Shortly after the manuscript for this chapter was completed, Bill Swanson died. He had a most distinguished career: following graduation from the University of Illinois and the University of California at Berkeley, he spent the first twenty years of his post-graduate career in high-energy physics. During this time he earned the respect of such luminaries as Luis Alvarez and Pief Panofsky.

By 1972 his interests had turned to radiation physics and the radiological safety aspects of the operation of particle accelerators. He carried out his research in these topics first at the Stanford Linear Accelerator Center and, since 1984, at the Lawrence Berkeley Laboratory. During his career he was author of more than 80 papers. He acquired an international reputation spending periods at CERN, DESY (Hamburg), GSF (Munich) and the University of Hamburg.

In 1977 the IAEA invited him to serve as a consultant and in that capacity he wrote the definitive text, "Radiological Safety Aspects of the Operation of Electron Linear Accelerators." In 1980 he was awarded the Farrington-Daniels Award of the American Association of Physicists in Medicine.

He served his profession well as a member of many committees and as a consultant to, among others, the DOE, NCRP and ICRU. He was instrumental in setting up the scholarship in honor of Professor Burton J. Moyer and was extremely active in the Health Physics Society.

This chapter is dedicated to his memory.

January 19, 1989

Acknowledgements

The authors wish to thank their many colleagues for advice and information during the preparation of this review article. We particularly wish to express our appreciation to our colleagues at the Lawrence Berkeley Laboratory, Mr. Joseph B. McCaslin, Leader of the Radiation Physics Group; Mr. Jensen Young, Head of the Environmental Health and Safety Department; Mr. Walter D. Hartsough, Associate Director Emeritus, and Dr. Richard H. Kropschot, Associate Director Engineering Division, for their support and encouragement. Several colleagues have offered valuable comments and suggestions on our original manuscripts: there were J.D. Cossairt, Fermilab; N.A. Greenhouse, Lawrence Berkeley Laboratory; M. Hofert, DERN; D.J. Perry, Rutherford-Appleton Laboratory; G.B. Stapleton, GEBAF; G.R. Stevenson, CERN; and K. Tesch, DESY. We are grateful to these colleagues who took the time the read our earlier drafts and help us to improve them.

One of us (RHT) wishes to thank Dr. Dennis F. Shaw, C.B.E., Keeper of the Scientific Books at the Radcliffe Science Library, Oxford, for allowing him to work as a Visiting Scholar at the Library during the time his contribution to this chapter was written. Thanks are also due to the Warden and Fellows of Keble College, Oxford, for electing him to a Visiting Fellowship during his stay at Oxford.

Partial support for this work was provided by the Central Electricity Generating Board of the United Kingdom, Pergamon Press, and the U.S. Department of Energy under Contract No. DE-AC03-76SF00098 with the Regents of the University of California.

CONTENTS

Abstract

The dosimetry of the radiation fields that can exist around particle accelerators presents one of the most formidable problems in radiological protection.

Two radiation fields are produced — the *prompt* field, which is present only during accelerator operation and the *remanent* field, produced by the interaction of the *prompt* field with matter to induce radioactivity remaining after accelerator turn-off. Both fields present their own individual but different problems for the dosimetrist. At high-energy installations the prompt radiation fields close to the primary beam and even outside shielding may be complex, being comprised of many different radiations distributed over a wide range of energy. The pulsed nature of the prompt radiation field often results in high instantaneous dose rates, even in fields of rather low intensity when averaged over time.

The prompt field may be detected at large distances from accelerators and the phenomenon called "skyshine" has been given considerable study so the environmental impact of accelerator operation may be understood. The remanent field, too, has environmental consequences and may be a considerable source of personnel exposure, for example during accelerator maintenance.

This chapter first discusses the special requirements for radiation dosimetry at high-energy particle accelerators, then describes the various types of particle accelerator and gives their radiological characteristics. The radiation fields that are observed at particle accelerator installations are described and the special instrumentation considerations they involve for dosimetry are discussed. Finally, the practical techniques of dosimetry found to be useful in accelerator radiation environments are described.

I. Introduction

A. HISTORY AND CONCEPTS

Since the invention of particle accelerators toward the end of the 1920s and their practical realization in 1932, there has been a steady increase in the energy of particles accelerated in the laboratory and available for experimental and other uses (Cockcroft and Walton, 1932a,b, 1934; Lawrence and Livingston, 1932; Lawrence *et al.*, 1932). In 1962 Livingston and Blewett presented a series of graphs showing the energies achieved by several types of particle accelerator plotted against the year in which the energy was first obtained. They concluded that "An envelope enclosing all the curves shows a tenfold increase every six years" (Livingston and Blewett, 1962). Some twenty years later, Panofsky confirmed their general conclusions and his revised version of the "Livingston plot" is shown in Fig. 1 (Panofsky, 1980).

The availability of intense sources of electrons and protons (and more recently other heavy ions) of increasing energy has presented dosimetrists with a continuing challenge and stimulated the evolution of the basic concepts, quantities, units, and techniques of radiation dosimetry. In 1937 the International Commission on Radiation Units and Measurements modified its earlier (1928) definition of the roentgen to remove its direct dependence on free-air ionization chambers, and thus make it more relevant to photons of energy higher than 300 keV (ICRU, 1928, 1938). This led to changes both in concepts and instrumentation because the long range of secondary electrons made the free-air ionization chamber ill-suited to such measurements and it was replaced by the cavity chamber (Gray, 1936, 1937; Boag, 1987; Burlin, 1968).

Despite the clarification intended by the 1937 definition of the roentgen, confusion arose in practice because this unit of exposure was used in two different ways and, as the result of continuing practice, came to express two different concepts — one describing the properties of the ambient field and the other quantifying the energy imparted to the absorbing medium, particularly human tissue. In radiological protection this latter quantity had been informally referred to as the "dose" of ionizing radiation even before 1937. Thus was born the conceptual dichotomy, which exists to this day, leading to the expression of ionizing radiation either in terms of field quantities, which quantify physical aspects of the ionizing radiation field, or dose-equivalent quantities (absorbed dose quantities modified by some biological weighting factors), which attempt to quantify ionizing radiation in terms of biological harm to humans.

Research in atomic and nuclear physics just prior to and during the Second World War led to dramatic increases in the quantity, energy, and quality of available radiation sources. Previously, radiation dosimetry had been largely concerned with photons of energy less than 3 MeV from naturally radioactive materials and x-ray generators. After 1945 the dosimetry of photons, electrons, neutrons and other heavily ionizing particles of ever-increasing energy became of great importance. As we have seen (Fig. 1), the maximum energy of particles available from accelerators increased from about 90 MeV to 6 GeV in the decade from 1945 to 1955.

By 1953 the energy deposition in an absorbing medium had been more precisely characterized by the introduction of the quantity "absorbed dose," measured in rads (1 rad = 100 erg/g), but it was not until 1956 that the ICRU introduced the quantity "exposure dose," measured in roentgens (later called, simply, "exposure") to point up the distinction between the properties of the radiation field and the energy deposition that can occur due to its interaction with matter.

The quantity *kerma* was introduced in 1962 to be able to specify the energy transferred to charged particles in matter by indirectly ionizing radiation, and has proved extremely useful in calculations.

Some twelve years after the suggestion by Cantril and Parker (1945) (see also Parker, 1948), the ICRU defined the quantity "RBE dose" to provide a common basis in radiological protection for quantifying the biological effects of different radiations (ICRU, 1957). This quantity was the precursor of *dose equivalent;* the distinction was drawn between experimentally determined values of RBE, on the one hand, and quality factors, designated for radiological protection, on the other (ICRP, 1959; ICRU, 1962; ICRP, 1963; ICRU, 1971a).

Many different dose-equivalent quantities have been used in radiological protection. The dose equivalent averaged over a single organ, used by the ICRP as the basis of a scheme of radiological protection (ICRP, 1959), has now been supplemented by the quantity *effective dose equivalent* (ICRP, 1977). The maximum dose equivalent (MADE) in a cylindrical tissue phantom was used as an operational quantity to measure neutrons (ICRU, 1971b) until the dose-equivalent index quantities were introduced (ICRU,

1973, 1976, 1980). Most recently the ICRU has defined further operational dose-equivalent quantities: the ambient and directional dose equivalents (ICRU, 1985, ICRU, (nd)).

Thus the need to improve both the accuracy and precision of the specification of the dose equivalent, as well as the necessity to deal with the increasing variety and energies of available ionizing radiations, has led to many changes both in theoretical concepts and techniques of measurement during the past 35 years. We are concerned here with the influence of these changes in the dosimetry for radiological protection associated with particle accelerators, especially for those with energies above 100 MeV.

B. RADIATION DOSIMETRY AT HIGH-ENERGY ACCELERATORS

The theoretical basis for radiation dosimetry has already been discussed in Volume I (Carlsson, 1986). However, there are several aspects that make radiation dosimetry at particle accelerators sufficiently different from other branches of dosimetry to warrant some separate discussion here. The most obvious differences lie in the variety of radiations (and/or particles)[1] to be considered, their energy distributions, and their distributions in time. In only one other branch of radiation physics — dosimetry during space missions — does the energy of the radiations to be measured extend as widely as in particle-accelerator environments. Furthermore, only at these high energies is dosimetry of muons, pions, and the rarer nuclear particles performed. The particular problems incurred because of pulsed radiation are discussed in Section IV.

At particle accelerators radiation dosimetry is performed for six distinct reasons (McCaslin and Thomas, 1981):

- Investigation of radiation accidents;
- Routine radiological protection surveys;
- Individual (personal) monitoring;
- Environmental monitoring;
- Beam intensity measurements;
- Radiation field quantification.

The first four items of this list are principally concerned with radiological protection, while the last two are more broadly based.

Measurements that are made solely for the purposes of radiological protection, i.e., to demonstrate compliance with protection limits, must ultimately be expressed in units of the quantities in which the limits are expressed. At present these limits are expressed in terms of a dose-equivalent quantity (ICRP, 1977). However, measurements made with other applications in mind — for example, the design of accelerator shielding, predictions of induced activity or radiation damage — are often more conveniently expressed by physical parameters that specify the radiation field (energy and spatial distributions of particle fluence) (see, for example, Moyer, 1954).

It is natural that, at high-energy laboratories, the latter more fundamental approach should be preferred because the necessary instrumentation is available for such measurements and the results of physical measurements of the radiation field may be applied to a variety of tasks, including radiological protection. The converse is not so (Moyer, 1954; Patterson and Thomas, 1973). Furthermore, the physical characterization of the radiation field will have a stability not yet achieved by dose-equivalent quantities (Rindi and Thomas, 1973). This argument is given additional emphasis by noting that there is a lively debate on the concept of dose equivalent (NCRP, 1981), the relationship between quality factor and relative biological effectiveness (RBE) (Mole, 1979), the relationship between quality factor and dosimetric quantities (Rossi, 1977; Blohm and Harder, 1985) and, finally, the implications of these quantities for the assignment of quality factors (Q) (Dennis, 1983; Dennis and Dunster, 1985; Sinclair, 1985). The ICRU has recently published a report entitled "The Quality Factor in Radiation Protection" in which changes are recommended in both the magnitude of Q and its functional relationship to microdosimetric quantities (ICRU, 1986). At

[1] In what follows the term "ionizing radiation" will be taken to include atomic or nuclear particles unless otherwise indicated.

the time of this writing the ICRP has not endorsed these recommendations but is beginning a broad review of its system of radiological protection to determine whether comprehensive changes should be made (Thorne, 1986).

This chapter will

- Review the special requirements for radiation dosimetry at high-energy particle accelerators;
- Describe and classify the various types of particle accelerators;
- Discuss the radiation fields that exist around particle accelerators and the special instrumentation considerations that arise;
- Review the practical dosimetric techniques that are available and have been found useful in accelerator radiation environments.

II. Particle Accelerators and Their Radiological Properties

A. TRENDS IN HIGH-ENERGY ACCELERATOR DESIGN

Particle accelerators may be discussed and categorized in terms of their technology, but the classifications of greatest relevance to the radiological physicist are the type(s) of particles accelerated; the maximum energy, maximum intensity, and duty factor of the accelerated particles; and the types of media in the vicinity of locations struck by the beams. Particle accelerators that operate above energies of 100 MeV are discussed here and divided into two groups:

- Proton accelerators, including heavy-ion accelerators where appropriate.
- Electron accelerators, discussed separately because of the different composition of their radiation fields.

Particle accelerators operating at energies above 100 MeV are generally synchrotrons, cyclotrons, or linear accelerators. Information on the design and operation of high-energy particle accelerators may be found in a variety of excellent texts including Lapostolle and Septier (1970), Livingood (1961), Livingston and Blewett (1962), Livingston (1966) and Wilson and Littauer (1960). Recent machine development is set forth in international conference proceedings (CERN, 1971a; SLAC, 1974; FNAL, 1983b) and summer schools organized by CERN (1977, 1985) and Fermilab (FNAL, 1982, 1983a, 1985). A complementary series of proceedings is sponsored by the Institute of Electrical and Electronic Engineers (IEEE, 1975, 1977, 1979a, 1981a, 1983a, 1985a). A recent overview is also given by Lawson and Tigner (1984).

The machines described have been mostly built for physics research although proton and heavy-ion accelerators have also found application in medicine for isotope production or for cancer therapy with pions, protons, or heavy ions (Amols *et al.*, 1980; Bewley *et al.*, 1976; Lam and Skarsgard, 1983; Larsson, 1980; Paciotti *et al.*, 1981; PART, 1977, 1982; Raju, 1980; Skarsgard, 1983; Tobias *et al.*, 1952, 1971; Tobias, 1985; and Wilson, 1964), and for medical imaging (Benton *et al.*, 1973; Llacer *et al.*, 1984; Tobias *et al.*, 1977). A recently revived proposal is for the production of nuclear fuel by spallation neutrons produced by positive-ion accelerators (Van Atta *et al.*, 1976; Steinberg, 1983).

An important innovation, quickly applied to accelerator design, was the development of superconducting (SC) materials, which found use in magnet windings and for rf accelerating cavities. The use of superconducting systems has made possible the construction of ever-larger facilities, greatly extending the range of energies possible. Examples of machines representing state-of-the-art SC technology are the Tevatron in operation at Fermi National Accelerator Laboratory (Fermilab) (Edwards, 1985), the Continuous Electron Beam Accelerator Facility (CEBAF, 1986) under construction at the time of writing, and the proposed Superconducting Super Collider (SSC, 1986). Examples of other projects using superconducting technology are given in Table III. The concept of cw acceleration (cw = continuous wave, i.e., continuous rather than pulsed beam) has been successfully realized in a number of facilities using both superconducting and normally conducting technology (Herminghaus, 1984). The 100% duty factor of such facilities eliminates the gross pulse structure of the radiation that usually needs to be considered although the

dosimetrist must be aware of the rf micropulse structure.

The energy of heavy-ion facilities is generally given in terms of "specific energy," i.e., the energy divided by the atomic mass of the projectile expressed in units of MeV/amu or GeV/amu. An example is GANIL (1986) in Caen, France, which comprises two identical separated-sector cyclotrons capable of accelerating light ions to 100 MeV/amu, but with decreasing specific energy with mass to about 10 MeV/amu for the heaviest naturally occurring nuclei. The Bevalac at Lawrence Berkeley Laboratory (LBL) gives a maximum beam energy of 2.1 GeV/amu. In late 1986 the CERN SPS succeeded in producing beams of oxygen and sulphur at energies up to 200 GeV/amu. The proposed Relativistic Heavy Ion Collider (RHIC) at Brookhaven National Laboratory (BNL) would have colliding beams at specific energies of 100 GeV/amu each.

Among the highest energy synchrotrons in operation are the 1000-GeV Tevatron at Fermilab (Edwards, 1985) and the 450-GeV Super Proton Synchrotron (SPS) at CERN, Geneva (CERN, 1971c, 1972) (later converted to operate as a 270×270 GeV collider, $S\bar{P}P S$). As shown in Table I, several multi-GeV particle-accelerator facilities have been in operation for many years. Others are in the design or construction phase. Examples of the highest-energy linear accelerators (Table II) are the 800-MeV proton machine LAMPF (1986) at Los Alamos National Laboratory (LANL), and the 22-GeV (now 40-GeV) electron accelerator at the Stanford Linear Accelerator Center (SLAC) (Neal et al., 1968). The highest-energy cyclotrons now in operation are the 520-MeV TRIUMF (1986) in Vancouver, the 590-MeV ring cyclotron at the Swiss Institute for Nuclear Research (SIN) the 660-MeV synchrocyclotron at Dubna (Zaitsev *et al.*, 1971; Biryukov, 1971), and the 1-GeV synchrocyclotron in Leningrad.

The trend over the past decade has been to develop the capability of "stacking" particle beams in storage rings (Sands, 1970). These are often constructed as "colliders," which can stack counter-rotating beams. This has the advantage of making the full accelerated energy available in the reaction center-of-mass system in studying particle-particle collisions. Some examples of the ambitious plans now under development are listed in Table III.

Synchrotron radiation, produced by high-energy electron-storage rings and circular accelerators, is used in physics, chemistry, materials science, metrology, and microelectronics and has been successfully used for diagnostic imaging (Hughes, 1983, 1986). A growing application is the production of integrated circuits by lithography. Many circular electron machines (synchrotrons, storage rings) are fully dedicated to utilization of their synchrotron radiation. Examples are given in Table IV. A recent review of $e^{\pm}e^{-}$ storage rings is given by Kohaupt and Voss (1983). An extensive treatment of synchrotron radiation and its sources is given by Krinsky *et al.* (1985). Papers from a major conference on synchrotron-radiation instrumentation are reported in SRI (1980), and all modern aspects are addressed in the Synchrotron Radiation Handbook edited by Koch (1983).

Recent decades have been marked by steady development towards higher energies, higher intensities, larger duty cycles, and significant technological advance. At the present there is a vigorous accelerator construction program around the world, and several technological advances, especially in superconductivity, make for growth in both complexity and reliability of particle accelerators. Steady progress and expansion of their capabilities and applications is clearly characteristic of the types of high-energy facilities addressed in this chapter, as well as the new technologies and applications of low-energy accelerators (see, for example, Scharf, 1986).

B. RADIOLOGICAL PROPERTIES

At the energies addressed in this chapter (>100 MeV), radiation fields are generally a manifestation of a cascade process. The electromagnetic cascade is always important with electron accelerators at these energies. The hadronic cascade produced by proton and heavy-ion accelerators is also important and becomes quite complex above the pion-production threshold. Although these cascades are usually discussed as if they were separate entities, they are to some degree coupled because they may transfer energy to each other — a hadronic cascade initiated by a high-energy proton transfers a significant fraction of its energy to the electromagnetic cascade, while part of the energy from a well shielded target struck by a primary electron beam ultimately produces a moderated spectrum of neutrons that emerges from the shield accompanied by capture gamma rays.

The prompt radiation fields have the following general characteristics:

- They are usually *pulsed* because of the periodic nature of the operation of most machines.
- They are *mixed fields* because of the variety of secondary particle fields that are possible.
- The particle fluences (neutrons, photons, muons, etc) are characterized by *broad spectra* extending from very low (e.g., thermal) energies to the highest ones energetically possible. Because of the cascade processes, the lower-energy spectral components dominate in most situations.

Proton (hadron) accelerators produce neutrons in copious quantities and the number of neutrons produced scales roughly as the total energy absorbed in the stopping materials. Electron machines also produce significant numbers of neutrons, but about a factor of 40 less than proton machines of comparable energy and beam current (Swanson, 1979b; Tesch, 1985). Despite their reduced production, neutrons can dominate the radiation fields at electron accelerators outside the thick shielding at high-energy, high intensity facilities (DeStaebler, 1965). If the primary particle energy is greater than 1 GeV, both types of accelerators produce strong fields of muons having pronounced directional properties. (At the higher energies the rarer particles may also be produced in significant intensities, e.g., pions, kaons.) Both categories of accelerator produce remanent radioactivity.

Information on the radiological aspects of high-energy accelerator operation is summarized by ICRU (1978), IEEE (1976), and in proceedings of major conferences held at Brookhaven (1965), SLAC (1969), and CERN (1971b). Radiological protection aspects are thoroughly treated by Patterson and Thomas (1973) for all types of high-energy accelerators; in Thomas and Stevenson (1988) for high-energy hadron accelerators; and Swanson (1979a) for electron accelerators. More recent topics are covered in proceedings of the Reno Meeting of the Health Physics Society (1987). Much of the information obtained at lower-energy (<100 MeV) accelerators is useful for radiological protection at higher-energy machines as well. Thus, NCRP-51 (1977) is also an excellent resource.

Since the impetus given particle-physics research by cosmic-ray studies in the 1930s (see, e.g., Puppi and Dallaporta, 1952), there has been a synergism between space and accelerator radiation science. Both disciplines share strong interests in radiation transport, radiation damage, and detector design. The series of conference proceedings by the Institute of Electrical and Electronic Engineers sets forth well the development of these areas of research (IEEE, 1978, 1979b, 1980, 1981b, 1982, 1983b, 1984, 1985b).

III. External Radiation Fields

A. INTRODUCTION

Two somewhat different external radiation fields at accelerators are of concern for radiological protection. They have been identified as *prompt* and *remanent*.

The prompt-radiation field exists only while the particle accelerator is operating: its characteristics are determined by the energy and type of particle accelerated, the duty cycle, and the shielding around the accelerator (see Section II). It may be complex in space (large fluence gradients) and time (duty cycle) and be composed of many different types of particles. As we shall show later, photons, neutrons, and muons present the principal problems.

Interaction of the prompt-radiation field with matter leads to the induction of radioactivity. This radioactivity is produced most intensely in the accelerator components, but may also be detected in the structural materials of the building and in the surrounding earth and ground water. This residual activity produces the remanent-radiation field.

In preparation for Section IV, which discusses techniques of measurement, we shall show in this chapter why it is not always prudent to apply those techniques of dosimetry that are known to work well for lower energy radiations (e.g., see Kase *et al.*, Vol. II, 1987), to the measurement of accelerator radiation without a clear understanding of the accelerator radiation environment and its interaction with the dosimeter to be used. Dosimeters that work perfectly well at low energies may often have responses to the high-energy particles present in accelerator environments that make the proper interpretation of their measurements more complicated than at lower energies. One example that demonstrates this point is the additional radioactivity produced by high-energy charged particles in activation detectors, normally used to measure

neutrons. Other examples are the response of LET-spectrometers to highly charged ions of high velocity and the interaction of neutrons with the walls and gases of ionization chambers used to measure photons.

In the 1950s this need to predict the radiation environments of high-energy accelerators led to a dilemma. The large synchrotrons then being designed or constructed were intended to explore the very phenomena that needed to be understood before adequate systems of radiological protection (including monitoring and shielding) could be established.[2] Moyer and his colleagues at Berkeley realized that cosmic radiation provided a model that might be used to resolve this difficulty (Solon, 1957; Hess *et al.*, 1959; Patterson *et al.*, 1959; Bonet-Maury *et al.*, 1962). Cosmic-ray studies are helpful in understanding the electromagnetic and hadronic cascades that are initiated by the interaction of galactic protons with the top of the earth's atmosphere. Of particular interest was the neutron spectrum generated by the hadronic cascade, and it was demonstrated that a large proportion of the dose equivalent was due to neutrons with energies between 0.1 MeV and 20 MeV (Hess *et al.*, 1959; Patterson *et al.*, 1959). Another important conclusion reached was that the attenuation length of the neutron fluence through the atmosphere was about 110 g cm^{-2} (Patterson and Thomas, 1973, Chapter 6).

The conclusions drawn from cosmic-ray studies and applied to the radiological protection systems at proton accelerators were largely confirmed by experience at the 184-Inch Synchrocyclotron of the University of California Radiation Laboratory (now LBL) and the early proton synchrotrons — the "Cosmotron" and the "Bevatron" — at Brookhaven and Berkeley. The qualitative features of their prompt radiation fields outside thick shielding were determined and quantitatively assessed (Lindenbaum, 1957; Moyer, 1957; Patterson, 1957, 1965; and Smith, 1958, 1962). To repeat a much-used quotation:

> "A general rule that has emerged from our studies is that fast neutrons (0.1 to 10 MeV) dominate the biological hazard of the radiation field existing near a well-shielded particle accelerator by contributing more than half the total rem dose. Gamma rays and low-energy neutrons contribute 10 to 20%, and high-energy neutrons make up the balance." (Patterson, 1965)

Subsequent experience around the newer proton synchrotrons has built upon this foundation and extended these early conclusions so that today we have a fairly good understanding of these phenomena (see, for example, Thomas and Stevenson, 1988).

B. THE PROMPT RADIATION FIELD

1. *Introduction*

The prompt-radiation environment close to a particle accelerator is dependent upon many factors, but particularly on the type and energy of particles accelerated and the amount of material through which they pass. In general, the higher the energy of the accelerated particles the more complex is the radiation field. The accelerated particles are essentially monoenergetic, and dosimetry of particles in the accelerator beam is therefore straightforward compared with the task of measuring radiation fields outside the accelerator structure and shielding, where extremely complex radiation fields may exist. Since no acceleration process is perfect, particles are lost during acceleration or when being stored or transported at maximum energy. The full-energy beam, which is used for experiments or measurements, interacts with targets and other components and generates electromagnetic and hadronic cascades.

2. *Photons*

a. *Introduction.* At electron accelerators of all energies, bremsstrahlung establishes the photon field that dominates the secondary radiation field. For the primary electron energies addressed in this chapter (>100 MeV), the radiation field is best approached through a discussion of the electromagnetic cascade. In this process, electrons and photons repeatedly interact, each time losing energy, to replenish their numbers until the degraded electrons are brought to rest by ionization and, finally, the photons are attenuated at a

[2]G.R. Stevenson (private communication, 1988) points out a current analogous situation to that which was true in 1950. The presence of charmed mesons, discovered only a few years ago, must now be considered in the design of beam dumps at SPS energies and in the shielding of collider interaction regions at CERN and the SSC. A similar situation exists for the bottom meson.

rate close to the minimum attenuation coefficient for the material.

For tables of electron energy loss, extensive data are presented by Berger and Seltzer (1964, 1966, 1982), Pages *et al.* (1972) and Seltzer and Berger (1982a,b). Report 37 of the International Commission on Radiation Units and Measurements (ICRU, 1984) contains extensive discussion and tabulations on stopping powers for electrons and positrons. The theory of electron bremsstrahlung has been set forth by Heitler (1954) and Jauch and Rohrlich (1976). A compendium of bremsstrahlung formulae is given by Koch and Motz (1959). Data on photon mass attenuation coefficients and related parameters are well explained and tabulated by Hubbell (1969, 1977, 1982), Hubbell *et al.* (1980), Plechaty *et al.* (1975), and Storm and Israel (1967). Although these tabulations emphasize the lower-energy behavior of electrons and photons, this information is essential to a complete understanding of dosimetry of high-energy electron beams, simply because the electromagnetic cascade contains electrons and photons of essentially all energies from zero up to the maximum energy possible; indeed particles of lower energy tend to dominate.

The electromagnetic cascade is copiously populated with low-LET particles and the quality factor for related absorbed doses is accepted as Q = 1. Metrology is therefore considerably simpler than, say, for neutron fields. [This simplicity may, however, disappear if the recommendations of ICRU Report 40 are implemented, in which the quality factor for photons and electrons may vary by as much as a factor of three (ICRU, 1986).] Readily available standard instruments can be used for radiological protection measurements in most cases. An outstanding body of work has been done related to accelerators that operate below 100 MeV (see, for example, NCRP, 1977) but the approach presented here is more appropriate for higher-energy facilities. A concise description of the electromagnetic cascade may be found in ICRU (1978).

In contrast to the situation at electron facilities, bremsstrahlung is a negligible effect at proton (or heavy-ion) accelerators. The radiative energy loss by protons is less than that by electrons by approximately the ratio of their masses squared, $(m_e/M_p)^2$.

b. *The Electromagnetic Cascade.* In what follows it is assumed that the primary beam energy is well above the critical energy of the material struck by the beam. The critical energy, E_c, is defined as the electron energy at which the average energy loss rates due to radiation and due to ionization are equal. Above E_c, the radiation losses will dominate those from ionization, so that showering can occur more readily, whereas, as the energy is decreased below E_c, bremsstrahlung production, and therefore showering, is increasingly suppressed. Values of E_c in MeV are approximately given by:

$$E_c = 800/(Z + 1.2) \quad , \tag{1}$$

where Z is the atomic number of the material.

Although, when examined in detail, the electromagnetic cascade is an exceedingly complicated stochastic phenomenon, it is possible to come to terms with it through generalizations that reflect average behavior. An intuitive picture is very helpful:

> An electron travels about one radiation length, X_0, and emits a photon with which it shares its energy about equally. The photon then travels approximately one radiation length (actually about 9/7 X_0), within which distance it produces an electron-positron pair. The pair members share the photon's energy about equally and the original electron emits a new photon. In each such interval the number of particles is approximately doubled and thereby the average energy per particle is similarly reduced. This multiplication results in a rapid rise in particle number (and absorbed dose to the medium) until the average electron energy is near the critical energy. At this depth the shower "tops out" at a maximum. Thereafter the electrons, having too low an energy, cannot actively participate in maintaining the shower. Photons thus remain as the particles which principally propagate the cascade. The photon energy at which the minimum attenuation coefficient occurs, called the "Compton minimum," is typically (1/2 to 1/3) E_c for all materials. Below this energy the probability for Compton scattering and resulting energy degradation becomes larger than for electron-positron pair production. When pair production occurs, the members have energies well below E_c. This ensures that photons in the tail of the shower cannot effectively replenish the shower.

The concepts and units with which the shower is characterized are summarized:

- *The radiation length*, X_0, is the distance an electron must travel so that its energy is reduced by an average factor of e by radiation at the high-energy limit:

$$X_0 = 716\ A[Z(Z+1)\ln(183\ Z^{-1/3})]^{-1} \quad , \tag{2}$$

where A and Z are the mass number and atomic number of the medium, respectively, and X_0 is expressed in units of g cm^{-2}. Accurate values of X_0 have been calculated by Knasel (1970), Tsai (1974), and Seltzer and Berger (1982b, 1985).

- *The Molière length*, X_M, is used to describe the transverse development of a shower:

$$X_M = X_0 \frac{E_s}{E_c} \quad , \tag{3}$$

where E_s is a constant equal to 21.2 MeV (Molière, 1948).

- *The Compton minimum*[3] is the minimum mass attenuation coefficient for photons in a given material. It occurs at a photon energy at which the cross sections for the Compton effect and electron-positron pair production are about equal. The energy at which it occurs, E_{Compt}, is less than the critical energy E_c, for all materials. Values can be found in Swanson (1979a, pp. 298–300).

- When the photon energy is much greater than the Compton minimum energy, E_{Compt}, the interaction length for pair-production, λ_p, is given by 9/7 X_0.

- The absorption length, λ_c, is used to describe the exponential attenuation of the "tail" of the electromagnetic cascade (see, for example, Bathow *et al.*, 1970 and Dinter and Tesch, 1977). In g cm^{-2}, it is approximately given by

$$\lambda_c = 325(\ln Z)^{-1.73} \quad , \tag{4}$$

where Z is the atomic number of the medium (Van Ginneken and Awschalom, 1974). Values of λ_c are somewhat larger than the inverse of the photon mass attenuation length at the Compton minimum just discussed; e.g., for Al, Cu and Pb, they are larger by factors of 1.37, 1.21 and 1.05, respectively.

- *Equivalent quantum*, for thin-target bremsstrahlung, is equal to the total energy radiated by all incident electrons divided by the incident energy of one electron, E_0. It is approximately equal to the thickness of the radiating target, measured in radiation lengths, multiplied by the number of incident electrons.

The dosimetric properties of an electromagnetic cascade shower may be summarized in curves that show the fluence of particles, the absorbed dose, or any other quantity of interest, as functions of shower depth or of distance from the shower axis. An example is the curve of Fig. 2 which shows the fraction of total energy deposited versus depth, from the work of Bathow et al. (1970) as adapted by Van Ginneken and Awschalom (1974). Energy deposition is integrated over all radii about the shower axis. Van Ginneken and Awschalom generalized this curve by defining a new parameter λ_1

$$\lambda_1 = 325(\ln Z)^{-1.73} \times (\ln E_0) \tag{5}$$

where λ_1 is in g cm^{-2}, and E_0 is in MeV. When depths are expressed in units of λ_1, all curves merge approximately into a universal curve. This formulation shows that the location of the dose maximum moves deeper into the medium, proportionately to the logarithm of the incident energy. This is because each doubling of incident energy adds approximately one unit of distance to that needed to reduce the average particle energy to E_c.

[3]The expression "Compton minimum" is conventionally used here but does not accurately describe the physical phenomenon. The Compton cross section is not at a minimum at the so-called "Compton minimum." It would be more accurate to describe the phenomenon as "the photon attenuation minimum."

The so-called *Approximation B* of analytic shower theory (Rossi and Greisen, 1941; Rossi, 1952) predicts that the number N of negative and positive electrons at the shower maximum should be nearly proportional to E_0/E_c in the following manner:

$$N = \frac{0.31\, E_0/E_c}{[\ln(E_0/E_c) - 0.37]^{1/2}} \quad . \tag{6}$$

This is consistent with the intuitive picture outlined above where, at the shower maximum, the energy of the incident electron, E_0, is divided among a number of particles having energy near E_c. As discussed, the location of shower maximum (X_{max}) should depend on the logarithm of the incident energy. Approximation B gives:

$$X_{max}/X_0 = 1.01[\ln(E_0/E_c) - 1] \quad . \tag{7a}$$

Experimentally, Bathow et al. (1967b) found:

$$X_{max}/X_0 = [\ln(E_0/E_c) - C] \quad , \tag{7b}$$

where C takes the values 0.77 and 0.47 for Cu and Pb, respectively.

Figure 3 shows a graph (Nelson et al., 1966; DeStaebler et al., 1968) of the fraction U/E_o of incident energy that escapes as a function of cylinder radius for showers caused by electrons of various energies. The abscissa is the cylinder radius in units of Molière-length. There is obviously a transition in this distribution from a steeper slope to a constant smaller slope at larger radii. The curve has been parameterized as:

$$U/E_0 = 0.8\, \exp(-3.45\, R/X_m) + 0.2\, \exp(-0.889\, R/X_m) \quad , \tag{8}$$

where X_m is the Molière length defined above. While there is no simple derivation for the first term of this expression, the second term, describing the radial "tail," must be related to the attenuation of photons near the Compton minimum.

Although these empirical observations are useful, the Monte Carlo approach to calculating problems related to the electromagnetic cascade is the most satisfactory in several ways (see, for example, Ford and Nelson, 1978 and Nelson *et al.*, 1985). Particular advantages are, first, that all of the several elementary physical processes of electrons and photons can be taken into account accurately, and second, that geometrical details can be modeled with utmost flexibility. Monte-Carlo calculations of the electromagnetic cascade, published in the literature, are summarized in Table V.

Experimental work on the electromagnetic cascade goes back several decades, having received early impetus from cosmic-ray research. References to earlier experimental work can be found, for example, in Bathow *et al.* (1967b, 1970). Additional experimental work has been described by Yuda *et al.* (1970), Jakeways and Calder (1970), Brockmann *et al.* (1971), Müller (1972), Ban *et al.* (1987), Hirayama *et al.* (1987), and Nakamura *et al.* (1987).

c. *External Bremsstrahlung Field.* The photon field in the environment of a high-energy electron accelerator is derived from the electromagnetic cascade, and the effects of passing through the accelerator machinery and any intervening shielding. Assuming that a substantial amount of material has been traversed, what is observed is

- A broad photon field that is forward-peaked in the direction of the electron beam but extends to backward angles as well with decreasing intensity. This is due to bremsstrahlung from electrons that have been turned by multiple Coulomb scattering and a large fraction of which must therefore come from electrons present in the maximum of the shower. This wide-angle field will be dominated by photons near the Compton minimum, and the attenuation is controlled by the attenuation coefficient near that energy.
- A very sharp forward spike, which is a remnant of the radiation produced by the incident electrons and contains photons of the highest energy possible for that primary energy. The characteristic angle of this radiation is given by $\theta_c = m_e/E_0$ (radians) or $29.28/E_0$ (degrees, if E_0 is in MeV). In the limit of very thin targets ($X/X_0 \ll 1$), the spike will have the spectrum and other characteristics of thin-target bremsstrahlung (Koch and Motz, 1959). For thick

targets, this spike stands above a background of photons from subsequent shower generations. Empirically, the angular width of the forward spike is somewhat wider, and given approximately by the relationship

$$E_0\theta_{1/2} \; 100 \;, \tag{9}$$

where $\theta_{1/2}$ is the angle in degrees of dose half-maximum and E_0 is in MeV.

d. *Absorbed Doses Related to the Forward Spike.* The spike in the direction of the initial electron beam was analyzed by Tesch (1966), who compared doses from thin-target bremsstrahlung with doses from monoenergetic photons and electrons (Fig. 4). Analyses of this type have received renewed attention because this radiation might be produced in the "maximum credible accident" at electron storage rings. An errant electron beam, if it strikes an internal component of the machine, can produce a large dose in a small solid angle. A more bizarre, but not far-fetched scenario, would result if a sudden vacuum leak occurred in a portion of the ring. While the beam tube remains at low pressure, the beam would continue circulating until virtually every electron had interacted with air in a limited region at the leak before the air could diffuse to fill the ring uniformly. This occurrence would produce the forward spike of thin-target bremsstrahlung already described. This phenomenon has been been studied at several accelerator laboratories including Adone at Frascati (Esposito *et al.*, 1978; Rindi, 1982; Esposito and Pelliccioni, 1982, 1986; Pelliccioni and Esposito, 1987), the NSLS at Brookhaven (Blumberg and Perlman, 1980) and Aladdin at Wisconsin (DeLuca *et al.*, 1987; Otte *et al.*, 1987; Schilthelm *et al.*, 1985 and Swanson *et al.*, 1985). Although there is disagreement over the magnitude of the maximum dose that might be imparted, all the studies agree that such an occurrence could have severe consequences with the beam intensities commonly achieved.

e. *Bremsstrahlung Doses at Large Angles.* Absorbed doses due to thick-target bremsstrahlung at large angles are important because of the large areas at high-energy electron accelerators that generally must be protected by radiation shielding. DeStaebler *et al.* (1968) presented the first significant information for the SLAC 20-GeV electron accelerator. Their data have been used for conceptual designs of several accelerator facilities. Figure 5 shows the photon dose rate, normalized to a distance of 1 m for 20-GeV electrons incident on various targets. The work at SLAC has been extended by Jenkins (1979, 1988) who expressed the photon dose at 15 GeV in a form in which all factors are explicit:

$$D = E_0 C \left[\frac{\sin\theta}{a+d}\right]^2 \left[\frac{1}{E_0}\frac{dN}{d\Omega}\right] B \exp\left[-\frac{\mu}{\rho}\frac{\rho d}{\sin\theta}\right] \;, \quad \text{(Gy/electron)} \;, \tag{10}$$

where

D	is the absorbed dose in Gy per incident electron,
E_0	is the incident electron energy (GeV).
C	is the fluence to absorbed-dose conversion factor, which is assumed constant after the depth of shower maximum within the shield. The value assumed is 2.14×10^{-15} Gy m^2 $photon^{-1}$.
θ	is the angle with respect to the beam direction in degrees.
a	is the target-to-shield distance (m).
d	is the shield thickness (m).
ρ	is the shielding material density (kg m^{-3}). For clarity, ρ is shown explicitly in the two factors of the exponential, (ρd) and (μ/ρ).
μ/ρ	is the attenuation coefficient, assumed constant and equal to the value at the Compton minimum (for concrete, it is 2.4×10^{-3} m^2 kg^{-1});
B	is a photon dose build-up factor, dependent on energy and material. In this context the value is not significantly different from unity and this factor is omitted in the discussion that follows.

$(1/E_0)dN/d\Omega$ is the yield of photons of all energies. This function is fitted by the expression

$$\frac{1}{E_0}\frac{dN}{d\Omega} = [4.58E_0^{-\theta/1.58} + 1.07e^{-\theta/72}] \text{ (photons} \cdot \text{sr}^{-1} \cdot \text{GeV}^{-1} \cdot \text{electron}^{-1}) \ . \quad (11)$$

The first term corresponds to yield at small angles, 0–5°, from 17 X_0 targets. The second fits the remaining angular range to 180°. Combining factors, this gives

$$D(\theta) = [98E_0^{-\theta/1.58} + 2.3e^{-\theta/72}] \times 10^{-15} E_0 \left[\frac{\sin\theta}{a+d}\right]^2 \exp\left[-\frac{\mu}{\rho}\frac{\rho d}{\sin\theta}\right] . \quad (12)$$

At 90°, the above formulation gives:

$$D(90°) = \frac{6.59 \times 10^{-16} E_0}{(a+d)^2} \exp(-\frac{\mu}{\rho}\rho d). \quad (13a)$$

Expressing this in terms of total incident electron energy, U (in J), we have:

$$D(90°) = \frac{4.11 \times 10^{-6} U}{(a+d)^2} \exp(-\frac{\mu}{\rho}\rho d). \quad (13b)$$

In a detailed study, Dinter and Tesch (1977) measured the absorbed dose from electromagnetic radiation around iron plates of thickness t = 0.2, 1.0, 5.0 and 10 cm (0.11, 0.57, 2.84 and 5.68 X_0, respectively), placed at various orientation angles, ϕ, to electron beams of E_0 = 3.0, 5.0 and 7.2 GeV. A portion of their measurements, obtained with ^{7}LiF TL dosimeters, are shown in Fig. 6 for E_0 = 5 GeV. At this energy, shower maximum is at about X_{max} = 7.6 cm (4.3 X_0). Because of the variety of geometries surveyed, several general conclusions can be drawn from these data; the strong dependence on target geometry is obvious.

- The absorbed doses decline with detector angle, θ, for all geometries. This is manifestly true for those orientations for which the detector is on the opposite side of the target from the point of beam incidence (Fig. 6, a-d). The dips seen in Fig. 6 (e-h) are due to self-absorption in the target when the plane of the target nearly coincides with the direction of observation; thus they can be considered as artifacts. Around $\theta = 90°$ the dose fall-off with angle can be approximately described by exponentials: D exp $(-\beta\theta)$. For glancing incidence, $(2° \le \phi \le 12°)$, on thin targets the slopes of the curves at 90° correspond to values of β between 1.6 and 1.7 radian^{-1}. For thicker targets smaller values of β are found. The rate of fall-off with observation angle is strongest for perpendicular incidence ($\phi \approx 90°$), for all target thicknesses. For all target thicknesses, the rate of fall-off with observation angle is strongest for perpendicular incidence ($\phi \approx 90°$).
- For effective target thicknesses t csc ϕ < 15 cm, the highest absorbed doses were found in the forward direction ($\phi = 0°$). For larger effective target thicknesses, absorbed doses due to radiation scattered from the point of incidence dominated (Fig. 6, e-h).

Analysis of the absorbed dose rates as a function of incident beam energy (not shown here) led to the following generalizations:

- For "thick" targets, (t csc ϕ > 8 cm), absorbed dose rates were proportional to incident electron energy over the range 3 GeV $\le E_0 \le$ 7 GeV.
- For "thin" targets (t = 0.2 cm and t csc ϕ < 2 cm), absorbed dose rates were independent of incident electron energy over the range 3 GeV $\le E_0 \le$ 7 GeV.

The following observations were made concerning the dose attenuation in shielding materials:

- For "thin" targets, as defined above, 99% of the absorbed dose was from very low-energy particles, as evidenced by rapid initial attenuation by relatively thin layers of shielding, before exponential attenuation began. For perpendicular incidence ($\phi \approx 90°$), the initial transmission factor ranged from 0.007 to 0.004 for target thicknesses $0.2 \text{ cm} \leq t \leq 5 \text{ cm}$.
- The absorption coefficient for the subsequent exponential attenuation μ_e/ρ, was independent of target arrangement. Observed values of μ_e/ρ were consistent with the minimum photon absorption coefficients μ_{Compt}/ρ, for the shielding materials investigated (lead, iron, heavy concrete, ordinary concrete and sand).

Fassò *et al.* (1984) reported Monte Carlo studies using the program EGS (Ford and Nelson, 1978) which gave the dose distribution about a tungsten target of 0.5-cm radius ($R = 1.43\ X_0$ or $0.69\ X_M$) and three thicknesses ($t = 1$, 4, and $10\ X_0$) struck by 200-MeV electrons. For this energy, shower maximum occurs at $X_{max} = 2.0\ X_0$. This distribution is shown in Fig. 7, where the dose as a function of angle about the target can be seen.

Calculations using the ESG4 code have subsequently been extended to cover the energy range from 0.15 GeV to 50 GeV. The electron-photon cascades in concrete, iron, and lead were studied and their dependence on primary energy, target configuration, and angle of observation determined. Comparisons between calculation and experimental observation were made at 5 GeV [Dinter et al. (1988)].

f. *Scaling of Doses from Thick-Target Bremsstrahlung.* Absorbed dose rates from thick-target bremsstrahlung at large angles (45°–180°) should scale as initial beam energy. The reason is that the photon doses at large angles are mainly due to radiation from electrons of relatively low energy that have been scattered to large angles. The number of such degraded particles, at energies near E_c, increases with initial particle energy, for constant beam current. This rule was confirmed by Dinter and Tesch (1977) for thick targets (see above).

The doses at and near 0° must scale as a higher power of primary energy because of the narrowing of the forward radiation "spike" with increasing E_0 as (m_e/E_0) discussed above. Swanson (1979a) has suggested rules of thumb that describe the photon radiation field, as follows:

- For 0°,

$$\dot{D} = 3 \times 10^2\ E_0\ P \quad \text{Gy m}^2\ \text{h}^{-1} \quad \text{or} \tag{14a}$$

$$D = 8.3 \times 10^{-5}\ E_0\ U \quad \text{Gy m}^2 \tag{14b}$$

and

- for 90°,

$$\dot{D} = 50\ P \quad \text{Gy m}^2\ \text{h}^{-1} \quad \text{or} \tag{15a}$$

$$D = 1.4 \times 10^{-5}\ U \quad \text{Gy m}^2\ . \tag{15b}$$

where P is the incident beam power in kW, U is the incident beam *total energy* in J, and E_0 is the electron energy in MeV. The coefficients in these expressions were obtained by taking published dose rates and extrapolating backward through the target self-shielding to the approximate location of shower maximum. They are meant to be used only for the calculation of thick shielding where detailed data are lacking and the attenuation of the shielding material is separately factored in. It is noted that the data of Fassò *et al.* (1984) agree with the rule of thumb for 0° for target thicknesses between $2\ X_0$ and $4\ X_0$, but at a thickness of $10\ X_0$ the rule of thumb would exceed the data of Fassò *et al.* by an order of magnitude.

The rule of thumb expresed by Eqs. (15a) and (15b) is meant to provide a source term when thick shielding is employed at 90° to a target. A comparison with the formula of Jenkins *et al.* [Eq. (13b)] shows consistency before the shield attenuation is accounted for; the data of Fassò *et al.* give absorbed doses

about a factor of two higher than Eq. (15) for the target radius used in the calculations; the data of Dinter and Tesch (1977) lie a factor of 2–5 higher at 90° than predicted by Eq. (15). However, after correction for the low-energy component, which is quickly absorbed, their data lie within a factor of 3–5 below those given by Eq. (15).

3. *Neutrons*

a. *Proton Accelerators (<1 GeV).* Much understanding concerning neutron production by proton (and heavy-ion) beams can be gained from the work in the region below 1 GeV. The neutrons of interest in radiological protection are generally not produced from thin targets in the beam but from scraping or stopping of the beam or a portion of the beam in a substantial amount of material — the *thick-target* situation. There the production of neutrons arises from many individual particle interactions, until the initial particle energy is dissipated. At lower energies (E 150 MeV), where the hadron cascade is less complex, the yield of neutrons is obtained from the "range-integrated" cross sections of beam particles for neutron production.

At accelerator energies below 1 GeV, two mechanisms are important, giving rise to distinctive spectra:

- "Intranuclear-cascade" neutrons are emitted by target nuclei following the direct impact of beam particles or other hadronic fragments (Metropolis, 1958a, 1958b; Bertini, 1963, 1969; Armstrong, 1980b); and
- "evaporation" neutrons are emitted from excited residual nuclei, which generally dominate the fluence close to the target, and have an average energy of a few MeV (Weisskopf, 1937).

Figures 8 and 9 show the number of neutrons emitted from the two mechanisms as a function of incident proton energy and for several target materials. The neutron spectra in Figure 10 illustrate how the continuum of intranuclear cascade neutrons extend, with diminishing intensity, up to the full beam energy for 450, 600 and 850 MeV protons on aluminum. This continuum is capped by the prominent "bulge" of evaporation neutrons at about 5 MeV.

Figure 11 summarizes total neutron yield (from both mechanisms) produced by protons and heavier particles, on a variety of materials, as a function of incident energy. Data for protons on copper have given the following rule of thumb, valid for 0.1–10 GeV and useful for scaling to other energies:

$$N/E_0 \approx 7 \text{ neutrons (proton·GeV)}^{-1}, \quad \text{or} \tag{16a}$$

$$N/U \approx 4.4\times10^{10} \text{ neutrons J}^{-1}, \tag{16b}$$

where N is the number of neutrons released, E_0 is the incident proton kinetic energy, and U is the total incident beam energy (J). A recent review by Tesch (1985) summarizes information on neutron source terms (to 10 GeV) and shielding information (to 1 GeV) for proton accelerators.

b. *The Hadronic Cascade.* For hadron accelerators operating at very high energies (several times the pion threshold at ~150 MeV), the hadronic cascade is the phenomenon that gives rise to the external radiation field. For a brief description, see, for example, ICRU (1978) and Armstrong (1980c). A fuller discussion is provided by Thomas and Stevenson (1988); also see collected papers in Nelson and Jenkins (1980).

The nuclear collision length is the mean free path between collisions of nucleons with nuclei and is given by $\lambda_c = A/(N_A \sigma)$, where A is the atomic mass number of the medium, N_A is Avogadro's number and σ is the total nucleon-nucleus cross section. For high energies (1 GeV) cross sections have little energy dependence and the cross sections of neutrons and protons are about equal [$\sigma(p) = \sigma(n)$]. Furthermore $\sigma(\pi^+) = \sigma(\pi^-) = 0.6\,\sigma(p)$. For materials commonly used in accelerator systems with Z higher than about 13, the distance within which hadronic cascade interactions occur is several times larger than for the electromagnetic cascade. To illustrate, a comparison of the radiation length for electrons and the nuclear collision length is shown in Table VI. For high Z materials, to a good approximation, the energy transferred to the electromagnetic cascade by the hadronic cascade can be considered locally deposited, except for materials with Z lower than that of aluminum. [In the design of high-energy electron beam-dumps low Z

materials such a beryllium (targets), lithium (magnetic lenses), and graphite (dumps) are used.]

The hadronic cascade involves competing processes that include several particle types (nucleons, pions and kaons, and muons). Multiplicities of reaction products are large and vary with energy. These factors make for considerable complexity. The most important hadronic cascade processes are as follows:

(i) The extranuclear cascade acts as the source of all other processes. The carriers are nucleons and mesons ($\pi^{\pm}$ and $K^{\pm}$), typically propagated with high energy, at small angles to the incident beam direction, and with high secondary-particle multiplicity per extranuclear event. The tight collimation of the extranuclear cascade follows from the small transverse momenta imparted in the elementary interactions (average of $\overline{P_T} = 0.3$–0.4 GeV/c). The multiplicity of secondary particles rises logarithmically with reaction energy. The extranuclear cascade is a high-energy phenomenon and depends upon copious meson production in each collision. It expires completely when the average particle kinetic energy decreases below about 150 MeV, near the pion-production threshold. Because, in addition, the hadron-hadron cross sections rise substantially when the energies are further reduced below this value, the attenuation of the lower energy components of the extra-nuclear cascade are sharply increased. In this regard, 150 MeV for the extranuclear cascade may be thought of as analogous to the critical energy for the electromagnetic cascade.

(ii) The π^0 mesons from the extranuclear cascade decay into two photons of high energy. These initiate an electromagnetic cascade in the vicinity of each extranuclear-cascade event in which π^0 mesons are produced. As the initial energy increases, the number of extranuclear cascade generations rises, meaning that a significant fraction of the total energy is eventually transferred. Because of this, the rule of thumb Eq. (16) will overestimate the neutron production at very high energies.

(iii) $\pi^{\pm}$ and $K^{\pm}$ mesons can decay before interacting; the fraction decaying will depend upn the length of the flight path made available. This meson decay will produce a field of mesons ($\mu^{\pm}$). Because the muons react predominantly electromagnetically in matter, the energy of the muon field is not returned to the hadronic cascade, and the only practical way for its abatement is by exhaustion through ionization or dispersion by multiple Coulomb scattering.

(iv) The intranuclear cascade gives rise to the neutron field discussed above containing energies up to about 1 GeV.

(v) The excited nuclei remaining after each cascade event emit evaporation particles, mostly low-energy (few-MeV) neutrons with an isotropic distribution (also discussed above).

(vi) The energy of the hadronic cascade is ultimately dissipated through ionization of the medium.

(vii) The resultant nucleus is usually unstable against radioactive decay, resulting in the remanent radiation field described in Section III.c.

Informative studies of the hadronic cascade are probably those performed by computer simulations. The most notable programs are CASIM (Van Ginneken, 1972; Van Ginneken and Awschalom, 1974; Van Ginneken, 1975, 1980; and Van Ginneken *et al.*, 1987), FLUKA (Ranft, 1972; Ranft and Routti, 1972, 1974; Aarnio *et al.*, 1984a,b and Ranft *et al.*, 1985) and HETC (Gabriel *et al.*, 1970; Chandler and Armstrong, 1972; Gabriel and Bishop, 1978; Armstrong, 1980a and Gabriel, 1985). Also see collected papers in Nelson and Jenkins (1980). Useful comparisons of these Monte Carlo codes are given by Mokhov and Cossairt (1986).

Results of this type of calculation are often related to "star density" (the number of interactions of the extranuclear cascade per unit volume of material). For example, cascade calculations published by Stevenson (1986) give conversion coefficients for dose-equivalent to unit star density for several materials, including dry or wet concrete, iron, aluminum, and tungsten. Table VII summarizes these and related hadronic-field conversion coefficients calculated or summarized by various authors.

High energy hadronic fields obviously transport mixtures of protons, neutrons, and mesons of various types, and gross averages over the hadronic components can be measured. For example parameters such as particle energy spectra, angular distributions, fluences, star densities, have been determined and their conversion to absorbed dose calculated.

To illustrate, Stevenson and his colleagues have reported measurements using various dosimeters around copper targets bombarded by incident protons of momentum from 8 GeV/c to as high as 400 GeV/c (Levine, *et al.*, 1972; Stevenson, *et al.*, 1971, 1983, 1986). Typical data presented include induced radioactivity, hadronic fluence and absorbed dose as a function of angle and radius from the target. Figure 12

summarizes some typical data obtained around a 1.3-cm diameter Cu target bombarded by 225-GeV/c protons. Absolute spectral information are given in integrated form over the full angular range for detectors with thresholds of 50, 70, 105, 126, 393, and 561 MeV. Similiar angular and spectral measurements have been made by Sandberg (1982).

Stevenson et al. (1986) have studied the distribution of energy inside a cylindrical aluminium target bombarded by 225-GeV protons. After exposure the target was disected into several small aluminium sections and the distribution of absorbed dose in the target determined (see Fig. 13).

Many other measurements have been reported using other detectors, for example, radiophotoluminesent glass (RPL) dosimeters (Ižisha and Schönbacher, 1979; Tesch, 1984). Good general agreement was found between measurements and simulations using the program FLUKA82 (Aarnio *et al.*, 1984b; Ranft, 1985). Tesch and Dinter (1986) give a discussion, with examples, of the use of star densities calculated by Monte Carlo methods.

Experimental work provides directly useful information and serves as a benchmark for the calculations. References to experimental studies are summarized in Table VIII.

c. *Electron Accelerators.* The production of neutrons by electron beams incident on thick targets has been discussed by Swanson (1978, 1979a, 1979b). The total neutron production is obtained by the integration of the photoneutron production cross section multiplied by the photon track length distribution of the electromagnetic cascade shower. The results for several materials are summarized in Fig. 14, which shows that the neutron production rate per unit beam power is nearly saturated at E_0 = 100 MeV for high-Z target materials, whereas it is still rising at this energy for Z < 50. However, the production rate per unit beam power for $E_0 \geq 500$ MeV is almost constant for all materials. Above this energy, a simple scaling by total electron beam energy (power) predicts the neutron production (rate).

The variation of photoneutron source with target material is indicated by a formula suggested by Swanson (1979b) which fits the behavior over a large range of atomic numbers (Z):

$$N = 1.21\times10^{8}Z^{0.66} \text{ neutrons } J^{-1} \ . \tag{17}$$

This formula is useful over most of the range of atomic numbers but will underestimate the source for very light materials (especially ^{3}H, Be) and for transuranic materials in which photofission processes become important.

In discussing photoneutron production mechanisms, it must be borne in mind that the electromagnetic cascade shower contains photons of all energies from zero up to the primary particle energy. The photon spectrum behaves approximately as k^{-2}, where k is the photon energy. Because of the preponderance of lower energy photons and because of the large cross sections at low photon energies, the dominant neutron source mechanism at all primary energies is the giant photonuclear resonance. However, other mechanisms play an important role when high-energy photons are present in the electromagnetic cascade shower. These secondary mechanisms are the quasi-deuteron effect, which is more important for photon energies in the range 30–300 MeV (DeStaebler et al., 1968; Swanson, 1979a), and neutrons released as a product of photopion reactions [threshold ≈ 150 MeV], which are more important at photon energies above 300 MeV (DeStaebler et al., 1968).

Photoneutron spectra from the giant-resonance process are often compared to a fission spectrum and are well described by a Maxwellian distribution, having a "temperature" in the range 0.5 MeV ≤ T ≤ 1.5 MeV. The Maxwellian energy spectrum is expressed in the equation

$$\frac{d\phi}{dE_n} = \frac{E_n}{T^2} \exp(-E_n/T) \tag{18}$$

which is normalized to unit fluence. For this distribution, the peak and average energies lie in the range

$$\hat{E}_n = T \approx 0.5\text{–}1.5 \text{ MeV and} \tag{19}$$

$$\overline{E_n} = 2\,T \approx 1\text{–}3 \text{ MeV} , \tag{20}$$

respectively. The Maxwellian distribution does not account for the high-energy tail produced by the secondary mechanisms described above. The behavior at photoneutron energies higher than about 10 MeV is summarized by Swanson (1979a) where references can be found. It has been described by a simple

exponential behavior:

$$\frac{dN}{dE_n} \approx E_n^{-\alpha}, \tag{21}$$

where α is in the range 1.7–3.6. There is a steeper decline than this as the neutron energy approaches the primary beam energy.

Although many more photoneutrons are produced via the giant resonance than from the higher-energy mechanisms, it is the neutrons above 100 MeV that are most capable of penetrating thick shields. Except for limited regions where muons may predominate, it is the high-energy neutrons that propagate the radiation field for shielding thicknesses greater than about 2 m of concrete. In so doing, they continually regenerate a "satellite" field: neutrons of lower energy and neutron-capture gamma rays.

d. *Spectra Within the Accelerator Enclosure.* The materials struck by the primary accelerator beam (targets, beam dumps, magnets) as well as the material of the accelerator enclosure, generally concrete or earth, will significantly alter the nature of the neutron spectrum. This phenomenon has been studied by McCall *et al.* (1979) for lower energy electron machines in which photoneutrons are filtered by tungsten and lead shielding (also see NCRP, 1984). Two effects are important — the neutron spectrum is softened by multiple inelastic scattering and the angular distribution becomes nearly isotropic. Other studies by McCall *et al.* (1979), McCaslin and Stephens (1976), McCaslin *et al.* (1983), Eisenhauer *et al.*(1982) and Stevenson *et al.* (1986), following on earlier work by Patterson *et al.* (1958), demonstrated the importance of scattered neutrons within a concrete enclosure. (See for example Patterson, 1957, and Perry and Shaw, 1965.) Elwyn and Cossairt (1986, 1987) have experimentally confirmed the existence of a peak in the distribution of neutrons leaking through an inner shield at the Tevatron. This peak in the energy spectrum in the range from about 0.1 MeV to 1 MeV was removed by the addition of 0.9-m concrete.

In calculations, Alsmiller and Barish (1973, 400-MeV electrons on Cu) and Gabriel and Santoro (1971, 500-GeV protons) furthermore predicted a very soft component of the neutron spectrum, caused by moderation by hydrogenous materials, namely concrete and earth. The particular spectral form, $1/E_n$, for these neutrons results from the "slowing-down" process and is known by that name (see, for example, Amaldi, 1959). Figure 15 shows energy spectra of neutrons and other hadrons within a volume of earth at the end of a concrete tunnel. The primary neutron source in this case is the cascade initiated by a 500-GeV proton beam incident on an iron target. Alsmiller and Barish (1973) also predicted a substantial moderating effect of iron (used in magnet yokes and beam stops) as well as an enhancement in the spectrum between 10 keV and 1 MeV due to a filtering effect of iron shielding. This effect had previously been observed at several particle accelerators. [See for example Patterson, 1957; Perry and Shaw, 1965). Elwyn and Cossairt (1986, 1987) have experimentally confirmed the existence of a peak in the distribution of neutrons leaking through an inner shield at the Tevatron.] This peak in the energy spectrum in the range from about 0.01 MeV to 1 MeV was removed by the addition of 0.9-cm concrete.

A definitive experiment by McCaslin *et al.* (1986, 1987) is very instructive in this regard. Measurements of the neutron fluence and spectrum were made in the Fermilab tunnel during Tevatron operation using Bonner spheres and other instruments. At the location of the experiment, there were no significant differences between spectra determined for Tevatron operation at 800 or 150 GeV, or for Main-Ring acceleration from 8 to 120–150 GeV. (The Main Ring is a separate accelerator that occupies the same tunnel and is used for injection into the Tevatron.

Five different spectra are shown which correspond to different operating conditions of the accelerators. When the unfolded spectra were plotted in lethargy units[4] (Fig. 16), dominant peaks between 0.2 and 1.3 MeV were evident in addition to the expected slowing-down component and enhancement of thermal neutrons. Hadron cascades in the surrounding iron of the accelerator structure, initiated by primary beam interactions with nitrogen gas in the vacuum chamber—identified by "Slope-(N_2)" in the figure—were

[4] "Lethargy is defined as $\ln(E_0/E)$, where E_0 is an arbitrary energy. Thus, plotting $E[d\phi(E)/dE]...[\equiv d\phi(E)/d(\ln E)]...$ versus the logarithm of E allows the spectrum to be displayed over a large range of energies in a way that preserves area representation of flux densities and gives a clear indication of the relative contributions of source neutrons, slowing down neutrons and thermal neutrons." (ICRU, 1969) Because natural and common logarithms differ by only a multiplicative constant, $\ln E = \ln 10 \times \log_{10} E$, the abscissa scale of Fig. 16 ($\Delta\phi/\Delta \log E$) provides these same properties.

analyzed separately from others at a location designated (A-17). Random beam events in accelerator component materials were compared at a remote location designated (A48). For typical neutron spectra filtered through iron about 30% of the fluence was contained between 100 keV and 1 MeV, and there was a surprising lack of high-energy neutrons (≈4% above 10 MeV) (Fig. 17). The median energy was about 0.06 MeV and the average quality factor close to 7, based on ICRP (1973) (see Shaw *et al.*, 1969; Patterson *et al.*, 1971; Rindi, 1974a, 1977). The same experiment yielded upper limits to the absorbed dose due to photons and minimum-ionizing particles. These measurements showed that the absorbed dose (in tissue) from photons is comparable to, or less than, the absorbed dose from the neutron field, and the absorbed dose from minimum-ionizing particles from the beam line is lower than that from neutrons by at least an order of magnitude.

In the particular location in which the measurements were made, the detector array was shielded from direct view of the beam line by a chain of magnets having iron yokes about 11 cm thick. The picture suggested by these results is that very little remained of the high-energy particles of the hadronic cascade (predominantly $\pi^{\pm}$ and $K^{\pm}$) or electromagnetic cascade (photons and $e^{\pm}$), but rather that the radiation field at the location of the detector was dominated by fast neutrons from the iron dipole magnets, subsequently scattered within the enclosure.

e. *Spectra Outside Shielding.* Experience at the highest energy proton synchrotrons has shown that it is possible to find radiation fields in which any one energy-component (e.g., thermal neutrons, intermediate-energy neutrons, or fast neutrons) dominates (Antipov *et al.*, 1978; McCaslin *et al.*, 1977; McCaslin and Thomas, 1981; Moritz, 1988). These differences between the radiation fields very much depend upon the thickness of shielding and the number and type of penetrations in the shielding between the primary source and the point of observation.

The neutron field reaches equilibrium through transverse shield thicknesses of about 500 g cm^{-2} and the properties of the field were studied in some detail at the early proton synchrotrons. Perry (Perry and Shaw, 1965; Perry, 1967) was one of the first to give a detailed description of the field outside the concrete shield (1.5 m to 3 m thick) for a 7 GeV, weak-focusing proton synchrotron and his results are given in Table IX. As the energy of the accelerated particles increased it was found that there were many departures from the simple rule given by Patterson (1965; see p. 15). For example, at CERN it was reported that the importance of fast neutrons relative to intermediate and thermal neutrons could significantly differ from what was indicated by earlier data (Baarli and Sullivan, 1965a,b; Capone *et al.*, 1965). It became clear that it would be necessary to determine neutron spectra before the dosimetric data could be fully understood.

Over the past twenty years, neutron spectra have been determined at several accelerators under different conditions of shielding. The spectra were obtained by using a variety of experimental techniques including nuclear emulsions, activation detectors, Bonner spheres, and fission counters (Gilbert *et al.*, 1968; Thomas, 1973; Thomas and Stevenson, 1985). Figures 18 through 21 show several spectra identified as follows:

- 1/E the familiar slowing-down energy spectrum.
- RT a neutron spectrum determined at the CERN 28-GeV proton synchrotron (CPS) above the earth shielding with a target intercepting the beam as a primary radiation source.
- PSB measured at the CPS above a concrete shield, again with a target acting as the primary source.
- BEV measured at the University of California Radiation Laboratory (now Lawrence Berkeley Laboratory) 6.3-GeV proton synchrotron outside thick concrete shielding.
- X2 measured at the 7-GeV proton synchrotron of the Rutherford Laboratory, outside concrete shielding.
- P1 measured as for X2 but outside steel shielding.
- PLA the ambient neutron spectrum around the 50-MeV proton linac of the Rutherford Laboratory, largely from skyshine.
- CR cosmic-ray neutron spectrum measured by Hess *et al.* (1959).
- PPA measured at the Princeton-Pennsylvania Proton Accelerator.

The features of these spectra will now be described and discussed. Figure 18 shows neutron spectra measured by the Lawrence Berkeley Laboratory Group during the middle 1960s (Gilbert *et al.*, 1968; Hess *et al.*, 1959; Patterson *et al.*, 1959). A combination of four detectors was used: a boron trifluoride (BF_3) counter in a cylindrical moderator, the ^{27}Al–^{24}Na and ^{12}C–^{11}C passive activation detectors, and a bismuth ionization chamber (see Section IV). These spectra are reasonably well constrained in the 0.1–100-MeV region. Outside this energy range the spectra are not well determined by the measurements but general physical principles are invoked to give reasonable spectral shapes. From these early measurements several features emerge. The "ring-top" spectrum (RT) was measured above the earth shielding of the CERN 28-GeV proton synchrotron (CPS). This earth contained more moisture than the concrete shield of the "PS bridge" — a concrete shielding structure around internal targets — at the same accelerator where the PSB spectrum was measured. The Bevatron spectrum (BEV) shows a broad peak in the 1–100 MeV region; the negative slope of the cosmic-ray spectrum (CR) in this energy region coupled with the response of the moderated BF_3 counter implies a peak in the spectrum below 1 MeV.

Spectra were obtained at the 7-GeV proton synchrotron accelerator "Nimrod" of the Rutherford Laboratory using the multisphere technique with a ^6LiI scintillator as the thermal neutron detector (Stevenson, 1967). The spectra in Fig. 19 are relatively flat in the lethargy plot (reflecting a 1/E differential energy spectrum). The X2 spectrum, taken directly outside the shield around a target struck by an extracted beam, is significantly harder than the P1 spectrum, which was measured in an environment where the outer surface of the shield was of iron and there was a significant contribution to the field from neutrons scattered by local concrete blocks.

Spectra obtained by the Princeton-Pennsylvania Health Physics Group, also using Bonner spheres (Fig. 20), show a much more oscillatory character (Awschalom, 1966), which may reflect the spectrum unfolding by the routine used, which was different from that used at the Rutherford Laboratory. The selection of unfolding routines is extremely important in ensuring the reliable and physical interpretation of Bonner-sphere measurements.

The neutron spectra described in Figs. 18–20 were obtained under conditions of great experimental difficulty. It is therefore valuable to have theoretical support in the analysis of such measurements that cannot only interpret the experimental data but guide further measurements. Figure 21 shows the results of calculation by O'Brien where the features of a 1/E type spectrum, coupled with a peak in the 1–10 MeV energy range, are confirmed. In addition, the calculation by O'Brien reveals a second peak in the 100-MeV energy region. None of the measurements described above would be expected to have sufficient resolution to detect this peak (O'Brien and McLaughlin, 1968; O'Brien, 1971), which was later confirmed experimentally by Madey *et al.* (1976), and also in calculations reported by Stevenson of the high-energy cascade in iron (Stevenson, 1984a).

All the spectra shown may be qualitatively understood in terms of the shielding configuration around the accelerators, but caution must be used in their detailed interpretation. It is not possible with the techniques available to obtain precise neutron spectra and the assumptions made in obtaining the spectra must be clearly understood. The spectra shown are, however, of great value in radiological protection and are of sufficient accuracy for that purpose.

Cossairt *et al.* (1987) have recently summarized neutron spectra measured around the Fermilab Accelerator. These measurements confirm the general conclusions reached by the earlier workers.

The thermal neutron fluence is particularly difficult to determine because it is greatly influenced by the presence of absorbers and scatterers (including the detectors themselves) and hence may show large fluctuations with location. Thermal neutrons are found near the openings of labyrinths and other shielding penetrations; these are effective in eliminating fast neutrons but thermal neutrons can scatter through them [see, for example, Cossairt *et al.* (1985b), Elwyn and Cossairt, (1987)]. At higher energies (>100 MeV) charged particles will be present and can influence the response of detectors.

4. *Protons*

Energy loss by ionization (mass stopping power) of protons can be calculated using the Bethe-Bloch formula and values are provided by Janni (1966, 1982), Bichsel (1968, 1972), and Bichsel and Porter (1982). Radiological protection must take into account the quality factor, which ranges between Q = 1 (above 15 MeV) and 15 (below 0.1 MeV). Conversion coefficients from fluence to dose equivalent are given in ICRP Publication 21 (1973) and recently revised in ICRP 51 (1987).

Although the primary hadron beam may be easily attenuated or even "ranged out" in the accelerator beam-stop, depending on the energy, a secondary proton field is generated by the cascade process, generally by the interaction of secondary neutrons. Tardy-Joubert (1965) cited the work of Puppi and Dallaporta (1952) to show that at energies above about 100 MeV, protons would appear in increasing numbers relative to neutrons of the same energy in the equilibrium field.

The presence of protons outside accelerator shields has been detected by counter telescopes (Penfold and Stevenson, 1968; Aleinikov *et al.*, 1975) and by spark chambers (Hajnal *et al.*, 1969; Rindi, 1974b; Mamont-Ciesla and Rindi, 1974). Figure 22 shows the proton spectrum measured outside a 2 meter thick concrete shield-wall of the 660-MeV Dubna synchrocyclotron using a proton telescope and (dE/dx) spectrometer (Aleinikov *et al.*, 1975). It is now possible to investigate the charged-particle spectrum using radiation transport codes (see for example, Aarnio *et al.*, 1984; Stevenson, 1984a, 1986).

Such theoretical and experimental studies are important because of the following reasons given by Thomas and Stevenson (1985).

> "During the past ten years the radiation environments around high energy accelerator facilities have undergone a subtle change. The external radiation fields from the earliest proton synchrotrons (Cosmotron, Bevatron) mainly came from the bulk shielding of the accelerators themselves. As the shielding of the accelerator proper was improved the dominant radiation sources came from the extracted primary beam lines (AGS, CPS, Nimrod). Secondary beams from these second generation proton synchrotrons were of little importance as radiation sources. However, at the highest energy facilities (Fermilab and the CERN SPS) it is possible for secondary beams to have intensities equal to or greater than the [primary] intensity of the early synchrotrons. These secondary beams are typically transported through lightly shielded areas, often without roof shielding, because beam losses are small. It is expected that quality of the radiation fields around these unshielded, or lightly shielded high energy (>100 GeV) beams will be very different from those found around the well shielded second generation proton synchrotrons. Theoretical cascade calculations predict the presence of protons and charged pions under certain circumstances. The existence of this charged component to the field is of great importance; the techniques currently used to measure dose equivalent may not be entirely adequate. The conventional interpretation of the readings of personal dosimeters (e.g., film) may be incorrect. Charged particle fluence to dose equivalent conversion coefficients (particularly for negatively charged pions) need to be determined."

5. *Muons*

a. *Introduction.* It was known early from studies of cosmic radiation, that muons would be present in the radiation environment around particle accelerators of sufficiently high primary energy. A brief review of the production, transport, and shielding of muons may be found in Thomas and Stevenson (1988).

The detection of muons within their characteristic "cone," downstream of the targets of large accelerators, is relatively easy. However, to pinpoint their origin may be difficult because of multiple sources of production and the presence of intense magnetic fields near the points of production (see, for example, the work of Moore and Velen, 1974).

Except for their higher mass, muons are similar in every respect to electrons. In principle, the dose from muons can be measured by normal ionization chamber techniques, but Höfert (1984b, 1987) noted discrepancies of up to 30% between the readings of different detector types in pure muon fields. The problem of muon dosimetry in general, and of fluence to dose-equivalent conversion in particular, is discussed by Stevenson (1983) (see also ICRP, 1987).

The energy loss by muons due to ionization is computed from the Bethe-Bloch formula [see, e.g., Bethe and Ashkin (1963)] with the density-effect correction of Sternheimer (well described in Sternheimer and Peierls, 1971). At higher energies (see below), muons lose significant energy by catastrophic radiative processes such as bremsstrahlung, direct electron or muon pair-production ($e^{\pm}, \mu^{\pm}$) and inelastic nuclear collisions (Barrett *et al.*, 1952; Hayman *et al.*, 1963). Muon mass stopping powers were calculated by Thomas (1964). Extensive tables of muon stopping powers and ranges in various materials have since been published by Barkas and Berger (1964), Berger and Seltzer (1966), Richard-Serre (1971), Stevenson (1984c) and Lohmann *et al.* (1985). Figure 23 shows a plot of average muon ranges in several materials as a function of energy. It is noted that muon ranges can be hundreds of meters in soil at the energies characteristic of new operating facilities [~2 km for the planned 20-TeV Superconducting Super Collider, (SSC)].

Muon transport calculations have taken two basic approaches: an analytic method involving numerical integrations based on Fermi-Eyges theory for energy loss with multiple scattering (Eyges, 1948), and the application of Monte Carlo techniques. Both methods give satisfactory agreement with experiment, but the agreement becomes less satisfactory as range straggling becomes more important at higher energies. The analytic approach has been pursued by Alsmiller *et al.* (1971) for proton accelerators (< 500 GeV), Alsmiller and Barish (1969) for electron accelerators (18 GeV), Nelson and Kase (1974), Stevenson (TOMCAT program, 1981b), Ladu *et al.* (1972) (100, 200 and 500 GeV muon energy), and Keefe and Noble (1968; 25, 70, 200, 300 GeV muon energy).

The Monte-Carlo approach has been developed by Van Ginneken (program CASIMU, 1975) at Fermilab, Mokhov *et al.* (program MUTRAN, 1981) and Maslov *et al.* (MUTRAN calculations for 1 and 3 TeV primary protons, 1983). The work of Alsmiller *et al.* (1968) for the design of a beam-stop for a 200-GeV proton accelerator, compares

- Monte Carlo calculations that include multiple Coulomb scattering and range straggling;
- Monte Carlo calculations that include multiple Coulomb scattering but neglect straggling;
- Analytic calculations that approximate multiple scattering and neglect straggling.

Although these approximations led to somewhat different results, all appeared to be sufficiently accurate for beam-stop and shielding design for facilities operating up to ≈200 GeV.

Experimental studies at electron accelerators are primarily those of Nelson (1968) and Nelson *et al.* (1974) at SLAC. At proton accelerators, related measurements have been reported by Green *et al.* (1986) (25–150 GeV/c muons through Pb and Fe), Nelson *et al.* (1979, 1983) (200–280 GeV muons through soil) and Cossairt (1983) (muons from 400 GeV primary protons, soil).

Stevenson (1983) has summarized present knowledge of the relationship of dose and dose-equivalent H to muon fluence. Based on a quality factor Q = 1, he recommended a nominal conversion factor of 40 fSv m^2 for muons between 100 MeV and 100 GeV, i.e.,

$$H(\mu^{\pm}) = 40\,\phi_{\mu}\ \text{fSv m}^2\,, \tag{22}$$

where ϕ_{μ} is the muon fluence in m^{-2}. Below 100 MeV, muons will stop in the human body, with increasing linear energy transfer as the energy decreases, and the dose equivalent will depend strongly upon spectrum and geometry. Below 100 MeV, Stevenson recommends a conversion factor of 260 fSv m^2 (Fig. 24). However, the muon spectra encountered at accelerators are generally very broad and contain only a small percentage of muons below 100 MeV, so this contribution can usually be neglected.

b. *Muons from Proton Accelerators.* Muons arise principally from the decay of pions and kaons produced in the hadronic cascade induced in the accelerator structure, surrounding equipment, and shielding, and particularly in beam-dumps. The decay of pions in secondary beam lines is a less important source of muons (Keefe, 1964; Keefe and Noble, 1968).

The threshold for pion production from proton reactions with nuclei is a little less than 200 MeV and muons are observed in the radiation environment of proton synchrocyclotrons. Muons interact electromagnetically with particles and, once produced, will be stopped only by reaching the end of their ranges. At accelerator energies below 10 GeV, muons have not presented a problem because the shielding thickness usually exceeds the range of the muons.

At particle accelerators with energies above about 20 GeV, muons should be expected, particularly in regions downstream of targets, beam-dumps or other locations where the beam interacts (Barbier and Hunter, 1971; Bertel and de Sérèville, 1971; Bertel *et al.*, 1971). Substantial muon intensities were observed downstream from targets when the 33-GeV Alternating-Gradient Synchrotron (AGS) first came into operation at Brookhaven National Laboratory (Cowan, 1962). Muons were also observed downstream of low-energy pion beams at the Nimrod accelerator at the Rutherford Laboratory. They are a regular feature of the radiation field at all the multi-GeV CERN accelerators (Bertel *et al.*, 1971; Nielsen, 1971) and at Fermilab (Cossairt, 1983; Kang *et al.*, 1972; Theriot *et al.*, 1971). At the highest energy accelerators, for example at Fermilab and the SPS, there are some special considerations. At energies above 1 GeV the so-called direct production of muons—the decay of charmed mesons—can become an important, or even dominant, source of high-energy muons.

The decay of pions in beam lines is the most important source of muons at these accelerators—these muons tend to be generally collimated around the transported beams but can be as large as several meters in lateral dimension. Radiation intensities as high as 50 μSv h^{-1} have been observed, making these muon beams readily detachable (Stevenson, 1988).

c. *Muons from Electron Accelerators.* Above about 211 MeV, muon pair-production (μ^+, μ^-) by photons becomes possible. This is a process analogous to ordinary e^+–e^- pair production, except that the cross sections are smaller by approximately the ratio of the particle masses squared, $(m_e/m_\mu)^2 \approx 40{,}000$. Muons also are produced by decay of $\pi^\pm$ and $K^\pm$ mesons but, depending upon the decay path available, these fluences are relatively small compared with fluences from direct muon pair-production. Just as for hadron accelerators, the photoproduced muon fluence is very highly peaked in the forward direction with typical beam diameters (at half-intensity) of 10–30 cm outside thick shielding.

Muon photoproduction and transport with specific application to electron accelerators have been discussed by Clément and Kessler (1965), Nelson (1968), the companion papers by Nelson and Kase (1974) and Nelson *et al.* (1974), and by Alsmiller and Barish (1969). Figure 25 shows calculated integral energy spectra of muons produced in a thick target of iron at various angles and primary electron energies. Figure 26 plots the $\mu^\pm$ fluence at 0°, integrated over all muon energies, as a function of primary electron energy, E_0. The fluence rate at 0° per kW of primary electron-beam power is approximately proportional to E_0 at energies up to about 30 GeV.

d. *Muons at Very High Energies.* At very high energies 100 GeV), processes other than the ionization loss as described by the Bethe-Bloch formula take on increasing significance (Hayman *et al.*, 1963; Thomas, 1984; Ladu *et al.*, 1972; ICRU, 1978; Mo and Tsai, 1969; Lohmann *et al.*, 1985; Van Ginneken, 1986). Among the additional processes, muon bremsstrahlung dominates to about 10 GeV, followed in importance by electron pair production and inelastic nuclear scattering (Fig. 27). Above 10 GeV, electron-pair production dominates. For these processes, the probability of a fractional energy loss in a collision has only a weak energy dependence. Therefore, the average muon mass stopping power is commonly written as

$$-\frac{1}{\rho}\frac{\langle dE\rangle}{\langle dx\rangle} = a(E) + b(E)\,E\,, \tag{23}$$

where ρ is the medium density, a(E) is the usual ionization energy loss rate and $b(E) = b_{brems}(E) + b_{pair}(E) + b_{nucl}(E)$ is the sum of the fractional energy losses due to bremsstrahlung, pair production and inelastic nuclear processes. The inverse of the slowly-varying coefficient b is analogous to a generalized "radiation length" for muons in the multi-GeV region; a reasonable approximation (to within a factor of ≈2) results if a is set equal to its value at 10 GeV and $b^{-1} \approx 1\times10^4\ X_0$, where X_0 is the radiation length for electrons (Tsai, 1974; Seltzer and Berger, 1985; Knasel, 1970). Values of the coefficients b for iron are shown in Fig. 27 (Groom, 1986).

Based mainly on work of Hayman *et al.* (1963), Jackson (1983) has suggested average values for a and b for soil (composition corresponding to $\bar{Z} = 11.3$, $\bar{A} = 22.6$), for muon energies from 10 GeV to 100 GeV, as

$a = 2.08 + 0.7675 \ln E$,
$b_{brems} = 1.84\times10^{-6}$,
$b_{pair} = 1.55\times10^{-6}$,
$b_{nucl} = 0.11\times10^{-6}$, and therefore
$b = 3.50\times10^{-6}$,

where E is in MeV, a is in MeV $cm^2\ g^{-1}$ and the coefficients b are in $cm^2\ g^{-1}$.

Given the slow variation of both a and b with energy, we may treat the coefficients as constant to obtain the average energy-range relationship for multi-TeV muons:

$$E \approx (a/b)\exp(b\bar{R} - 1)\,, \text{ or,} \tag{24a}$$

$$\bar{R} \approx \frac{1}{b}\ln\left[1 + \frac{bE}{a}\right] \tag{24b}$$

where $\bar{R}$ is the muon average range in the same units as b^{-1}. It should be emphasized that processes

represented by the second term of Eq. (23) involve catastrophic energy losses that are variable and often large. This introduces considerable range straggling for muons in the multi-TeV region. To a first approximation, one may consider the spectrum of muons, resulting from these processes, to be the same as that for electrons of the same primary energy following bremsstrahlung. Fluctuations in energy loss and resultant range straggling may be important to the dosimetrist in some circumstances (ICRU, 1978). Van Ginneken *et al.* have given useful information on range straggling of muons at very high energies (Van Ginneken *et al.*, 1987).

6. *Synchrotron Radiation*

a. *Introduction.* When charged particles pass through transverse magnetic fields, they experience a transverse acceleration equivalent to a series of regular accelerations of fixed magnitude. This acceleration is accompanied by the emission of synchrotron radiation. Synchrotron radiation can thus be considered similar to bremsstrahlung in its underlying physical origin, except that for bremsstrahlung, the accelerations are random and, on average, much larger. At currently operating electron facilities, the spectrum of synchrotron radiation (Green, 1976) covers typically the eV (visible light) to keV region, i.e. it is much softer than the bremsstrahlung spectrum emitted by electrons of the same energy.

The theory of synchrotron radiation, in a form easily applicable to circulating electron beams, was developed by Schwinger (1949). A basic theoretical treatment is given by Jackson (1975). Because of the interest in synchrotron radiation as a research tool, there is an extensive and growing body of literature about its sources, characteristics and applications. The short review by van Steenbergen (1979) is a good introduction to the subject. An extensive description of synchrotron radiation and its sources is given by Krinsky *et al.* (1985). The proceedings of major conferences on synchrotron radiation instrumentation are available (e.g., SRI, 1980). Another valuable source of current information is the Handbook of Synchrotron Radiation, edited by Koch (1983).

At relativistic energies, the primary synchrotron radiation resembles a searchlight beam, tightly bundled about the tangent to the orbit, sweeping the orbital plane (Fig. 28). The characteristic angle is $\theta_c = 1/\gamma \equiv \sqrt{1-\beta^2} = m_e c^2/E_0$ radians, where E_0 is the electron's total energy, and the polarization is such that $\vec{E}$ lies in the orbital plane. However, upon striking the first solid material (e.g., the vacuum vessel, typically at glancing angles), the synchrotron radiation is multiply Compton-scattered, if not absorbed. The scattered field therefore tends to be more isotropic than the primary radiation, and resembles the field from an isotropic ring source, or in close, an isotropic line source. With high energy electron rings, the primary radiation is sufficiently intense to cause radiation damage.

Synchrotron radiation is of a steady predictable nature and its characteristics are easily calculated for a given beam current, magnetic field, and particle mass. Two parameters are of primary importance in determining the effects of synchrotron radiation: the characteristic energy and the radiated power. The characteristic energy, ε_c, is defined as the median energy of the power spectrum and characterizes the "hardness" of the radiation. It increases as the third power of the particle energy. For electrons:

$$\varepsilon_c = 2.218\, E_0^3/\rho \ , \tag{25}$$

where ε_c is in keV, E_0 is in GeV and ρ is the bending radius in meters. The radiated power, P (in watts), for a circulating electron current, I (in mA), is

$$P = 88.46\, E_0^4 I/\rho. \tag{26}$$

The differential photon spectrum for a single electron is given by the expression:

$$\frac{d^2N}{d\varepsilon dt} = \left[\frac{\alpha}{\pi\ \sqrt{3}}\right](1/\gamma^2)\int_r^{\infty} K_{5/3}(\eta)d\eta \ , \tag{27}$$

where N is the number of photons, ε is the photon energy, α and hbar are the fine-structure constant (1/137.036) and Planck's constant (6.626176×10^{-34} J·s), respectively, $\gamma = E_0/m_e c^2$, the integrand is the modified Bessel function of order 5/3 and the integration is over the dimensionless dummy variable η. The lower limit of integration is the ratio of the photon energy to the characteristic energy, $r \equiv \varepsilon/\varepsilon_c$. The differential power spectrum can be written in universal form as

$$\varepsilon \frac{d^2N}{d\varepsilon dt} = C(\gamma)\, G_2(r)\,, \tag{28a}$$

where $C(\gamma)$ is a function of electron speed only and

$$G_2(r) \equiv r^2 \int_r^\infty K_{5/3}(\eta)d\eta \tag{28b}$$

Values of G_2 are plotted in Fig. 29. Simplified forms have been suggested to avoid dealing with the Bessel function (e.g. Stevenson, 1981a). The spectrum peaks near the characteristic energy, ε_c and falls off rapidly above it; about 95% of the radiated power is contained between $0.1\varepsilon_c$ and $5\varepsilon_c$. Therefore, for qualitative assessment of dosimetric consequences of synchrotron radiation, the spectrum can be considered to consist of photons of energy near ε_c. The spectrum is considered useful for research purposes to about $5\varepsilon_c$.

An "insertion device" is a magnetic device placed in a straight section of an electron ring to enhance the synchrotron radiation. Two types are frequently used: A "wiggler" consists of short sections of alternating-polarity magnetic field, usually provided by high-field permanent magnets or superconducting magnets. The beam orbit suffers no net deflection by this device but, because the local magnetic fields are strong, a synchrotron radiation spectrum at a significantly higher characteristic energy can result. Achievable fields can increase ε_c values by up to a factor of 4 above what is obtained from bends in conventional electromagnets. Wigglers can be oriented to produce polarization in any plane containing the beam direction. An "undulator" is composed of many low-field wigglers in sequence. The radiation intensity is proportional to the square of the number of undulator periods; enhancements in intensity of as much as two to three orders of magnitude can be achieved.

b. *Electron Accelerators and Rings.* Although present in noticeable amounts in all circular electron accelerators, synchrotron radiation was not considered a troublesome phenomenon until the multi-GeV rings, such as SPEAR, DORIS, PETRA, PEP and LEP, were constructed. Attention was drawn to the radiological protection considerations in an early paper by Golde and Warren (1980). In PETRA, corrosive agents formed by radiolysis of air caused damage to magnet pole faces (Tesch, 1986) until protective coatings were applied. For PEP (1976), possible damage to coils by radiolytic gases produced by synchrotron radiation was examined by Nelson *et al.* (1975). In LEP, the highest-energy electron accelerator now under construction (Fassò *et al.*, 1984), provision is made to shield the synchrotron radiation with lead incorporated into the vacuum vessel, in order to prevent radiation damage to nearby magnets and electronics (Burn *et al.*, 1982; Chapman *et al.*, 1983). In LEP, enhanced photoneutron production is also a result of synchrotron radiation for 100-GeV operation.

Typical synchrotron-radiation spectra are shown in Fig. 30 for LEP energies (51.5, 86 and 100 GeV), and relevant parameters for selected large rings are shown in Table X. Because of the large variation in photoelectric absorption among materials at synchrotron-radiation energies, absorbed dose measurements must be interpreted with care and the medium should be specified. Spectral modifications due to materials (beam windows, air, etc.) are significant and should be taken into account. These and other general dosimetric considerations are described by Esposito and Pelliccioni (1982).

In work at the storage ring ADONE (Frascati), Cannata *et al.* (1983) used thin films of commercially available blue and green cellophane in dosimetric studies of synchrotron radiation in the low-energy x-ray region (ε_c = 2.7 keV). Ionizing radiation bleaches these films irreversibly and they are useful for absorbed doses above about 10^4 Gy. Following exposure, the optical density profiles were read at 6328 from a low power He-Ne laser. The blue and green films were only 15 and 30 μm thick, respectively, and therefore especially suitable for measurements in fields with large gradients for field mapping and depth-dose distribution studies.

Series of measurements were performed at the rings DORIS and PETRA at DESY (Yamaguchi, 1981, 1982; Dinter *et al.*, 1982; Dinter, 1982, 1983, 1984, 1985a,b) with silver-activated radiophotoluminescence (RPL) glass dosimeters. The composition of this material gives mass-energy absorption coefficients similar to Al, a common material in accelerator or ring environments. This type of glass dosimeter is capable of measuring absorbed dose of a range of ten orders of magnitude and is widely used at CERN, DESY and in Japan (K. Tesch, 1984, 1988). Dosimetric properties are illustrated in Fig. 31 (Dinter *et al.*, 1982; Yamaguchi, 1982 in which the calculated kerma is compared to the calculated absorbed dose to the same material, either unshielded or shielded by thin (1.7 mm) layers of air, CH_2, or

Al. Below 30 keV, the average dose is less than the kerma, owing to rapid absorption in outer layers. Above 1–3 MeV, the absorbed dose is again reduced below the kerma, because energy is transported out of the material by secondary electrons.

The results of dosimetry for storage rings is commonly normalized to units of circulated beam "charge" in units of A·h. In the measurements made at the 5-GeV electron storage ring DORIS at DESY (bending radius of 32 m) (Tesch, 1986; CEBAF 1987), the absorbed dose was measured at several locations 10 cm outside the 3-mm thick aluminum vacuum chamber of dipole magnets. The locations were also shielded by 14 mm of Cu absorber. The average absorbed dose was found to be 700 Gy per A·h of beam operation.

Absorbed dose measurements were made at PETRA at 17–23.5 GeV over an extensive grid (Dinter *et al.*, 1982; Dinter 1985a). In particular, measurements in the median plane, near the aluminum vacuum chamber, are of interest because of potential radiation damage. For 17–GeV operation absorbed dose rates per unit beam charge were about 4.8×10^{6} Gy $(A\cdot h)^{-1}$ and 1.5×10^{5} Gy $(A\cdot h)^{-1}$, for locations to the outside (≈6 cm) and inside (≈18 cm) of the ring, respectively (Dinter, 1985a). (Distances quoted are measured from the *projected point of synchrotron radiation impact* on the vacuum vessel.) Additional shields of 3-mm Pb reduced these values by more than 3 orders of magnitude towards the outside and more than 2 orders of magnitude towards the inside of the ring. These results should be considered only as indicative, as the absorbed doses will vary with the type and thickness of actual walls, cooling water channel, and shielding employed.

The distribution of scattered synchrotron radiation is illustrated by the set of isodoses for a tunnel section shown in Fig. 32 for 17-GeV operation (Dinter, 1985a). As the ring locally resembles a line source, a 1/R dependence on distance is expected. This was found to be approximately true, with some flattening at distances greater than 1 m due to scattering from tunnel walls. Over a range up to 170 cm from the beam line, the average dependence on distance varied more closely as $R^{-0.8}$. In the regions studied, the dose was practically all from scattered photons. Absorption of the general tunnel field was also studied as a function of Pb shielding thickness. An exponential attenuation for 1–10 mm of Pb was found at beam height at the tunnel wall, and analysis of the data gave an effective energy of about 300 keV, consistent with expectations for scattered photons.

In conjunction with these studies, the geometry was also simulated using the Monte-Carlo program EGS (Ford and Nelson, 1978), for PETRA over the range 17–30 GeV (Dinter, 1982, 1984, 1985a) and for HERA at 30 GeV (Dinter, 1982, 1984). Although the true geometry could be simulated only approximately, agreement with the PETRA measurements was usually within a factor of 2, when a comparison could be made. In a parallel set of calculations with a Monte Carlo program that took into account the intrinsic polarization of the synchrotron radiation (Kötz, 1981), acceptable agreement with measurements was also found.

Dinter (1985a) also studied the dependence of synchrotron radiation absorbed dose on PETRA beam energy at nine locations in the tunnel, both with RPL glass dosimetry and in calculations with EGS (Fig. 33). The energy range of the measurements was 17–22.8 GeV, and for the calculations 17–30 GeV. The dependence of dose on beam energy varied approximately as E_0^n, where $n \approx 9$ (range 7–10). Such a dependence is considerably higher than the dependence of radiated power per unit length, reflecting in addition the greater penetrating power of the radiation with increasing ε_c.

c. *Proton Accelerators and Rings.* Synchrotron radiation was not a consideration at proton (or heavier-ion) accelerators before planning began for the proposed 20-TeV Superconducting Super Collider (SSC, 1986). There the protons are sufficiently relativistic (i.e., the ratio of total energy to rest mass is high enough) that significant synchrotron radiation must be anticipated. Although the radiated power in the SSC will be much less than in electron storage rings, it will be sufficient to have an impact on the cryogenic system and the vacuum system. Parameters for the synchrotron radiation from protons can be obtained from those for electrons of the same energy by the following scaling:

- The characteristic energy is increased by the inverse ratio of masses raised to the third power: $(m_e/M_p)^3$.
- The energy loss is obtained by scaling by the inverse ratio of masses raised to the 4th power: $(m_e/M_p)^4$.

For the SSC (Table X), with an energy of 20 TeV at a bending radius of 10.1 km, the characteristic energy will be ε_c=284 eV and, for a total current per beam of I = 73 mA, the average power radiated per beam will be 9 kW.

7. *Radiation from RF Cavities*

In addition to the familiar production of x rays from klystrons and similar rf generators, Swanson (1979b) has reported, "Any vacuum containing high-power microwave fields, such as an rf separator or accelerator cavity, can produce x-ray emissions which may be intense. This radiation is unpredictable and may be erratic, depending on microscopic surface conditions which change with time. The x-ray output is a rapidly increasing function of rf power."

Measurements have been reported from several laboratories. At SLAC measurements at 90° to a test cavity to be used on PEP showed that the absorbed dose, D, due to x rays was proportioned to the fifth power of the radio-frequency power, P ($D(90°) \sim P^5$) (Swanson, 1975; Busick, 1978).

Tesch (1988) has reported that at DESY measurements on the axis of single cavity showed dose equivalent rates as high as 100 rem/h, at a distance of 10 cm from the axis, with an rf pulse power of 200 kW and a duty factor of 8%. Here the dose equivalent rate was said to be proportional to the tenth power of the rf power applied to special copper cavities.

The exposure rates around rf sources are not entirely predictable and strongly depend upon specific designs. Users are strongly advised to make adequate measurements before routine use. Ionization chambers that are sensitive to low-energy x rays should be used; thermoluminescent dosimeters are valuable integrating devices.

8. *Skyshine*

High-intensity high-energy accelerators are potent radiation sources and their operation may be detected, even at large distances, by sensitive detectors. For example, Fig. 34, shows the response of a photon detector and a moderated BF_3 neutron detector as a function of time at a distance of about 500 meters from the Experimental Area of the 20-GeV electron Stanford Linear Accelerator. At periods of intense operation the neutron dose-equivalent rate exceeds background by more than an order of magnitude, but the increase in photon dose-equivalent rate is only 10–20%.

DeStaebler (1965) stated the basic reasons for expecting that neutrons should be the dominant source of dose equivalent outside the shielding of high-energy high-intensity accelerators, whether they accelerate electrons or protons. Measurements have amply confirmed that expectation at both proton accelerators (see, for example, Patterson and Thomas, 1973 and Thomas and Stevenson, 1988) and electron accelerators, in particular at the Stanford Linear Accelerator Center (SLAC) (Nelson and Jenkins, 1976).

As another example, this time for a proton accelerator, Fig. 35 shows contours of equal dose equivalent due to neutrons (Fig. 35a) and photons (Fig. 35b) taken from environmental monitoring data at CERN during 1974 (Bonifas *et al.*, 1974; see also Tuyn, 1977 and Tuyn, 1982). At the time these measurements were made, three accelerator facilities were in operation: a synchrocyclotron (identified as SC), a 28-GeV proton synchrotron (PS), and intersecting storage rings (ISR). Radiation levels of 100 μSv/y were observed some 500 m from the proton synchrotron, as compared with the background level of about 30 μSv/y (Hewitt *et al.*, 1980). The annual dose equivalent due to photons is more than an order of magnitude lower than that due to neutrons. These observations may be explained by the fact that the neutron source strengths, even from shielded accelerators, are high, and the natural neutron background is low. For instance, it has been estimated from radiation surveys that 10^9 neutrons s^{-1} leak from the roof shield of the Bevatron when it accelerates 10^{12} protons s^{-1} to an energy of 6 GeV (Smith, 1977). At a distance of about 1 km, a neutron source of this magnitude generates a fluence comparable to that of neutrons at sea level produced by cosmic rays (Thomas, 1978a,b).

The word "skyshine," as commonly used in the literature, describes all radiation reaching a point distant from an accelerator, whether the radiation is unscattered or scattered (from the ground, air, or even buildings). Because of the dominance of neutrons as a source of dose equivalent, neutron skyshine has been most studied.

An early theoretical study by Lindenbaum (1957) used neutron diffusion theory to characterize the neutron field around the Cosmotron of the Brookhaven National Laboratory. The absence of overhead

shielding at this 3-GeV proton synchrotron resulted in a radiation field different from that found around well-shielded high-energy accelerators. Lindenbaum's treatment was intended to describe a situation in which the neutron-leakage spectrum in the air was largely composed of neutrons with energy below a few MeV. Leakage from the magnet steel of the Cosmotron provided an intense source of such neutrons and Lindenbaum's use of diffusion theory proved to be adequate (within a factor of two or so) to describe the variation of neutron dose equivalent with distance out to about 200 m from the accelerator.

However, when an accelerator is well-shielded, and the radiation field is consequently controlled by neutrons of energy > 100 MeV, Lindenbaum's treatment fails. Moyer discussed the transport of high-energy neutrons through the atmosphere but showed, because of the magnitude of the physical parameters involved, that the forms of the variation of neutron fluence with distance, both for the diffusion-neutron group and the high-energy neutron group, were very similar (Moyer, 1962, see Fig. 36). Mere inspection of the shape of the variation of neutron fluence with distance from an accelerator is therefore an insensitive test of any theoretical predictions—absolute measurements of flux density are required and measurements of the energy spectrum highly desirable. This fact may explain the use of empirical formulae by some workers which, although they apparently fit experimental data quite well, are nevertheless not based upon complete theoretical models (Bathow *et al.*, 1967a; Jenkins, 1974; Nakamura, 1981a,b).

In the absence of a comprehensive theoretical treatment of skyshine an empirical approach must be adopted. Figure 37 summarizes some of the experimental data obtained around several particle accelerators (Rindi and Thomas, 1975). At distances greater than about 200 m from the accelerator all the observed sets of data may be fitted with an empirical equation of the form:

$$\dot{\phi}(r) = \frac{aQ \exp(-r/\lambda)}{4\pi r^2} \tag{29a}$$

or

$$\dot{H}(r) = \frac{gaQ \exp(-r/\lambda)}{4\pi r^2} \tag{29b}$$

where $\dot{\phi}(r)$ and $\dot{H}(r)$ are the fluence rate and the dose equivalent rate, respectively. Here,

- Q is the leakage neutron source strength,
- a source enhancement factor. (This dimensionless factor accounts for possible "buildup" of the neutron field.),
- r is the distance from the accelerator
- λ is the effective attenuation length of the skyshine neutrons in air
- g is a fluence-to-dose equivalent conversion coefficient.

Equations (29a) and (29b) give a plausible, physical interpretation of observation and require knowledge of four parameters: the leakage source strength Q, the source enhancement factor a, the attenuation length λ, and the conversion coefficient g, which is energy-spectrum dependent.

The values of λ observed vary from about 250 m to nearly 1000 m (Rindi and Thomas, 1975). For conditions where low-energy neutrons dominate the shield leakage spectra, values towards the lower end of the range are obtained [cf., values of λ obtained at large distances from nuclear reactors or D-D and D-T neutron sources (Stephens and Aceto, 1963; Sanders *et al.*, 1962; Auxier *et al.*, 1963; Haywood *et al.*, 1964, 1965; French and Mooney, 1971)]. Examples of such accelerator conditions are a 50 MeV proton beam from the Rutherford Laboratory linear accelerator stopped in a thick copper target with no overhead shielding (Simpson and Laws, 1962; Thomas *et al.*, 1962); a 6-GeV electron beam of the Deutches Elektronen-Synchrotron striking a target in an experimental area with no overhead shielding [giant-resonance neutrons] (Bathow *et al.*, 1967a); and the Dubna 10-GeV proton synchrotron, with no overhead shielding and a thick magnet that produces an iron-leakage neutron spectrum (Lebedev *et al.*, 1965; Komochkov, 1970).

Under conditions where high-energy neutrons dominate the leakage spectrum and transport the cascade through the air, the values of λ obtained are close to the value of the high-energy mean free path in air (100 g cm^{-2} or 800 m at STP).

The transport of neutrons through air and ground might be well treated by neutron transport codes. Most of the studies published to date, however, are limited in scope [for a summary see Thomas and Stevenson (1988), Chapter 6]. To be complete, a numerical treatment of skyshine must address neutron and photon transport for neutrons with energies up to several hundreds of MeV, with realistic shielding geometries and with sources simulating accelerator conditions. Many published calculations are limited to neutrons with energy < 20 MeV (Kinney, 1962; Ladu *et al.*, 1968). Nakamura and his colleagues (1981a,b) used the MORSE computer code to study accelerator skyshine. All the calculations are in general agreement with the diffusion theory treatment by Lindenbaum and lead one to the view that the transport of low-energy (few MeV) neutrons produced at an air-ground interface is reasonably well understood.

Alsmiller *et al.* (1981) have made calculations for monoenergetic neutrons up to 400 MeV using the discrete ordinates transport (DOT) code (Rhoades *et al.*, 1978). For selected distances from the skyshine source up to about 1 km, the dose equivalent was calculated as a function of the solid angle open to the sky for emission. The results are expressed as "neutron importance functions" and tabulated in terms of dose equivalent/source neutron for selected energy-intervals over the neutron and photon spectra.

Stevenson and Thomas (1984) have reviewed the calculations of Alsmiller *et al.* (1981) and Nakamura and his colleagues (1981a,b). By combining the calculations with a variety of experimental data (Distenfeld and Colvett, 1966; Hack, 1969; Thomas *et al.*, 1962; Simpson and Laws, 1962) they suggested that a conservative upper bound to the values of dose equivalent, per neutron emitted from the source, as a function of distance from the source may be evaluated from

$$H(r) = 3\times10^{-15} \exp(-r/\lambda) \quad \text{Sv neutron}^{-1} \quad . \tag{30}$$

The number of neutrons emitted from the skyshine source must be determined and may be inferred from the dose equivalent and surface area of the skyshine source. The value of the attenuation length, λ, may be obtained from inspection of Fig. 38 (Stevenson and Thomas, 1984).

C. THE REMANENT RADIATION FIELD

1. *Activation*

Bombardment of materials by charged particles of energies of at least a few MeV can induce radioactivity. At accelerated energies above 10 MeV, induced radioactivity is to be suspected around all accelerators[5] and, of course, whenever neutrons are produced radioactivity will be found in targets and the surrounding accelerator structure and components (Fermi *et al.* 1934).

At higher energies, when electromagnetic and hadronic cascades are generated, the cascade-products, which give rise to the prompt radiation field, penetrate surrounding material and induce radioactivity in it, often at great distance from the accelerator. A radiation field produced by the decay of this radioactivity lingers on when the prompt radiation field ceases. This lingering radiation field has become known in the literature as the *remanent radiation field.* Its precise characteristics depend upon many parameters, such as the intensity, type and energy of the particles accelerated, and the materials irradiated. Barbier (1969) has reviewed the mechanisms for the production of radioactivity by high-energy particles.

The number of radionuclides that may be produced in this way is so large that Sullivan and Overton (1965) have had some success in treating the problem as a continuum of radioactive decay constants.

The variation of dose rate with time, $\dot{D}(t)$, resulting from the decay of a single radionuclide is given by

$$\dot{D}(t) = G\phi(1 - e^{-\lambda T})\, e^{-\lambda t} \tag{31}$$

where

[5]For a convenient means of deciding whether an accelerator may produce significant quantities of radioactivity, see NBS Handbook 107 (National Bureau of Standards, 1970).

ϕ is the irradiating fluence rate (assumed constant),

T is the irradiation time,

t is the decay time,

λ is the decay constant, and

G is a materials constant, the value of which depends upon many parameters.

If there exists a relationship between the number of radionuclides n and their decay constants λ that is known, and if the assumption is made that G does not depend strongly on λ, we write the contribution to the dose rate from those radionuclides with radioactive decay constants between λ and $\lambda + d\lambda$ as

$$d\{\dot{D}(t)\} = G\phi(1 - e^{-\lambda T})\, e^{-\lambda t}\, dn \quad . \tag{32}$$

Sullivan and Overton noted that for medium mass-number materials (e.g., iron, copper) the number of radionuclides, n, with decay constants greater than λ induced in the target material is represented quite well by the empirical relationship

$$n = a \ln \lambda \tag{33}$$

where a is a constant. Equation (33) is accurate to about 10% for nuclei of medium mass number, and for half-lives between 15 minutes and 100 years. Differentiating Eq. (33), substituting into Eq. (32) and integrating the result gives

$$\dot{D}(t) = B\,\phi \ln\left[\frac{T+t}{t}\right] \tag{34}$$

where B is a constant. However, Eq. (34) has several interesting approximations:

$$\text{When} \quad t \gg T, \quad \dot{D}(t) = \frac{B\phi T}{t} \tag{35}$$

(i.e., the dose rate is inversely proportional to the decay time, Sullivan, 1983), and

$$\text{when} \quad T \gg t \quad \dot{D}(t) = B\phi \ln(T/t) \tag{36}$$

(a logarithmic decrease in dose rate with decay time).

For intermediate values of $x \equiv T/t$ an effective half-life, T_E, may be calculated (Freytag, 1968):

$$T_E = t\left[\frac{1+x}{x} \ln(1+x)\right] \ln 2 \quad . \tag{37}$$

These equations give a good overall description of the variation of dose rate from accelerator structures, which are largely composed of materials of medium mass number (aluminum, copper, steel).

A more extensive discussion on the time dependence of the remanent radiation fields may be found in Tesch and Dinter (1986). The work of these authors is based upon experimental data from CERN and calculations from ORNL.

2. *Solid Materials*

Table XI summarizes the radionuclides commonly identified in solid materials irradiated by accelerator radiations (radionuclides with half-lives less than about 10 minutes are excluded). Most of these radionuclides are produced by simple nuclear reactions [e.g., (n,xn); (n,xnyp); (p,xnyp) etc., where x and y are integers] but spallation, fragmentation, or capture reactions are also important. When the radioactivity is produced under simple conditions, for example monoenergetic beam irradiation, the radioactivity induced may be readily estimated from published values of the reaction cross sections (Brunix, 1961, 1962, 1964; Rudstam, 1966). Such calculations have been discussed in detail by Barbier (1969; see also Patterson and Thomas, 1973, Chapter 7).

Although, in principle, many radionuclides may be produced the number of concern for radiological protection is limited by consideration of production cross-section and radioactive half-life. As we have

already seen (Table XI) only a limited number of radionuclides are commonly identified around particle accelerators. Of the principal radionuclides about two thirds are photon emitters (Charalambus and Rindi, 1967). For those radionuclides that decay by $\beta^{\pm}$ emission, special care must be taken to estimate correctly the absorbed dose from the electrons emitted (Sullivan, 1982, 1983).

The accelerator environment in which particle cascades are developed is complex, and computer programs are necessary to study the production of radioactivity in detail. A great deal of work has been carried out at the Neutron Physics Division of the Oak Ridge National Laboratory, where the High-Energy Transport Code (HETC) has been written to study the development of the hadronic cascade and the production of radioactivity (Coleman, 1968; Chandler and Armstrong, 1972; Armstrong, 1980a). Over the years HETC has been continually improved: the present version incorporates the EVAP-4 code of Guthrie (1970) to treat nuclear evaporation and the MECC-7 code to treat the intranuclear cascade (Bertini, 1969). This process of modification continues and at present a better treatment of high-energy interactions (E > 3 GeV) is underway with the code FLUKA82 (Aarnio *et al.*, 1984a,b; Ranft *et al.*, 1985; Thomas and Stevenson, 1988). When combined with lower energy neutron and photon transport codes (e.g., 05R or MORSE) HETC may be applied to the detailed calculation of the production of radioactivity and dose rates from irradiated materials (Irving *et al.*, 1965)

Many examples of the application of HETC to the calculation of radioactivity induced by high-energy particles in solids (e.g., concrete, iron, lead) have been published (Armstrong, 1969; Armstrong and Alsmiller, 1968, 1969; Armstrong and Barish, 1969a,b). Also, comparisons have been made between measured data and calculations with HETC (Shen, 1964; Armstrong and Alsmiller, 1968; Armstrong and Alsmiller, 1969; Armstrong *et al.*, 1972) and indicate fair to good agreement between measurement and calculation, demonstrating that HETC is an extremely helpful tool in accelerator component design. Figure 39 shows the results of an early comparison of measured and calculated estimates of the production of ^{54}Mn in iron, irradiated by 1 GeV and 3 GeV protons (Shen, 1964; Armstrong and Alsmiller, 1969).

3. *Earth*

Earth is often used as a shielding material for high-energy accelerators. The radioactivity induced in earth is generally treated separately from other solid materials because of the implications for environmental contamination; if the accelerator and its experimental areas are buried underground, particles produced by the electromagnetic and hadronic cascades and transmitted through the accelerator shielding will pass into the surrounding earth.

Middlekoop (1966) was one of the first to draw attention to the possibility that activity induced in earth might enter ground-water systems and be transported far beyond the accelerator structures. He estimated the specific activity due to thermal-neutron irradiation of impurities from chalky soil dissolved in ground water. This study was extended by Stapleton and Thomas (1971, 1972, 1973) to high-energy irradiation of dissolved solids in ground water and earth, as part of the design study for a 300-GeV proton synchrotron. Several studies in other soils than chalk and for a variety of particle accelerators followed: Hoyer (1968) at the CERN 28-GeV proton synchrotron; Borak *et al.* (1972b) at the 500-GeV proton synchrotron of the Fermi National Accelerator Laboratory; Thomas (1972) at the 1-GeV electron linear accelerator of the High Energy Physics Laboratory at Stanford University. Table XII summarizes the radionuclides identified either in earth or as solutes in ground water by these studies. Baker (1976) reported on the use of Monte-Carlo hadronic cascade computer codes to estimate the induced activity in soil and found reasonable agreement with measurement. The experimental data obtained at Stanford were consistent with electromagnetic cascade theory (Thomas, 1972).

The precise mixture of radionuclides generated in earth will depend upon many factors, most importantly the chemical composition of the earth. Table XII does show, however, that several radionuclides identified are common to more than one soil type. The total activity induced in the soil will depend greatly upon the accelerator design. For proton synchrotrons, such as the 28-GeV CERN PS or the 30-GeV AGS at Brookhaven, the total activity produced at an operating proton intensity of 5×10^{12} s^{-1}, is 150 TBq (4000 Ci) (Moore, 1966; Thomas and Stevenson, 1988). Of this total, it has been estimated that about 5% is produced in earth close to the accelerator building (Stapleton and Thomas, 1972).

Several studies of the implications of the radioactivity induced in earth have concluded that the potential for contamination of ground-water supplies is extremely small (Hoyer, 1968; Borak *et al.*, 1972b; Thomas 1970, 1978a; Stapleton and Thomas, 1972, 1973; Thomas and Rindi, 1979). Experience, gleaned

from environmental monitoring programs at large accelerator laboratories has confirmed this expectation.

4. *Water*

Radioactivity may be induced in water in two locations:

- Water used in cooling circuits for accelerator elements such as beam-stops, magnets, collimators or septa.
- Water in earth shielding close to the accelerator room.

a. *Cooling Water*. The radioactivity induced in cooling water is of concern for two reasons: first, the external dose rate may be high close to pipes of the cooling circuits, and second, the possibility exists for leaks or spills and eventual release to the environment.

Table XIII summarizes the radionuclides that are produced by hadron-reactions in oxygen. Extensive experience has confirmed the production of these radionuclides. For a compilation of references see Stapleton and Thomas, 1967; Thomas and Rindi, 1979; Thomas and Stevenson, 1988. During the first five hours after irradiation, the induced activity is dominated by the short-lived positron emitters, particularly ^{11}C. It is these short-lived radionuclides that will contribute significantly to the external dose rates. The only γ-emitter produced that has a half-life > 10 hours is ^{7}Be. Under certain circumstances it may contribute to the external dose rate from pipes and heat-exchangers (Rindi, 1972a) and it is absorbed on the ion exchange resins of cooling circuits.

Radioactive corrosion-products, particularly from steel, have been identified in cooling water, for example at CERN and Dubna (Borak, 1972a; Komochkov and Teterev, 1972).

The production of radionuclides in water may be calculated in the same manner as for solid materials by the use of Monte-Carlo transport programs. Studies using the transport code FLUKA (Aarnio *et al.*, 1984a,b) for the particular accelerator structure of the SPS at CERN, have shown that 0.3% of all inelastic interactions produced in the hadronic cascade occur in water (Stevenson, 1984b). This supports the conservative rule-of-thumb used at CERN that 1% of the total activity is induced in the cooling water. Christensen *et al.* (1978) applied this information to determine the quantities of radionuclides ($T_{1/2}$ > few minutes), produced in a cooling water system of the CERN PS for two beam-loss conditions. Their results are given in Table XIV.

b. *Ground Water*. The direct induction of radioactivity in ground water is an obvious potential source of contamination and has been studied extensively (Stapleton and Thomas, 1972; Thomas, 1970; Patterson and Thomas, 1973; Thomas and Rindi, 1979). The radionuclides directly produced in ground water from the spallation of ^{16}O have already been listed in Table XIII. Estimates made for the CPS and AGS show that 1 TBq (27 Ci) of activity is produced in the ground water at saturation, to be compared with a total activity produced in the surrounding earth of 150 TBq (4000 Ci) (30 GeV, 5×10^{12} protons s^{-1}) (Thomas and Stevenson, 1988). Of this total activity, about 0.74 TBq (20 Ci) is present as tritium (Stapleton and Thomas, 1972) and is mobile in the ground water.

Leaching of the radionuclides produced in the ground, particularly ^{22}Na and ^{45}Ca, has been reported by Hoyer (1968) and Baker (1974, 1975, 1976, 1985). An extensive monitoring program for radioactivity in earth and ground water has been conducted at the 500-GeV proton synchrotron of the Fermi National Accelerator Laboratory since its operation began. No accelerator-produced radionuclides have been detected in water samples collected from nearby wells and creeks. However, tritium is routinely found in some sumps designed to collect run-off water from the footings of accelerator tunnels and enclosures. On occasion ^{45}Ca and ^{22}Na are detected (Baker, 1975, 1976).

Studies of the solubility, distribution coefficients and migration of these radionuclides produced in earth suggest that the quantities in which they are produced adjacent to accelerators, and in which they might appear in ground water systems, make them of little environmental significance (Borak *et al.*, 1972b; Stapleton and Thomas, 1972; Thomas, 1970, 1972).

5. *Air and Dust*

a. *Introduction.* There are three principal sources of air-borne radioactivity at particle accelerators:

- Interaction of the products of the electromagnetic and hadronic cascades with the constituents of air and airborne dust.
- Dust formed by natural erosion or wear of radioactive materials or by maintenance of accelerator components that may be radioactive.
- Emission of radioactive gases, aerosols or droplets from irradiated liquids.

b. *Direct Production in Air.* Table XV summarizes the radionuclides with half life greater than 1 minute that may be produced by the irradiation of air around particle accelerators (Rindi, 1972b). Most of the radionuclides produced from the oxygen and nitrogen in the air have been observed (Table XVI).

The radionuclides of most importance for exposure of personnel at accelerators are those with half-lives long enough that the radionuclides may reach occupied areas, but with half-lives short enough that a significant fraction of saturation activity can be reached in the running time available. Thus, the short-lived positron-emitters ^{11}C, ^{13}N and ^{15}O together with ^{41}Ar, produced by thermal neutron capture in ^{40}Ar, are quite important. ^{7}Be is produced in sufficient quantities to be observed in some areas close to accelerators (Prantl and Baarli, 1972), but the half-life of ^{3}H is so long that accelerator-produced airborne tritium is of little environmental consequence.

The mechanisms for production of radioactivity in air are well understood (Patterson and Thomas, 1973) and good agreement between estimated and measured values can be obtained when airflow distributions and ventilation rates are known (Peetermans and Baarli, 1974).

c. *Radioactivity in Dust.* Experience at many large high-energy accelerators suggests that, with normal good housekeeping, the radiation exposure of maintenance crews and other accelerator workers from radioactive dust is negligible (Thomas and Rindi, 1979). At the CERN 28-GeV proton synchrotron the radionuclides identified in dust in the accelerator room were ^{54}Mn (~50%), ^{7}Be (~25%), ^{51}Cr (~7%), ^{59}Fe (~9%), and ^{48}V (~9%) (Charalambus and Rindi, 1967). Similar results were obtained at the 50-MeV electron accelerator at Saclay, where radionuclides produced in iron formed the largest component of the radioactivity in dust (Vialettes, 1969).

The specific activity of these dusts is not high: for example Charalambus and Rindi (1967) reported concentrations of ~200 MBq m^{-3} (~5 nCi cm^{-3}). In some cases, for example at LAMPF, higher levels have been observed. Despite the small probability of internal contamination from dust, it is valuable to monitor accelerator workers by periodic whole-body counts in order to demonstrate that effective contamination control procedures are in operation. Patterson and Thomas (1973) have reviewed the results of such studies at the Lawrence Berkeley and Lawrence Livermore Laboratories, which show individual uptakes to be extremely small (Patterson *et al.*, 1965; Van Dilla and Engelke, 1960; Anderson and Schmidt, 1966; Sargent, 1962).

In addition to the induction of radioactivity in the air it has been observed that recoil nuclei generated from accelerator components (e.g., beam-line vacuum enclosures) are often a greater source of airborne radioactivity than dust (Moritz, 1988).

Experience has shown that, save for very exceptional cases, the emission of radioactive gases, droplets, or aerosols from irradiated liquids is a negligible hazard at particle accelerators.

In summary, operational experience at many large accelerators suggests that the potential radiation exposure during maintenance caused by radioactive dust in the accelerator environment is negligible. Furthermore, Busick and Warren (1969) have pointed out that chemical toxicity may often be a more important criterion for limiting the exposure to dust rather than its radioactivity.

IV. Techniques of Dosimetry

A. SPECIAL CONSIDERATIONS FOR ACCELERATOR ENVIRONMENTS

The radiation environments at particle accelerators differ from those usually found in radiological protection in that they result from cascade phenomena and therefore typically consist of several types of ionizing radiation, distributed over a broad range of energies and extending to higher energies. In addition

the radiation fields have a complex time structure, which depends upon the accelerator repetition rate, the details of the radiofrequency accelerating system, and the beam extraction systems.

Several general statements concerning accelerator radiation fields can be made:

- If muons are produced, neutrons will always be present;[6]
- High-energy neutrons are always accompanied by intermediate, fast and thermal neutrons;
- Neutron fields, regardless of their origin, are *always* accompanied by photons.

Apart from DC accelerators (e.g., Cockcroft-Walton or Van de Graaff generators), accelerator operation uses a pulse structure that can vary from the picosecond regime to full cw ("continuous wave," i.e., 100% duty factor) operation, but even cw operation contains "microstructure" features determined by the phase stability requirement of rf acceleration. The dosimetry of pulsed radiation is reviewed in ICRU Report 34 (1982), where other references to published literature can be found.

The use of sophisticated instruments in mixed fields is discussed below, but here we mention a variation on the game "Paper, Stone and Scissors," namely, "Air, Lead and Wood," that is useful in practical field situations. In an unknown radiation field that is producing a reading on an ionization chamber, the dominant field component (as regards absorbed dose) will produce the responses given in Table XVII when a 5-cm thick slab of lead or wood is introduced between the source and the instrument. In addition to these tests, thin sheets of these materials (e.g., a few mm of Pb) may actually produce an increase in reading in a photon field if dose buildup occurs, while producing no significant changes in the other fields. Furthermore, in the absence of magnetic fields, a muon field can be distinguished from a neutron field by its tight collimation.

Because the instruments and techniques discussed here are extensively described in the open literature and in other chapters of this series, the approach adopted here will be to discuss them only briefly, giving references to the literature but providing examples of their use at high energy accelerators and their characteristics in these situations. The volumes by Knoll (1979) and Tait (1980) are basic references that discuss the principles of a range of modern radiation detection instruments.

B. STANDARD INSTRUMENTS

1. *Introduction*

The so-called "standard instruments" include the ionization chamber, Geiger-Müller counter, proportional counter, and thermoluminescent dosimeter. All of these are sensitive to the types of radiation produced by accelerators but their measurements must be interpreted with care.

2. *Ionization Chambers*

The single dosimetric instrument of greatest overall utility at accelerator facilities is the ionization chamber. This instrument in its many forms is well understood, reliable and gives real-time indications of absorbed dose. Perhaps the simplest experimental approach to the determination of dose equivalent, H, in accelerator radiation fields is to measure the absorbed dose, D, with a suitable ionization chamber and multiply the result by an appropriate quality factor, Q:

$$H = QD \quad . \tag{38}$$

Many different means of determining absorbed dose by ionization chambers have been developed including the use of paired ion chambers, high pressure argon-filled chambers, and cavity chambers (Burlin, 1968; Goodman and Rossi, 1968; and Patterson and Thomas, 1973). However the use of only one chamber to determine dose equivalent in accelerator environments is fraught with difficulty, because of the variable contributions from low-LET radiations (photons and muons) and high-LET radiations (principally

[6]Although both muons and neutrons will be produced, they need not necessarily appear at the same location. At Fermilab and CERN, for example, essentially pure muon beams exist—several kilometers from locations of neutron production, because muon production is highly collimated whereas neutron production is quite diffuse.

neutrons). At proton accelerators, and often at high-energy electron accelerators, when neutrons dominate the radiation field and a single ionization instrument is used, one should ensure that the materials of the chamber (walls, gas filling) have a reasonable response to neutrons. Thus at accelerators, the absorbed dose is often determined by a tissue-equivalent chamber, following the original work of Failla and Rossi (1950; also Rossi and Failla, 1956).

The shortcoming of this technique is that it gives only a measurement of D but no information on Q. A conservative approach in the evaluation of dose equivalent is to assume a quality factor of 10, but this can be unreasonably conservative as experience shows values of Q that range between 1 and 6 in accelerator environments. Either some detailed knowledge of the radiation environment is required to estimate Q or resort must be made to an empirical determination of Q using, for example recombination chambers (see Section IV.C.5). Both methods require additional measurements.

Practical problems that arise with the use of ionization chambers in accelerator fields include

- Radio-frequency interference: Ionization chambers are low-signal high-gain detectors, sensitive to electromagnetic interference caused by the stray fields from the radio-frequency cavities used with particle accelerators.
- Pulsed radiation fields: The electric field strength in the ion chamber may be insufficient to ensure complete charge collection in pulsed radiation fields of low duty cycle. Even though the average absorbed dose rates may be low, the rates during pulses may be extremely high. Phase stability requires that acceleration takes place only at a limited time interval during each rf (or microwave) cycle. This results in an rf "microstructure" in the beam pulse that may exacerbate the problem of charge collection.
- Small beam cross sections: Particle beams, whether primary (direct from the accelerator) or secondary (produced in a target or converter), can have cross sectional areas that are very small compared to standard instrument sizes; beam diameters of ~ 1 mm or even smaller are not uncommon. When an instrument is placed in such a beam, two effects must be appreciated: First, the true in-beam dose will be higher than the nominal instrument reading by a factor given by the ratio of the instrument's sensitive volume divided by the beam volume within the instrument. Second, the true dose rate within the beam volume may be so high that sizable corrections are required (e.g., for ion recombination).
- Boag (1950, 1952, 1987) has discussed the fundamental problems of pulsed radiation dosimetry and a review of the literature appears in ICRU Report 34 (1982). Tesch (1984) has discussed volume recombination effects in typical conditions around accelerators while recent measurements of collection efficiencies in accelerator radiation fields have been made by Oda *et al.* (1982).

3. *Geiger-Müller Counters*

Geiger-Müller counters are among the oldest instruments used for the detection of ionizing radiation, and their design, construction, and operation is well understood (Emery, 1966). The greatest utility of Geiger-Müller counters in accelerator environments is in the assessment of remanent radioactivity. Their use for this purpose is no different from their use with any type of radioactive source and will not be discussed.

For prompt radiation, the Geiger-Müller counter can be of great help in the detection and localization of fields, but it may be of little use for quantifying the fields unless the counting rate of the instrument is substantially below the accelerator pulse rate. Otherwise, the problems of counting losses due to dead time effects severely limit the use of these counters. Furthermore, their calibration is often unknown in the mixed and variable fields near accelerators.

The great advantage of the Geiger-Müller counter is its simplicity. It is relatively stable and one does not need to control its voltage very closely. Its chief limitation, as suggested above, is that its dead time is of the order of 100 microseconds, because of the time required for the discharge to be quenched. With suitable techniques, this limitation can be overcome or minimized, thus permitting Geiger-Müller counters to be used in areas of high instantaneous radiation fields. However, such methods must be used with care and with complete understanding of the instrument. The Geiger-Müller counter has found wide

application in measuring radiation fields at large distances from accelerators where the intensity is low (see Section D).

4. *Thermoluminescent Dosimeters*

Thermoluminescent dosimeters (TLDs) have applications at particle accelerators that parallel those in other branches of radiological protection (Tuyn, 1982). TLDs are predominantly used in personal dosimetry as an alternative to photographic film, particularly in the monitoring of exposures from β-particles and photons (Kathren nd). Some success has been achieved in using TLDs for individual monitoring of neutrons, particularly in the intermediate energy region, by variations on the albedo principle (Piesch and Burghardt, 1985).

The ability to produce individual dosimeters that are small in size is a significant advantage of TLDs. At particle accelerators this is of particular value in measuring electron and photon exposures to the hands and fingers when maintenance is carried out. It is sometimes the case that contact with irradiated accelerator components cannot be avoided, and in regions where the dose gradient is high the exposure to the hands must be monitored (Thomas and Stevenson, 1988). In particular, this is the case when severe dose gradients occur near accelerator components due to the emission of weakly penetrating radiations. Thus, Sullivan (1982, 1983) has shown that the surface absorbed-dose resulting from electrons (including β^- and β^+), emitted by accelerator-irradiated metal foils, is an order of magnitude higher than the absorbed dose from photons. Even at thicknesses as great as 1 mm the electron and photon contribution to the doses are equal (Sullivan 1982, 1983). In general, TLDs are extremely useful in estimating electron doses.

TLDs have been used for individual monitoring of neutron exposures, but their application in the broad neutron spectra typical of high energy accelerators has been less successful. At the Stanford Linear Accelerator Center (SLAC) a combination of ^{6}LiF and ^{7}LiF in one badge has been used for many years. This combination works well if the neutron dose equivalent is much smaller than the photon dose equivalent and the ratio of thermal neutron to fast neutron flux densities is constant. If these criteria are not met considerable overestimation of dose equivalent results (Busick *et al.*, 1975). Hack (1971) has reported the use of a ^{6}LiF, ^{7}LiF, and NTA film combination to improve the accuracy of neutron personal dose measurement at a 7-GeV proton synchrotron. Despite these limited successes, the difficulties of using TLD are serious enough to ensure that the use of nuclear emulsions in the individual monitoring of neutrons at accelerators still continues (Patterson and Thomas, 1973; Höfert, 1984a; Höfert and Piesch, 1985).

TLDs have also been applied to beam monitoring. The response of TLDs is known to be a function of the LET of the incident charged particles (see, for example, Jähnert, 1972). However, in monoenergetic charged particle beams, as produced by accelerators, this is of no consequence for relative absorbed dose measurements. For example, in beams produced by proton accelerators, TLDs have been applied to exploration of the spatial variation of irradiating fields (Smith *et al.*, 1977). At SLAC, TLDs have been used to study the detailed distribution of dose within electromagnetic cascades (Nelson *et al.*, 1966). Further, TLDs have been used as transfer dosimeters from high to low doses to measure activation cross sections (Smith and Thomas, 1976), for absolute dosimetry in radiobiological experiments (Patrick *et al.*, 1975; Ainsworth *et al.*, 1983), and for the determination of W, the average energy required to create an ion pair in gas (Thomas *et al.*, 1980; Thomas, 1981).

Kalef-Ezra and Horowitz (1982) have stressed that there is a great deal of variation in response between individual LiF dosimeters, between different batches of dosimeters, and for any particular dosimeter, depending upon its thermal and radiation history. Nevertheless it is possible, with careful experimental technique, to derive an empirical relationship for the response of TLDs as a function of LET of the incident charged particles. This has been done, for example, in the particular case of ^{7}LiF and agreement with the predictions of theory obtained (Jähnert, 1972; Henson and Thomas, 1978) (see Fig. 40). With such an empirical relationship TLD may be used for beam dosimetry when the LET of the beam particles is known.

C. NEUTRON DOSIMETRY

1. *Introduction*

Neutron dosimetry is better understood in the region below 20 MeV than at higher energies. This is largely due to the fact that most of the experience with neutron exposure has been obtained from radioactive neutron sources, nuclear reactors, and low-energy accelerators where the significant dose equivalent is

produced by neutrons well below this energy.

For high-energy accelerators, it is often convenient to consider two energy regions, both bounded at 20 MeV. The choice of 20 MeV roughly corresponds to the upper limit of moderated thermal neutron instruments (e.g., the moderated BF_3 counter), but, more importantly, it is the threshold of the very convenient activation reaction $^{12}C(n, 2n)^{11}C$, which is widely used at particle accelerators. In consequence, the spectrum of high energy accelerators is often characterized by the fractions of dose equivalent due to neutrons above and below 20 MeV.

Excellent references that review modern aspects of neutron dosimetry are *Neutron Dosimetry* (Ing and Piesch, eds., 1985) and, more recently, Burger *et al.* (nd, this volume). Valuable discussions of neutron dosimetry can also be found in NCRP Reports 38 and 79 (1971, 1984), and the texts by Patterson and Thomas (1973), Swanson (1979a) and Thomas and Stevenson (1988).

2. *Passive Detectors*

a. *Nuclear Emulsions.* A valuable tutorial on nuclear emulsion technique is available in Patterson and Thomas (1973). Also recommended are the texts by Yagoda (1949), Powell *et al.* (1959) and Barkas (1963). The sensitivity of thin (25 μm) nuclear emulsions, used for personal dosimetry (NTA or NTB), is limited to neutrons of energy between approximately 0.5 and 15 MeV. Protons with energies aprless 0.5 MeV produce tracks too short to observe, whereas above about 15 MeV few tracks are observed because the (n,p) cross section decreases with increasing energy. For these reasons, an important preliminary step in the use of nuclear emulsions is a "calibration" for the particular spectrum. This is ideally done by determining the true dose equivalent in the field to be monitored by a spectral measurement, and comparison with the reading from emulsions simultaneously exposed in conjunction with a suitable phantom (see, e.g., Greenhouse *et al.*, 1987).

NTA film is frequently used as a personal dosimeter and passive area monitor. In environmental conditions where both the temperature and relative humidity are high, fading of the latent image before development of the film — the so-called "track fading" — may lead to serious error (Becker, 1966, 1973; Bartlett and Creasy, 1977). However, studies in moderate climates, such as at Berkeley, California, show the magnitude of this effect to be small and manageable (Rindi and Henson, 1976). In those areas where the effect might be serious, the problems of fading can be minimized by proper humidity control (Stevenson and Marshall, 1964; Höfert, 1984a; Lehmann, 1983; Kooiman and Höfert, 1982).

In his evaluation of the NTA emulsion, Höfert (1984a) summarizes: "Under the present circumstances the NTA film is considered to be the second-best choice of personnel dosimeter around high-energy proton accelerators, the perfect one still awaiting realization."

b. *Activation Detectors.* Activation detectors are among the most important types of passive detectors in accelerator radiation dosimetry. They have the advantage that their response is not influenced by the high duty cycles of some accelerator radiation fields. Activation detectors often offer good discrimination against radiations other than neutrons (for example, the $^{32}S(n,p)^{32}P$ reaction). If variation in the accelerator beam is significant within an irradiation time comparable to the activation product half-life, corrections must be made in normalizing the measured activation to the integrated beam current. A hand correction can be made if an associated beam monitor is available that records beam intensity as a function of time. Alternatively, the correction can be made in an analog fashion by setting the time constant of the beam-current integrator equal to the decay time of the product nuclide, i.e., $RC = t_{decay} = t_{1/2}/\ln 2$, where C is the integrating capacitor, R is a resistance in parallel with C and $T_{1/2}$ is the half-life (see, e.g., Knoll, 1979, p. 82).

Some activation detectors, particularly those with high-energy thresholds, are somewhat insensitive, depending upon the production cross section and half-life of the radionuclide produced. Significant ingenuity is often required to measure intensities at the level of interest in radiological protection, for example, using the production of ^{149}Tb from gold or mercury (McCaslin *et al.*, 1968; Shave, 1970).

Other reactions that are widely used at accelerators to measure high-energy neutrons include: $^{32}S(n,p)^{32}P$; $^{27}Al(n,\alpha)^{24}Na$; $^{27}Al(n,2p4n)^{22}Na$; $^{12}C(n,2n)^{11}C$ $^{12}C(n,spall)^{7}Be$. In addition, the $^{198}Hg(n,spall)^{149}Tb$ reaction has been attempted with some success, but it involves difficult separation techniques (McCaslin and Stephens, 1967). Table XVIII gives the properties of these reactions together with

the sensitivity of detectors used at the Lawrence Berkeley Laboratory (Gilbert *et al.*, 1968).

Activation techniques are also familiar in the measurement of thermal neutrons, usually by (n,capture) reactions. Holt (1985) has reviewed the slow neutron reactions in common use and Table XIX summarizes the three thermal neutron reactions most frequently used at accelerator laboratories and the sensitivities of the detectors, as used at the Lawrence Berkeley Laboratory.

Figure 41 shows the excitation functions for the activation reactions most frequently used at accelerators. Of these the $^{12}C(n,2n)^{11}C$ reaction has a special place because its threshold at 20 MeV represents a convenient boundary between "conventional" neutron dosimetry and the dosimetry of particular interest only at particle accelerators. This reaction was first employed to monitor the intensity of cyclotron beams (Sharpe and Stafford, 1951). They also showed that a neutron fluence rate of about 15 n $cm^{-2}s^{-1}$ could be measured using a 4.5-g anthracene crystal. The sensitivity was improved by the use of a liquid scintillator (Baranov *et al.*, 1957) and solid plastic scintillators (McCaslin, 1960, 1973; Shaw, 1962). With scintillators of increased size (2.7 kg) developed by McCaslin (as reported by Gilbert *et al.*, 1968) the ability to measure a fluence rate of less than 1 n $cm^{-2}s^{-1}$ was achieved. The experimental techniques used have been described in detail by McCaslin (1960, 1973).

An important disadvantage of the method is that ^{11}C is also produced by photons, protons and charged pions (see Fig. 42). Stevenson (1984a) has investigated the production of ^{11}C in plastic scintillators in radiation fields outside the shielding of a 30-GeV accelerator (Stevenson 1984a). In this work he was able to use the most recent cross section data and a consistent definition of dose equivalent. He found that in fields that were in equilibrium (containing a charged-particle component of protons and pions) the calculated fluence to dose-equivalent conversion coefficient was 45 fSv m^2, to be compared with his previous value of 50 fSv m^2 (Stevenson, 1971) and with an early value suggested by Shaw *et al.* (1969) of 60 fSv m^2.

c. *Threshold Detectors.* A "threshold detector" can be any detector having a specific well known reaction threshold and, to the extent possible, well-known reaction cross sections. Several of the "real-time" detectors described in Section 3 must therefore be considered to be threshold detectors (e.g., Bi-fission, Th-fission). The combination of an etch track detector, such as polycarbonate (see Section e below), with a radiator of fissile material (e.g., ^{238}U or Bi) gives a threshold detector, with reasonable sensitivity and low background. For example, with a bismuth radiator achieved sensitivities of 600 μSv and 100 μSv may be achieved with 60 MeV and 100 MeV neutrons respectively (Tesch, 1988). Another group is a subset of activation detectors, already discussed. A small number of threshold detectors can be used for crude spectral characterization, or, together with unfolding techniques, for more elaborate spectral studies. Table XX lists materials commonly used for this purpose.

d. *Moderated Detectors.* A commonly used arrangement, utilizing a thermal-neutron-sensitive activation detector, is an indium or gold foil placed within a spherical or cylindrical moderator. Many variations on the original adaptation by Stephens and Smith (1958) have been reported (Bathow *et al.*, 1967b; Carter *et al.*, 1970; Simpson, 1964; Smith, 1958, 1961, 1965b, 1966). The radioactivity of the foil placed at the center of the moderator is assayed afterwards by a thin end-window Geiger-Müller counter, gas-flow proportional counter (better for high count rates), or other suitable monitor. Indium foils of 2.54 cm (1 inch) diameter and 0.014 cm thick (mass 0.5 g) give a counting rate of ~5 cpm at saturation and zero decay time for unit neutron fluence rate when used with a thin-end-window counter of π sterad solid angle acceptance. Gold foils of 2.54 cm (1 inch) diameter and 0.020 cm thick (mass 2 g) give about one third the sensitivity of the In foils when counted under the same conditions. ^6LiF can also be used as a detector of thermalized neutrons within a moderator to similar effect. The detector may be calibrated with an isotopic neutron source of known strength, or by accelerator-produced neutrons (e.g., from the D-D, D-T reactions).

e. *Etch Track Detectors.* Etch track detectors function by the production of pits or holes in insulators irradiated with neutrons or heavily ionizing charged particles. The material is then etched with a suitable acid or base to enlarge the region thus sensitized. Early studies of this technique have been described by Fleischer *et al.* (1963, 1965, 1975) and Price and Walker (1962, 1963). An excellent review by Griffith and Tommasino (nd) is contained in this volume.

Many insulating solids are suitable and, among those investigated are cellulose nitrate, Lexan, and high-grade muscovite mica. Many of these have the advantage that they can be read automatically by use of the spark-through method described, for example, by Cross and Tommasino (1972). The spark counting technique depends on having a thin film that has been etched until its tracks have become holes all the way through or nearly so. Electronic equipment permits rapid, automatic counting of tracks in a detector film that might otherwise require hours or days of microscopic work. Parameters that affect reproducibility include foil thickness, diameter of the etched tracks, voltage applied, atmospheric condition, and length of time between sparks. Improved track resolution and higher maximum hole densities are obtained in a sparking atmosphere of helium. Percentage counting losses are proportional to hole density up to about 5000 tracks per cm^2.

The method is not in routine use in accelerator radiation dosimetry but has been used experimentally.

f. *CR-39 Dosimeters.* An interesting alternative to the use of NTA film for personal or area monitoring of accelerator-produced neutrons is a system based on CR-39 casting resin[7] (Tommasino *et al.* 1984, Harrison and Tommasino 1985, Cross 1986). This is a transparent highly-crosslinked, thermoset (as distinguished from thermoplastic) amorphous polymer of allyl diglycol carbonate that is sensitive to recoil protons from neutron interactions (Cross *et al.* 1986). The dosimeter is fabricated from thin (~ 0.625 mm) sheets. As described by Tommasino and Harrison (1985), "[It] ... satisfies the requirements of (a) being highly sensitive to radiation by chain scission reactions; (b) having a closed packed and uniform molecular structure; (c) having a nonsolvent chemical etchant; and (d) being optically transparent (its major use is in making eyeglass lenses). CR-39, being by far the most sensitive [damage track] detector yet discovered, registers recoil protons of energies up to about 15 MeV and it appears to be the most successful candidate as a personnel neutron dosemeter." A review of its use and properties for this application is provided by Hankins *et al.* (1984, 1985, 1986).

After being exposed to a neutron field it is etched electrochemically to develop the latent tracks into pits or holes. The etching medium is a solution of KOH in a special etching cell. In the procedure described by Hankins *et al.* (1984, 1985), an alternating voltage (~ 3000 V) is applied to the etching arrangement at frequencies of about 60 or 2000 Hz, in different parts of the development cycle (electrochemical etching, blowup, post-etch). After development, the holes can be counted in a manner amenable to easy automation (Griffith *et al.*, 1984, Tommasino and Harrison, 1985). Some of the characteristics of CR-39 dosimeters that can be used to advantage are:

- The energy response is relatively flat between about 0.1–4 MeV with a 40% drop in sensitivity at about 14-MeV neutron energy (Hankins, 1978). Indeed useful response over the range 0.050–20 MeV has been reported, but there is lack of information about the response curve in the range 6–12 MeV. Preliminary experimental data suggest a lack of response to neutrons between 6.25 MeV and 10 MeV, but more measurements need to be made (Greenhouse *et al.*, 1988). In particular, the lower limit is an improvement over the lower limit experienced with NTA film (0.5–0.6 MeV).
- Its sensitivity is adequate in the range normally encountered in personal dosimetry; in the neutron energy range for which the response is reasonably flat, the sensitivity is about 7×10^5 tracks cm^{-2} per Sv, based on ^{252}Cf calibration. However the track density per unit dose equivalent is reduced by as much as a factor of two in high-energy spectra (Höfert *et al.*, 1987; Greenhouse, 1988).
- Its response is linear with dose-equivalent up to at least 4 mSv and can be usefully corrected to dose equivalents at least as high as 10 rem. Linearity can be extended to higher dose equivalents by the use of less sensitive track-etch procedures.
- Track fading, such as reported for NTA film, is small or nonexistent.
- The evaluation can be automated by available technology. Instrumentation has been developed for counting of pits by spark-counting methods (Tommasino and Harrison, 1985) and by utilizing a biological colony reader (Hankins *et al.*, 1985, Griffith *et al.*, 1984).

---

[7]Trademark of PPG Industries, Inc., Pittsburgh, PA from whom the liquid monomer can be obtained. The designation "CR-39" signifies "Columbia Resin, Batch No. 39," a material developed for spectacle lenses.

- Excellent reproducibility can be achieved; ±3.2% has been reported at a dose equivalent of 4 mSv (Hankins *et al.*, 1985).
- As the base material is inexpensive, several individual dosimeters can readily be incorporated into a single dosimeter package. Some can be held in reserve for later development in case problems are suspected with the initial processing.
- The individual dosimeters can be saved to form a permanent record.

Apparent disadvantages are:

- There is a strong dependence of response on orientation to the neutron field; the relative sensitivity at grazing incidence decreases to about 15–30% of that at perpendicular incidence. Special calibrations or corrections must therefore be made for fields encountered in practice.
- Background tracks, contributed in part by natural Rn and/or surface defects give a variable background reading which, with good quality CR-39 material, is equivalent to about 8 mrem.
- The number of developed tracks is strongly dependent on parameters of the etching process and therefore this must be carefully controlled. There is a strong dependence on the etching temperature and some dependence on the thickness of the material. Details of one such electrochemical development process are outlined by Hankins *et al.* (1984, 1985).
- Labeling of individual films may present some difficulties.

Preliminary evaluations in an accelerator environment were carried out by Greenhouse *et al.* (1987), placing the dosimeters in a well shielded (by concrete) area in the proximity of a beam stop struck by argon ions at 8.5 MeV per nucleon from the LBL SuperHILAC. This particular accelerator was chosen because it provided the softest accelerator-produced neutron spectrum conveniently available at the time. Bonner sphere spectrometer measurements indicated that the average neutron energy was about 0.5 MeV and the maximum about 20 MeV. About 60% of the dose equivalent was contributed by neutrons having energies greater than 1 MeV. More significantly, about 83% and 71% of the dose-equivalent were contributed by the fractions of the neutron fluence above the thresholds for the CR-39 and NTA dosimeters, respectively. The report concluded that "... it appears that with proper calibration, NTA and CR-39 can provide satisfactory radiation protection dosimetry around medium-energy particle accelerators having ambient neutron spectra similar to that of this experiment at the SuperHILAC. The apparent paucity of response in CR-39 for neutrons between 5 and 14 MeV suggests that it should be used with caution in some high-energy accelerator environments."

Evidently, CR-39 dosimeters have not yet been evaluated in a sufficient variety of representative accelerator environments, but the preliminary indications are encouraging. Refinements in the development procedure have already served to enhance the neutron energy range. It is believed that more may be gained by additional research in this area.

g. *Bubble Detectors.* The bubble-damage polymer detector is similar to a bubble chamber in that a liquid whose normal boiling point is below room temperature is kept under pressure. When pressure is released, bubbles form along the path of a charged particle that has traversed it (Cross and Ing, 1984; Ing, 1986). In order to increase the sensitive time, superheated droplets of a volatile liquid are dispersed in a gelatinous medium (Apfel, 1979). In the detector developed by Ing and Birnboim (1984), superheated droplets of, for example, one of the Freons, are dispersed in a transparent, elastic solid that prevents the droplets from vaporizing and keeps them fixed in location. The solid medium, an acrylamide polymer, also maintains the bubbles at the sites of formation.

In his evaluation of the present state of personnel dosimetry, Griffith (1987) states: "Bubble detectors are an exciting development. The polymer or gel is worn in a clear vial. When a neutron interacts with the medium, a bubble is created that expands to optical dimensions. The detectors are easy to count, very sensitive, have no angular dependence, and the energy response can be tailored to the needs of the dosimetrist. Possible problems include temperature dependence, unit cost, sensitivity to mechanical shock, and potential difficulty in counting high bubble densities resulting from moderate to high doses. However, many of their characteristics are highly attractive and bubble detector development should be followed closely. It is possible that a hybrid dosimetry system using the advantages of both CR-39 and bubble detectors would provide the radiation protection community with the sensitive, accurate dosimeter it has

needed for so long."

According to Ing (1987), the temperature dependence has been overcome and detectors are produced with constant response over a temperature range of 15°–35°C. Recently developed dosimeters can be used as personal or area dosimeters for a 4-week period making them suitable for routine use. The material can be tailored to a chosen neutron energy threshold, as low as 10 keV or less. Indeed, dosimeter sets have been produced having arbitrarily chosen thresholds of 0.010, 0.100, 0.500, 1, 3 and 10 MeV. Neutron sensitivity can be adjusted in production to be in the range 0.1–3 bubbles/μSv (1–30 bubbles/mrem) for a dosimeter volume of 4 ml. Automated readout by means of a video system with pattern recognition has been achieved with a capability of up to 1000 bubbles per 4–ml dosimeter. Special bubble detectors have also been developed that can be used for the detection of gamma rays.

Bubble detectors have not yet been tested in accelerator environments but, at the time of writing, three such tests are scheduled (mid-1987). The first is in the context of a comparison between CR-39 and other dosimeters at the Bevalac at Lawrence Berkeley Laboratory (Greenhouse *et al.*, 1988), the second is at the Proton Synchrotron (PS) at CERN, operated with relativistic beams of argon, and the third is at the 500-MeV proton cyclotron at TRIUMF.

3. *Active Detectors*

a. *BF-3 Counters.* The boron-trifluoride (BF_3) counter has found the widest application of any instrument for measuring neutron fluence or dose equivalent. It can be used as a handy, self-contained portable instrument or fixed-mounted as an area or site monitor. Its sensitivity to neutrons is based on the reaction

$$n_{th} + {}^{10}B \rightarrow {}^{7}Li + \alpha + 2.78\ \text{MeV}\ , \tag{39}$$

which has a high cross section for thermal neutrons (3000 b) but drops as $E_n^{-1/2}$ by about four orders of magnitude at fast neutron energies. Several types of information can be obtained with a simple BF_3 counter arrangement. When used with no moderator the BF_3 counter is effectively sensitive only to ambient thermal neutrons ($E_n \approx 0.025$ eV). The sensitivity of a counter of typical dimensions (about 2 cm diam × 15 cm long) is of the order of 2–3 counts per neutron cm^{-2} and is proportional to volume, pressure, and degree of enrichment in ^{10}B.

With a moderator of, for example, paraffin, polyethylene or water, fast neutrons are thermalized and counted (see for example, Nachtigall and Burger, 1972). This indirect sensitivity to fast neutrons depends upon the moderator arrangement, but is of the same order as the sensitivity of the unmoderated counter to thermal neutrons. With a paraffin moderator about 6.5 cm thick, the sensitivity is almost independent of energy (factor of 2) over a large range from about 20 keV to 20 MeV (Hanson and McKibben, 1947). Interference from incident thermal neutrons can be eliminated by an 0.5-mm Cd shield covering the outside of the moderator. BF_3 counters are subject to interference from photons that can simulate a 2–3 MeV pulse in the chamber, which is operated as a proportional counter. This interference is caused predominantly by "pile-up" of several prompt photons of lower energy; containment of sufficient energy from a single high-energy photon within the counter volume to give a pulse corresponding to 2-3 MeV is less frequent. This interference can usually be minimized by optimal setting of the pulse-height discriminator level.

More elaborate, tailored moderator arrangements (about 11.5 cm thick) give the counter a sensitivity that closely resembles the ICRP (1973, 1977) dose-equivalent energy curve over a useful energy range up to about 6 MeV. Instruments designed for this purpose have been built by: DePangher and Nichols (1966); Andersson and Braun (1963, 1964); Ladu *et al.* (1963, 1965); and Leake (1967, 1968).

Hankins and Cortez (1975) studied the energy responses of four types of remmeter instruments and found that they approximate the shape of the dose-equivalent to neutron-fluence conversion coefficient reasonably well up to 7 MeV, after which the response drops rapidly. In a critique of the neutron remmeter that considered both conceptual and operational aspects of its use, Rogers (1979) stated "...remmeters give adequate indications of the dose equivalent index only in the range 100 keV–6 MeV" and indicated that they can also overestimate the dose equivalent in situations that are not unusual. These shortcomings arise, in part, from directional properties of the instruments *vis-a-vis* the directionality of the calibration field. Other problems are related to the "additivity in a mixed field, specification of the dose equivalent index curve and the instrumental energy response." Subsequent comparisons were made by Cosack and Lesiecki (1981) of the energy and angular response of eight dose equivalent survey meters. In this work, the instruments were found to be very similar to each other in their dose-equivalent energy response, showing a

decreasing response with increasing energy. Large differences were found among the instruments regarding their angular response. Some attempts to reduce this angular dependence have been reported (see for example Hankins, 1978)

The possibility of important spectral contributions above 6–7 MeV means that remmeter instruments should not be relied upon in accelerator environments without some knowledge of the neutron spectrum at each location they are used. In addition, their directionality should be taken into account in the interpretation of measurements.

As mentioned in Section A, the short duty cycle encountered at many accelerators is an important consideration for radiation measurements. Dinter and Tesch (1976) have examined this question in regard to moderated remmeters in pulsed accelerator fields. Because the intrinsic dead time of such instruments (2–7 μs) is long compared to the beam pulse length for many accelerator types one might think that this would render the instruments incapable of registering more than one count per machine pulse. In fact, the diffusion time of thermal neutrons within the moderator introduces a randomly distributed delay between the neutrons' time of arrival at the instrument and their registration. This delay is not attributable to the slowing to thermal energies but from the diffusion of thermal neutrons within the moderator. Therefore the delay is practically independent of the ambient neutron spectrum. As stated by Dinter and Tesch (1976, op. cit. p. 1), "Although the dose during an accelerator pulse ... [may] ... be very high for a given averaged dose rate, the counting losses will be small because the neutrons are 'stored' as thermal neutrons ... and can reach the detector hundreds of microseconds later." Knowledge of this time distribution permits estimation of the necessary dead-time correction.

The time for reduction of count rates by factors of ten from the rates at zero delay is about 65, 180, 520, and 560 μs for the four types of instruments studied (Fig. 43). These were the instruments designed by Leake (1968); 20.8-cm diameter spherical moderator), that by Andersson and Braun (1963, 1964; 20.2 cm diameter cylinder), and detectors with spherical moderators of 30 and 45 cm, respectively. The distributions appear to decrease nearly exponentially with time, but changes in the slopes occur when the count rates have declined by a factor of about 1/10 from the rate at zero delay. Jenkins (1969) has reported a similar study showing consistent results.

b. *Fission Counters.* The fission reactions of ^{235}U, ^{232}Th or ^{237}Np have long been used in the detection of neutrons, particularly at energies of a few MeV and below. One of their major advantages is that a large amount of energy (about 200 MeV) is released in every fission and this amount of energy is not strongly dependent upon the energy of the incident neutron. About 80% of the energy released is usually shared by two highly charged and therefore heavily ionizing fission fragments. These fragments have short ranges in solid materials but may be detected if the fissionable material is embedded within the detector, as is the case in nuclear emulsions, or is adjacent to the detector, as is the case in damage track detectors (Wollenberg and Smith, 1969, 1973; Harrison and Tommasino, 1985; Griffith and Tommasino, nd); or when the fissile material is plated on electrodes of a gas-filled ionization-chamber or pulse counter. Passive detectors previously mentioned, such as ^{238}U and Bi with polycarbonate etch track material, can be supplemented with on-line pulse-shape discriminators (Tesch, 1970, 1988).

At energies of 200 MeV or more, substances not normally thought of as fissionable, such as tantalum, gold, and bismuth, will fission when bombarded by neutrons or other particles, such as protons or pions. Figure 44 shows the fission cross sections for several substances as a function of neutron or proton energy.

The fission of ^{209}Bi by high-energy neutrons or protons has a threshold at about 50 MeV and the fission cross section rises with energy until, at about 1 GeV, it reaches a constant value (see Fig. 44). The best evidence suggests that the proton and neutron cross sections are similar (de Carvalho *et al.*, 1963; Hess *et al.*, 1957 and Moyer, 1952). These characteristics make the fissioning of bismuth extremely valuable in the detection of the high-energy radiation environment — in particular neutrons and protons with energies above 50 MeV.

The fact that the fission fragments are highly energetic but of short range suggest that they might be detected in a suitably designed ionization chamber. Several papers in the literature describe the features of practical instruments (Beasley, 1959; Hess *et al.*, 1957; Kelly and Wiegand, 1948; McCaslin *et al.*, 1968 and Wiegand, 1949).

Fission chambers have been extremely useful in measuring the intensity of particle beams or monitoring regions close to beams where the radiation intensities are high. However, the limited sensitivity of such small detectors does not permit their application to the measurement of the rather low fluence rates that typically appear outside accelerator shielding. For the latter purpose, larger chambers, with a greater amount of fissionable material, have been designed to monitor low fluences. Operation of the detectors in pulsed mode provides discrimination against photons and low-energy events. The range of fission fragments generated in bismuth is about 4 mg cm^{-2} and, to provide optimum sensitivity for a given amount of bismuth, it is necessary to spread the fissionable material thinly over a large area. The design of such instruments and the means of compensating for their high capacitance have been discussed by Moyer (1952), Hess *et al.* (1957), de Carvalho *et al.* (1963) and McCaslin *et al.* (1968). Although experience at Berkeley has shown the great value of using a detector with a threshold of 50 MeV in determining neutron spectra (Gilbert *et al.*, 1968), bismuth fission chambers have not been widely applied to radiation protection dosimetry at other laboratories.

As we have already seen, materials other than bismuth may be used in fission chambers. For example, thorium fission chambers have been applied to a study of the neutron field around a patient treated by heavy-ion radiotherapy (Smith *et al.*, 1981). When using natural uranium, the presence of ^{235}U produces a response of the fission chamber to thermal neutrons as well as to fast neutrons (Wollenberg and Smith, 1969).

4. *Neutron Spectrometry*

a. *Bonner Spheres.* Bonner and his colleagues first described a neutron spectrometer based upon the detection of thermal neutrons at the center of neutron moderators of differing sizes (Bramblett *et al.*, 1960). Polyethylene, $(CH_2)_n$, was chosen as the material for the moderator because it is rich in hydrogen, is physically and chemically stable, and can be consistently manufactured to specifications [but see Griffith and Fisher (1976) for a discussion of variations in the density of polyethylene]. More recently, calculations have been performed that also permit the use of water as a moderator for this purpose. In its original form the thermal neutron detector was a 4 mm-diameter × 4 mm-thick ^{6}LiI(Eu) crystal that could be placed at the center of any of five spherical polyethylene moderators with diameters ranging between 5.08 cm (2 in.) and 30.5 cm (12 in.). An approximately isotropic response was obtained by the choice of a spherical moderator, but the presence of the scintillator and its light pipe can significantly perturb the angular response, particularly for the smaller moderators. It is not feasible to determine the response functions of the Bonner spheres by experimental means because of the lack of adequate monoenergetic neutron sources over the energy range of interest (thermal to 150 MeV). Consequently, the response functions are determined by calculation using neutron transport codes.

Bramblett *et al.* (1960) calculated the variation of response with neutron energy for five spheres of various diameters: 5.08, 7.62, 12.7, 20.3, and 30.5 cm (2, 3, 5, 8, and 12 in.). Limited experimental confirmation of the calculated response functions has been reported (Bramblett *et al.*, 1960; Griffith and Fisher, 1976). Awschalom and Sanna (1985) have summarized both the calculated and the measured response data. Only five sets of calculated response data extend beyond neutron energies of 20 MeV (Burrus, 1962; O'Brien *et al.*, 1965; McGuire, 1966; and Sanna, 1973) and it is these that are of particular value in accelerator neutron spectrometry. The additional advantage of both the McGuire and Sanna response functions is that a 45.7-cm (18-in.) diameter moderator is included in the set, increasing the upper energy limit of the spectrometer. Sanna also calculated the response functions for water moderators and for gold-foil thermal neutron detectors used with both polyethylene and water moderators. Figure 45 gives typical response functions derived from the work of Sanna (1973) for polyethylene spherical moderators and a ^{6}LiI scintillator. A recent critical compilation of published response functions has been given by Alevra and Siebert (1986). Some measurements of response functions using time of flight techniques have been reported by Kosako, *et al.* (1985).

Determination of the overall response functions for a variety of moderator/detector systems is important because there are often good reasons to use detectors other than the ^{6}LiI(Eu) scintillator originally used by Bramblett *et al.* (1960). For example, in fields with high charged-particle or photon contamination, detectors with little or no response to these radiations are desirable. Alternative detectors that have been used to improve the discrimination in favor of neutrons include activation detectors such as gold, tantalum, or cobalt (Smith, 1961, 1962, 1965b, 1966); track detectors (Hewitt *et al.*, 1980); thermoluminescent

dosimeters (Weinstein *et al.*, 1970; Distenfeld, 1975); proportional counters and Geiger-Müller counters (Awschalom and Sanna, 1985). In circumstances in which it is necessary to gate out competing radiation sources, active counters such as LiI scintillators must be used, rather than activation counters.

b. *Unfolding Methods.* Neutron counting rates, measured with a set of detectors with differing energy response functions such as a set of Bonner spheres, are related to the neutron spectrum through the Fredholm equation

$$C_r = \int_0^\infty N(E)R_r(E)dE \quad , \tag{40}$$

where C_r is the counting rate in a detector surrounded by a spherical moderator of radius r, N(E) is the neutron spectrum and $R_r(E)$ is the energy-dependent response function for a sphere of radius r. Given C_r and R_r, N(E) can be obtained by standard unfolding techniques. (See, for example, Awschalom and Sanna, 1985; or Routti and Sandberg, 1980a, 1980b, 1985.)

In practice, Eq. (40) is converted to a discrete form:

$$C_r = \sum_{i=1}^{n} N(E_i)R_r(E_i)\Delta E_i \quad , \tag{41}$$

where $N(E_i)$ is the differential neutron fluence for the ith energy bin ΔE_i, and the response functions are obtained from a separate calculation (Sanna, 1973; Awschalom and Sanna, 1985). These functions are defined for either 31 or 40 discrete energy groups, depending upon the unfolding program that is used. The unfolding problem is thus reduced to solving 8 equations (i.e., data from the 8 spheres) for either 31 or 40 unknowns.

The same unfolding principles apply to other detectors such as threshold or activation detectors, used either separately or in combination with the sphere set.

Equation (41) does not have a unique solution, and it is well known that there are inherent difficulties due to the underdetermined and sometimes ill-conditioned nature of such a problem. Three different programs are representative of the several approaches that have been attempted to derive neutron spectra from the measured counting rates:

- BUNKI uses the SPUNIT iterative recursion procedure along with an algorithm that allows a choice of different starting solutions (Lowry and Johnson, 1984);
- LOUHI is a least-squares method that allows user-controlled constraint conditions (Routti, 1969; Routti and Sandberg, 1980a);
- SWIFT is based on a Monte-Carlo method that allows a broad sampling of possible neutron spectra with no *a priori* assumptions about their character, apart from non-negativity (Sanna and O'Brien, 1971; O'Brien and Sanna, 1981; Chambless and Broadway, 1983; O'Brien and Sanna, 1983).

Other unfolding methods are described in works by Draper (program SAND, 1971) and Perey (program STAY'SL, 1977).

From a neutron spectrum derived in this manner that acceptably reproduces the measured counting rates for a given data set, one can determine the neutron fluence, absorbed dose (kerma)[8] and dose equivalent, and thus the quality factor associated with the neutron field.

Discussions of unfolding procedures in accelerator environments have been published by Nakamura *et al.* (1978), Birattari and Salomone (1985), Cossairt *et al.* (1985b), Thorngate and Griffith (1985), Elwyn and Cossairt (1986), and McCaslin *et al.* (1986). For a complete discussion of neutron spectra, see Cross and Ing (1987).

---

[8] *Kerma* is defined as the "...quotient of dE_{tr} by dm where dE_{tr} is the sum of the initial kinetic energies of all the charged ionizing particles liberated by uncharged ionizing particles in a material of mass dm." (ICRU 1980). The unit for kerma is the gray [1 Gy = 1 J kg^{-1}] or the rad [1 Gy = 100 rad].

c. *Proton Recoil Counters.* Nuclear emulsions, discussed above, can be used to record recoil proton spectra from neutron interactions. Recoil proton spectra have also been measured in real time using bulk plastic scintillation detectors (Thorngate and Griffith, 1985). Both these techniques are able to give neutron spectral information in the energy range range 2–20 MeV. At higher energies, star-prong counting has been utilized to give crude spectral slope information (Remy, 1965; Patterson *et al.*, 1969).

At higher energies special counter telescope arrangements (Aleinikov *et al.*, 1974, 1975, 1979; Madey and Waterman, 1973; Penfold and Stevenson, 1968) or spark chamber arrays (Lim, 1973; Mamont-Ciesla and Rindi, 1974; Rindi, 1969, 1974b) are required. Both of these techniques derive directly from high-energy physics detectors and require a complex infrastructure, typically beyond the capabilities of small accelerator laboratories.

5. *Mixed Field Dosimetry*

a. *Introduction.* As mentioned, the radiation fields around accelerators are complex, often consisting of many different ionizing radiations extending over a broad range of energies (Baarli, 1969). Zielczynski (1971) has discussed the uncertainties in mixed radiation field dosimetry and cites two major difficulties:

- determination of response functions of detectors.
- interpretation of measurements and determination of accuracy.

More specifically, dosimetric techniques that span the wide range of accelerator radiation environments suffer from all or some of the following drawbacks:

- interference from radiations other than those to be measured,
- response-rate dependence in intense radiation fields,
- complexity,
- incomplete instrument response function data,
- uncertainties in instrument response interpretation.

In the search for a single dosimeter that would permit direct accurate measurement of the entire accelerator radiation field, imaginative attempts have been made, including the LET spectrometer of Rossi and Rosenzweig (1955), the modified LET spectrometer of Kuehner *et al.* (Baum *et al.*, 1969, 1970; Kuehner and Chester, 1973; Kuehner *et al.*, 1972, 1973), the differential recombination chambers of Zielczynski (1962, 1963), Zielczynski *et al.* (1964) and of Sullivan and Baarli (1963), and the scintillation method of Pszona (1971).

b. *Recombination Chambers.* Absorbed dose, D and dose equivalent, H, are related by a dimensionless quality factor, Q, according to the equation

$$H = DQ \quad . \tag{42}$$

For many years there has been some interest in developing ionizing chambers that may determine empirically the value of Q in particular radiation fields. A possible method is based upon the recombination of ions produced in gases. Recombination phenomena have been given considerable study (Boag, 1950, 1952, 1987; Jaffé, 1913, 1929a,b, 1940).

In the irradiated gas of an ionization chamber the signal (current) from the chamber may be reduced by ion recombination. Jaffé pointed to two distinct types of recombination:

- Inter-columnar recombination or recombination of ions from different tracks before collection. This phenomenon is dose-rate dependent and can be of importance in a pulsed radiation field of short duty cycle (Boag, 1966).
- Intra-columnar recombination occurs between ions within a single track. While generally of little significance when measuring low LET radiations, this can become important in

chambers operated at high gas pressures or when high-LET radiations such as neutrons (recoil protons) are to be measured (Jaffé, 1913, 1929a, 1929b, 1940; Zanstra, 1935).

The phenomenon of intra-columnar recombination may be utilized to determine the average LET of charged particles. This possibility arises because, for an unsaturated ionization chamber, over a considerable range of field strength due to the applied collection potential V, the collected ionization current, i, is given by the empirical equation

$$i = kV^n \quad , \tag{43}$$

where k is a constant for a given absorbed dose rate and radiation field and n is the "recombination number," which is a function only of unrestricted LET (L_∞). Because the quality factor Q is also defined only in terms of L_∞ (ICRP, 1963, 1977), it follows that the recombination number is also a function of Q, i.e., n = n(Q), a function that may be empirically derived. The empirical nature of the function n(Q) must be stressed because the relationship of Q and L is defined by consideration of a wide variety of biological data, and there is no direct theoretical connection between the two functions $Q(L_\infty)$ and n(Q).

Some twenty years ago work at Brookhaven National Laboratory (Distenfeld and Markoe, 1965), at CERN (Sullivan and Baarli, 1963) and in Warsaw and Dubna (Zielczynski, 1962, 1963; Zielczynski *et al.*, 1964) suggested that the quality factor could be estimated to within about 20% by recombination chambers. The various chambers developed at these laboratories had significantly different plate structures and used different collection potentials. Figure 46 shows the response of the chamber constructed at CERN. This was a large parallel plate chamber, with electric field gradients up to 2000 V cm^{-1} and operated with tissue-equivalent gas at pressures up to 6 atm.

These chambers were quite large and because of the large mass of the chamber itself and associated equipment, could perturb the radiation field in which they were placed. In addition, the operation of large chambers at moderately high pressure with thin windows made them something of a hazard.

Cossairt *et al.* (1984, 1985b; Cossairt and Elwyn, 1987) at Fermilab have used the recombination chamber developed by Zielczynski (1962, 1963, 1971; Zielczynski *et al.*, 1964), in conjunction with other instruments, to determine the quality factor of radiation fields in which neutrons were the main component. Consistency was found between the value of Q so determined and the value derived from detailed knowledge of the radiation field, in particular the neutron spectrum.

Interest in "Q meters" has declined somewhat over the past decade and they are now rarely if ever used at accelerator laboratories except for experimental purposes. In addition to the practical difficulties mentioned above, discussions suggest that the relationship between Q and L_∞ needs to be changed (Dennis and Dunster, 1985; ICRU, 1986), or even that lineal energy, y, rather than linear energy transfer, L, be the physical parameter used to specify quality factor (ICRU, 1986).

c. *Other Techniques for Direct Assessment of Q.* The light output from a plastic scintillator may be utilized to obtain an estimate of radiation quality. The method devised by Pszona (1969, 1971) and Pszona and Höfert (1977) relies on the simultaneous measurement of currents from an ionization chamber and a photomultiplier tube attached to a plastic scintillator. The ratio of the currents is a complex function of LET, but it can be used to give a measure of an average Q in an unknown field, provided the system is properly calibrated.

Yet another technique, described by Tesch (1970), is to use pulse-shape discrimination on the pulses coming from an organic scintillator to discriminate against photons and to choose a suitable discriminator threshold so that the pulse rate is proportional to dose equivalent.

d. *Universal Dose-Equivalent Instrument.* All of the techniques discussed above have given satisfactory estimates of quality factor and dose equivalent in near-laboratory conditions of exposure. However, as yet there is no universal dose-equivalent meter that is sensitive and robust enough to withstand the rigors of measurement in the field, while giving reliable results at occupational radiation levels. This is to be contrasted with the multiple detector systems described, which have been shown to be reliably consistent for more than 20 years.

D. ENVIRONMENTAL MONITORING

1. *Introduction*

"The dose received from external sources of ionizing radiation originates from cosmic rays and from gamma-emitting radionuclides in the earth's crust. The United Nations (UNSCEAR, 1982) estimates the external annual effective dose equivalent from all naturally occurring radiation in 'normal' parts of the world to be 30 mrem/year from cosmic sources and 35 mrem/year from terrestrial radiation" (Eisenbud, 1987). Thus there is a nominal background of external radiation due to photons of about 650 μSv/year (65 mrem/year) that must be subtracted from site environmental measurements. In addition, the fluence of cosmic-ray neutrons at sea level at mid-latitudes (41°–46° N) is about 65–84 neutrons $m^{-2}s^{-1}$ (measurements quoted by Hewitt *et al.* 1980, p. 868), corresponding to dose-equivalents in the range 50–60 μSv/year (5–6 mrem/year). These values are based on a fluence to dose-equivalent conversion coefficient of 2.3×10^{-14} Sv m^2 $neutron^{-1}$ (2.3×10^{-8} rem cm^2 $neutron^{-1}$ for the presumed cosmic-ray spectrum (Gilbert *et al.*, 1968, p. 126). A very useful monograph that summarizes the natural environmental radiation field as well as measurement procedures is NCRP-50 (1976).

Experience at many high-energy particle accelerators around the world has shown that accelerators impose their primary radiological impact on the environment in the form of prompt radiation. While each accelerator facility is an individual case, generally the magnitudes of population exposure from prompt radiation, radioactive gases, and radionuclides in water occur roughly in the ratio of 100 : < 10 : < 1. Experience has shown that the population exposure due to radioactivity induced in materials that are recycled, for example magnet iron, copper conductors, and other accelerator components, is even smaller (Thomas, 1978a, 1978b; Thomas and Rindi, 1979). Major consideration is thus given to determine the prompt radiation field in environmental monitoring at particle accelerators.

As we have seen in Section III there are three components to the prompt radiation field that are of environmental concern. These are muons, neutrons, and photons; and of these three neutrons are usually most important. In addition, the presence of any induced radioactivity in air and water is monitored at many high-energy installations.

2. *Neutrons*

a. *BF_3 counters.* Neutrons are most readily monitored by moderated BF_3 counters based on versions of the "long counter." These counters have a fairly flat energy dependence per unit fluence from 20 keV up to about 20 MeV and may be calibrated either in terms of fluence or dose equivalent. As at Lawrence Berkeley Laboratory, the primary neutron detector for environmental monitoring may be a moderated BF_3 proportional counter, the moderator consisting of 6.3 cm of paraffin wax. This detector is considered sensitive to neutrons from 0.1 to about 20 MeV (Wallace *et al.*, 1961; Thomas, 1976). Figure 47 shows the typical response record of such a neutron detector placed at the site boundary of LBL. Periods of accelerator operation are clearly evident. Dose-equivalent rates comparable with those due to cosmic ray neutrons, 50–60 μSv/year (5–6 mrem/year) are detectable with a system such as this. Similar detectors are used at many other accelerator laboratories. See, for example, Rau and Wittekind (1982b) and Cossairt and Coulson (1985).

b. *Thermoluminescent Dosimeters.* The high thermal neutron capture cross-section of ^6Li has led to the application of ^6LiF phosphors to the detection of neutrons. The response of the ^6LiF phosphors to photons may be corrected for by the use of ^6LiF–^7LiF pairs. Neutrons are detected by ^6LiF after thermalization in a suitable moderator surrounding the detector pair. Such a system has been used at CERN (Bonifas *et al.*, 1974; Tuyn, 1977, 1982). For typical data see Fig. 35.

One major disadvantage of this technique is that it is difficult to measure dose-equivalent rates below 100–200 μSv per annum. Extreme care must be taken to prevent the dosimeters from being exposed to thermal neutrons during transport to and from the monitoring site. A successful way of handling TLD pairs is to load them into polyethylene inserts and put the inserts inside Cd cylinders for temporary storage upon reaching the measurement site. The inserts are rapidly removed from the Cd cylinders. Upon completion of the measurements the procedure is reversed (Sanna *et al.*, 1980; Rohloff and Heinzelmann, 1973; Awschalom and Sanna, 1985).

3. *Photons*

a. *Introduction.* Whatever technique is used to measure photons, the measurements must be carefully interpreted. The total accelerator-produced radiation level at high energy accelerator boundaries is in many cases administratively limited to levels as low as 0.1 mSv per year (10 mrem/y). Of this only

10–20% is likely to be due to photons. The task of identifying 10 μSv/y (1 mrem/y) due to accelerator operation in a background some 50 to 100 times higher is formidable. Variations in the geology within an accelerator site may easily produce local fluctuations of 0.2 mSv/y (20 mrem/y) or more (Stephens *et al.*, 1975, 1976; Thomas, 1976). Variations in water content in the soil and contributions from radon daughters washed out by rainfall may also significantly perturb the radiation background to an extent much greater than is done by accelerator operation (Beck *et al.*, 1971; de Planque-Burke, 1975a, 1975b; de Planque-Burke and O'Brien, 1974). It is imperative that these fluctuations in natural background be understood before any attribution of detector readings to radiation sources (natural or man-made) is attempted.

b. *Ionization Chambers.* The natural instrument of choice for real-time measurements of environmental photon fields is the ionization chamber. Special chambers have been constructed having sensitivity and stability that are capable of measuring the low dose rates characteristic of environmental radiation, of range 30–200 nGy/h (3–20 μrad/h). In particular, we mention one type of chamber that has received wide acceptance at accelerator laboratories, as well as at nuclear facilities, and has an accuracy of better than ± 1% in fields as low as 100 nGy/h (10 μrad/h). The Health and Safety Laboratory of the U.S. Atomic Energy Commission (de Campo *et al.*, 1972) developed a high-pressure argon-filled steel-walled ionization chamber of fairly large volume, coupled with an electrometer based on MOS field-effect transistors capable of measuring currents as low as $\sim 10^{-15}$ A (McCaslin, 1964; Negro *et al.*, 1967). For adequate sensitivity, the chamber proper is constructed as a stainless steel sphere (either 7 or 10 inch-diameter) and is filled with argon gas at 25 atm (range 10–44 atm). The center electrode is an aluminum sphere of either 0.75 or 2 inch–diameter, held in place by a thinner aluminum rod. The chambers exhibit essentially complete ion collection at a collecting potential of 300 V for dose rates up to several μGy/h (several hundred μrad/h).

The 10-inch, 25-atm, steel-argon chamber described has been found to be nearly optimum because of the following properties:

- nearly flat photon energy response over 0.050–10 MeV;
- nearly complete ionization collection up to 10 μGy/h (1 mrad/h);
- sensitivity of $\sim 2.2 \times 10^{-15}$ A/(nGy/h) [22×10^{-15} A/(μrad/h)];
- can be calibrated with standard radium sources generally available;
- MOSFET electrometer is adaptable for *in-situ*, real-time environmental conditions;
- also useful as muon dosimeter without modification;
- neutron sensitivity is minimized by the use of a steel shell and argon gas filling.

Chambers based on the HASL design have been integrated into complete systems having extended exposure-rate ranges and are available from Reuter-Stokes Instruments, Inc., Twinsburg, OH.

c. *Geiger-Müller Counters.* Geiger-Müller counters are extremely reliable instruments for determining environmental radiation levels at accelerator laboratories. At LBL an energy-compensated Geiger-Müller counter of the type designed by Jones (1962) is used. The detector assembly consists of a thin window GM tube in a stainless steel cylinder and the associated transistorized circuitry and scaler units. Each dosimeter is packaged in a metal box 6 in. × 6 in., with the GM tube assembly, 6 in. × 1–1/2 in., mounted on top of the box. The units, while normally operated from domestic AC power, also contain a rechargeable battery that can run the detector for about 6 weeks in the event of a domestic power outage. The detector and scaler units provide a sensitivity of about 2 μR per register count. Each Geiger-Müller unit is calibrated with an NBS standard 1.35 milligram radium source.

d. *Thermoluminescent Dosimeters.* Thermoluminescent dosimeters have been widely used to monitor photon intensities around nuclear power stations and have been successfully adapted for use at particle accelerators (Bonifas *et al.*, 1974; Tuyn, 1977, 1982). Lithium fluoride is usually the material of choice due to its favorable energy response but it has lower sensitivity than other materials such as calcium fluoride (CaF_2). CaF_2:nat is about 23 times as sensitive to cobalt-60 radiation as LiF (Cameron *et al.*, 1968) and the readily available CaF_2:Dy (marketed by Harshaw as TLD-200) is 15–30 times as sensitive as LiF, depending upon the readout system employed (see, for example, Portal, 1981). However, CaF_2 materials also have the disadvantage of significant "fading," whereas fading for LiF is not significant in

most applications.

The Environmental Measurements Laboratory of the U.S. Department of Energy has reported extensive studies of the application of LiF to the measurements of external radiation levels due to photons and muons. The use of Harshaw TLD-700 dosimeters, evaluated monthly, was able to determine background levels to an accuracy estimated at ± 3.5%. Variations in natural background due to moisture content in the soil are readily observed with these detectors (de Planque-Burke, 1975a, 1975b; de Planque-Burke and O'Brien, 1974).

4. *Muons*

a. *Introduction.* Muons are routinely observed outside the shielding of accelerators with operating energies greater than 10 GeV (Cowan, 1962; Bertel *et al.*, 1971; Nelson *et al.*, 1974; Cossairt, 1983). In limited regions, muons may be the dominant component of the radiation at the site boundary, as is the case, for example, at the Fermi National Accelerator Laboratory (Baker, 1974; Cossairt, 1983, 1987; Elwyn and Freeman, 1984), or the CERN SPS (Rau and Wittekind, 1982a; Nelson *et al.*, 1979, 1983; Stevenson, 1985). Indeed, the boundary muon dose is an important consideration in site requirements for the proposed Superconducting Super Collider (SSC, 1987).

b. *Ionization Chambers.* Muons, apart from having higher mass, are similar to electrons and may, in principle, be measured using ionization chambers. However, in measurements of muon fields, Höfert (1984b) has reported differences in determination of absorbed dose of up to 30% between different instruments. It is possible that values of W, the average energy required to create an ion pair in gas, need to be more precisely evaluated for muons because the estimates of absorbed dose in tissue usually assume values of W for the gas in the ionization chamber identical with those for photons.

c. *Counter Telescopes.* The directionality of stray muon fields suggests the use of scintillation counter telescopes, commonly used in nuclear and high-energy physics experiments to detect energetic charged particles. These were first applied to the detection of protons outside accelerator shielding by Penfold and Stevenson (1968). The technique has been subsequently applied to the detection of muons by Höfert and Baarli (1974) at CERN and Cossairt and his colleagues at Fermilab (Cossairt, 1983; Moore and Velen, 1974). Nelson *et al.* (1974) used scintillator paddles (not really a telescope) for the detection of muons through thick shielding at SLAC.

Cossairt (1983) has described a muon telescope of moderate directional sensitivity used at the Fermi National Accelerator Laboratory consisting of two scintillator paddles approximately $20 \times 20 \times 1$ cm separated by 38 cm and operated in coincidence. A 2.5-cm-thick aluminum plate is placed between the scintillators to reduce false coincidences due to δ-rays. Coincidence data are obtained both during beam-on and beam-off phases of operation, using gates synchronized with the accelerator duty cycle. The gating is operated by a microwave transmitter, which also provides beam intensity data. This detector is mobile and has been used to explore the muon fields at Fermilab in some detail (Cossairt, 1983).

d. *Other Techniques.* Several other techniques commonly used to detect ionizing radiation have also been used in muon fields. We briefly mention some examples:

i) Nelson *et al.* (1974) used nuclear emulsions to study muon fields (particularly the angular distributions) emerging from thick concrete and iron shields at SLAC.

ii) A detector system based on silicon detectors developed by Heijne (1983) was applied to study muon fields through thick soil shields at CERN (Nelson *et al.*, 1979).

iii) Thermoluminescence dosimeters are well suited as passive detectors of muons. For example, as part of the routine environmental monitoring program at CERN (Goebel, 1985; Rau and Wittekind, 1982a), as many as 90 CaF_2:Dy TL dosimeters are suspended in an array at beam height (2.0–5.5 m above ground) at the site boundary downstream of the SPS West Experimental Hall.

iv) A study that illustrated the use of a variety of instruments in a mixed field of neutrons and muons produced by a 400-GeV proton beam was performed by Cossairt and Elwyn (1987) at Fermilab. In this field the proportions of absorbed dose were D(muons):D(neutrons) = 92%:8%. The instrumentation consisted of a recombination ionization chamber, self-reading pocket ion-chamber dosimeters, and ordinary gamma film "badges." Plastic scintillator paddles and Bonner multisphere system were used to study the muon

and neutron fluences. It was concluded that simple instrumentation, *viz.* the pocket dosimeters and gamma films, "provide an adequately accurate record of adsorbed dose equivalent in a muon radiation field... even when the spectrum is not well known. [However,...] neutron contamination... will complicate the dosimetry considerably."

5. *Monitoring of Gaseous Emissions*

a. *Radioactive Gas Monitors.* Moy *et al.* (1980) described the radioactive gas and aerosol monitors used at air-extraction points of the CERN accelerators. Air is diverted from the extraction ducts at a rate of about 16 m^3h^{-1}, filtered to remove aerosols greater than about 0.3 μm in size, and passed through a 1-m^3 measuring chamber. Two Geiger-Müller counters are placed inside the measuring chamber to determine the radioactivity of the gas. Because the principal radionuclides emit $\beta^{\pm}$ particles, one counter is thin-walled and responds to both electrons and photons; the second counter is covered by a plexiglass tube with a wall thickness of 5 mm, and responds to photons only. The difference between the readings of these two counters gives the activity from $\beta^{\pm}$ particles and also compensates for any fluctuation in the photon background. The system is calibrated by introducing a known quantity of ^{85}Kr into the measuring chamber (Ribes *et al.*, 1974, 1976). Two types of GM tubes are used, having calibrated sensitivities of 440 Bq/pulse (12 nCi/pulse) and 4.3×10^6 Bq/pulse (116 μCi/pulse). The less sensitive detectors are placed where the concentrations of radioactivity in air are usually high during accelerator operation (for example at outlets from target stations).

Two digital outputs are provided from the electronics — the instantaneous concentrations of radioactivity and, by multiplying the concentration by the flow-rate of air through the ventilation duct, the total activity release. Specifications of the gas monitor are shown in Table XXI.

b. *Radioactive Aerosols.* The concentration of radioactive aerosols in the released air may be determined by pumping the air through a filter system. At CERN, for example, air is pumped through a 200-mm diameter filter paper (Schleiter and Schull No. 6) that is clamped in a special cartridge. The total volume of air passing through the filter is measured by a gas counter. A differential manometer connected across the filter indicates whether the filter cartridge is clogged, broken, or improperly placed. For ventilation ducts the air flow through the filters is 16 m^3h^{-1} but for routine low-level air sampling a rate of 30 m^3h^{-1} is used. Filter-cartridges are removed every fortnight and the activity measured in a low-level counting laboratory (Moy *et al.*, 1980).

V. Summary

We conclude, as we began, by claiming that it is at particle accelerators where the science and technology of radiation dosimetry is at its most sophisticated. In only one other class of radiation environments — those met in extra-terrestrial exploration — do such novel and diverse dosimetric challenges need to be faced. Even here, the dosimetrist does not encounter the range of particle intensities, variety of radiation environments, or the pulsed nature characteristic of accelerator radiation fields.

This article has stressed the importance of a sound physical understanding of accelerator environments and so has largely dealt with the causes and characteristics of these fields. When the character of the radiation fields is understood, it is often possible to use instruments and techniques familiar to other fields of radiation dosimetry. This should, however, only be attempted when the response of any instrument in such radiation environments is fully understood.

At particle accelerators, the application of radiation dosimetry goes beyond attempts to quantify individual radiation exposure. Dosimetric data are often needed to determine what changes in accelerator operation or shielding are needed to modify (usually to reduce) radiation environments. It is not surprising therefore, to find that instruments developed for nuclear-physics and particle-physics research are often applied to radiation dosimetry at accelerator laboratories. The results of such measurements quantify radiation fields in physical terms — particle type, energy, fluence, and angular distributions.

It would be inappropriate to end without reminding the reader that, having the benefit of some thirty years of experience, there is general agreement at accelerator laboratories with Moyer's (1954) view that physical characterization of the accelerator radiation environment is to be preferred to attempts to reduce

its great complexity to a single scalar quantity, such as dose-equivalent. As we have already said, dosimetrists continue their quest for techniques by which a single dosimeter can be applied to an accurate and sufficient specification of the high-energy accelerator radiation field. While keeping an open mind, the authors remain sceptical that such a goal can be achieved. Indeed, the debates concerning the dose-equivalent system that have taken place in the past five years may lead one to doubt its permanence. The system is now so complex that it has perhaps lost its original intended virtue of simplicity.

VI. REFERENCES

Aarnio P.A., Ranft J., and Stevenson G.R. (1984a). "First Up-date of FLUKA82 Including Particle Production with a Multi-Chain Fragmentation Model (EVENTQ)." European Organization for Nuclear Research CERN, Geneva, CERN Divisional Report TIS-RP/129.

Aarnio, P.A., Ranft, J., and Stevenson, G.R. (1984b). "A Long Write-Up of the FLUKA Program." European Organization for Nuclear Research CERN, Geneva, CERN Divisional Report TIS-RP/106(Rev).

Ainsworth, E.J., Kelly, L.S., Mahlmann, L.J., Schooley, J.C., Thomas, R.H., Howard, J., and Alpen, E. (1983). "Response of colony forming units — spleen to heavy charged particles." *Radiation Research 96*, 180–197.

Aleinikov, V.E., Gerdt, V.P., and Komochkov, M.M. (1974). "Neutron Spectra Outside the Shielding of High-Energy Proton Accelerators." Joint Institute for Nuclear Research, Dubna, U.S.S.R., Report JINR P16-8176.

Aleinikov, V.E., Gerdt, V.P., and Timoshenko, G.N. (1975). "Measurement of Spectra of High-Energy Protons Generated in the Shielding of a 680 MeV Synchrocyclotron." Joint Institute for Nuclear Research, Dubna, U.S.S.R., Report JNIR-P16-9400.

Aleinikov, V.E., Komochkov, M.M., Krilov, A.R., Timoshenko, G.H., and Hahn, G. (1979). "The Energy-Angle Distributions of the Proton Component of the Radiation Field Behind the 660 MeV Synchrotron Shielding." Joint Institute for Nuclear Research, Dubna, U.S.S.R., Report JINR P-16-12732.

Alevra, A.V., and Siebert, B.R.L. (1986). "Influence of Neutron Spectra and Fluence Response Data on the Determination of Dose Equivalent with Bonner Spheres." Physikalisch-Technische Bundesanstalt, Braunschweig, F.R.G., Report PTB-NB-28.

Allen, A.J., Nechaj, J.F., Sun, K.-H., and Jennings, B. (1951). Thick target fast neutron yield from 15-MeV deuteron and 30-MeV alpha-bombardment. *Phys. Rev. 81*, 536–539.

Alsmiller, R.G., Jr., and Barish, J. (1969). High-energy (<18 GeV) muon transport calculations and comparison with experiment. *Nucl. Instrum. Methods 71*, 121–124.

Alsmiller, R.G., Jr., and Barish, J. (1973). Shielding against the neutrons produced when 400-MeV electrons are incident on a thick copper target. *Particle Accelerators 5*, 155–159.

Alsmiller, R.G., Jr., and Moran, H.S. (1966). "Electron-Photon Cascade Calculations and Neutron Yields from Electrons in Thick Targets." Oak Ridge National Laboratory Report ORNL-TM-1502 (1966). [See also Alsmiller and Moran 1967a. The ORNL report contains extensive tables not included in the published version.]

Alsmiller, R.G., Jr., and Moran, H.A. (1967a). Electron-photon cascade calculations and neutron yields from electrons in thick targets. *Nucl. Instrum. Methods 48*, 109–116.

Alsmiller, R.G., Jr., and Moran, H.S. (1967b). "Dose Rate from High-Energy Electrons and Photons." Oak Ridge National Laboratory Report ORNL-TM-2026; also, *Nucl. Instrum. Methods 58*, 343–344 (1968).

Alsmiller, R.G., Jr., and Moran, H.S. (1968). "The Electron-Photon Cascade Induced in Lead by Photons in the Energy Range 15 to 100 MeV." Oak Ridge National Laboratory Report ORNL-4192.

Alsmiller, R.G., Jr., and Moran, H.S. (1969). "Calculation of the Energy Deposited in Thick Targets by High-Energy (1 GeV) Electron-Photon Cascades and Comparison with Experiment." Oak Ridge

National Laboratory Report ORNL-TM-2559; also, *Nucl. Sci. Eng. 38*, 131–134 (1969). This report is superseded by Alsmiller and Moran (1970a).

Alsmiller, R.G., Jr., and Moran, H.S. (1970a). "Calculation of the Energy Deposited in Thick Targets by High-Energy (1 GeV) Electron-Photon Cascades and Comparison with Experiment II." Oak Ridge National Laboratory Report ORNL-TM-2843; also, *Nucl. Sci. Eng. 40*, 483–485 (1970). This report supersedes Alsmiller and Moran (1969).

Alsmiller, R.G., Jr., and Moran, H.S. (1970b). "Energy Deposition by 45-GeV Photons in Be and Al." Oak Ridge National Laboratory Report ORNL-4631.

Alsmiller, R.G., Jr., Alsmiller, F.S., Barish, J., and Shima, Y. (1971). "Muon transport and the shielding of high-energy (500 GeV) proton accelerators." *In* op.cit. CERN (1971b), 601–640.

Alsmiller, R.G., Jr., Barish, J., and Childs, R.L. (1981). Skyshine at neutron energies ≤400 MeV. *Particle Accelerators 11*, 131–141.

Alsmiller, R.G., Jr., Barish, J., and Dodge, S.R. (1974). "Energy Deposition by High-energy Electrons (50–200 MeV) in Water." Oak Ridge National Laboratory Report ORNL-TM-4419.

Alsmiller, R.G., Jr., Leimdorfer, M., and Barish, J. (1968). "High-Energy Muon Transport and the Muon Backstop for a 200-GeV Proton Accelerator." Oak Ridge National Laboratory Report ORNL-4322.

Amaldi, E.(1959). The production and slowing down of neutrons. *In* "Encyclopedia of Physics." 38(2), pp. 1–659, Springer, New York.

Amols, H.I., Kittell, R., Paciotti, M.A., Hellend, J.A., Hogstrom, K.R., Collier, M., and Heller, P. (1980). Preclinical studies of dynamic treatment modes in pion therapy. *Med. Phys. 7*, 621–626.

Andersson, I.O., and Braun, J. (1963). A neutron rem counter with uniform sensitivity from 0.025 MeV to 10 MeV. *In* "Neutron Dosimetry. Proc. Symp. Neutron Detection and Dosimetry Standards," Harwell (Dec. 1962), Vol. 2, p. 87–95, IAEA, Vienna.

Andersson, I.O., and Braun, J. (1964). A neutron rem counter. *Nucleonik 6*, 237–241.

Anderson, A.L., and Schmidt, C.T. (1966). "^{65}Zn Content in 90 Inch Cyclotron Workers at Livermore." Lawrence Livermore National Laboratory Hazards Control Progress Report No. 25, UCRL-5007.

Antipov, A.V., Bajshev, I.S., Golovachik, V.T., Krupnyji, G.I., Kustarev, V.M., Lebedev, V.N., and Höfert, M. (1978). "Comparison of Dose Equivalent Measurements Behind the IHEP Accelerator Shielding Using Different Methods." Institute of High Energy Physics, Serpukhov, Report IFVEORI 78-15 (in Russian). Available in English Translation by B.C. Hodge as CERN Internal Report CERN TRANS 78-01.

Apfel, R.E. (1979). The superheated drop detector. *Nucl. Instrum. Methods 162*, 603–608.

Arakita, Y., Hirayama, H., Inagaki, T., and Miyajima, M. (1979). Study of an iron beam stop for 500 MeV protons. *Nucl. Instrum. Methods 164*, 255–265.

Armstrong, T.W. (1969). Monte-Carlo calculations of residual nuclei production in thick iron targets bombarded by 1 and 3 GeV protons and comparison with experiment. *J. Geophys. Res. 74*, 1361–1373.

Armstrong, T.W. (1980a). The HETC hadronic cascade code. *In* "Computer Techniques in Radiation Transport and Dosimetry." (W.R. Nelson and T.M. Jenkins, eds.), pp. 373–385.

Armstrong, T.W. (1980b). The intranuclear cascade-evaporation model. *In* op.cit. (W.R. Nelson and T.M.

Jenkins, eds.). pp. 311–322.

Armstrong, T.W. (1980c). Introduction to hadronic cascades. *In* op. cit. (W.R. Nelson and T.M. Jenkins, 1980), Computer Techniques in Radiation Transport and Dosimetry, Plenum Press, New York and London.

Armstrong, T.W., and Alsmiller, R.G., Jr. (1968). Monte-Carlo calculations of the nucleon-meson cascade in iron initiated by 1 and 3 GeV protons and comparison with experiment. *Nucl. Sci. Eng. 33*, 291–296.

Armstrong, T.W., and Alsmiller, R.G., Jr. (1969). Calculation of the residual photon dose rate around high-energy proton accelerators. *Nucl. Sci. Eng. 38*, 53–62.

Armstrong, T.W., and Barish, J. (1969a), Calculation of the residual photon dose rate induced in iron by 200 MeV protons. *Nucl. Sci. Eng. 38*, 271–272.

Armstrong, T.W., and Barish, J. (1969b), Calculation of the residual photon dose rate due to the activation of concrete by neutrons from a 3-GeV proton beam in iron. *Nucl. Sci. Eng. 38*, 265–270.

Armstrong, T.W., Alsmiller, Jr., R.G., Chandler, K.C., and Bishop, B.L. (1972). Monte Carlo calculations of high-energy nucleon-meson cascades and comparison with experiment. *Nucl. Sci. Eng. 49*, 82–92.

Auxier, J.A., Haywood, F.F., and Gilley, L.W. (1963). "General Correlative Studies—Operation BREN." Oak Ridge National Laboratory, USAEC Report CEX 62.03.

Awschalom, M. (1966). "The Use of Multisphere Neutron Detector for Dosimetry of Mixed Radiation Fields." Princeton-Pennsylvania Accelerator Laboratory Report PPAD 596E.

Awschalom, M., and Sanna, R.S. (1985). Application of Bonner sphere detectors in neutron field dosimetry. *Radiat. Prot. Dosim. 10* (1–4), 89–101.

Awschalom, M., Larsen, F.L., and Sass, R.E. (1965). "Health physics problems at the Princeton-Penn Synchrotron." *In* Proc. USAEC First Symposium on Accelerator Radiation Dosimetry and Experience. Brookhaven, November 1965, USAEC Report CONF-651109, p. 57–79.

Baarli, J. (1969). Dosimetry of very high energy radiation. *In* "Health Physics." (A.M.F. Duhamel, ed.), Vol. 2, p. 291–320, Pergamon Press, Oxford.

Baarli, J., and Sullivan, A.H. (1965a). Radiation dosimetry for protection purposes near high-energy particle accelerators. *Health Physics 11*, 353–361.

Baarli, J., and Sullivan, A.H. (1965b). Health physics survey methods for the measurement of stray radiation around the CERN high-energy accelerators. *In* "Proceedings of the First Symposium on Accelerator Radiation Dosimetry and Experience," USAEC Report CONF 651109, p. 103–116.

Baker, S.I. (1974). Fermi National Accelerator Laboratory environmental monitoring report. *In* "Environmental Monitoring at Major USERDA Contractor Sites—CY 1974." USERDA, Washington, D.C., Report ERDA-54, TID-26775, pp. 561–594.

Baker, S.I. (1975). Soil activation measurements at Fermilab. *In* "Proc. Third Environmental Protection Conference," Chicago, Sept. 23-26, 1975, USERDA, Washington, D.C., Report ERDA-92, Vol. 1, pp. 329–347.

Baker, S.I. (1976). Fermi National Accelerator Laboratory environmental monitoring report for calendar year 1975. *In* "Environmental Monitoring at Major U.S. Energy Research and Development Administration Contractor Sites Calendar Year 1975." USERDA, Washington, D.C., Report ERDA-76-104, Vol. 1, pp. 562–603.

Baker, S.I. (1985). Fermilab soil activation experience. *In* "Proceedings of the 5th DOE Environmental Protection Information Meeting," Albuquerque, NM, Nov. 6–8, 1984, pp. 673–684.

Baranov, P.S., Goldanskii, V.I., and Roganov, V.S. (1957). Dosimeter for high-energy neutrons. *Rev. Sci. Instrum. 28*, 1029–1032.

Ban, S., Hirayama, H., and Miura, S. (1987). Measurement of absorbed dose in water irradiated by 2.5-GeV bremsstrahlung. *Health Physics 53*, 67–72.

Barbier, M. (1969). "Induced Radioactivity." North Holland, Amsterdam.

Barbier, M., and Hunter, R. (1971). Numbers and spectrum of muons from proton-induced extranuclear cascades in shields. *In op. cit.* CERN (1971b), 652–677.

Barkas, W.H. (1963). "Nuclear Research Emulsions." Vol. 1: "Techniques and Theory;" Vol. 2: "Particle Behavior and Emulsion Applications." Academic Press, New York.

Barkas, W.H., and Berger, M.J. (1964). "Tables of energy losses and ranges of heavy charged particles." National Aeronautics and Space Administration, Washington, D.C., Report NASA SP-3013.

Barrett, P.H., Bollinger, L.M., Cocconi, G., Eisenberg, Y., and Greisen, K. (1952). Interpretation of cosmic-ray measurements far underground. *Rev. Mod. Phys. 24*, 133–178.

Bartlett, D.T., and Creasey, F.L. (1977). Latent image fading in nuclear emulsions. *Phys. Med. Biol. 22*, 1187–1188.

Bathow, G., Clausen, U., Freytag, E., and Tesch, K. (1967a). Skyshine-Messungen und ihr Vergleich mit Abschätzungen aus der Diffusionstheorie. *Nukleonik 9*, 14–17.

Bathow, G., Freytag, E., and Tesch, K. (1967b). Measurements on 6.3 GeV electromagnetic cascades and cascade-produced neutrons. *Nucl. Phys. B2*, 669–689.

Bathow, G., Freytag, E., Köbberling, M., Tesch, K., and Kajikawa, R. (1970). Measurements of the longitudinal and lateral development of electromagnetic cascades in lead, copper and aluminum at 6 GeV. *Nucl. Phys. B20*, 592–602.

Baum, J.W., Woodcock, R.C., and Kuehner, A.V. (1969). Factors affecting pulse size in sealed tissue-equivalent counters. *In op. cit.* "Proceedings of the Second Int. Conference on Accelerator Dosimetry and Experience," Stanford Linear Accelerator Center, Nov. 5–7, 1969, USAEC, Washington, D.C. Report No. CON-691101, pp. 648–659.

Baum, J.W., Kuehner, A.V., and Chase, R.L. (1970). Dose equivalent meter designs based on tissue equivalent proportional counters. *Health Physics 19*, 813–824.

Beasley, J.W. (1959). "The Mean Fission-Fragment Range in Bismuth as Applied to Pulse-Type Ion Chambers." Lawrence Berkeley Laboratory Internal Report UCRL-8760.

Beck, H.L. (1970a). A new calculation of dose rates from high energy electrons and photons incident on 30 cm water slabs. *Nucl. Instrum. Methods 78*, 333–334.

Beck, H.L. (1970b). The influence of the density effect on electron-induced cascade showers in water and aluminum. *Nucl. Sci. Eng. 39*, 120–121.

Beck, H.L. (1971). Monte-Carlo calculations of electromagnetic shower transition effects. *Nucl. Instrum. Methods 91*, 525–531.

Beck, H.L., Lowder, W.M., and McLaughlin, J.E. (1971). In situ external environmental gamma-ray

measurements utilizing Ge(Li) and NaI(Tl) spectrometry and pressurized ionization chambers. *In* "Proc. Int. Symposium on Rapid Methods for Measurement of Radioactivity in the Environment," 5–9 July 1971, Neuherberg, International Atomic Energy Agency, Vienna, IAEA Report STI/PUB/289, pp. 499–513.

Becker, K. (1966). "Photographic Film Dosimetry." (The Focal Press, London and New York, 1961 in German; 1966 in English).

Becker, K. (1973). "Solid State Dosimetry." CRC Press, Cleveland, Ohio.

Bennett, G.W., Foelsche, H., Lazarus, D., Levine, G., Moore, W., Toohig, T., Thomas, R., and Kostoulas, J. (1971). Study of a uniform steel beam dump at 28 GeV. *IEEE Trans. Nucl. Sci. NS-18* (3) 776–777.

Bennett, G.W., Brown, H.N., Foelsche, H.W.J., Fox, J.D., Lazarus, D.M., and Levine, G.S. (1973). Particle distribution in a steel beam stop for 28 GeV protons. *Particle Accelerators 4*, 229–238.

Benton, E.V., Henke, R.P., and Tobias, C.A. (1973). Heavy particle radiography. *Science 182*, 474–476.

Berger, M.J., and Seltzer, S.M. (1964). "Tables of Energy Losses and Ranges of Electrons and Positrons." National Aeronautics and Space Administration, Washington, D.C., Report NASA-SP-3012.

Berger, M.J., and Seltzer, S.M. (1966). "Additional Stopping Power and Range Tables for Protons, Mesons and Electrons." National Aeronautics and Space Administration, Washington, D.C., Report NASA SP-3036.

Berger, M.J., and Seltzer, S.M. (1970). Bremsstrahlung and photoneutrons from thick tungsten and tantalum targets. *Phys. Rev. C2*, 621–631.

Berger, M.J., and Seltzer, S.M. (1982). "Stopping Powers and Ranges of Electrons and Positrons." National Bureau of Standards, Washington, D.C., Report NBSIR 82-2550.

Bertel, E., and de Séréville, B. (1971). Un programme de calcul de flux de muons dans les configurations réelles. *In op.cit.* CERN (1971b), 678–696.

Bertel, E., Freytag, E., de Séréville, B., and Wachsmuth, H. (1971). Shielding against Muons. Chapter 6 in "Radiation Problems Encountered in the Design of Multi-GeV Research Facilities." (K. Goebel, ed.) CERN Internal Report 71-21, p. 79–90.

Bertini, H.W. (1963). Low energy intranuclear cascade calculation. *Phys. Rev. 131*, 1801–1821. Erratum, *Phys. Rev. 138*, AB2 (1965).

Bertini, H.W. (1969). Intranuclear cascade calculations of the secondary nucleon spectra from nucleon-nucleus interactions in the energy range 340 to 2900 MeV and comparison with experiments. *Phys. Rev. 188*, 1711–1730.

Bethe, H.A., and Ashkin, J. (1963). Passage of radiations through matter. *In* "Experimental Nuclear Physics," Vol. 1 (E. Segrè, ed.), pp. 166–357. Wiley and Sons, New York.

Bewley, D.K., Cullen, B., Field, S.B., Hornsey, S., Page, B.C., and Berry, R.J. (1976). A comparison for use in radiotherapy of neutron beams generated with 16 and 42 MeV deuterons on beryllium. *Br. J. Radiol. 49*, 360–366.

Bichsel, H. (1968). Charged particle interactions. *In* "Radiation Dosimetry" (F.H. Attix and W.C. Roesch, eds.), Vol. I, pp. 157–228. Academic Press, New York.

Bichsel, H. (1972). Passage of charged particles through matter. *In* "American Institute of Physics

Handbook." 3rd Ed., Section (8d). McGraw Hill, New York, pp. 8-142 to 8-189.

Bichsel, H., and Porter, L. (1982). Stopping power of protons and alpha particles in H_2, He, N_2, O_2, CH_4 and air. *Phys. Rev. 25*, A2499–2510.

Birattari, C., and Salomone, A. (1985). Neutron spectrum measurements at a 40-MeV proton cyclotron. *Health Physics 49*, 919–936.

Biryukov, V. (1971). "Joint Institute for Nuclear Research." Progress, Moscow, 80 pp.

Blohm, R., and Harder, D. (1985). Restricted LET: Still a good parameter of radiation quality for electrons and photons. *Radiat. Prot. Dosim. 13*(1–6), 377–381.

Blumberg, L., and Perlman, M.L. (1980). "Maximum Credible Radiation Accident." NSLS Memo dated 15 May, 1980, National Synchrotron Light Source, Brookhaven National Laboratory, Upton, New York.

Boag, J.W. (1950). Ionization measurements at very high intensities. I. Pulsed radiation beams. *Brit. J. Radiol. 23*, 601–611.

Boag, J.W. (1952). The saturation curve for ionization measurements in pulsed radiation beams. *Brit. J. Radiol. 25*, 649–650.

Boag, J.W. (1966). Ionization Chambers. Chapter 9 in "Radiation Dosemetry, Vol. II, Instrumentation," pp. 2-72 (F.H. Attix and W.C. Roesch, eds.) Academic Press, New York.

Boag, J.W. (1987). Ionization dosimetry. Chapter 3 in Vol. II, "The Dosimetry of Ionizing Radiation." (K.R. Kase, B.E. Bjärngard and F.H. Attix, eds.) Academic Press, New York.

Bonet-Maury, P., Duhamel, M., and Perrin, F. (eds.) (1962). Proc. "Premier Colloque International sur la Protection auprès des Grands Accélérateurs." Paris, France, January 18–20, 1961, Presses Universitaires de France, 108 Bd. Saint-Germain, Paris.

Bonifas, A., Géroudet, J.M., Marchal, H., and Tuyn, J.W.N. (1974). "On the Use of Thermoluminescence Dosimetry for Stray Radiation Monitoring on the CERN Site." European Organization for Nuclear Research CERN, Geneva, Internal Report HA-74-138.

Borak, T.B. (1972a). "Measurement of Induced Radioactivity in Cooling Waters for the CERN PS and External Beam Magnets." European Organization for Nuclear Research CERN, Geneva, Internal Report HP-72-112.

Borak, T.B., Awschalom, M., Fairman, W., Iwami, F., and Sedlet, J. (1972b). The underground migration of radionuclides produced in soil near high energy proton accelerators. *Health Physics 23*, 679–687.

Bramblett, R.L., Ewing, R.I., and Bonner, T.W. (1960). A new type of neutron spectrometer. *Nucl. Instrum. Methods 9*, 1–12.

Brockmann, R., Keil, P., Knop, G., and Wucherer, P. (1971). Elektron-Photon-Kaskaden in Blei bei Primäenergien von 100, 200 und 400 MeV. *Z. Physik 243*, 464–479.

Brookhaven (1965). "Proc. Symposium on Accelerator Radiation Dosimetry and Experience." Held at Brookhaven National Laboratory, Nov. 3–5, 1965, U.S.A.E.C., Washington, D.C., Report CONF-691109.

Bruninx, E. (1961). "High-Energy Nuclear Reaction Cross Sections." Vol. 1, CERN Report CERN 61-1.

Bruninx, E. (1962). "High-Energy Nuclear Reaction Cross Sections." Vol. 2, CERN Report CERN 62-9.

Bruninx, E. (1964). "High-Energy Nuclear Reaction Cross Sections." Vol. 3, CERN Report CERN 64-17.

Burfeindt, H. (1967). "Monte-Carlo-Rechnung für 3-GeV-Schauer in Blei." Deutsches Elektronen-Synchrotron, Hamburg, F.R.G., Report DESY-67/24.

Burger, G., Schraube, H., and Morhardt, A. (nd). Neutron dosimetry for radiation protection. *In* "The Dosimetry of Ionizing Radiation." Vol. III (Eds. K.R. Kase, B.E. Bjärngard and F.H. Attix), Academic Press, New York (in preparation).

Burlin, T.E. (1968), Cavity chamber theory. *In* "Radiation Dosimetry" (F.H. Attix and W.C. Roesch, eds), Vol. 1, Academic Press, New York, pp. 331–392.

Burn, K., Fassò, A., Goebel, K., Höfert, M., Janssens, J., Schönbacher, H., and Ye Sizong (1982). "Dose Estimations for the LEP Main Ring." European Organization for Nuclear Research CERN, Geneva, Reports HS-RP/071 and LEP-348.

Burrus, W.A. (1962). "Bonner Spheres and Threshold Detectors for Neutron Spectroscopy." Oak Ridge National Laboratory Neutron Physics Division Annual Report for Period ending September 1, 1962, Report ORNL-3360, pp. 296–305.

Busick, D.D. (1978). Stanford Linear Accelerator Center. Private communication.

Busick, D.D., and Warren, G.J. (1969). Operational health physics associated with induced radioactivity at the Stanford Linear Accelerator Center. *In* "Proc. II Int. Conf. on Accelerator Dosimetry and Experience," Stanford, November 1969, USAEC Report CONF-691101, p. 139–145.

Busick, D.D., Jenkins, T.M., and Swanson, W.P. (1975). Personnel neutron dosimetry at SLAC. *In* "Proc. 5th ERDA Workshop on Personnel Neutron Dosimetry," held in Washington, D.C., May 6–7, 1975, Battelle Northwest Laboratories, Report BNWL-1934, p. 60–63.

Butcher, J.C., and Messel, H. (1960). Electron number distribution in electron-photon showers in air and aluminum absorbers. *Nucl. Phys. 20*, 15–128.

Cameron, J.R., Suntharalingam, N., and Kenney, G.N. (1968). "Thermoluminescent Dosimetry." University of Wisconsin Press, Madison, Wisconsin.

Cannata, A., Esposito, A., Merolli, S., and Pelliccioni, M. (1983). Synchrotron radiation beams dosimetry by TFD. *Nucl. Instrum. Methods 204*, 549–552.

Cantril, S.T., and Parker, H.M. (1945). "The Tolerance Dose." US Atomic Energy Commission Report MDDC-1100 (Technical Information Division, Atomic Energy Commission, Oak Ridge, Tennessee).

Capone, T., Baarli, J., Charalambus, S., Dutrannois, J., Freeman, J.Y., Goebel, K., Middelkoop, W.C., Overton, T.R., Rindi, A., and Sullivan, A.H. (1965). "A Radiation Survey Inside and Outside the CPS Tunnel." CERN Internal Report DI/HP/71.

Carlsson, G.A. (1986). Theoretical basis for dosimetry. Chapter 1 in Vol. I, pp. 1–75, "The Dosimetry of Ionizing Radiation." (K.R. Kase, B. Bjärngard, and F.H. Attix, eds.) Academic Press, New York.

Carter, T.G., Chakalian, V.M., and Thomas, R.H. (1970). "Stanford Mark I Moderator Calibration Using Tantalum." Stanford University Internal Report RHT/TN/70-2.

CEBAF (1986). "CEBAF Conceptual Design Report." Continuous Electron Beam Accelerator Facility, Southeastern Universities Research Association, Newport News, Virginia.

CEBAF (1987). "CEBAF Workshop on Radiation Safety." Swanson, W.P. (Chm.), Cossairt, J.D., Crook, K., Höfert, M., Jenkins, T.M., Johnson, C.D., Lee, D.W., McCaslin, J.B., McGee, R.P., Page, L.P., Reed, L., Stapleton, G.B., and Tesch, K., Continuous Electron Beam Accelerator Facility, Newport News, VA. (Revised April 1987)

CERN (1971a). "Proc. 8th Int. Conf. on High Energy Accelerators CERN 1971." Geneva, Sept. 20–24, 1971 (M. H. Blewett and N. Vogt-Nilsen, eds.), European Organization for Nuclear Research CERN, Geneva.

CERN (1971b). "Proc. Int. Congress on Protection Against Accelerator and Space Radiation," Geneva, April 26–30, 1971, European Organization for Nuclear Research CERN, Geneva, Report 71-16.

CERN (1971c). "Radiation Problems Encountered in the Design of Multi-GeV Research Facilities." Laboratory II, European Organization for Nuclear Research CERN, Geneva, Report 71-21.

CERN (1972). "Le Programme 300 GeV." European Organization for Nuclear Research CERN, Geneva, Report CERN/1050.

CERN (1977). Theoretical aspects of the behaviour of beams in accelerators and storage rings. *In* "Proc. First Course of the International School of Particle Accelerators of the Ettore-Majorana Centre for Scientific Culture," Erice, 10–22 Nov., 1976 (M.H. Blewett, ed.). European Organization for Nuclear Research CERN, Geneva, Report CERN 77-13.

CERN (1985). "Proceedings of the CERN Accelerator School," Gif-sur-Yvette, Paris, 3–14 September, 1984 (P. Bryant and S. Turner, eds.). European Organization for Nuclear Research CERN, Geneva. Report CERN 85-19 (2 vols.).

Chambless, D.A., and Broadway, J.A. (1983). Comments on 'Neutron spectral unfolding using the Monte Carlo method.' *Nucl. Instrum. Methods 214*, 543-545.

Chandler, K.C., and Armstrong, T.W. (1972). "Operating Instructions for the High-Energy Nucleon-Meson Transport Code HETC." Oak Ridge National Laboratory Report ORNL-4744.

Chapman, G., Gröbner, O., Linser, G., Perry, T., and Schmidlin, G. (1983). Synchrotron radiation lead shielding in the vacuum chambers for LEP. *In op. cit. IEEE Trans. Nucl. Sci. NS-30*, 2340–2342.

Charalambus, St., and Rindi, A. (1967). Aerosol and dust radioactivity in the halls of high-energy accelerators. *Nucl. Instrum. Methods 56*, 125–135.

Childers, R.L., Zerby, C.D., Fisher, C.M., and Thomas, R.H. (1965). Measurement of the nuclear cascade at 10 GeV/c with emulsions. *Nucl. Instrum. Methods. 32*, 53–56.

Christensen, G.C., Fassò, A., and Stevenson, G.R. (1978). "Radioactivity in the Cooling Water from the NAHIF Installation." CERN Internal Report HS-RP/IR/78-46.

Cioni, G., and Treves, A. (1969). A simplified method of simulating electromagnetic showers. *Nuovo Cimento 62B*, 371–378.

Citron, A., Hoffmann, L., and Passow, C. (1961). Investigation of the nuclear cascade in shielding materials. *Nucl. Instrum. Methods 14*, 97–100.

Citron, A., Hoffmann, L., Passow, C., Nelson, W.R., and Whitehead, M. (1965). A study of the nuclear cascade in steel initiated by 19.2 GeV/c protons. *Nucl. Instrum. Methods. 32*, 48–52.

Clément, G., and Kessler, P. (1965). Electroproduction de muons de très haute énergie. *Nuovo Cimento 37*, 876–887.

Cockcroft, J.D., and Walton, E.T.S. (1932a). Experiments with high velocity positive ions. I: Further developments in the method of obtaining high velocity positive ions. *Proc. Roy, Soc.* (London) *A136*, 619–630.

Cockcroft, J.D., and Walton, E.T.S. (1932b). Experiments with high velocity positive ions. II: The disintegration of elements by high velocity protons. *In Proc. Roy. Soc.* (London) *A137*, 229–242.

Cockcroft, J.D., and Walton, E.T.S. (1934). Experiments with high velocity positive ions. III: The disintegration of lithium, boron and carbon by heavy hydrogen ions. *In Proc. Roy. Soc.* (London) *A144*, 704–720.

Coleman, W.A. (1968). "Thermal-Neutron Flux Generation by High-Energy Protons." Oak Ridge National Laboratory Report ORNL-TM-2206.

Cosack, M., and Lesiecki, H. (1981). Dependence of the response of eight neutron dose equivalent survey meters with regard to the energy and direction of incident neutrons. *In* "Proc. Fourth Symposium on Neutron Dosimetry," Munich-Neuherberg, 1–5 June, 1981. Commission of the European Communities, Luxembourg, Report EUR-7448, pp. 407–420.

Cossairt, J.D. (1983). Recent muon fluence measurements at Fermilab. *Health Physics 45*, 651–658.

Cossairt, J.D. (1987). Shielding design at Fermilab; calculations and measurements. *In* "Proc. of the 20th Midyear Topical Meeting of the Health Physics Society on the Health Physics of Radiation Generating Machines," 8–12 Feb. 1987, Reno, Nevada (D.D. Busick and W.P. Swanson, eds.), pp. 642–658.

Cossairt, J.D., and Coulson, L.V. (1985). Neutron skyshine measurements at Fermilab. *Health Physics 48*, 175–181.

Cossairt, J.D., and Elwyn, A.J. (1987). Personal dosimetry in a mixed field of high-energy muons and neutrons.
Health Physics 52, 813–818. Fermi National Accelerator Laboratory, Batavia, Illinois, Report FN-431.

Cossairt, J.D., Butala, S.W., and Gerardi, M.A. (1985a). Absorbed dose measurements at an 800 GeV proton accelerator; comparison with Monte-Carlo calculations. *Nucl. Instrum. Methods Phys. Res. A238*, 504–508. Fermi National Accelerator Laboratory, Batavia, Illinois, Report FN-414.

Cossairt, J.D., Couch, J.G., Elwyn, A.J., and Freeman, W.S. (1985b). Radiation measurements in a labyrinth penetration at a high energy proton accelerator. *Health Physics 49*, 907–917.

Cossairt, J.D., Grobe, D.W., and Gerardi, M. (1984). "Measurements of Radiation Quality Factors Using a Recombination Chamber." Fermi National Accelerator Laboratory, Batavia, Illinois, Report TM-1248.

Cowan, F.P. (1962). A preliminary report on health physics problems at the Brookhaven Alternating Gradient Synchrotron. *In op. cit.* Bonet-Maury *et al.* (1962), pp. 143–146.

Crandall, W.E., Millburn, G.P., and Schechter, L. (1957). Neutron yields from thick targets bombarded by 24-MeV deuterons and 12-MeV protons. *J. App. Phys. 28*, 273–276.

Crawford, D.F., and Messel, H. (1962). Energy distribution in low energy electron-photon showers in lead absorbers. *Phys. Rev. 128*, 2352–2360.

Crawford, D.F., and Messel, H. (1965). The electron-photon cascade in lead, emulsion and copper absorbers. *Nucl. Phys. 61*, 145–172.

Cross, W.G. (1986). Characteristics of track detectors for personnel neutron dosimetry. *In* "Proc. 13th Int.

Conference on Solid State Nuclear Track Detectors," Rome, 23–27 Sept., 1985 (L. Tommasino, G. Baroni and G. Campos-Venuti, eds.), *Nucl. Tracks Radiat. Measurements 12*, 533–542.

Cross, W.G., and Ing, H. (1984). Overview of neutron dosimetry in Canada. *In* "Tenth DOE Workshop on Personnel Neutron Dosimetry." Acapulco, August 30–Sept. 1, 1983, Pacific Northwest Laboratory, Battelle Memorial Institute, Richland, Washington, Report CONF-8308140, PNL-SA-12352, pp. 13–28.

Cross, W.G., and Ing, H. (1987). Neutron Spectra. *In* "The Dosimetry of Ionizing Radiation." K.R. Kase, B.E. Bjärngard and F.H. Attix, eds., Vol. II, Ch. 2, Academic Press, New York, NY.

Cross, W.G., Arneja, A., and Ing, H. (1986). The response of electrochemically-etched CR-39 to protons of 10 keV to 3 MeV. *In* "Proc. 13th Int. Conference on Solid State Nuclear Track Detectors," Rome, 23–27 Sept., 1985 (L. Tommasino, G. Baroni and G. Campos-Venuti, eds.), *Nucl. Tracks Radiat. Measurements 12*, 649–652.

Cross, W.G., and Tommasino, L. (1972). Improvements in the spark counting technique for damage track neutron dosimeters. *In* "Proceedings of the First Symposium on Neutron Dosimetry in Biology and Medicine," Munich, 15–19 May, 1972 (G. Burger, H. Schraube and H.G. Ebert, eds.), Vol. I, pp. 283–301, Commission of the European Communities, Luxembourg, Report EUR-4896.

de Campo, J.A., Beck, H.L., and Raft, P.D. (1972). "High Pressure Argon Ionization Chamber Systems for the Measurement of Environmental Radiation Exposure Rates." Health and Safety Laboratory, USAEC, New York, Report HASL-260.

de Carvalho, H.G., Cortini, G., Muchnik, M., Potenza, G., Rinzivillo, R., and Lock, W.O. (1963). Fission of uranium, thorium, and bismuth by 20-GeV protons. *Nuovo Cimento 27*, 468–474.

DeLuca, P.M., Jr., Otte, R.A., Swanson, W.P., Schilthelm, S.W., and Rogers, G. (1987). Radiation measurements at Aladdin, a 1-GeV electron storage ring. *In* "Proceedings of the 20th Midyear Topical Meeting on Health Physics of Radiation Generating Machines" (D.D. Busick and W.P. Swanson, eds.) held in Reno, Nevada, 8–12 Feb., 1987, pp. 486–494.

Dennis, J.A. (1983). Biological effects of neutron radiation and their implications for the nuclear power industry. *Nucl. Energy. 22*(2), 87–93.

Dennis, J.A., and Dunster, H.J. (1985). Radiation quality and radiation protection: Implications of changes in quality factors. *Radiat. Prot. Dosim. 13*(1–4), 327–334.

DePanger, J., and Nichols, L.L. (1966). "A Precision Long Counter for Measuring Fast Neutron Flux Density." Battelle Memorial Institute, Pacific Northwest Laboratory, Richland, Washington, Report BNWL-260.

de Planque-Burke, G. (1975a). Thermoluminescent dosimeter measurements of perturbations of the natural radiation environment. *In* "Proc. Second International Symposium on the Natural Radiation Environment," Vol. II, USAEC Symposium Series CONF-720805-P-1, pp. 305–315.

de Planque-Burke, G. (1975b). "Variations in Natural Environmental Gamma Radiation and its Effect on the Interpretability of TLD Measurements Made near Nuclear Facilities." Health and Safety Laboratory, New York, USERDA Report HASL-289.

de Planque-Burke, G., and O'Brien, K. (1974). "Operating Manual for GRANIA, a Code for the Analysis of Climatic Effects on Natural Environmental Gamma Ray Exposure Rates." Health and Safety Laboratory, New York, USAEC Report HASL-283.

DeStaebler, H. (1965). Similarity of shielding problems at electron and proton accelerators. *In* "Proc. Symp. on Accelerator Dosimetry and Experience," Brookhaven, November 1965, USAEC Report

651109, p. 429–441.

DeStaebler, H., Jenkins, T.M., and Nelson, W.R. (1968). Shielding and radiation. *In* "The Stanford Two-Mile Accelerator," (R.B. Neal, ed.) Ch. 26 (Benjamin, New York), pp. 1029–1067.

Dinter, H. (1982). "Synchrotron Radiation in the PETRA Tunnel for Beam Energies up to 30 GeV." Deutsches Elektronen-Synchrotron DESY, Hamburg, F.R.G., Report D03-42.

Dinter, H. (1983). "Strahlungsdosen im HERA-Tunnel durch Synchrotronstrahlung." Deutsches Elektronen-Synchrotron DESY, Hamburg, F.R.G., Report DESY D3-47.

Dinter, H. (1984). "Synchrotron Radiation in the PETRA Tunnel." Deutsches Elektronen-Synchrotron DESY, Hamburg, F.R.G., Report DESY D3-52.

Dinter, H. (1985a). Absorbed doses due to synchrotron radiation in the tunnel of the storage ring PETRA. *Nucl. Instrum. Methods Phys. Res. A239*, 597–604.

Dinter, H. (1985b). "Synchrotronstrahlung im HERA Tunnel." Deutsches Elektronen-Synchrotron, DESY, Hamburg, F.R.G., Report DESY D3-56.

Dinter, H., and Tesch, K. (1976). "Moderated Rem Meters in Pulsed Neutron Fields." Deutsches Elektronen-Synchrotron, DESY, Hamburg, F.R.G., Report DESY-76/08.

Dinter, H., and Tesch, K. (1977). Dose and shielding parameters of electron-photon stray radiation from a high-energy electron beam. *Nucl. Instrum. Methods 143*, 349–355.

Dinter, H., Tesch, K., and Yamaguchi, C. (1982). Absorbed radiation dose due to synchrotron radiation in the storage ring PETRA. *Nucl. Instrum. Methods 200*, 437–442.

Dinter, H., Pang, J., and Tesch, K. (1988). "Calculations of Doses due to Electron-Photon Stray Radiation from a High-Energy Electron Beam behind Lateral Shielding." Deutsches Elektronen-Synchrotron DESY, Hamburg, F.R.G., Report DESY-88-117.

Distenfeld, C. (1964). Modifications required by high intensity: Shielding. *In* "A Proposal for Increasing the Intensity of the Alternating-Gradient Synchrotron at the Brookhaven National Laboratory." Brookhaven National Laboratory, Report BNL-7956, May, 1964.

Distenfeld, C.H. (1975). "Improvements and Tests of the Bonner Sphere Multisphere Spectrometer." Brookhaven National Laboratory Report BNL-21292.

Distenfeld, C.H., and Colvett, R.D. (1966). Skyshine considerations for accelerator shielding design. *Nucl. Sci. Eng. 26*, 117–121.

Distenfeld, C.H., and Markoe, A.M. (1965). Determination of quality factor through the utilization of a balanced, tissue-equivalent, ionization chamber. *In* "Proceedings of First Symposium on Accelerator Dosimetry and Experience," Brookhaven, November 1965, USAEC Report CONF-651109, p. 181–198.

Draper, E.L., Jr. (1971). Integral reaction rate determinations - Part I. *Nucl. Sci. Eng. 46*, 22–30. [Program SAND].

Edwards, H.T. (1985). The Tevatron Energy Doubler. *Ann. Rev. Nucl. Part. Sci. 35*, 605–660 (Annual Reviews, Inc., Palo Alto, CA).

Eisenbud, M. (1987). "Environmental Radioactivity from Natural, Industrial and Military Sources." 3rd ed., Academic Press, New York, NY.

Eisenhauer, C.M., Schwartz, R.B., and Johnson, T. (1982). Measurement of neutrons reflected from the surface of a calibration room. *Health Physics 42*, 489–495.

Elwyn, A.J., and Cossairt, J.D. (1986). A study of neutron leakage through an Fe shield at an accelerator. *Health Physics 51*, 723–735.

Elwyn, A.J., and Cossairt, J.D. (1987). Neutron leakage through an iron shield at a high energy accelerator. *In* "Health Physics of Radiation Generating Machines—Proc. 20th Mid-Year Topical Symposium of the Health Physics Society," Reno, Nevada, Feb. 8–12, 1987, CONF-8602106, Eds. D.D. Busick and W.P. Swanson, pp. 424–431.

Elwyn, A.J., and Freeman, W.S. (1984). "Muon Fluence Measurements at 800 GeV." Fermi National Accelerator Laboratory, Batavia, Illinois, Report TM-1288.

Emery (1966). "Radiation Dosimetry," Vol. II, Chapter 10, Attix, Roesch, and Toshilin eds., Academic Press, New York.

Esposito, A., and Pelliccioni, M. (1982). Radiation protection problems at a synchrotron radiation facility. *Health Physics 42*, 703–711.

Esposito, A., and Pelliccioni, M. (1986). "Gas Bremsstrahlung Production in the Adone Storage Ring." Instituto Nazionale di Fisica Nucleare, Laboratori Nazionali di Frascati, Report LNF-86/23(NT).

Esposito, A., Pelliccioni, M., and Rindi, A. (1978). "Radiation Doses at an Electron and Positron Linac and Storage Ring." INFN, Laboratori Nazionali di Frascati, Report LNF-78/39(R).

Eyges, L. (1948). Multiple scattering with energy loss. *Phys. Rev. 74*, 1534–1535.

Failla, G., and Rossi, H.H. (1950). Dosimetry of Ionizing Particles. *Am. J. Roent. Radium Therapy 64*, 489–491.

Fassò, A., Goebel, K., Höfert, M., Rau, G., Schönbacher, H., Stevenson, G.R., Swanson, W.P., and Tuyn, J.W.N. (1984). "Radiation Problems in the Design of the Large Electron-Positron Collider (LEP)." European Organization for Nuclear Research, Technical Inspection and Safety Commission, Report CERN 84-02.

Fermi, E., Amaldi, E., D'Agostino, O., Rosetti, F., and Segrè, E. (1934). Artificial radioactivity produced by neutron bombardment. *In Proc. Roy. Soc. A 146*, 483–500.

Fleischer, R.L., Price, P.B., and Walker, R.M. (1963). Method of forming fine holes of near atomic dimensions. *Rev. Sci. Instrum. 34*, 510–512.

Fleischer, R.L., Price, P.B., and Walker, R.M. (1965). Tracks of charged particles in solids. *Science 149*, 383–393.

Fleischer, R.L., Price, P.B., and Walker, R.M. (1975). "Nuclear Tracks in Solids: Principles and Applications." Univ. of California Press, Berkeley, California.

FNAL (1982). "Physics of High Energy Particle Accelerators." Fermilab Summer School, 1981 (R.A. Carrigan, F.R. Huson, and M. Month, eds.), AIP Conference Proceedings, No. 87, American Institute of Physics, New York.

FNAL (1983a). "Physics of High Energy Particle Accelerators." SLAC Summer School, 1982 (M. Month, ed.), AIP Conference Proceedings, No. 105, American Institute of Physics, New York.

FNAL (1983b). "Proceedings of the 12th Int. Conf. on High-Energy Accelerators," Fermilab, August 11–16, 1983 (F. T. Cole and R. Donaldson, eds.) Fermi National Accelerator Laboratory, Batavia,

Illinois.

FNAL (1985). "Physics of High Energy Particle Accelerators." BNL/SUNY Summer School, 1983 (M. Month, P.F. Dahl, and M. Dienes, eds.), AIP Conference Proceedings, No. 127, American Institute of Physics, New York.

Ford, R.L., and Nelson, W.R. (1978). "EGS Code System: Computer Programs for the Monte-Carlo Simulation of Electromagnetic Cascade Showers." Stanford Linear Accelerator Center, Report SLAC-210.

French, R.L., and Mooney, L.G. (1971). Differential measurements of fast-neutron air-ground interface effects. *Nucl. Sci. Eng. 43*, 273–280.

Freytag, E. (1968). Halbwertszeiten der Aktiverung bei Beschleunigern. *Health Physics 14*, 267–269.

Gabriel, T.A. (1985). The high energy transport code HETC. Presented at the CERN Workshop on Shower Simulation for LEP Experiments, Jan. 29–31, 1985, Oak Ridge National Laboratory Report ORNL-TM-9727.

Gabriel, T.A., and Alsmiller, R.G., Jr. (1969). "Photonucleon and Photopion Production from High-energy (50–400 MeV) Electrons in Thick Copper Targets." Oak Ridge National Laboratory Report ORNL-4443-UC34.

Gabriel, T.A., and Bishop, B.L. (1978). Calculated hadronic transmission through iron absorbers. *Nucl. Instrum. Methods 155*, 81–92.

Gabriel, T.A., and Santoro, R.T. (1971). Calculation of the long-lived activity in soil produced by 500-GeV protons. *Nucl. Instrum. Methods 95*, 275–283.

Gabriel, T.A., and Santoro, R.T. (1973). Photon dose rates for the interaction of 200 GeV protons in iron and iron-lead beam stops. *Particle Accelerators 4*, 169–186.

Gabriel, T.A., Alsmiller, R.G., Jr., and Guthrie, M.P. (1970). "An extrapolation method for predicting nucleon and pion differential production cross sections from high-energy (>3 GeV) nucleon-nucleus collisions." Oak Ridge National Laboratory Report ORNL-4542.

GANIL (1986). "GANIL, 1972–1982, Conception et Realisation." Grand Accélérateur National d'Ions Lourds, Caen, France.

Gilbert, W.S., Keefe, D., McCaslin, J.B., Patterson, H.W., Smith, A.R., Stephens, L.D., Shaw, K.B., Stevenson, G.R., Thomas, R.H., Fortune, R.D., and Goebel, K. (1968). "1966 CERN-LRL-RHEL Shielding Experiment at the CERN Proton Synchrotron." Lawrence Berkeley Laboratory Report UCRL-19741.

Goebel, K. (ed.) (1985). "Radiation Protection Group Annual Report (1984)." European Organization for Nuclear Research CERN, Geneva, Report TIS-RP/146.

Goebel, K., and Ranft, J. (1970). "Radiation Measurements around a Beam Stopper Irradiated by 19.2 GeV/c Protons, and Neutron Energy Spectra from Monte Carlo Nucleon-Meson Cascade Calculations." European Organization for Nuclear Research CERN, Geneva, Report CERN 70-16.

Golde, A., and Warren, G.J. (1980). Experimental enclosures for synchrotron radiation: Design considerations. *Nucl. Instrum. Methods 172*, 375–378.

Gollon, P.J., Awschalom, M., Baker, S.I., Coulson, L., Moore, C., and Velen, S. (1981). Measurements of radial and longitudinal hadron shower development at 300 GeV. *Nucl. Instrum. Methods 189*, 387–394.

Goodman, L.J., and Rossi, H.H. (1968). The measurement of dose equivalent using paired ionization chamber. *Health Physics 14*, 168–170.

Gray, L.H. (1936). An ionization method for the absolute measurement of gamma-ray energy. *Proc. Roy. Soc.* (London) *A156*, 578–596.

Gray, L.H. (1937). Radiation dosimetry. *Brit. J. Radiol. 10*, Part I: pp. 600–612 and Part II: pp. 721–742.

Green, D., Fenker, H., Martin, P., Takasaki, M., Yamada, R., Kunori, S., Rapp, P., Owen, D., Grannis, P., and Hedin, D. (1986). Hadron showers and muon trajectories in thick absorber from 25 to 150 GeV/c. *Nucl. Instrum. Methods Phys. Res. A244*, 356–366.

Green, G.K. (1976). "Spectra and Optics of Synchrotron Radiation." Brookhaven National Laboratory, Upton, New York, Report 50522.

Greenhouse, N.A. (1988). Lawrence Berkeley Laboratory. Private communication.

Greenhouse, N.A., de Castro, T.M., McCaslin, J.B., Smith, A.R., Sun, R.-K., and Hankins, D.E. (1987). An evaluation of NTA film in an accelerator environment and comparisons. *Radiat. Prot. Dosim. 20*, 143–147.

Greenhouse, N.A., Busick, D.D., de Castro, T.M., Elwyn, A.J., Hankins, D.E., Ipe, N.E., La Plant, P.R., McCaslin, J.B., Renner, T.R., Smith, A.R., Sun, R-K.S., and Swanson, W.P. (1988), "Field Characterization and Personal Dosimetry at a High-Energy Ion Accelerator." Lawrence Berkeley Laboratory Report LBL-24941.

Griffith, R.V. (1987). Personnel dosimetry developments. *In* "Summary and Minutes of DOE Accelerator Contractor's Planning Meeting on Accelerator Health Physics Research Needs," Reno, Nevada, February 12, 1987 (L. Coulson, ed.), Fermi National Accelerator Laboratory, Batavia, Illinois.

Griffith, R.V., and Fisher, J.C. (1976). "Measurement of the Responses of Multisphere Detectors with Monoenergetic Neutrons, 0.1 to 18.5 MeV." Lawrence Livermore National Laboratory, Hazards Control Department Report No. 55, UCRL-50007-75-2, pp. 219–233.

Griffith, R.V., McMahon, T.A., and Espinosa, G. (1984). A commercial bacterial colony counter for semiautomatic track counting. *In* "Proc. 12th Int. Conference on Solid State Nuclear Track Detectors," Acapulco, 4–10 Sept. 1983 (G. Espinosa, R.V. Griffith, L. Tommasino, S.A. Durrani, and E.V. Benton, eds.), *Nucl. Tracks Radiat. Measurements 8*(1-4), 215–218.

Griffith, R.V., and Tommasino, L. (nd). Etch track detectors. *In* "Dosimetry of Ionizing Radiation." Vol III. (K.R. Kase, B.E. Bjärngard and F.H. Attix, eds.), Academic Press, New York [this volume; in preparation].

Groom, D.E. (1986). Superconducting Super Collider, Central Design Group, Berkeley, California. Private communication.

GSI (1984). Proceedings of the 1984 Linear Accelerator Conference, Seeheim, F.R.G., May 7–11, 1984 (N. Angert, ed.), Gesellschaft für Schwerionenforschung, Darmstadt, F.R.G, Report GSI-84-11.

Guthrie, M.P. (1970). "EVAP-4: Another Modification of a Code to Calculate Particle Evaporation from Excited Compound Nuclei." Oak Ridge National Laboratory Report ORNL-TM-3119.

Hack, R.C. (1969). "Radiation Protection Group (Operations) Progress Report for 1968." Rutherford Laboratory Report RHEL/M 171.

Hack, R.C. (1971). "Personal Fast-Neutron Dosimetry Around Nimrod." Rutherford Laboratory Report RHEL/MR8.

Hajnal, F., Awschalom, M., Bennett, B.G., McLaughlin, J.E., O'Brien, K., Raft, P.D., and Schimmerling, W. (1969). A study of the neutron cascade in iron. *Nucl. Instrum. Methods 69*, 245–253.

Hankins, D.E. (1978). A modified A-B remmeter with improved directional dependence and thermal neutron sensitivity. *Health Physics 34*, 249–254.

Hankins, D.E. (1987). Hazards Control Department, Lawrence Livermore National Laboratory. Private communication.

Hankins, D.E., and Cortez, J.R. (1975). Energy dependence of four neutron remmeter instruments. *Health Physics 28*, 305–307.

Hankins, D.E., Homann, S.G., and Davis, J. (1984). Use of CR-39 foils for personnel neutron dosimetry: New electrochemical etching chambers and procedures. *In* "Annual Technology Review 1984," (R.V. Griffith and K.J. Anderson, eds.), Hazards Control Department, Lawrence Livermore National Laboratory Report UCRL 50007-84, pp. 11–19.

Hankins, D.E., Homann, S.G., and Westermark, J. (1985). Use of CR-39 foils for personnel neutron dosimetry: Improved electrochemical etching chambers and procedures. *In* "Annual Technology Review 1985," (R.V. Griffith and K.J. Anderson, eds.), Hazards Control Department, Lawrence Livermore National Laboratory Report UCRL 50007-85, pp. 79–87.

Hankins, D.E., Homann, S.G., and Westermark, J. (1986). "Personnel Neutron Dosimetry Using Electrochemical Etched CR-39 Foils." Hazards Control Department, Lawrence Livermore National Laboratory Report UCRL 95350.

Hanson, A.O., and McKibben, J.L. (1947). A neutron detector having uniform sensitivity from 10 keV to 3 MeV. *Phys. Rev. 72*, 673–677.

Harrison, K.G., and Tommasino, L. (1985). Damage track detectors for neutron dosimetry: II. Characteristics of different detection systems. *Radiat. Prot. Dosim. 10* (1-4), 219–235.

Hayman, P.J., Palmer, N.S., and Wolfendale, A.W. (1963). The rate of energy loss of high-energy cosmic ray muons. *Proc. Royal Soc.* (London) *275A*, 391–410.

Haywood, F.F., Auxier, J.A., and E.T. Loy (1964). "An Experimental Investigation of the Spatial Distribution of Dose in an Air-Over-Ground Geometry." Oak Ridge National Laboratory, USAEC Report CEX 62-14.

Haywood, F.F., Provenzano, T.G., and Auxier, J.A. (1965). "Operations Plan — HENRE." Oak Ridge National Laboratory, USAEC Report CEX-65.03.

Health Physics Society (1987). Health physics of radiation generating machines. *In* "Proceedings of the 20th Midyear Topical Symposium of the Health Physics Society," Reno, Nevada, 8–12 February, 1987 (D.D. Busick and W.P. Swanson, eds.). Available from D.D. Busick, Stanford Linear Accelerator Center, Stanford, CA 94305.

Heijne, E.H.M. (1983). "Muon Flux Measurement with Silicon Detectors in the CERN Neutrino Beams." European Organization for Nuclear Research CERN, Geneva, Report CERN 83-06.

Heitler, W. (1954). "The Quantum Theory of Radiation." Oxford University Press, Oxford.

Henson, A.M., and Thomas, R.H. (1978). Measurement of the efficiency of ^{7}LiF thermoluminescent dosimeters to heavy ions. *Health Physics 34*, 389–390.

Herminghaus, H. (1984). Survey on cw electron accelerators. *In op. cit.* GSI (1984), pp. 275–281.

Hess, W.N., Patterson, H.W., and Wallace, R. (1957). Delay-line chamber has large area, low capacitance. *Nucleonics 15*(3), 74–79.

Hess, W.N., Patterson, H.W., Wallace, R., and Chupp, E.L. (1959). Cosmic-ray neutron energy spectrum. *Phys. Rev. 116*, 445–457.

Hewitt, J.E., Hughes, L., McCaslin, J.B., Smith, A.R., Stephens, L.D., Syvertson, C.A., Thomas, R.H., and Tucker, A.B. (1980). Exposure to cosmic ray neutrons at commercial jet aircraft altitudes. *In* "Natural Radiation Environment III", Vol. 2, pp. 855–881, Proceedings of a Symposium held at Houston, Texas, April 23–28, 1978, T.F. Gesell and W.M. Lowder, eds., U.S. Dept. of Energy, Washington, D.C., Report CONF-780422 (Vol. 2).

Hirayama, H., Ban, S., and Miura, S. (1987). Investigations of electromagnetic cascades produced in lead by 2.5-GeV bremsstrahlung. *Nucl. Sci. Eng. 96*, 66–72.

Höfert, M. (1969). Radiation hazards of induced radioactivity in air as produced by high-energy accelerators. *In* "Proc. Second. International Conference on Accelerator Dosimetry and Experience," Stanford, California, USAEC Report CONF-691101, pp. 111–120.

Höfert, M. (1980). European Organization for Nuclear Research CERN, Geneva. Private communication as quoted by Tesch and Dinter (1986).

Höfert, M. (1984a). The NTA emulsion: An ill-reputed but misjudged neutron detector. *In* "Proceedings of the 10th DOE Workshop on Personnel Neutron Dosimetry," Acapulco, 30 Aug.–1 Sept., 1983. Battelle Pacific Northwest Laboratory Report PNL-SA-12352 (CONF-8308140), pp. 107–121. Also European Organization for Nuclear Research CERN, Geneva, Report TIX-RP/110/CF.

Höfert, M. (1984b). "Muons and Exposure Dose." CERN Internal Report TIS-RP/IR/84-23.

Höfert, M. (1987). Dosimeter response to muons. *Radiat. Prot. Dosim. 20*, 149–154.

Höfert, M., and Baarli, J. (1974). Some preliminary investigations on the contribution of muons to the stray radiation level around the CERN 28 GeV Proton Synchrotron. *In* "Proc. Third Int. Congress of IRPA," September 9–14, 1973 (W.S. Snyder, ed.), Washington D.C. USAEC Report CONF-730907-P1, Washington, D.C., Part II. pp. 841–845.

Höfert, M., and Piesch, E. (1985). Neutron dosimetry with nuclear emulsions. *In op. cit.* Ing, H., and Piesch, E., eds. Neutron dosimetry. *Radiat. Prot. Dosim. 10* (1-4), 189–195.

Höfert, M., and Raffnsøe, C. (1980). Measurement of absolute absorbed dose and dose-equivalent response for instruments used around high-energy proton accelerators. *Nucl. Instrum. Methods 176*, 443–448.

Höfert, M., and Stevenson, G.R. (1984). Dose equivalent measurements around GeV accelerators. *Radiat. Prot. Dosim. 9*, 235–239.

Höfert, M., Bartlett, D.T., and Piesch, E. (1987). Personnel neutron monitoring around high energy accelerators. *Radiat. Prot. Dosim. 20*, 103–108.

Holt, P.D. (1985). Passive detectors for neutron fluence measurement. *Radiat. Prot. Dosim. 10*(1–4), 251–264.

Hoyer, F.E. (1968). "Induced Radioactivity in the Earth Shielding on Top of High-Energy Particle Accelerators." European Organization for Nuclear Research CERN, Geneva, Report CERN 68-42.

Hubbell, J.H. (1969). "Photon Cross Sections, Attenuation Coefficients, and Energy Absorption Coefficients from 10 keV to 100 GeV." U.S. National Bureau of Standards, Washington, D.C., Publication

No. NSRDS-NBS 29.

Hubbell, J.H. (1977). Photon mass attenuation and mass energy-absorption coefficients for H, C, N, O, Ar and seven mixtures from 0.1 keV to 20 MeV. *Radiat. Res. 70*, 58–81.

Hubbell, J.H. (1982). Photon mass attenuation and energy-absorption coefficients from 1 keV to 20 MeV. *Int. J. Appl. Radiat. Isot. 33*, 1269–1290.

Hubbell, J.H., Gimm, H.A., and Øverbø, I. (1980). Pair, triplet, and total atomic cross sections (and mass attenuation coefficients) for 1 MeV-100 GeV photons in elements Z = 1 to 100. *J. Phys. Chem. Ref. Data 9*, 1023–1147.

Hudis, J., and Katcoff, S. (1969). High-energy-proton fission cross sections of U, Bi, Au and Ag measured with mica track detectors. *Phys. Rev. 180*, 1122–1130.

Hughes, E.B., Zeman, H.D., Campbell, L.E., Hofstadter, R., Meyer-Berkhout, U., Otis, J.N., Rolfe, J., Stone, J.P., Wilson, S., Rubenstein, E., Harrison, D.C., Kernoff, R.S., Thompson, A.C., and Brown, G.S. (1983). The application of synchrotron radiation to non-invasive angiography. *Nucl. Instrum. Methods 208*, 665–675.

Hughes, E.B., Rubinstein, E., Zeman, H.D., Brown, G.S., Buchbinder, M., Harrison, D.C., Hofstadter, R., Kernoff, R.S., Otis, J.N., and Thompson, A.C. (1986). The angiography program at Stanford. *Nucl. Instrum. Methods Phys. Res. A246*, 719–725.

ICRP (1959). "Recommendations of the International Commission on Radiological Protection," Pergamon Press, Oxford.

ICRP (1963). Report of the RBE Committee to the International Commissions on Radiological Protection and on Radiological Units and Measurements. *Health Physics 9*, 357–386.

ICRP (1965). "Recommendations of the International Commission on Radiological Protection (adopted September 17, 1965)." ICRP Publication 9, Pergamon Press, Oxford.

ICRP (1973). "Data for Protection Against Ionizing Radiation from External Sources." Supplement to ICRP Publication 15, Report of ICRP Committee 3, ICRP Publication 21, International Commission on Radiological Protection, Pergamon Press, Oxford.

ICRP (1977). "Recommendations of the International Commission on Radiological Protection." ICRP Publication 26, Annals of the ICRP, Vol. 1, No. 3 (reprinted with revisions, 1981), Pergamon Press, Oxford.

ICRP (1987). "Data for Use in Protection Against External Radiation." ICRP Publication 51, Pergamon Press, Oxford.

ICRU (1928). "Recommendations of the International X-Ray Unit Committee, Stockholm Congress, 23–27 July 1928." *Brit. J. Radiol. 1*, 363–364.

ICRU (1938). "Recommendations of the International Committee for Radiological Units (Chicago, 1937)." *Am. J. Roetgenol. Radium Ther. 39*, 295–298.

ICRU (1957). "Report of the International Commission on Radiation Units and Measurements." NBS Handbook 62. National Bureau of Standards, U.S. Department of Commerce, Washington, D.C.

ICRU (1962). "Radiation Quantities and Units." ICRU Report 10a, published as NBS Handbook 84, Washington, D.C.

ICRU (1969). "Neutron Fluence, Neutron Spectra and Kerma." ICRU Report 13, International

Commission on Radiation Units and Measurements, Washington, D.C.

ICRU (1971a). "Radiation Quantities and Units." ICRU Report 19, International Commission on Radiation Units and Measurements, Washington, D.C. [Superseded by "Radiation Quantities and Units." ICRU Report 33, Washington, D.C. (1980)].

ICRU (1971b). "Radiation Protection Instrumentation and its Application." ICRU Report 20, International Commission on Radiation Units and Measurements, Washington, D.C.

ICRU (1973). "Dose Equivalent — Supplement to ICRU Report 19." ICRU Report 19S, Washington, D.C. See also: ICRU (1971a). "Radiation Quantities and Units." ICRU Report 19, International Commission on Radiation Units and Measurements, Washington, D.C. [Superseded by ICRU Report 33 (1980)].

ICRU (1976). "Conceptual Basis for the Determination of Dose Equivalent." ICRU Report 25, International Commission on Radiation Units and Measurements, Washington, D.C.

ICRU (1978). "Basic Aspects of High Energy Particle Interactions and Radiation Dosimetry." ICRU Report 28, International Commission on Radiation Units and Measurements, Washington, D.C.

ICRU (1980). "Radiation Quantities and Units." ICRU Report 33, International Commission on Radiation Units and Measurements, Washington, D.C.

ICRU (1982). "The Dosimetry of Pulsed Radiation." ICRU Report 34, International Commission on Radiation Units and Measurements, Washington, D.C.

ICRU (1984). "Stopping Powers for Electrons and Positrons." ICRU Report 37, International Commission on Radiation Units and Measurements, Washington, D.C.

ICRU (1985). "Determination of Dose Equivalents Resulting from External Radiation Sources." ICRU Report 39, International Commission on Radiation Units and Measurements, Washington, D.C.

ICRU (1986). "The Quality Factor in Radiation Protection." ICRU Report 40, International Commission on Radiation Units and Measurements, Washington, D.C.

ICRU (1988). "Determination of Dose Equivalents Resulting from External Radiation Sources — Part II." ICRU Report No. 43, International Commission on Radiation Units and Measurements, Washington, D.C.

IEEE (1975). 1975 Particle Accelerator Conference, Accelerator Engineering and Technology. Washington, D.C., March 12–14, 1975, *IEEE Trans. Nucl. Sci. NS-22*(3).

IEEE (1976). First Course on High Energy Radiation Dosimetry and Protection. Erice, Sicily, October 1–10, 1975, *IEEE Trans. Nucl. Sci. NS-23*(4).

IEEE (1977). 1977 Particle Accelerator Conference, Accelerator Engineering and Technology. Chicago, Illinois, March 16–18, 1977, *IEEE Trans. Nucl. Sci. NS-24*(3).

IEEE (1978). Annual Conference on Nuclear and Space Radiation Effects. Univ. of NM, Albuquerque, New Mexico, July 18–21, 1978. *IEEE Trans. Nucl. Sci. NS-25*(6).

IEEE (1979a). 1979 Particle Accelerator Conference, Accelerator Engineering and Technology, San Francisco, California, March 12–14, 1979, *IEEE Trans. Nucl. Sci. NS-26*(3) (in 2 parts).

IEEE (1979b). IEEE Annual Conference on Nuclear and Space Radiation Effects, Santa Cruz, California, July 17–20, 1979, *IEEE Trans. Nucl. Sci. NS-26*(6).

IEEE (1980). IEEE Annual Conference on Nuclear and Space Radiation Effects, Univ. of New Mexico, Albuquerque, New Mexico, July 18–21, 1980. *IEEE Trans. Nucl. Sci. NS-27*(6).

IEEE (1981a). 1981 Particle Accelerator Conference, Accelerator Engineering and Technology, Washington, D.C., March 11–13, 1981, *IEEE Trans. Nucl. Sci. NS-28*(3) (in 2 parts).

IEEE (1981b). Annual Conference on Nuclear and Space Radiation Effects, Seattle, Washington, July 21–24, 1981, *IEEE Trans. Nucl. Sci. NS-28*(6).

IEEE (1982). Annual Conference on Nuclear and Space Radiation Effects, Las Vegas, Nevada, July 20–22, 1982, *IEEE Trans. Nucl. Sci. NS-29*(6).

IEEE (1983a). 1983 Particle Accelerator Conference, Accelerator Engineering and Technology, Santa Fe, New Mexico, March 21–23, 1983, *IEEE Trans. Nucl. Sci. NS-30*(4).

IEEE (1983b). Annual Conference on Nuclear and Space Radiation Effects, Gatlinburg, Tennessee, July 18–21, 1983, *IEEE Trans. Nucl. Sci. NS-30*(6).

IEEE (1984). Annual Conference on Nuclear and Space Radiation Effects, Colorado Springs, Colorado, July 23–25, 1984, *IEEE Trans. Nucl. Sci. NS-31*(6).

IEEE (1985a). 1985 Particle Accelerator Conference, Accelerator Engineering and Technology, Vancouver, B.C., May 13–16, 1985, *IEEE Trans. Nucl. Sci. NS-32*(5).

IEEE (1985b). Annual Conference on Nuclear and Space Radiation Effects, Monterey, California, July 22–24, 1985, *IEEE Trans. Nucl. Sci. NS-32*(6).

Ing, H. (1986). The status of the bubble damage polymer detector. "Proc. 13th Int. Conference on Solid State Nuclear Track Detectors," Rome, 23–27 Sept., 1985 (L. Tommasino, G. Baroni and B. Campos-Venuti, eds.), *Nucl. Tracks Radiat. Measurements 12*, 49–54.

Ing, H. (1987). "A new bubble detector for the detection of gamma rays." Presented at the 32nd Annual Meeting of the Health Physics Society, July 5–10, 1987, Salt Lake City, UT.

Ing, H., and Birnboim, H.C. (1984). A bubble-damage polymer detector for neutrons. *In* "Proceedings of the 12th Int. Conference on Solid State Nuclear Track Detectors," Acapulco, 4–10 Sept., 1983 (G. Espinosa, R.V. Griffith, L. Tommasino, S.A. Durrani, and E.V. Benton, eds.), *Nucl. Tracks Radiat. Measurements 8*(1-4), 285–288.

Ing, H., and Piesch, E. (eds.) (1985). Neutron dosimetry. *Radiat. Prot. Dosim. 10* (1–4).

Irving, D.C., Freestone, R.M., Jr., and Kam, F.B.K. (1965). "O5R, A General Purpose Monte Carlo Neutron Transport Code." Oak Ridge National Laboratory Report ORNL-3622.

Ižycka, A., and Schönbacher, H. (1979). "High-Level Dosimetry for Radiation Damage Studies at High-Energy Accelerators." European Organization for Nuclear Research CERN, Geneva, Report HS-RP/040/CF. See also "Proceedings Third ASTM-Euratom Symposium for Reactor Dosimetry," ISPRA 1979. Euratom Report EUR 6813, ISPRA 1980.

Jackson, J.D. (1975). "Classical Electrodynamics." 2nd ed., John Wiley & Sons, New York.

Jackson, J.D. (1983). "Range-Energy Relation and Multiple Scattering for TeV Muons in Soil." Internal Memo: Physics Notes JDJ/83-1, Lawrence Berkeley Laboratory, Berkeley, CA.

Jaffé, G. (1913), Zur Theorie der Ionisation in Kolonnen, *I. Ann. Physik* (4th Series) *42*, 303–344.

Jaffé, G. (1929a). Zur Theorie der Ionisation in Kolonnen, II. *Ann. Physik* (5th Series) *1*, 977–1008.

Jaffé, G. (1929b). Kolonnenionisation in Gasen bei erhöhtem Druck. *Physik. Z. 30*, 849–856.

Jaffé, G. (1940). On the theory of recombination. *Phys. Rev. 58*, 968–976.

Jähnert, B. (1972). The response of TLD-700 thermoluminescent dosimeters to protons and alpha particles. *Health Physics 23*, 112–115.

Jakeways, R. and Calder, I.R. (1970). An experimental study of the longitudinal development of electron initiated cascades in lead in the energy range 0.5–4.0 GeV. *Nucl. Instrum. Methods 84*, 79–82.

Janni, J.F. (1966). "Calculations of Energy Loss, Range, Pathlength, Straggling, Multiple Scattering, and the Probability of Inelastic Nuclear Collisions for 0.1 to 1000-MeV Protons." Air Force Weapons Laboratory, Kirtland Air Force Base, New Mexico, Report AFWL-TR-65-150.

Janni, J.F. (1982). Proton range-energy tables 1 keV – 10 GeV. *At. Data Nucl. Data Tables 27*, 147–529.

Jauch, J.M., and Rohrlich, F. (1976). "The Theory of Photons and Electrons." (2nd ed.), (Springer-Verlag, New York).

Jenkins, T.M. (1969). Stanford Linear Accelerator Center, Stanford, California. Private communication.

Jenkins, T.M. (1974). Accelerator boundary doses and skyshine. *Health Physics 27*, 251–257.

Jenkins, T.M. (1979). Neutron and photon measurements through concrete from a 15 GeV electron beam on a target — Comparison with models and calculations. *Nucl. Instrum. Methods 159*, 265–288.

Jenkins, T.M. (1988). Stanford Linear Accelerator Center, Stanford, California. Private communication.

Jones, A.R. (1962). Pulse counters for gamma dosimetry. *Health Physics 8*, 1–9.

Kalef-Ezra, J., and Horowitz, Y.S. (1982). Heavy charged particle thermoluminescence dosimetry: Track structure theory and experiments. *Int. J. Appl. Radiat. Isot. 33*, 1085–1100.

Kang, Y., Lee, K., Roberts, A., Snowdon, S.C., Theriot, D., and Meyer, S.L. (1972). Design of a magnetized iron muon shield for a high energy neutrino laboratory. *Particle Accel. 4*, 31–41.

Kase, K.R., Bjärngard, B.E., and Attix, F.H.(eds.) (1987). "The Dosimetry of Ionizing Radiation." Vol. II, Academic Press, New York.

Kathren, R.L. (nd). External Beta-Photon Dosimetry for Radiation Protection. *In* "Dosimetry of Ionizing Radiation." Vol. III (K.R. Kase, B.E. Bjärngard, and F.H. Attix, eds.), Academic Press, New York [in preparation].

Katoh, K. (1977). National Laboratory for High-Energy Physics, Tsukuba, Japan, Private communication.

Keefe, D. (1964). "Mu-Meson Shielding Problems at 200 GeV: Approximate Calculations." Lawrence Berkeley Laboratory Internal Report UCID-10018.

Keefe, D., and Noble, C.M. (1968). Radiation shielding for high energy muons: The case of a cylindrically symmetrical shield and no magnetic field. *Nucl. Instrum. Methods 64*, 173–180.

Kelly, E.L., and Wiegand, C. (1948). Fission of elements from Pt to Bi by high-energy neutrons. *Phys. Rev. 73*, 1135–1139.

Kinney, W.E. (1962). "A Monte Carlo Calculation of Scattered Neutron Fluxes at an Air-Ground Interface due to Point Isotropic Sources on the Interface." Oak Ridge National Laboratory Internal Report ORNL-3287.

Knasel, T.M. (1970). Accurate calculation of radiation lengths. *Nucl. Instrum. Methods 83*, 217–220.

Knoll, G.F. (1979). "Radiation Detection and Measurement." Wiley, New York.

Koch, E-.E. (ed.) (1983). "Handbook on Synchrotron Radiation." North Holland Publishing Co., Amsterdam.

Koch, H.W., and Motz, J.W. (1959). Bremsstrahlung cross-section formulas and related data. *Rev. Mod. Phys. 31*, 920–955.

Kohaupt, R.D., and Voss, G.-A. (1983). Progress and problems in performance of e^+e^- storage rings. *Annual Review of Nuclear and Particle Science 33*, 67–104. Annual Reviews, Inc., Palo Alto, CA.

Komochkov, M.M. (1970). The Dubna Synchrophasotron. *In* "Engineering Compendium on Radiation Shielding, Vol. III: Shield Design and Engineering," pp. 171–174, R.G. Jaeger (ed.), International Atomic Energy Agency (sponsor), Springer-Verlag, New York.

Komochkov, M.M., and Teterev, Yu.G. (1972). "Activation of Water Cooling the Synchrocyclotron Units." Joint Institute for Nuclear Research Report JNIR-P16-6314, Dubna.

Kon'shin, V.A., Matusevich, E.S., and Regushevskiĭ, V.I. (1965). Cross sections for fission of Ta^{181}, Re, Pt, Au^{197}, Pb, Bi^{209}, Th^{232}, U^{235} and U^{238} by 150–660 MeV protons. *J. Nucl. Phys. (U.S.S.R.) 2*, 682–686. Engl. transl. in *Soviet. J. Nucl. Phys. 2*, 489–492 (1966).

Kooiman, M., and Höfert, M. (1982). "The Influence of Development Conditions on the Fading Behaviour of the NTA Nuclear Emulsion." European Organization for Nuclear Research CERN, Geneva, Report HS-RP/TM/82-31.

Kosako, T., Nakamura, T., and Iwai, S. (1985). Estimation of time-of-flight method combined with a large lead pile. *Nucl. Instrum. Methods A235*, 103–122.

Kötz, U. (1981). "Energy Deposition and Dose Calculations for Synchrotron Radiation Produced in the HERA Bending Magnet." Report DESY HERA 81/09. Deutsches Elektronen Synchrotron DESY, Hamburg.

Krinsky, S., Perlman, M.L., and Watson, R.E. (1985). Characteristics of synchrotron radiation and of its sources. *In* "Handbook on Synchrotron Radiation" (E.-E. Koch, ed.), Vol. 1A, Ch. 2, pp. 65–171, North Holland, Amsterdam.

Kuehner, A.V., and Chester, J.D. (1973). "Dose Equivalent Meter Operating Instructions." Informal report, Health and Safety Division, Brookhaven National Laboratory, Upton, NY.

Kuehner, A.V., Chester, J.D., and Baum, J.W. (1972). "Portable Mixed Radiation Dose Equivalent Meter." Brookhaven National Laboratory, Upton, New York, Report BNL-17298.

Kuehner, A.V., Chester, J.D., and Baum, J.W. (1973). Portable mixed radiation dose-equivalent meter for protection monitoring. *In* "Proc. Symp. on Neutron Monitoring for Protection Purposes," International Atomic Energy Agency, Vienna, pp. 233–246.

Ladu, M., Pelliccioni, M., and Rotondi, E. (1963). On the response to fast neutrons of a BF_3 counter in a paraffin spherical-hollow moderator. *Nucl. Instrum. Methods 23*, 173–174.

Ladu, M., Pelliccioni, M., and Rotondi, E. (1965). Flat response to neutrons between 20 keV and 14 MeV of a BF_3 counter in a spherical hollow moderator. *Nucl. Instrum. Methods 32*, 173–174.

Ladu, M., Pelliccioni, M., Picchi, P., and Verri, G. (1968). A contribution to the skyshine study. *Nucl.*

Instrum. Methods 62, 51–56.

Ladu, M., Pelliccioni, M., Picchi, P., and Roccella, M. (1972). Shielding for ultrarelativistic muons. *Nucl. Instrum. Methods 104*, 5–10.

Lam, G.K.Y., and Skarsgard, L. (1983). "Physical aspects of the pion beam at TRIUMF." *In op. cit.* Skarsgard (1983), 83–90.

LAMPF (1986). "Progress at LAMPF." (J.C. Allred and B. Talley, eds.), Progress Report LA-10738-PR, Clinton P. Anderson Meson Physics Facility, Los Alamos National Laboratory, Los Alamos, NM.

Lapostolle, P.M., and Septier, A.L. (eds.) (1970). "Linear Accelerators." North Holland Publishing Co., Amsterdam.

Larsson, B. (1980). Dosimetry and radiobiology of protons as applied to cancer therapy and neurosurgery. *In op. cit.*, Thomas and Perez-Mendez (1980), 367–394.

Lawrence, E.O., and Livingston, M.S. (1932). The production of high speed light ions without the use of high voltages. *Phys. Rev. 40*, 19–35.

Lawrence, E.O., Livingston, M.S., and White, M.G. (1932). The disintegration of lithium by swiftly-moving protons. *Phys. Rev. 42*, 150–151.

Lawson, J.D., and Tigner, M. (1984). The physics of particle accelerators. *Annual Rev. Nucl. Part. Sci. 34*, 99–123. Annual Reviews, Inc., Palo Alto, CA.

Leake, J.W. (1967). Portable instruments for the measurement of neutron dose-equivalent rate in steady-state and pulsed neutron fields. *In* "Proc. Symp. Neutron Monitoring for Radiological Protection," Vienna, August 29–Sept. 2, 1966, IAEA (Vienna), pp. 313–326.

Leake, J.W. (1968). An improved spherical dose equivalent neutron detector. *Nucl. Instrum. Methods 63*, 329–332.

Lebedev, V.N., Zolin, L.S., and Salatskaya, M.I. (1965). "Distribution of the Penetrating Radiation Field over the Protective Zone of the 10 GeV Synchrophasotron." Joint Institute for Nuclear Research, Dubna, USSR, Internal Report JNIR-P-2177.

Lehmann, F. (1983). "Perte d'Information sur les Films à Neutron (Fading)." European Organization for Nuclear Research CERN, Geneva, Report TIS-RP/TM/83-37.

Levine, G.S., Squier, D.M., Stapleton, G.B., Stevenson, G.R., Goebel, K., and Ranft, J. (1972). The angular dependence of dose and hadronic yields from targets in 8 GeV/c and 24 GeV/c extracted proton beams. *Part. Accel. 3*, 91–101.

Lim, C.B. (1973). "The development of a Neutron Spectrometer Using Multi-Wire Spark Chambers." Ph.D. Thesis, Nuclear Engineering Department, University of California, Lawrence Berkeley Laboratory Report LBL 1719.

Lindenbaum, S.J. (1957). Brookhaven National Laboratory Proton Synchrotron. *In* "Proc. Conference on Shielding of High-Energy Accelerators," New York, April 11–13, 1957, USAEC TID-7545, pp. 28–37.

Livingood, J.J. (1961). "Principles of Cyclic Particle Accelerators." D. Van Nostrand Co., Inc. Princeton, New Jersey.

Livingston, M.S. (ed.) (1966). "The Development of High Energy Accelerators." Classics of Science, Vol. III, Dover Publictions, Inc., New York.

Livingston, M.S., and Blewett, J.P. (1962). "Particle Accelerators." McGraw Hill, New York.

Llacer, J., Chatterjee, A., Alpen, E.L., Saunders, W., Andreae, S., and Jackson, H.C. (1984). Imaging by injection of accelerated radioactive particle beams. *IEEE Trans. Med. Imaging MI-3*, 80–90.

Lohmann, W., Kopp, R., and Voss, R. (1985). "Energy Loss of Muons in the Energy Range 1–10,000 GeV." European Organization for Nuclear Research CERN, Geneva, Report CERN 85-03.

Lowry, K.A., and Johnson, T.L. (1984). "Modification to Iterative Recursion Unfolding Algorithms and Computer Codes to Find more Appropriate Neutron Spectra." Naval Research Laboratory, Washington, D.C., Report NRL-5340.

Madey, R., and Waterman, F.M. (1973). Neutron spectroscopy from 1 MeV to 1 GeV. *In* "Proc. Symp. on Neutron Monitoring for Radiation Protection Purposes," Vol. 1, International Atomic Energy Agency, Vienna, pp. 113–121.

Madey, R., Baldwin, A.R., and Waterman, F.M. (1976). Neutron spectrum from 20 to about 600 MeV above the Brookhaven National Laboratory AGS shielding. *Trans. Am. Nucl. Soc. 23*, 612–613.

Mamont-Čiesla, K., and Rindi, A. (1974). "Spark Chamber Neutron and Proton Spectrometer: First Report on Performance." Lawrence Berkeley Laboratory Report LBL-3343.

Maslov, M.A., Mokhov, N.V., and Uzunian, A.V. (1983). Calculation of muonic fields around large high energy proton accelerators. *Nucl. Instrum. Methods 217*, 419–424.

McCall, R.C., Jenkins, T.M., and Shore, R.A. (1979). Transport of accelerator produced neutrons in a concrete room. *IEEE Trans. Nucl. Sci. NS-26*, 1593–1602.

McCaslin, J.B. (1960). A high-energy neutron-flux detector. *Health Physics 2*, 399–407.

McCaslin, J.B. (1964). Electrometer for ionization chambers using metal-oxide-semiconductor field-effect transistors. *Rev. Sci. Instrum. 35*, 1587–1591.

McCaslin, J.B. (1973). Detection of neutrons greater than 20 MeV from the production of ^{11}C. *In* "Laboratory Manual Experiment 8," Patterson, H.W., and Thomas, R.H., "Accelerator Health Physics." Academic Press, New York, pp. 621–626.

McCaslin, J.B., and Stephens, L.D. (1967). "High-Sensitivity Neutron and Proton Flux Detector with a Practical Threshold near 600 MeV, Using Hg (spallation) ^{149}Tb." Lawrence Radiation Laboratory, Berkeley, California, Report UCRL-17505.

McCaslin, J.B., and Stephens, L.D. (1976). "Effect of Neutron Scattering on the Calibration of Moderated BF_3 Detectors." Lawrence Berkeley Laboratory Internal Note HPN-57 (22 Dec. 1976).

McCaslin, J.B., and Thomas, R.H. (1981). Practical neutron dosimetry at high energies. *In* "Proceedings of the European Seminar on Radiation Protection Quantities for External Exposure," Braunschweig, Fed. Rep. of Germany, October 13–15, 1980. EUR 7101-EN, pp. 137–175, Harwood Academic Publishers, Chur, Switzerland.

McCaslin, J.B., Patterson, H.W., Smith, A.R., and Stephens, L.D. (1968). Some recent developments in technique for monitoring high-energy accelerator radiation. *In* "Proceedings of the First International Congress of Radiation Protection," International Radiation Protection Association, Pergamon Press, New York, Part 2, pp. 1131–1137.

McCaslin, J.B., Smith, A.R., Stephens, L.D., Thomas, R.H., Jenkins, T.M., Warren, G.J., and Baum, J.W. (1977). An intercomparison of dosimetry methods in radiation fields at two high-energy accelerators.

Health Physics 33, 611–620.

McCaslin, J.B., Stephens, L.D., and Thomas, R.H. (1983). Ground scattering contribution in neutron calibrations. *Health Physics 44*, 437-439.

McCaslin, J.B., Sun, R.-K.S., Swanson, W.P., Cossairt, J.D., Elwyn, A.J., Freeman, W.S., Jostlein, H., Moore, C.D., Yurista, P.M., and Groom, D.E. (1988). "Radiation Environment in the Tunnel of a High-Energy Proton Accelerator at Energies near 1 TeV." Lawrence Berkeley Laboratory Report LBL-24640; Conf. International Radiation Protection Association IRPA on Radiation Protection Practice, Sydney, Australia, 10-17 April 1988, pp. 137-140 (Pergamon Press, Sydney).

McCaslin, J.B., Sun, R.-K.S., Swanson, W.P., Elwyn, A.J., Freeman, W.S., and Yurista, P.M. (1986). "Measurement of Neutron Spectra and Doses in the Tevatron Tunnel for 800 GeV Circulating Proton Beams." Superconducting Super Collider Central Design Group (c/o Lawrence Berkeley Laboratory) Report SSC-58.

McGuire, S.A. (1966). "A Dose Monitoring Instrument for Neutrons from Thermal to 100 MeV." Los Alamos National Laboratory Internal Report LA-345 (March 1, 1966).

Messel, H., and Crawford, D.F. (1970). "Electron-Photon Shower Distribution Function, Tables for Lead, Copper and Air Absorbers." Pergamon Press, Oxford.

Messel, H., Smirnov, A.D., Varfolomeev, A.A., Crawford, D.F., and Butcher, J.C. (1962). Radial and angular distributions of electrons in electron-photon showers in lead and in emulsion absorbers. *Nucl. Phys. 39*, 1–88.

Metropolis, N., Bivins, R., Storm, M., Turkevich, A, Miller, J. M., and Friedlander, G. (1958a). Monte Carlo calculations on intranuclear cascades. I. Low-energy studies. *Phys. Rev. 110*, 185–203.

Metropolis, N., Bivins, R., Storm, M., Turkevich, A, Miller, J. M., and Friedlander, G. (1958b). Monte Carlo calculations on intranuclear cascades. II. High-energy studies and pion processes. *Phys. Rev. 110*, 204–219.

Middlekoop, W.C. (1966). "Remarks about Groundwater Activation by a 300 GeV Proton Synchrotron." CERN Internal Report ISR/INT BT/66-3.

Mo, L.W., and Tsai, Y.-S. (1969). Radiative corrections to elastic and inelastic ep and μp scattering. *Rev. Mod. Phys. 41*, 205–235.

Mokhov, N.V., and Cossairt, J.D. (1986). A short review of Monte Carlo hadronic cascade calculations in the multi-TeV energy region. *Nucl. Instrum. Methods Phys. Res. A244*, 349–355.

Mokhov, N.V., Semenova, G.I., and Uzunian, A.V. (1981). Muon production and transport in matter in the energy range 10^1-10^5 GeV. *Nucl. Instrum. Methods 180*, 469–481.

Mole, R.H. (1979). RBE for carcinogenesis by fission neutrons. *Health Physics 36*, 463–464.

Molière, G. (1948). Theorie der Streuung schneller geladener Teilchen II. Mehrfach- und Vielfachstreuung. *Z. Naturforschg. 3a*, 78–97.

Moore, C., and Velen, S. (1974). "Muon Beam Halo Studies." Fermilab Internal Report TM-497.

Moore, W.H. (1966). "Source of High-Energy Particles from an Internal Target in the AGS." Brookhaven National Laboratory Internal Report AGSCD-62.

Moritz, L. (1988). TRIUMF, Vancouver, B.C. Private communication.

Moy, B., Rau, G., and Schwenke, D. (1980). "The Instrumentation for Monitoring the Environment Around CERN." European Organization for Nuclear Research CERN, Geneva, Internal Report HS-RP/050 (25 Aug. 1980).

Moyer, B.J. (1952). Survey methods for fast- and high-energy neutrons. *Nucleonics 10*(5), 14–19.

Moyer, B.J. (1954). Neutron physics of concern to the biologist. *Radiat. Res. 1*, 10–22.

Moyer, B.J. (1957). Buildup factors. *In* "Conference on Shielding of High-Energy Accelerators," held at New York, April 11–13, 1957, USAEC Report TID-7545, pp. 96–100.

Moyer, B.J. (1962). Method of calculation of the shielding enclosure for the Berkeley Bevatron. *In* "Premier Colloque International sur la Protection auprès des grands Accélérateurs." Presses Universitaires de France. Paris, pp. 65–70.

Müller, D. (1972). Electron showers of high primary energy in lead. *Phys. Rev. 5*, 2677–2683 [Electrons: $E_0 = 2 - 15$ GeV].

Muraki, Y., Kasahara, K., Yuda, T., Hotta, N., Ohta, I., Mizutani, K., Torii, S., Sakata, M., Yamamoto, Y., and Dake, S. (1985). Radial and longitudinal behaviour of hadronic cascade showers induced by 300 GeV protons in lead and iron absorbers. *Nucl. Instrum. Methods Phys. Res. A236*, 47–54.

Nachtigall, D., and Burger, G. (1972). Dose equivalent determinations in neutron fields by means of moderator techniques (F.H. Attix, ed.). *In* "Topics in Radiation Dosimetry," Supplement 1, Academic Press, New York, pp. 385–459.

Nagel, H.-H. (1965). Elektron-Photon-Kaskaden in Blei. *Z. Phys. 186*, 319–346. Copies of complete shower tables may be obtained from: Bibliothek des Physikalischen Institutes, 53 Bonn, Nussallee 12, F.R.G.

Nagel, H.H., and Schlier, Ch. (1963). Berechnung von Elektron-Photon-Kaskaden in Blei für eine Primärenergie von 200 MeV. *Z. Phys. 174*, 464–471.

Nakamura, T., and Kosako, T. (1981a). A systematic study on the neutron skyshine from nuclear facilities. Part I: Monte Carlo analysis of neutron propagation in air-over-ground environment from a monoenergetic source. *Nucl. Sci. Eng. 77*, 168–181.

Nakamura, T., Kosako, T., Hayashi, K., Ban, S., and Katoh, K. (1981b). A systematic study on the neutron skyshine from nuclear facilities. Part II: Experimental approach to the behavior of environmental neutrons around an electron synchrotron. *Nucl. Sci. Eng. 77*, 182–191.

Nakamura, T., Ohkubo, T., and Uwamino, Y. (1987). Spatial distribution of radionuclides produced in copper by photonuclear spallation reactions. *Nucl. Instrum. Methods Phys. Res. A256*, 505–512.

Nakamura, T., Yoshida, M., and Shin, K. (1978). Spectral measurements of neutrons and photons from thick targets of C, Fe, Cu and Pb by 52 MeV protons. *Nucl. Instrum. Methods 151*, 493–503.

National Bureau of Standards (1970). "Radiological Safety in Design and Operation of Particle Accelerators." NBS Handbook 107 and American National Standard N43.1.-1969. Also see *op. cit.* ANSI (1978).

NCRP (1971). "Protection Against Neutron Radiation." NCRP Report 38, National Council on Radiation

Protection and Measurements, Washington, D.C.

NCRP (1976). "Environmental Radiation Measurements." NCRP Report 50, National Council on Radiation Protection and Measurements, Washington, D.C.

NCRP (1977). "Radiation Protection Design Guidelines for 0.1–100 MeV Particle Accelerator Facilities." NCRP Report 51, National Council on Radiation Protection and Measurements, Washington, D.C.

NCRP (1981). Quantitative risk in standards setting. "Proceedings of the Sixteenth Annual Meeting," 2–3 April 1980, National Council on Radiation Protection and Measurements, Washington, D.C.

NCRP (1984). "Neutrons from Medical Accelerators." NCRP Report 79, National Council on Radiation Protection and Measurements, Washington, D.C.

Neal, R.B. (Gen. ed.), Dupen, D.W., Hogg, H.A., Loewe, G.A. (eds.) (1968). "The Stanford Two Mile Accelerator." Benjamin, New York.

Negro, V.C., Cassidy, M.E. and Graveson, R.T. (1967). A guarded insulated gate field effect electrometer. *IEEE Trans. Nucl. Sci. NS-14*, 135–142.

Nelson, W. R. (1968). The shielding of muons around high energy electron accelerators: Theory and measurement. *Nucl. Instrum. Methods 66*, 293–303.

Nelson, W.R., and Jenkins, T.M. (1976). Similarities between the radiation fields at different types of high-energy accelerators. *IEEE Trans. Nucl. Sci. NS23*, 1351–1354.

Nelson, W.R., and Jenkins, T.M. (eds.) (1980). Computer Techniques in Radiation Transport and Dosimetry. *In* "Proc. 2nd Int. School of Radiation Damage and Protection," Erice, Italy, Oct. 25–Nov. 3, 1978. Plenum Press, New York.

Nelson, W.R., and Kase, K.R. (1974). Muon shielding around high-energy electron accelerators. Part I. Theory. *Nucl. Instrum. Methods 120*, 401–411.

Nelson, W.R., Hirayama, H., and Rogers, D.W.O. (1985). "The EGS4 Code System." Stanford Linear Accelerator Center, Stanford, California, Report SLAC-265.

Nelson, W.R., Jenkins, T.M., McCall, R.C., and Cobb, J.K. (1966). Electron-induced cascade showers in copper and lead at 1 GeV. *Phys. Rev. 149*, 201–208.

Nelson, W.R., Kase, K.R., and Svensson, G.K. (1974). Muon shielding around high-energy electron accelerators. Part II. Experimental investigation. *Nucl. Instrum. Methods 120*, 413–429.

Nelson, W.R., Warren, G.J., and Ford, R.L. (1975). "The Radiation Dose to Coil Windings and the Production of Nitric Acid and Ozone from PEP Synchrotron Radiation." Stanford Linear Accelerator Center, Stanford, California, Report PEP-109.

Nelson, W. R., Stevenson, G. R., Heijne, E. H. M., Jarron, P., Liu, K.-L., and Nielsen, M. (1979). "Preliminary Profile Measurements of High-Energy Muon Beams in a Soil Shield." European Organization for Nuclear Research CERN, Geneva, Report HS-RP/042.

Nelson, W.R., Jenkins, T.M., Stevenson, G.R., Nielsen, M., Heijne, E.H. M., Jarron, P., Lord, J., and Anderson, S. (1983). "Transport of High Energy Muons in a Soil Shield." European Organization for Nuclear Research CERN, Geneva, Report CERN-TIS-RP/100/PP, and *Nucl. Instrum. Methods 215*,

385–396.

Nielsen, B. (1971). "Muon Measurements for Radiation Protection." European Organization for Nuclear Research CERN, Geneva, Internal Report HP-74-135.

O'Brien, K. (1971). Neutron Spectra in the Side-Shielding of a Large Particle Accelerator. USAEC Health and Safety Laboratory, New York, Report HASL-240.

O'Brien, K., and McLaughlin, J.E. (1968). The propagation of the neutron component of the nucleonic cascade at energies less than 500 MeV: Theory and a solution to the accelerator transverse shielding problem. *Nucl. Instrum. Methods 60*, 129-140.

O'Brien, K., and Sanna, R. (1981). Neutron spectrum unfolding using the Monte Carlo method. *Nucl. Instrum. Methods 185*, 277-286.

O'Brien, K., and Sanna, R. (1983). Reply to Chambless and Broadway. *Nucl. Instrum. Methods 214*, 547-549.

O'Brien, K., Sanna, R.S., and McLaughlin, J.E. (1965). "Inference of accelerator stray neutron spectra from various measurements." *In* Proc. USAEC First Symposium on Accelerator Radiation Dosimetry and Experience, Brookhaven National Laboratory, November 1965, USAEC Report CONF-651109, pp. 286-305.

Oda, K., Kobayashi, H., Yamamoto, T., and Kawanishi, M. (1980). Experimental determination of collection efficiency on ionization chamber in field of pulsed x-rays. *J. Nucl. Sci. Tech. (Japan) 19*, 89-95.

Oda, K. *et al.* (1982). *J. Nucl. Science Techn. (Japan) 19*, 9.

Ollendorf, W. (1964). "A Study of Radiation Levels at the CERN Site." European Organization for Nuclear Research CERN, Geneva, Internal Report DI/HP/66.

Otte, R.A., Swanson, W.P., Rowe, E.M., and DeLuca, P.M., Jr. (1987). Aladdin, a 1-GeV electron storage ring: An opportunity to understand its radiation patterns. *In* "Proceedings of the 20th Midyear Topical Meeting on Health Physics of Radiation Generating Machines" (D.D. Busick and W.P. Swanson, eds.) held in Reno, Nevada, 8-12 Feb., 1987.

Paciotti, M., Bradbury, J., Inoue, H., Rivera, O., and Sandford, S. (1981a). Beam characteristics in the LAMPF biomedical channel. *op.cit. IEEE Trans. Nucl. Sci. NS-28*, 3150-3152.

Pages, K., Bertel, E., Joffre, H., and Sklavenitis, L. (1972). Energy loss, range, and bremsstrahlung yield for 10-keV to 100-MeV electrons in various elements and chemical compounds. *At. Data Nucl. Data Tables 4*, 1-127.

Panofsky, W.K.H. (1980). Needs versus means in high-energy physics. *Physics Today 33*(6), 24-33.

Parker, H.M. (1948). Health physics, instrumentation, and radiation protection. *Adv. Biol. Med. Phys. 1* (J.H. Lawrence and J.G. Hamilton, eds.), Academic Press, New York, pp. 223-285.

PART (1977). Proceedings of the 2nd Int. Conf. on Particles and Radiation Therapy, *Int. J. Radiat. Oncol. Biol. Phys. 3* (entire volume).

PART (1982). Proceedings of the 3rd Int. Conf. on Particles and Radiation Therapy, *Int. J. Radiat. Oncol. Biol. Phys. 8* (entire volume).

Patrick, J.W., Stephens, L.D., Thomas, R.H., and Kelly, L.S. (1975). The design of an experiment to study carcinogenesis and hematological effects in mice irradiated by energetic heavy ions. *Radiat. Res. 64*, 492-508.

Patterson, H.W. (1957). "The University of California Radiation Laboratory Synchrocyclotron." *In op. cit.* Solon. L.R. (1957), pp. 3-7.

Patterson, H.W. (1965). Accelerator radiation monitoring and shielding at Lawrence Radiation Laboratory, Berkeley. *In* "Proceedings First Symposium on Accelerator Radiation Dosimetry and Experience," Brookhaven National Laboratory, November 1965, USAEC Report CONF-651109, p. 3–19.

Patterson, H.W., and Thomas, R.H. (1973). "Accelerator Health Physics." Academic Press, New York.

Patterson, H.W., and Wallace, R.W. (1958). "A Method of Calibrating Slow-Neutron Detectors." Lawrence Radiation Laboratory, Berkeley, California, Report UCRL-8359.

Patterson, H.W., Hess, W.N., Moyer, B.J., and Wallace, R.W. (1959). The flux and spectrum of cosmic ray produced neutrons as a function of altitude. *Health Physics 2*, 69–72.

Patterson, H.W., Low-Beer, A.D., and Sargent, T.W. (1965). Whole body counting and bioassay determination of accelerator workers. *Health Physics 17*, 621–625.

Patterson, H.W., Heckman, H.H., and Routti, J.T. (1969). New measurements of star production in nuclear emulsions and applications to high-energy neutron spectroscopy. *In op. cit.* Proceedings of the Second Int. Conference on Accelerator Dosimetry and Experience, Stanford Linear Accelerator Center, Nov. 5-7, 1969, Report No. CONF-691101, U.S.A.E.C., Washington, D.C., pp. 750-763.

Patterson, H.W., Routti, J.T., and Thomas, R.H. (1971). What quality factor? *Health Physics 20*, 517-527.

Peetermans, A., and Baarli, J. (1974). Radioactive gas and aerosol production by the CERN high-energy accelerators and evaluation of their influences on environmental problems. *In* "Environmental Surveillance around Nuclear Installations." Vol. 1, p. 433, International Atomic Energy Agency, Vienna.

Pelliccioni, M., and Esposito, A. (1987). Measurements of gas bremsstrahlung in the Adone storage ring. *In* "Proceedings of the 20th Midyear Topical Meeting on Health Physics of Radiation Generating Machines" (D.D. Busick, and W.P. Swanson, eds.) held in Reno, Nevada, 8-12 Feb. 1987, pp. 495-501.

Penfold, J., and Stevenson, G.R. (1968). "Preliminary Measurements of the Angular Distribution of the Stray Radiation Field." Rutherford Laboratory Internal Report RP/PN/29.

PEP (1976). "PEP Conceptual Design Report." Stanford Linear Accelerator Center Report No. SLAC-189 and Lawrence Berkeley Laboratory Report No. LBL-4288.

Perey, F.G. (1977). "Least-Square Dosimetry Unfolding: the Program STAYL'SL." RSIC Computer Code Collection No. CCC-113, Oak Ridge National Laboratory Report ORNL/TM-6062.

Perry, D.R. (1967). Neutron dosimetry methods and experience in the 7 GeV proton synchrotron, Nimrod. *In* "Proceedings of the Symposium on Neutron Monitoring for Radiological Protection," International Atomic Energy Agency, Vienna, pp. 355-374.

Perry, D.R., and Shaw, K.B. (1965). Radiation levels in and around Nimrod. *In* "Proceedings First Symposium on Accelerator Radiation Dosimetry and Experience," USAEC Report CONF-651109, p. 20–33.

Piesch, E., and Burghardt, B. (1985). Albedo neutron dosimetry. *Radiat. Prot. Dosim. 10* (1-4), pp. 175-188.

Plechaty, E.F., Cullen, D.E., and Howerton, R.J. (1975). "Tables and Graphs of Photon Interaction Cross Sections from 1.0 keV to 100 MeV Derived from the LLL Evaluated Nuclear Data Library." Lawrence Livermore Laboratory, Report UCRL-50400, Vol. 6, Rev. 1.

Portal, G. (1981). Preparation and properties of principal TL products. *In* "Applied Thermoluminescence Dosimetry." Lectures at the Joint Research Center, Ispra, Italy, 12-16 November 1979 (M. Oberhofer and A. Scharmann, eds.). Commission of the European Communities (Adam Hilger, Ltd., Bristol).

Powell, C.F., Fowler, P.H., and Perkins, D.H. (1959). "The Study of Elementary Particles by the Photographic Method." Pergamon Press, New York.

Prantl, F.A., and Baarli, J. (1972). "Control of Radioactive Pollution in the Environment of the CERN Accelerators." European Organization for Nuclear Research CERN, Geneva, Report CERN 72-15.

Price, P.B., and Walker, R.M. (1962). Observations of charged-particle tracks in solids. *J. Appl. Phys. 33*, 3400-3406.

Price, P.B., and Walker, R.M. (1963). A simple method of measuring low uranium concentrations in natural crystals. *Appl. Phys. Letters 2*, 23-25.

Pszona, S. (1969). A new approach for determining quality factor and dose equivalent in mixed radiation fields. *Health Physics 16*, 9-11.

Pszona, S. (1971). The Ne-102A organic scintillation detector as an acceptable LET dependent detector for quality factor and dose equivalent determination in mixed radiation fields. *In op. cit.* Int. Congress on Protection Against Accelerator and Space Radiation, CERN, April 26-30, 1971, Report CERN 71-16, European Organization for Nuclear Research CERN, Geneva, Vol. 1, pp. 388-402.

Pszona, S., and Höfert, M. (1977). A rapid method for the determination of dose equivalent in mixed radiation fields. *Nucl. Instrum. Methods 146*, 509-512.

Puppi, G., and Dallaporta, N. (1952). The equilibrium of the cosmic ray beam in the atmosphere. *In* "Progress in Cosmic Ray Physics." Vol. 1 (J.G. Wilson, ed.), North-Holland, Amsterdam, pp. 315-391.

Raju, M.R. (1980). "Heavy Particle Radiotherapy." Academic Press, New York.

Ranft, J. (1972). Estimation of radiation problems around high energy accelerators using calculations of the hadronic cascade in matter. *Particle Accel. 3*, 129-161.

Ranft, J. (1980a). Particle production models, sampling high-energy multiparticle events from inclusive single-particle distributions. *In op. cit.* (Nelson and Jenkins, 1980). pp. 279-310.

Ranft, J. (1980b). The FLUKA and KASPRO hadronic cascade codes. *In op.cit.* (Nelson and Jenkins, 1980). pp. 339-372.

Ranft, J. (1985). Karl-Marx Universität, Leipzig. Private communication.

Ranft, J., and Routti, J.T. (1972). Hadronic cascade calculations of angular distributions of integrated secondary particle fluxes from external targets and new empirical formulae describing particle production in proton-nucleus collisions. *Particle Accel. 4*, 101-110.

Ranft, J., and Routti, J.T. (1974). Monte Carlo programs for calculating three-dimensional high-energy (50 MeV - 500 GeV) hadron cascades in matter. *Comput. Phys. Commun. 7*, 327-342.

Ranft, J., Aarnio, P.A., and Stevenson, G.R. (1985). "FLUKA82." Paper presented at the CERN Workshop on Shower Simulation for LEP Experiments, 19-31 January 1985, European Organization for Nuclear Research CERN, Geneva, CERN Divisional Report TIS-RP/156/CF.

Rau, G., and Wittekind, D. (1982a). "Environmental Radiation Monitoring on the CERN Sites During 1981." European Organization for Nuclear Research CERN, Geneva, Report No. HS-RP/IR/82-13.

Rau, G., and Wittekind, D. (1982b). "Proposal for Measuring the Natural Radiation Around the Future LEP." European Organization for Nuclear Research CERN, Geneva, Report No. HS-RP/TM/82-28.

Remy, R. (1965). "Neutron Spectroscopy by the Use of Nuclear Stars from 20 to 300 MeV." Lawrence Radiation Laboratory, Berkeley, California, Report No. UCRL-16325 (M.S. Thesis).

Rhoades, W.A., Simpson, D.B., Childs, R.L., and Engle, W.W. (1978). "The DOT-IV Two-Dimensional Discrete Ordinates Transport Code with Space-Dependent Mesh and Quadrature." Oak Ridge National Laboratory Technical Memorandum ORNL/TM-6529.

Ribes, J.G., Moy, B., and Rau, G. (1974). "Système de Mesure de la Radioactivité de l'Air." European Organization for Nuclear Research CERN, Geneva, Internal Report LAB II-RA/Note/74-6.

Ribes, J.G., Moy, B., and Rau. G. (1976). "Etalonnage du Système de Ventilation." European Organization for Nuclear Research CERN, Geneva, Internal Report SPS/CA/SDM/76-18.

Richard-Serre, C. (1971). "Evaluation de la Perte d'Energie Unitaire et du Parcours pour des Muons de 2 à 600 GeV dans un Absorbant Quelconque." European Organization for Nuclear Research CERN, Geneva, Report CERN 71-18.

Rindi, A. (1969). Present and projected uses of multiwire spark chambers in health physics. *In* "Proc. Second Symposium on Accelerator Dosimetry and Experience," Stanford, CA, November 1969, USAEC Report CONF-691101, p. 660–671.

Rindi, A. (1972a). "Induced Radioactivity in the Cooling Waters of the 300 GeV SPS." European Organization for Nuclear Research CERN, Geneva, Internal Report Lab II-RA/Note/72-13.

Rindi, A. (1972b). "La Radioactivé Induite dans l'Air de l'Accélérateur de Protons de 300 GeV du CERN." European Organization for Nuclear Research CERN, Geneva, Internal Report CERNLABII RA/72-5.

Rindi, A. (1974a). An analytical expression for the neutron flux-to-dose [equivalent] conversion factors. *Health Physics 27*, 322-323.

Rindi, A. (1974b). A spectrometer for measuring charged particles and neutrons. *Nucl. Instrum. Methods 116*, 471-475.

Rindi, A. (1977). An analytical expression for the neutron flux-to-absorbed-dose conversion factor. *Health Physics 33*, 264-265.

Rindi, A. (1982). Gas bremsstrahlung from electron storage rings. *Health Physics 42*, 187–193.

Rindi, A., and Baarli, J. (1963). "Scattered Radiation at Large Distance from the CERN 600 MeV

Synchrocyclotron." European Organization for Nuclear Research CERN, Geneva, CERN Internal Report DI/HP/19.

Rindi, A., and Charalambus, S. (1967). Airborne radioactivity produced at high-energy accelerators. *Nucl. Instrum. Methods 47*, 227-232.

Rindi, A., and Thomas, R.H. (1973). The radiation environment of high-energy accelerators. *Ann. Rev. Nucl. Sci. 23*, pp. 315-346. Annual Reviews, Inc., Palo Alto, California.

Rindi, A., and Thomas, R.H. (1975). Skyshine — a paper tiger? *Particle Accel. 7*, 23-39.

Rindi, A., and Henson, A.M. (1976). "The Fading of Tracks in NTA Film." Lawrence Berkeley Laboratory Health Physics Dept. Note HPN-55.

Rogers, D.W.O. (1979). Why not to trust a rem-meter. *Health Physics 37*, 735-742.

Rohloff, F., and Heinzelmann, M. (1973). Influence of detector types and equipment on the sensitivity of Bonner spheres. *In* "Neutron Monitoring for Radiation Protection Purposes." International Atomic Energy Agency, Vienna, pp. 269–277.

Rossi, B. (1952). "High-Energy Particles." Ch. 5, Prentice-Hall, Englewood Cliffs, New Jersey.

Rossi, B., and Greisen, K. (1941). Cosmic-ray theory. *Rev. Mod. Phys. 13*, 240-309.

Rossi, H.H. (1977). A proposal for revision of the quality factor. *Radiat. and Environm. Biophys. 14*, 275-283.

Rossi, H.H., and Rosenzweig, W. (1955). A device for the measurement of dose as a function of specific ionization. *Radiology 64*, 404-411.

Rossi, H.H., and Failla, G. (1956). Tissue-equivalent ionization chamber. *Nucleonics 14*(2), 32-37.

Routti, J.T. (1969). "High-Energy Neutron Spectroscopy with Activation Detectors Incorporating New Methods for the Analysis of Ge(Li) Gamma-Ray Spectra and the Solution of Fredholm Integral Equations." Lawrence Berkeley Laboratory, Berkeley, California, Report No. UCRL-18514, (Ph.D. Thesis).

Routti, J.T., and Sandberg, J.V. (1980a). General purpose unfolding program LOUHI 78 with linear and nonlinear regularisations. *Compt. Phys. Commun. 21*, 119-144.

Routti, J.T., and Sandberg, J.V. (1980b). Unfolding techniques for activation detector analysis. *In op. cit.* (W.R. Nelson and T.M. Jenkins, 1980), "Computer Techniques in Radiation Transport and Dosimetry" (Plenum, New York and London), pp. 389-407.

Routti, J.T., and Sandberg, J.V. (1985). Unfolding activation and multisphere detector data. *Radiat. Prot. Dosim. 10* (1-4), 103-110.

Rudstam, G. (1966). Systematics of spallation yields. *Z. Naturforschg. 21a*, 1027-1041.

Russell, J.E., and Ryan, R.M. (1965). Radioactive gas production from the R.P.I. electron linear accelerator. *IEEE Trans. Nucl. Science NS-12* (3), 678-682.

Sandberg, J.V. (1982). Angular and energy distribution measurements of second hadron fluxes with

multireaction spallation detectors at CERN SPS. *Nucl. Instrum. Methods 200*, 211–218.

Sanders, F.W., Haywood, F.F., Lundin, M.I., Gilley, L.W., Cheka, J.S., and Ward, D.R. (1962). "Operation Plan and Hazards Report—Operation BREN." Oak Ridge National Laboratory, USAEC Report CEX-62.02.

Sands, M. (1970). "The Physics of Electron Storage Rings." Stanford Linear Accelerator Center, Stanford, California, Report SLAC-121.

Sanna, R.S. (1973). "Thirty-one Group Response Matrices for the Multisphere Neutron Spectrometer over the Energy Range Thermal to 400 MeV." Health and Safety Laboratory, New York, USAEC Report HASL-267 (March 1973).

Sanna, R., and O'Brien, K. (1971). Monte-Carlo unfolding of neutron spectra. *Nucl. Instrum. Methods 91*, 573-576.

Sanna, R.S., Hajnal, F., McLaughlin, J.E., Gulbin, J.G., and Ryan, R.M. (1980). "Neutron Measurements inside PWR Containments." Environmental Measurements Laboratory, New York, USDOE Report EML-379,

Sargent, T.W. (1962). Lawrence Berkeley Laboratory. Private communication, quoted in Patterson *et al.* (1969).

Scharf, W. (1986). "Particle Accelerators and their Uses." In two parts. Part 1: Accelerator Design; Part 2: Applications of Accelerators. Harwood Academic Publishers, Chur.

Schilthelm, S.W., DeLuca, Jr., P.M., Swanson, W.P., Otte, R.A., and Pedley, R.T. (1985). "Steady State Radiation Survey Measurements at Aladdin Synchrotron Light Source." Synchrotron Radiation Center, University of Wisconsin, Stoughton, Wisconsin, Technical Note SRC-32.

Schwinger, J. (1949). On the classical radiation of accelerated electrons. *Phys. Rev. 75*, 1912-1925.

Seltzer, S.M., and Berger, M.J. (1982a). Evaluation of the collision stopping power of elements and compounds for electrons and positrons. *Int. J. Appl. Radiat. Isot. 33*, 1189-1218.

Seltzer, S.M., and Berger, M.J. (1982b). Procedure for calculating the radiation stopping power for electrons. *Int. J. Appl. Radiat. Isot. 33*, 1219–1226.

Seltzer, S.M., and Berger, M.J. (1985). "Bremsstrahlung spectra from electron interactions with screened atomic nucleii and orbital electrons." *Nucl. Instrum. Methods in Phys. Res. B12*, 96-134.

Sharpe, J., and Stafford, G.H. (1951). The $^{12}C(n,2n)^{11}C$ reaction in an anthracene crystal. *Proc. Phys. Soc. (London) A64*, 211-212.

Shave, A.J. (1970). "The Extraction of Terbium from Mercury by a Chemical Method." Rutherford Laboratory Internal Report RP/PN/43.

Shaw, K.B. (1962). "High-Energy Flux Measurements Using Plastic Scintillators." European Organization for Nuclear Research CERN, Geneva, Internal Report DI/HP/6.

Shaw, K.B., and Thomas, R.H. (1964). "Shielding Experiment at 6 GeV — Parts I and II." Lawrence Berkeley Laboratory Internal Reports UCID-10021 and UCID-10023.

Shaw, K.B., and Thomas, R.H. (1967). Radiation problems associated with a high-energy extracted proton beam. *Health Physics 13*, 1127–1132.

Shaw, K.B., Stevenson, G.R., and Thomas R.H. (1969). Evaluation of dose equivalent from neutron energy spectra. *Health Physics 17*, 459–469.

Shen, S.P. (1964). "Passage of High-Energy Particles in Matter: Nuclear Cascades Induced in Dense Media by 1 and 3 GeV Protons." Brookhaven National Laboratory Report BNL-8721.

Simpson, P.W. (1964). "The Measurement of Accelerator Produced Neutron Flux by Activation of Indium, Gold and Cobalt." Rutherford Laboratory Report NIRL/M/70.

Simpson, P.W., and Laws, D. (1962). "Neutron Surveys around the Rutherford Laboratory." Rutherford Laboratory Internal Report, Addendum to NIRL/M/30 (Thomas et al., 1962).

Sinclair, W.K. (1985). Experimental RBE values of high LET radiations of low doses and the implications for quality factor assignment. *Radiat. Prot. Dosim. 13*(1–4), 319–326.

Skarsgard, L. (ed.) (1983). "Pion and Heavy Ion Radiotherapy: Pre-Clinical and Clinical Studies." Elsevier, North Holland, Amsterdam.

SLAC (1969). "Proc. 2nd Int. Conf. on Accelerator Dosimetry and Experience," held at Stanford Linear Accelerator Center, Nov. 5-7, 1969, USAEC, Washington, D.C., Report CONF-691101.

SLAC (1974). "Proc. 9th Int. Conf. on High Energy Accelerators," Stanford Linear Accelerator Center, May 2–7, 1974 (R.B. Neal, Chairman), Stanford Linear Accelerator Center Report CONF-740522.

Smith, A.R. (1958). "The Stray Radiation Field of the Bevatron." Lawrence Berkeley Laboratory Internal Report UCRL-8377 (July, 1958).

Smith, A.R. (1961). A cobalt neutron flux integrator. *Health Physics 7*, 40–47.

Smith, A.R. (1962). "Measurements of the Radiation Field Around High-Energy Accelerators." Lawrence Berkeley Laboratory Internal Report UCRL-10163.

Smith, A.R. (1965a). Some experimental shielding studies at the 6.2 BeV Berkeley Bevatron. *In op.cit.*, "Proc. First Symposium on Accelerator Radiation and Experience," Brookhaven National Laboratory, Nov. 3-5, 1965, USAEC, Washington, D.C., Report CONF-651109, pp. 365-409.

Smith, A.R. (1965b). Threshold detector applications to neutron spectroscopy at the Berkeley accelerators. *In* "Proceedings of First Symposium on Accelerator Dosimetry and Experience," Brookhaven National Laboratory, November 1965, USAEC Report CONF-651109, 224–273.

Smith, A.R. (1966). "A Tantalum Fast Neutron Integrator." Lawrence Berkeley Laboratory Internal Report UCRL-17051.

Smith, A.R. (1977). Lawrence Berkeley Laboratory. Private communication.

Smith, A.R., and Thomas, R.H.(1976). The production of ^{11}C by the interaction of 375 MeV/amu Ne^{10+} ions with carbon. *Nucl. Instrum. Methods 137*, 459-461.

Smith, A.R., McCaslin, J.B., and Pick, M. (1965). "Radiation Field inside a Thick Concrete Shield for 6.2 BeV Incident Protons." Lawrence Radiation Laboratory, Berkeley, California, Report UCRL-11331.

Smith, A.R., Stephens, L.D., and Thomas, R.H. (1977). Dosimetry for radiobiological experiments that use energetic heavy ions. *Health Physics 32*, 343-350.

Smith, A.R., Schimmerling, W., Kanstein, L.L., McCaslin, J.B., and Thomas, R.H. (1981). "Neutron flux density and secondary particle spectra at the 184-inch synchrocyclotron medical facility." *Medical Physics 8*, 668–676.

Smith, L.W., and Kruger, P.G. (1951). Thick target yields from the (d,n) reaction at 10 MeV. *Phys. Rev. 83*, 1137–1140.

Solon, L.R. (ed.) (1957). "Proc. Conf. on Shielding of High-Energy Accelerators." New York, April 11–13, 1957, USAEC Report TID-7545.

SRI (1980). Proc. National Conf. Synchrotron Radiation Instrumentation, Gaithersburg, Maryland, June 4-6, 1979 (D.L. Ederer and J.B. West, eds.) *Nucl. Instrum. Methods 172*(1,2), 1–406.

SSC (1986). "Conceptual Design of the Superconducting Super Collider." (J.D. Jackson, ed.). SSC Central Design Group (c/o Lawrence Berkeley Laboratory) Report SSC-SR-2020.

SSC (1987). "SSC Environmental Radiation Shielding." Superconducting Super Collider Central Design Group (c/o Lawrence Berkeley Laboratory) Task Force Report SSC-SR-1026 (J.D. Jackson, ed.).

Stapleton, G.B., and Thomas, R.H. (1967). "Radioassay for ^{7}Be and ^{3}H of Nimrod Cooling Water." Rutherford Laboratory Internal Note RP/PN/45.

Stapleton, G.B., and Thomas, R.H. (1971). The production of ^{7}Be by 7 GeV proton interactions with oxygen. *Nucl. Phys. A175*, 124-128.

Stapleton, G.B., and Thomas, R.H. (1972). Estimation of the induced radioactivity of the groundwater system in the neighbourhood of a proposed 300-GeV high-energy accelerator situated on a chalk site. *Health Physics 23*, 689–699.

Stapleton, G.B., and Thomas, R.H. (1973). The effect of sorption on the migration of ^{7}Be from a high-energy accelerator constructed on a chalk site. *Water Research 7*, 1259-1268.

Steinberg, M. (1983). The spallator and APEX nuclear fuel cycle — a new option for nuclear power. *IEEE Trans. Nucl. Sci. NS-30(1)*, 14-19.

Stephens, L.D., and Aceto, H., Jr. (1963). Variation of a fission-neutron flux and spectrum from a fast reactor measured over large distances. *In* "Neutron Dosimetry, Proc. Symposium on Neutron Detection, Dosimetry and Standardization," 10-14 Dec. 1962, Harwell, U.K., Vol. 1, pp. 535-545, International Atomic Energy Agency, Vienna.

Stephens, L.D., and Miller, A.J. (1969). Radiation studies at a medium energy accelerator. *In op.cit.* "Proc. 2nd Int. Conf. on Accelerator Dosimetry and Experience," Stanford Linear Accelerator Center, Nov. 5-7, 1969, USAEC, Washington, D.C., Report CONF-691101, pp. 459-485.

Stephens, L.D., and Smith, A.R. (1958). "Fast Neutron Surveys Using Indium Foil Activation." Lawrence Berkeley Laboratory Report UCRL-8418.

Stephens, L.D., Smith, A.R., and Thomas, R.H. (1976). An analytical approach to environmental radiation measurements. *IEEE Trans. Nucl. Sci. 23*(1), 719-725.

Stephens, L.D., Thomas, R.H., and Thomas, S.B. (1975). Population exposure from high energy accelerators. *Health Physics 29*, 853–860.

Stephens, L.D., Thomas, R.H., and Thomas, S.B. (1976). A model for estimating population exposures due to the operation of high energy accelerators at the Lawrence Berkeley Laboratory. *Health Physics 30*, 404–407.

Sternheimer, R.M., and Peierls, R.F. (1971). General expression for the density effect for the ionization loss of charged particles. *Phys. Rev. B3*, 3681-3692.

Stevenson, G.R. (1967). "Neutron Spectrometry from 0.025 eV to 25 GeV." Rutherford Laboratory Report RHEL/R-154.

Stevenson, G.R. (1971). "Evaluation of Neutron Dose Equivalent Around Nimrod." Rutherford Laboratory Internal Report RP/PN/56.

Stevenson, G.R. (1981a). "Analytic Expressions for the Synchrotron Spectrum." European Organization for Nuclear Research CERN, Geneva, Report HS-RP/IR/81-15.

Stevenson, G.R. (1981b). "A Description of the TOMCAT Muon Transport Program." European Organization for Nuclear Research CERN, Geneva, Report HS-RP/IR-81-28.

Stevenson, G.R. (1983). "Dose and Dose Equivalent from Muons." European Organization for Nuclear Research CERN, Geneva, Report TIS-RP/099.

Stevenson, G.R. (1984a). The estimation of dose equivalent from the activation of plastic scintillators. *Health Physics 47*, 837–847.

Stevenson, G.R. (1984b). "Estimation of Star Densities in the Cooling Water of Certain SPS Machine Components." European Organization for Nuclear Research CERN, Geneva, Report TIS-RP/IR/84-12.

Stevenson, G.R. (1984c). "Calculations of dE/dx and Muon Ranges in Concrete and Earth." European Organization for Nuclear Research CERN, Geneva, Report TIS-RP/IR/74-07.

Stevenson, G.R. (1985). European Organization for Nuclear Research CERN, Geneva. Private communication.

Stevenson, G.R. (1986). "Dose Equivalent per Star in Hadron Cascade Calculations." European Organization for Nuclear Research CERN, Geneva, Report No. TIS-RP/173.

Stevenson, G.R. (1988). European Organization for Nuclear Research CERN, Geneva. Private communication.

Stevenson, G.R., and Marshall, T.O. (1964). "A Study of Latent Image Fading in the Kodak Personal Neutron Film, Type B." Radiological Protection Service, Sutton, Surrey (U.K.), Internal Report No. RPS/I/3.

Stevenson, G.R., and Thomas, R.H. (1984). A simple procedure for the estimation of neutron skyshine from proton accelerators. *Health Physics 46*, 115–122.

Stevenson, G.R., Fassò, A., Sandberg, J., Regelbrugge, A., Bonifas, A., Muller, A., and Nielsen, M. (1983). "Measurements of the Dose and Hadron Yield from Copper Targets in 200 GeV/c and 400 GeV/c Extracted Proton Beams. An Altas of the Results Obtained." European Organization for Nuclear Research

CERN, Geneva, Report No. TIS-RP/112.

Stevenson, G.R., Aarnio, P.A., Fassò, A., Ranft, J., Sandberg, J., and Sievers, P. (1985). "Comparison of Angular Hadron Energy Spectra, Induced Activity and Dose with FLUKA82 Calculations." Presented at the CERN Workshop on Shower Simulation for LEP Experiments, Jan. 29-31, 1985, European Organization for Nuclear Research CERN, Geneva, Report TIS-RP/158/CF.

Stevenson, G.R., Aarnio, P.A., Fassò, A., Ranft, J., Sandberg, J.V., and Sievers, P. (1986). Comparison of measurements of angular hadron energy spectra, induced activity and dose with FLUKA82 calculations. *Nucl. Instrum. Methods A245*, 323–327.

Stevenson, G.R., Squier, D.M., and Levine, G.S. (1971). "Measurements of the Angular Dependence of Dose and Hadron Yield from Targets in 8 GeV/c and 24 GeV/c Extracted Proton Beams." Rutherford Laboratory, Chilton, U.K., Report No. RHEL/MR-7.

Storm, E., and Israel, H.I. (1967). "Photon Cross Sections from 0.001 to 100 MeV for Elements 1 through 100." Los Alamos Scientific Laboratory Report LA-3753; and (1970) "Nuclear Data Tables A7," Academic Press, New York, pp. 565-681.

Sullivan, A.H. (1982). "Dose Rates from Radioactivity Induced in Thin Foils." European Organization for Nuclear Research CERN, Geneva, Internal Report HS-RP/IR/82-46.

Sullivan, A.H. (1983). "Some Ideas on Radioactivity Induced in High-Energy Particle Accelerators." European Organization for Nuclear Research CERN, Geneva, Internal Report TIS-RP/TM/83-27.

Sullivan, A.H., and Baarli, J. (1963). "An Ionization Chamber for the Estimation of the Biological Effectiveness of Radiation." European Organization for Nuclear Research CERN, Geneva, Report CERN 63-17.

Sullivan, A.H., and Overton, T.R. (1965). Time variation of the dose rate from radioactivity induced in high-energy particle accelerators. *Health Physics 11*, 1101–1105.

Swanson, W.P. (1975). "X-Ray Radiation Observed around a PEP Cavity." Stanford Linear Accelerator Center, Stanford, California, Internal Report.

Swanson, W.P. (1978). Calculation of neutron yields released by electrons incident on selected materials. *Health Physics 35*, 353-367.

Swanson, W.P. (1979a). "Radiological Safety Aspects of the Operation of Electron Linear Accelerators." Technical Report Series No. 188, International Atomic Energy Agency, Vienna.

Swanson, W.P. (1979b). Improved calculation of photoneutron yields released by incident electrons. *Health Physics 37*, 347-358.

Swanson, W.P., DeLuca, P.M., Jr., Otte, R.A., and Schilthelm, S.W. (1985). "Aladdin Upgrade Design Study." Synchrotron Radiation Center, Univ. of Wisconsin, Stoughton, Wisconsin.

Tai, Y.-K., Millburn, G.P., Kaplan, S.N., and Moyer, B.J. (1958). Neutron yields from thick targets bombarded by 18- and 32-MeV protons. *Phys. Rev. 109*, 2086-2091.

Tait, W.H. (1980). "Radiation Detection." Butterworths, London.

Tamura, M. (1965). A study of electron-photon showers by the Monte Carlo method. *Prog. Theor. Phys.*

34, 912-941.

Tardy-Joubert, Ph. (1965). Methods and experience acquired in dosimetry at the synchrotron Saturne. *In* "Proc. First Symposium on Accelerator Radiation Dosimetry and Experience," USAEC Report CONF-651109, pp. 117–143.

Tesch, K. (1966). Dosisleistung und Toleranzflussdichte hochenergetischer Elektronen- und Gammastrahlen. *Nukleonik 8*, 264-266.

Tesch, K. (1970). Neutron dosimetry in the energy range between 10 and 100 MeV. *Nucl. Instrum. Methods 83*, 295-299.

Tesch, K. (1984). Measurement of doses between 10^{-2} and 10^{8} Gy with glass dosemeters. *Rad. Prot. Dosim. 6*, 347–349.

Tesch, K. (1985). A simple estimation of the lateral shielding for proton accelerators in the energy range 50 to 1000 MeV. *Radiat. Prot. Dosim. 11*, 165-172.

Tesch, K. (1986). Deutsches Elektronen-Synchrotron, Hamburg, F.R.G. Private communication.

Tesch, K. (1988). Deutsches Elektronen-Synchrotron, Hamburg, F.R.G. Private connumication.

Tesch, K., and Dinter, H. (1986). Estimation of radiation fields at high energy proton accelerators. *Radiat. Prot. Dosim. 15*, 89-107.

Theriot, D., Awschalom, M., Lee, K. (1971). Muon shielding calculations: Heterogeneous passive and active shields, applications to experimental beams and areas. *In* "Proc. Int. Cong. Radiat. Prot. Accel. and Space Radiat.," European Organization for Nuclear Research CERN, Geneva, Report CERN 71-16, p. 641–651.

Thomas, R.H. (ed.) (1963). "Report of the Shielding Conference Held at the Rutherford Laboratory 26–27th September 1962." Rutherford Laboratory Internal Report NIRL/R/40.

Thomas, R.H. (1964). "Energy Loss of High-Energy Muons." Lawrence Radiation Laboratory, Berkeley, California, Report UCID-10010.

Thomas, R.H. (1970). Possible contamination of groundwater system by high-energy accelerators. *In* "Proc. Fifth Annual Health Physics Soc., Mid-Year Topical Symposium on the Health Physics Aspects of Nuclear Facility Siting," November 3–6, Idaho Falls, p. 93 (1970). Also published as Lawrence Berkeley Laboratory Internal Report UCRL-20131.

Thomas, R.H. (1972). Radioactivity in earth induced by high-energy electrons. *Nucl. Instrum. Methods 102*, 149-155.

Thomas, R.H. (1973). Neutron dosimetry at high-energy particle accelerators. *In* "Neutron Monitoring for Radiation Protection Purposes," International Atomic Energy Agency, Vienna, Report IA-SM-167/49, Vol. 1, pp. 327-353.

Thomas, R.H. (ed.) (1976). "The Environment Surveillance Program of the Lawrence Berkeley Laboratory." Lawrence Berkeley Laboratory Internal Report LBL-4678.

Thomas, R.H. (1978a). "The Radiological Impact of High-Energy Accelerators on the Environment." Lawrence Berkeley Laboratory Report LBL-8101.

Thomas, R.H. (1978b). Environmental radiation from particle accelerators. *Research Accelerators 3*(6), pp. 14-21. (Lawrence Berkeley Laboratory, PUB-300.)

Thomas, R.H. (1981). The value of $\overline{W}(E)$ in nitrogen for high-energy ions. *Radiat. Res. 90*, 437-440.

Thomas, R.H., and Rindi, A. (1979). Radiological environmental impact of high-energy accelerators. *Critical Reviews of Environmental Control 9*(1), 51-95.

Thomas, R.H., and Perez-Mendez, V. (eds.) (1980). "Advances in Radiation Protection and Dosimetry in Medicine." Plenum Press, New York.

Thomas, R.H., and Stevenson, G.R. (1985). Radiation protection around high-energy accelerators. *Radiat. Prot. Dosim. 10* (1–4), 283-301.

Thomas, R.H., and Stevenson, G.R. (1988). "Radiological Safety Aspects of the Operation of Proton Accelerators." International Atomic Energy Agency, Vienna, IAEA Technical Report No. 283.

Thomas, R.H., Shaw, K.B., Simpson, P.W., and MacEwan, J.F. (1962). "Neutron Surveys around the Rutherford Laboratory 50 MeV Proton Linear Accelerator." Rutherford Laboratory Report NIRL/M/30 (March 1962).

Thomas, R.H., De Castro, T.M., and Lyman, J.T. (1980). A measurement of the average energy required to create an ion pair in nitrogen by high-energy ions. *Radiat. Res. 82*, 1-12.

Thorne, M.C. (1986). Scientific Secretary ICRP, London. Private communication.

Thorngate, J.H., and Griffith, R.V. (1985). Neutron spectrometers for radiation monitoring at Lawrence Livermore National Laboratory. *Radiat. Prot. Dosim. 10* (1-4), 125-135.

Tobias, C.A. (1985). The future of heavy-ion science in biology and medicine. (20th Failla Memorial Lecture, 1983 Meeting of the Radiation Research Society, San Antonio, Texas), *Radiat. Res. 103*, 1-33.

Tobias, C.A., Anger, H.O., and Lawrence, J.H. (1952). Radiological use of high-energy deuterons and alpha particles. *Am. J. Roentgenol. 67*, 1-27.

Tobias, C.A., Lyman, J.T., and Lawrence, J.H. (1971). Some considerations of physical and biological factors in radiotherapy with high-LET radiations including heavy particles, pi mesons, and fast neutrons. *Prog. Atomic Medicine: Recent Advances in Nuclear Medicine 3*, 167-218. Grune and Stratton, Orlando, FL.

Tobias, C.A., Benton, E.V., Capp, M.P., Chatterjee, A., Cruty, M.R., and Henke, R.P. (1977). Particle radiography and autoactivation. *Int. J. Radiat. Oncol. Biol. Phys. 3*, 35-44.

Tommasino, L., and Harrison, K.G. (1985). Damage track detectors for neutron dosimetry: I. Registration and counting methods. *Radiat. Prot. Dosim. 10*(1-4), 207-217.

Tommasino, L., Zapparoli, G., Djeffal, S., and Griffith, R.V. (1984). A simple and sensitive fast neutron dosimeter using CR-39. *In* "Proc. of the 10th DOE Workshop on Personnel Neutron Dosimetry," Acapulco, 30 Aug.–1 Sept. 1983. Battelle Pacific Northwest Laboratory Report No. PNL-SA-12352 (CONF-8308140), pp. 141-155.

TRIUMF (1986). Cyclotron Division. "TRIUMF Annual Report Scientific Activities 1985." TRIUMF, Vancouver, B.C. Canada, pp. 90-112.

Tsai, Y.-S. (1974). Pair production and bremsstrahlung of charged leptons. *Rev. Mod. Phys. 46*, 815-851.

Tuyn, J.W.N. (1977). The use of thermoluminescent dosimeters for environmental monitoring around high energy accelerators. *In* "Proc. of the 5th International Conference on Luminescence Dosimetry," 14-17 Feb. 1977, Saõ Paulo, Brazil, pp. 288-297.

Tuyn, J.W.N. (1982). Radiation protection monitoring around high energy proton accelerators using thermoluminescence dosemeters. *Radiat. Prot. Dosim. 2*, 69-74.

UNSCEAR (1982). "Ionizing Radiation. Sources and Biological Effects." United Nations Scientific Committee on the Effects of Atomic Radiation, Report of 37th Session, Suppl. No. 45 (A/37/45), United Nations, New York.

Van Atta, C.M., Lee, J.D., and Heckrotte, W. (1976), "The Electronuclear Conversion of Fertile to Fissile Material." Lawrence Livermore Laboratory Report UCRL-52144.

Van Dilla, M.A., and Engelke, M.J. (1960). Zinc-65 in cyclotron workers. *Science 131*, 830-832.

Van Ginneken, A. (1972). "Weighted Monte-Carlo Calculations of Hadronic Cascades in Thick Targets." Fermi National Accelerator Laboratory, Batavia, Illinois, Report NAL-FN-250.

Van Ginneken, A. (1975). "CASIM, Program to Simulate Hadronic Cascades in Bulk Matter." Fermi National Accelerator Laboratory, Batavia, Illinois, Report FN-272.

Van Ginneken, A. (1975). "Penetration of Prompt and Decay Muon Components of Hadronic Cascades through Thick Shields." Fermi National Accelerator Laboratory, Batavia, Illinois, Report TM-630.

Van Ginneken, A. (1980). Calculation of the average properties of hadronic cascades at high energies (CASIM). *In* "Computer Techniques in Radiation Transport and Dosimetry" (W.R. Nelson and T.M. Jenkins, eds.), Plenum Press, New York and London, pp. 323-338.

Van Ginneken, A. (1986). Energy loss and angular characteristics of high energy electromagnetic processes. *Nucl. Instrum. Methods Phys. Res. A251*, 21-39.

Van Ginneken, A., and Awschalom, M. (1974). "High Energy Particle Interactions in Large Targets." Vol. 1, Fermi National Accelerator Laboratory Report (unnumbered).

Van Ginneken, A., and Borak, T. (1971). Beamstop experiment at 29.4 GeV. *IEEE Trans. Nucl. Sci. NS-18*(3), 746-747.

Van Ginneken, A., Yurista, P., and Yamaguchi, C. (1987). "Shielding Calculations for Multi-TeV Hadron Colliders." Fermi National Accelerator Laboratory, Batavia, Illinois, Report FN-447 (SSC-106).

van Steenbergen, A. (1979). Synchrotron radiation sources. *IEEE Trans. Nucl. Sci. NS-26(3)*, 3785-3790.

Varfolomeev, A.A., and Drabkin, L.B. (1966). "Calculations of Electromagnetic Showers in Lead with an Initial Energy of 6 GeV." Institute of Atomic Energy, USSR, Report IAE-1201. Transl. Oak Ridge National Laboratory Report ORNL-tr-1923 (1968).

Varfolomeev, A.A., and Svetlolobov, I.A. (1959). Monte Carlo calculations of electromagnetic cascades with account of the influence of the medium on bremsstrahlung. *Zh. Ekhsp. Teor. Fiz. 36*, 1771-1781. Transl. *Sov. Phys.-JETP 36*, 1263-1270 (1959).

Viallettes, H. (1969). "Gas and dust activation in the target room of the Saclay electron linac — Identification of the produced radioactive nuclei and determination of the rejected activities." *In* "Proc. Second Int. Conference on Accelerator Dosimetry and Experience," Stanford, November 1969, USAEC Report CONF-691101, p. 121–138.

Völkel, U. (1965). "Elektron-Photon-Kaskaden in Blei für Primärteilchen der Energie 6 GeV." Deutsches Elektronen-Synchrotron DESY, Hamburg, F.R.G., Report DESY-65/6.

Völkel, U. (1967). "A Monte Carlo Calculation of Cascade Showers in Copper Due to Primary Photons of 1 GeV, 3 GeV and 6 GeV, and to a 6-GeV Bremsstrahlung Spectrum." Deutsches Elektronen-Synchrotron DESY, Hamburg, F.R.G., Report DESY-67/16.

Volynchikov, A.I., Getmanov, V.B., Kuznetsov, A.A., Krupnyi, G.I., Lukahihn, V.S., Rastsvetalov, Ya, N., and Tatarenko, V.H. (1983). "Secondary Radiation Field Measurements in a Steel Block Absorbing 69 GeV/c Proton Beams." Institute for High Energy Physics, Serpukhov, U.S.S.R., Report IFVE-83-86. Transl. I. Schulz-Dahlen, Deutsches Elektron-Synchrotron DESY, Hamburg, F.R.G., Report DESY-L-Trans-284 (1983).

Wadman, W.W. (1964). "Angular Distribution of Neutrons Produced by 40- and 80-MeV α Particles on a Thick Tantalum Target." Lawrence Radiation Laboratory, Berkeley, California, Report UCRL-11375.

Wallace, R., Moyer, B.J., Patterson, H.W., Smith, A.R., and Stephens, L.D. (1961). The dosimetry of high-energy neutrons produced by 6.2-GeV protons accelerated in the Bevatron. *In* "Proc. Symposium on Selected Topics in Radiation Dosimetry," Vienna, 7-11 June 1960, pp. 579-588, International Atomic Energy Agency, Vienna, IAEA Publication STI/PUB/25.

Weinstein, M., Hajnal, F., McLaughlin, J., and O'Brien, K. (1970). "Neutron Dose Equivalent from Multisphere Accelerator Shield Leakage Spectra." USAEC Report HASL-223, March 1970.

Weisskopf, V. (1937). Statistics and nuclear reactions. *Phys. Rev. 52*, 295-303.

Wiegand, C.W. (1949). High-energy neutron detector. *Rev. Sci. Instrum. 19*, 790-792.

Wilson, R.R. (1952). Monte Carlo study of shower production. *Phys. Rev. 86*, 261-269. [E_0 = 20, 50, 100, 200, 300, 500 MeV].

Wilson, R.R. (1964). Radiological use of fast protons. *Phys. Med. Biol. 47*, 487-491.

Wilson, R.R., and Littauer, R. (1960). "Accelerators - Machines of Nuclear Physics." Anchor Books, Doubleday and Co., Inc., Garden City, New York.

Woischnig, W., and Burmeister, H. (1964). Berechnung von Elektronen-Photonen-Kaskaden nach der Monte-Carlo Methode. *Z. Phys. 117*, 151-156.

Wollenberg, H.A., and Smith, A.R. (1969). Energy and flux determinations of high-energy nucleons. *In* "Proc. Second. International Conference on Accelerator Dosimetry and Experience," Stanford, November 1969, USAEC Report CONF-691101, pp. 586–594.

Wollenberg, H.A., and Smith, A.R. (1973). Fission track detectors. "Experiment 12 in Accelerator Health Physics" (Patterson, H.W. and Thomas, R.H.), pp. 656–660. Academic Press, New York.

Yagoda, H. (1949). "Radioactive Measurements with Nuclear Emulsions." John Wiley, New York; Chapman and Hall, London.

Yamaguchi, C. (1981). "Absorbed Dose and Energy Deposition Calculation Due to Synchrotron Radiation from PETRA, HERA and LEP." Deutsches Elektronen-Synchrotron DESY, Hamburg, F.R.G., Report D3-38.

Yamaguchi, C. (1982). Comparison of absorbed dose to RPL glass dosimeter calculated by EGS code and kerma. *Nucl. Instrum. Methods 197*, 473-476.

Yuda, T., Masaike, A., Kusumegi, A., Murata, Y., Ohta, I., and Nishimura, J. (1970). Electron-induced cascade showers in lead, copper and aluminum. *Nuovo Cimento 65A*, 205-228.

Zaitsev, L.N., Komochkov, M.M., and Sychev, B.S. (1971). "Fundamentals of Shielding for Accelerators." Atomizdat, Moscow.

Zanstra, H. (1935). Ein kurzes Verfahren zur Bestimmung des Sättigungsstromes nach der Jaffé'schen Theorie der Kolonnenionisation. *Physica 2*, 817-824.

Zerby, C.D., and Moran, H.S. (1962a). "Monte-Carlo Calculation of the Three-Dimensional Development of High-Energy Electron-Photon Cascade Showers," Oak Ridge National Laboratory Report ORNL-422.

Zerby, C.D., and Moran, H.S. (1962b). "A Monte Carlo Calculation of the Three Dimensional Development of High Energy Electron Photon Cascade Showers." Oak Ridge National Laboratory Report ORNL-3329; also *J. Appl. Phys. 34*, 2445-2457 (1963). The ORNL report contains extensive tables not included in the published version.

Zielczynski, M. (1962). Use of columnar recombination to determine the biological effectiveness of radiation. *Nukleonika 7*, 175-182 (in Russian). English transl. in *Nukleonika* Vol. 7 (1-12), pp. 213-223 (1965). Available from Office of Technical Services, U.S. Dept. of Commerce, Washington, D.C.]

Zielczynski, M. (1963). Recombination method for determination of linear energy transfer (LET) of mixed radiation. *In* "Neutron Dosimetry, Proceedings of the Symposium on Neutron Detection, Dosimetry and Standardization," 10-14 Dec. 1962, Harwell, U.K., Vol. 2 (International Atomic Energy Agency, Vienna) pp. 397-404 (in Russian).

Zielczynski, M. (1971). Integral signal methods for determination of dose equivalent. *In* "Radiation Dosimetry, Proceedings of the International Summer School on Radiation Protection," Cavtat, Yugoslavia, September 21-30, 1970, Vol. 2, pp. 60-74.

Zielczynski, M., Lebedev, V.N., and Salatskaya, M.I. (1964). Instrument for determination of recommended relative biological effectiveness of radiation. *Pribory i Tekhn. Eksperim. 6*, 73-76. [English Transl. *Instruments and Experimental Techniques 6*, pp. 1217-1220 (1965).]

VII. TABLES

Table I. High-energy hadron synchrotrons and storage rings (≥1 GeV).

Designation	Location	Particle type	Energy (GeV)	Status (mid-1987)
PSR	LANL	p	0.8 GeV	In operation
RI Cybernetic	Moscow, USSR	p	1	In operation
Saturne	Saclay, France	p	3	In operation
Bevatron	LBL, USA	p	6.2	Converted to Bevalac
ITEP-PS	Moscow, USSR	p	7	In operation
Nimrod	RHEL, U.K.	p	7	Decomissioned
Booster	FNAL	p	8	In operation
JINR-Synchrophasatron	Dubna, USSR	p	10	In operation
KEK-PS	KEK, Japan	p	12	In operation
CPS	CERN	p	28	In operation
AGS	BNL, USA	p	33	In operation
IHEP-PS	Serpukhov, USSR	p	76	In operation
SPS	CERN (Geneva)	p	450	Converted to $\bar{S}$PPS
Main Ring	FNAL	p	500	In operation
Tevatron	FNAL, USA	p, $\bar{p}$	1000×1000	In operation
Bevalac	LBL, USA	Heavy ions	2.1/amu[(a)]	In operation
SPS	CERN (Geneva)	Heavy ions	200/amu	In operation
$\bar{S}$PPS	CERN	p, $\bar{p}$	270×270	In operation
Cosmotron	BNL	p	3	Decommissioned
PPA	Princeton-Penn	p	3	Decommissioned
ZGS	Argonne	p	12.7	Decommissioned
ISR	CERN	p	31×31	Decommissioned

(a) Maximum energy per nucleon for heavy ions.

Table II. High-energy linear accelerators (≥ 1 GeV).

Designation	Location	Particle type	Energy (GeV)	Status (mid-1987)
LAMPF	LANL, USA	p	0.8	In operation
Mark III	Stanford, USA	e^-	1	In operation
Linear Accelerator	Kharkov, USSR	e^-	2	In operation
Linear Accelerator	Orsay, France	e^-	2	In operation
SLAC	Stanford, USA	e^+,e^-	40	In operation

Table III. Multi-GeV accelerators and storage rings being planned or constructed.

Name of machine	Location	Particle type	Energy	Status (turn-on)
LHC	CERN (Geneva)	p, p	8×8 TeV	Proposed
UNK	Serpukhov (USSR)	p, p	3×3 TeV	Under construction (1993)
LEP	CERN (Geneva)	e^+, e^-	51 - 100 GeV	Under construction (1989)
HERA	DESY (Hamburg)	e^-, p	30×820 GeV	Under construction (1990)
SSC	(unknown) USA	p, p	20×20 TeV	Design stage
SLC	Stanford, USA	e^+, e^-	50×50 GeV	Construction (1987)
CEBAF	Newport News, USA	e^-	4-6 GeV	Under construction (1992)
RHIC	Brookhaven, USA	Heavy ions	100×100 GeV·A	Proposed
KAON	Triumf (Canada)	$k^{\pm}, \bar{p}$	30 GeV	Proposed
	KEK (Japan)	Hadrons	3 GeV	Proposed

Table IV. Electron synchrotrons and storage rings operating at present.

Name of machine	Location	Energy	Type	Main Use[a]
N-100	Kharkov, USSR	100 MeV	Ring	SR
TANTALUS I	Wisconsin, USA	240 MeV	Ring	SR
SURF II	Washington, USA	250 MeV	Synchrotron	SR
EROS	Saskatoon, Canada	300 MeV	Ring	NP
SOR	Tokyo, Japan	400 MeV	Ring	SR
BONN II	Bonn, FRG	500 MeV	Synchrotron	PP and SR
FIAN	Moscow, USSR	700 MeV	Synchrotron	SR
NSLS-VUV	Brookhaven, USA	700 MeV	Ring	SR
BESSY	Berlin, FRG	800 MeV	Ring	SR
ALADDIN	Wisconsin, USA	1 GeV	Ring	SR
FRASCATI	Frascati, Italy	1.1 GeV	Synchrotron	PP
LUSY	Lund, Sweden	1.1 GeV	Synchrotron	PP and SR
INS-ES	Tokyo, Japan	1.3 GeV	Synchrotron	PP and SR
PAKHRA	Moscow, USSR	1.3 GeV	Synchrotron	SR
SIRIUS	Tomsk, USSR	1.5 GeV	Synchrotron	SR
SRS	Daresbury, U.K.	2.0 GeV	Ring	SR
BONN I	Bonn, FRG	2.5 GeV	Synchrotron	PP and SR
NSLS-X-RAY	Brookhaven, USA	2.5 GeV	Ring	SR
Photon Factory	Tsukuba, Japan	2.5 GeV	Ring	SR
NINA	Daresbury, U.K.	5.2 GeV	Synchrotron	PP
DORIS	Hamburg, FRG	5.6 GeV	Ring	PP and SR
ARUS	Yerevan, USSR	6.1 GeV	Synchrotron	SR

Table IV. Electron synchrotrons and storage rings operating at present.

CEA	Cambridge, USA	6.3 GeV	Synchrotron	PP
DESY	Hamburg, FRG	7.5 GeV	Synchrotron	PP and SR
CHESS	Cornell, USA	8 GeV	Ring	SR
CORNELL	Cornell, USA	10 GeV	Synchrotron	PP
ACO	Orsay, France	540×540 MeV	Collider	SR
VEPP2M	Novosibirsk, USSR	700×700 MeV	Collider	SR
VEPP3	Novosibirsk, USSR	1.1×1.1 GeV	Collider	SR
ADONE	Frascati, Italy	1.5×1.5 GeV	Collider	PP and SR
DCI	Orsay, France	1.7×1.7 GeV	Collider	SR
CEA-Bypass	Cambridge, USA	3.5×3.5 GeV	Collider	PP, SR
VEPP4	Novosibirsk, USSR	3.5×3.5 GeV	Collider	PP and SR
SPEAR	Stanford, USA	4.2×4.2 GeV	Collider	PP and SR
CESR	Cornell, USA	8×8 GeV	Collider	PP and SR
PEP	Stanford, USA	18×18 GeV	Collider	PP and SR
PETRA	Hamburg, FRG	20×20 GeV	Collider	PP and SR
Tristan	KEK, Japan	30×30 GeV	Collider	PP and SR

(a) NP: Nuclear physics; PP: Particle physics research.

Table V. Monte-Carlo Calculations of the electromagnetic cascade.

Authors and year	Data[a]	Medium	Initial particle Type[b]	Initial particle Energy[a]
Wilson (1952)	I	Pb	e,γ	20, 50, 100, 200, 300, 500 MeV
Varfolomeev and Svetlolobov (1959)	D	Emulsion	e	1, 10, 100, 500, 1000, 3000 GeV
Butcher and Messel (1960)	D	Air, Al	e,γ	50, 100, 200, 500 MeV; 1, 2, 5, 10, 20, 50 GeV
Crawford and Messel (1962)	D	Pb	e,γ	50, 100, 200, 500, 1000 MeV
Messel et al. (1962)	D	Emuls., Pb	e	1 GeV
Zerby and Moran (1962a)	I	Be, Pb	e	100 MeV
	I	Sn	e	185 MeV
Zerby and Moran (1962b)	I	Air	e	200 MeV
	I	Al	e,γ	50, 100, 200, 500 MeV
	I	Pb	e	50, 100, 185, 200, 300, 500 MeV; 1 GeV
	I	Pb	γ	50, 100, 200, 300, 500 MeV
	D	Cu	e,γ	50, 100, 200, 400, 700 MeV; 1.4, 3, 5, 10, 20, 45 GeV
Nagel and Schlier (1963)	D	Pb	e	200 MeV
Woischnig and Burmeister (1964)	I	Pb	e,γ	100, 200, 380 MeV
Crawford and Messel (1965)	D	Emulsion, Cu, Pb	e,γ	50, 100, 200, 500 MeV; 1, 2 GeV
Nagel (1965)	D	Pb	e	100, 200, 400, 1000 MeV
Tamura (1965)	D	Al	e,γ	204 MeV
Völkel (1965)	D	Pb	e,γ	6 GeV

Table V. Monte-Carlo Calculations of the electromagnetic cascade.

Authors and year	Data[a]	Medium	Initial particle Type[b]	Initial particle Energy[a]
Alsmiller and Moran (1966)	Y	Cu	e	34 MeV
	DY	Ta	e	30, 100, 150, 200 MeV
	Y	Pb	e	34, 100 MeV
Varfolomeev and Drabkin (1966)	D	Pb	e	6 GeV
Alsmiller and Moran (1967a)	E	H_2O	e	100, 200, 500 MeV;
				1, 5.2, 10, 20 GeV
	E	H_2O	γ	10, 20, 50, 100, 200, 500 MeV;
				1, 5.2, 10, 20 GeV
Burfeindt (1967)	D	Pb	e	3 GeV
Völkel (1967)	D	Cu	γ	1, 3, 6 GeV
	D	Cu	B	6 GeV
Alsmiller and Moran (1968)	D	Pb	γ	15, 25, 35, 45, 60, 75, 100 MeV
Alsmiller and Moran (1969)	E	H_2O, Al	e	1 GeV
Cioni and Treves (1969)	I	Pb-glass	e	50, 150, 300, 500 MeV, 1 GeV
Gabriel and Alsmiller (1969)	DY	Cu	e	50, 100, 200, 300, 400 MeV
Alsmiller and Moran (1970a)	E	H_2O, Al	e	1 GeV
Alsmiller and Moran (1970b)	E	Be, Al	γ	45 GeV
Beck (1970a)	E	H_2O	e,γ	100, 200, 500 MeV;
				1, 5.2, 10, 20 GeV
Beck (1970b)	E	H_2O, Al	e	1 GeV
Berger and Seltzer (1970)	DY	Ta, W	e	2, 5, 10, 15, 20, 30, 60 MeV
Messel and Crawford (1970)	D	Air	e,γ	500 MeV; 1, 10, 50 GeV
	D	Cu	e,γ	50, 100, 200, 500 MeV; 1, 2 GeV
	D	Pb	e,γ	50, 100, 200, 500 MeV; 1, 2, 10 GeV

Table V. Monte-Carlo Calculations of the electromagnetic cascade.

Authors and year	Data[a]	Medium	Initial particle Type[b]	Initial particle Energy[a]
Beck (1971)	E	Pb + H_2O[c]	e	1 GeV
	I	Air + Al	e	200, 500 MeV; 1 GeV
	I	Air + Fe	e	200, 500 MeV; 1 GeV
Alsmiller et al. (1974)	E	H_2O	e	50, 100, 150, 200 MeV
Ford and Nelson (1978)	D	Various	e,γ	Various
Nelson et al. (1985)	D	Various	e,γ	Various
Nakamura et al. (1987)	D	Cu	e	900 MeV

[a]Type of cascade data given:

E: Distribution of energy deposition (absorbed dose) in medium only.

I: Data on electron and/or photon track length, but integrated over energy.

D: Data on electron and/or photon track length, differential in energy or in such a form that some information on differential track length can be derived.

Y: Yield of some type of secondary particle is given, in addition to cascade data.

[b]Particle type: e: electron (or positron); γ: monoenergetic photon; B: Bremsstrahlung beam of indicated end-point energy.

[c]Two-material medium.

Table VI. Comparison of radiation length, X_0, for electrons and nuclear collision length, X_c, for nucleons.

Material	Z	A	Density ($g\ cm^{-3}$)	X_0 (cm)	X_c (cm)
Hydrogen	1	1.01	0.0708	~865	611
Lithium	3	6.94	0.53	155	102
Berylium	4	9.01	1.85	35.3	30.2
Carbon	6	12.01	2.27	18.8	26.6
Aluminum	13	27	2.70	8.9	25.5
Iron	26	55.8	7.87	1.76	10.2
Copper	29	63.5	8.96	1.44	9.3
Lead	82	207.2	11.35	0.56	9.9
Uranium	92	238.0	18.95	0.32	6.2

Table VII. Approximate conversion coefficients (from stars or star densities).

Energy deposition	0.6 – 1.4 GeV $star^{-1}$	Thomas and Stevenson (1988)
H (neutrons) (W)	1.19×10^{-8} Sv $star^{-1}cm^3$	Stevenson (1986)
H (neutrons) (Fe)(a)	3.5×10^{-8} Sv $star^{-1}$ cm^3	Van Ginneken and Awschalom (1974)
H (neutrons) (Fe)	2.10×10^{-8} Sv $star^{-1}cm^3$	Stevenson (1986)
H (neutrons) (Fe)	1.2×10^{-8} Sv $star^{-1}$ cm^3	Thomas and Stevenson (1988)
H (neutrons) (Al)	4.62×10^{-8} Sv $star^{-1}cm^3$	Stevenson (1986)
H (neutrons) (Concr.)	9.0×10^{-8} Sv $star^{-1}$ cm^3	Van Ginneken and Awschalom (1974)
H (neutrons) (Concr.)	4.5×10^{-8} Sv $star^{-1}$ cm^3	Stevenson and Thomas (1987)
H (neutrons) (average)	4.4×10^{-8} Sv $star^{-1}$ cm^3	Tesch and Dinter (1986)
ϕ_n (conc., $E_n > 20$ MeV)	50 neutrons cm $star^{-1}$	Tesch and Dinter (1986)
ϕ_n (conc., $E_n > 1$ MeV)	80 neutrons cm $star^{-1}$	Tesch and Dinter (1986)
ϕ_n (conc., $E_n > 0$ MeV)	140 neutrons cm $star^{-1}$	Tesch and Dinter (1986)
$\dot{H}$ (activation, Fe)(b)	1.2×10^{-8}Sv $h^{-1}stars^{-1}cm^3sec$	Ranft (1980a,b)
$\dot{H}$ (activation, Fe)	2.5×10^{-8}Sv $h^{-1}stars^{-1}cm^3sec$	Gabriel and Santoro (1973)
$\dot{H}$ (activation, Fe)	4.5×10^{-9}Sv $h^{-1}stars^{-1}cm^3sec$	Tesch and Dinter (1986)
$\dot{H}$ (activation, Fe)	6.1×10^{-9} Sv h^{-1} $stars^{-1}$ cm^3 sec	Höfert (1980)
$\dot{H}$ (activation, Pb)	9.3×10^{-9}Sv $h^{-1}stars^{-1}cm^3sec$	Höfert (1980)
$\dot{H}$ (activation, Pb)	1.8×10^{-9}Sv $h^{-1}stars^{-1}cm^3sec$	Tesch and Dinter (1986)
$\dot{H}$ (activation, conc.)	4.8×10^{-9}Sv $h^{-1}stars^{-1}cm^3sec$	Tesch and Dinter (1986)
Global radioactivity(c)	$\approx$ 0.5 Bq $star^{-1}$	—

(a) Dose equivalent in tissue for transport in medium indicated.

(b) Absorbed dose rate due to gamma-rays at surface of medium from induced radioactivity.

Irradiation and decay times assumed: 30 and 1 days, respectively.

(c) For half-lives between several minutes and a few years.

Table VIII. Experimental studies of the hadronic cascade initiated by protons.

Initial Energy or Momentum	Medium	Reference
500 MeV	Iron	Arakita et al. (1979)
1, 3 GeV	Iron	Shen (1964)
6.2 GeV	Concrete	Shaw and Thomas (1964)
		Smith (1965a), Smith et al. (1965)
9.0 GeV/c	Concrete	Thomas (1963)
10, 19.2 GeV/c	Steel	Childers et al. (1965),
		Citron et al. (1965)
19.2 GeV/c	Iron	Goebel and Ranft (1970)
20-24 GeV/c	Concrete and Earth	Citron et al. (1961)
		Thomas (1963)
28 GeV	Steel	Bennett et al. (1971, 1973)
29.4 GeV	Iron	Van Ginneken and Borak (1971)
69 GeV/c	Steel	Volynchikov et al. (1983)
200 GeV	Aluminum	Stevenson et al. (1985)
200 GeV	Copper	Stevenson et al. (1986)
300 GeV	Al, Fe, Pb	Gollon et al. (1981)
300 GeV	Fe, Pb	Muraki et al. (1985)
400, 800 GeV	Iron	Cossairt et al. (1985)

Table IX.

Radiation spectrum above Nimrod extracted proton beam shielding (Perry, 1967). [See text]

Type of radiation	Energy range	Estimated % of neutron flux density	Estimated % of total dose-equivalent
Neutrons	<1 eV	<7	<1
Neutrons	1 eV-0.7 MeV	70	20
Neutrons	0.7–3 MeV	15	35
Neutrons	3–7 MeV	7	25
Neutrons	7–20 MeV	1.5	5
Neutrons + protons	20–100 MeV	1	5
Neutrons + charged particles	>100 MeV	0.5	4
Other particles + gammas	—	—	<2

Table X. Synchrotron radiation parameters for selected large storage rings.

Machine	PETRA	HERA	LEP			SSC
Particle type	$e^{\pm}$	e^{-}	$e^{\pm}$	$e^{\pm}$	$e^{\pm}$	p
Beam energy (GeV)	19	30	51.5	86	100	20,000
Bending radius (m)	192	550	3099	3099	3099	10,100
I (per beam) (mA)	10	56	3.0	3.3	5.5	73
ε_c (keV)	79	109	97.8	455.2	715.7	0.284
Total SR power (kW)	1,196	7250	1,200	10,265	31,275	18

Table XI. Radionuclides commonly identified in solid materials irradiated around accelerators (adapted from Patterson and Thomas, 1973).

Irradiated material	Radionuclides
Plastics, oils	^{7}Be, ^{11}C
Concrete, aluminum	As above, plus ^{22}Na, ^{24}Na, ^{32}P, ^{42}K, ^{45}Ca
Iron, steel	As above, plus ^{44}Sc, ^{44m}Sc, ^{46}Sc, ^{47}Sc, ^{48}V, ^{51}Cr, ^{52}Mn, ^{52m}Mn, ^{54}Mn, ^{56}Mn, ^{57}Co, ^{58}Co, ^{60}Co, ^{57}Ni, ^{55}Fe, ^{59}Fe
Copper	As above, plus ^{65}Ni, ^{61}Cu, ^{64}Cu, ^{63}Zn, ^{65}Zn

Table XII

Radionuclides identified in earth or water at accelerator laboratories.

Laboratory	Accelerator	Soil type	Radionuclides identified		Reference
			In soil	In water	
CERN	28 GeV proton synchrotron	Molasse	^{7}Be,^{45}Ca,^{54}Mn,^{22}Na	^{22}Na	Hoyer, 1968
Rutherford Laboratory	300 GeV proton synchrotron	Chalk	^{7}Be,^{47}Ca,^{43}K ^{32}P,^{47}Sc	^{7}Be,^{11}C, ^{3}H	Stapleton and Thomas, 1972
FNAL Batavia	500 GeV proton synchrotron	Glacial till, various clays	^{7}Be,^{45}Ca,^{60}Co, ^{51}Cr,^{55}Fe,^{59}Fe,^{3}H, ^{22}Na,^{46}Sc,^{48}V	^{45}Ca,^{3}H, ^{54}Mn, ^{22}Na	Borak et al., 1972b
Stanford HEPL	1 GeV electron linear accelerator	Sandstone	^{7}Be,^{58}Co,^{59}Fe, ^{54}Mn,^{22}Na,^{46}Sc	^{54}Mn,^{22}Na	Thomas, 1972

Table XIII

Radionuclides produced from ^{16}O.

Isotope	$T_{1/2}$ (s)	Beta decay	Gamma energies (MeV)	Gamma-emission probability (%)
^{10}C	19.1	100% β^+	0.717	100
			1.023	1.7
^{14}O	71.1	100% β^+	2.313	99
^{15}O	124	100% β^+	none	
^{13}N	600	100% β^+	none	
^{11}C	1220	100% β^+	none	
^{7}Be	4.60×10^{6}	100% EC	0.477	10.3
^{3}H	3.76×10^{8}	100% β^-	none	
^{14}C	1.76×10^{11}	100% β^-	none	
^{10}Be	7.88×10^{13}	100% β^-	none	

Table XIV

Quantities of radioactivity produced in cooling water of the CERN SPS by 300-GeV protons. (After Christensen et al. [1978])

Radionuclide	Instantaneous loss of 10^{13} protons	Continuous loss of 10^{11} protons/s for 5000 hours
^{13}N	73 GBq	630 GBq
^{11}C	71 GBq	1.3 TBq
^{7}Be	18 MBq	1.2 TBq
^{3}H	760 kBq	200 GBq
^{14}C	95 Bq	25 MBq
^{10}Be	98 mBq	25 kBq

Table XV. Radionuclides with half-life > 1 minute that can be produced in air at accelerators (after Rindi, 1972b).

Radionuclide	Half-life	Emission	Parent element	Production reaction	Cross section (mb)
^{3}H	12.3 y	β^-	N	spallation	30
			O	spallation	30
^{7}Be	53.3 d	γ,EC	N	spallation	10
			O	spallation	5
			Ar	spallation	0.6
^{11}C	20.4 m	β^+	N	spallation	10
			O	spallation	5
			Ar	spallation	0.7
^{14}C	5730 y	β^-	N	(n,p)	1640
^{13}N	9.96 m	β^+	N	spallation	10
			N	(γ,n)	10
			O	spallation	9
			Ar	spallation	0.8
^{14}O	70.6 s	β^+,γ	O	spallation	1
			Ar	spallation	0.06
^{15}O	2.03 m	β^+	O	spallation	40
			O	(γ,n)	10
			Ar	spallation	
^{18}F	1.83 h	β^+,EC	Ar	spallation	6
^{24}Ne	3.4 m	β^-,γ	Ar	spallation	0.12
^{22}Na	2.6 y	β^+,γ	Ar	spallation	10

Table XV.
(continued)

Radionuclide	Half-life	Emission	Parent element	Production reaction	Cross section (mb)
^{24}Na	15.0 h	β^-	Ar	spallation	7
^{27}Mg	9.46 m	β^-,γ	Ar	spallation	2.5
^{28}Mg	20.9 h	β^-,γ	Ar	spallation	0.4
^{28}Al	2.25 m	β^-,γ	Ar	spallation	13
^{29}Al	6.6 m	β^-,γ	Ar	spallation	4
^{31}Si	2.62 h	β^-,γ	Ar	spallation	6
^{30}P	2.50 m	β^+,γ	Ar	spallation	4.4
^{32}P	14.3 d	β^-	Ar	spallation	25
^{33}P	25.3 d	β^-	Ar	spallation	9
^{35}S	87.5 d	β^-	Ar	spallation	23
^{34m}Cl	32.0 m	β^-,γ	Ar	spallation	0.6
^{38}Cl	37.2 m	β^-,γ	Ar	(γ,pn)	4
^{39}Cl	55 m	β^-,γ	Ar	(γ,p)	7
^{41}Ar	1.8 h	β^-,γ	Ar	(n,γ)	660

Table XVI

Radionuclides identified in the air around several accelerators.

Laboratory	Accelerator	Radionuclides identified	Reference
RPI	50-MeV electron linac	^{15}O,^{13}N	Russell and Ryan (1965)
Saclay	330- to 560-MeV electron linac	^{13}N,^{15}O,^{11}C, ^{41}Ar,^{38}Cl,^{7}Be	Viallettes (1969)
CERN	600-MeV proton synchrotron	^{11}C,^{13}N,^{41}Ar	Rindi and Charalambus (1967)
PPA	3-GeV proton synchrotron	^{14}O,^{15}O,^{13}N,^{11}C	Awschalom et al. (1965)
RHEL	7-GeV proton synchrotron	^{16}N,^{15}O,^{13}N,^{11}C	Shaw and Thomas (1967)
CERN	25-GeV proton synchrotron	^{13}N,^{11}C,^{41}Ar	Höfert (1969)
BNL	30-GeV proton synchrotron	^{13}N,^{11}C,^{41}Ar	Distenfeld (1964)

Table XVII. The "Air, Wood, Lead" game.

Material introduced	Photons	Neutrons	Muons
Air	Reference reading	Reference reading	Reference reading
Lead	Large decrease	Little or no change	Little or no change
Wood	Small decrease	Moderate decrease	Little or no change

Table XVIII. Important characteristics of various activation-detector techniques.

Detector	Reaction	Energy range (MeV)	Half-life	Detector size	Response to unit fluence rate[a]	Background response
Sulphur	$^{32}S(n,p)^{32}P$	>3	14.3 d	1-in. diam 4 g disk	0.049 cpm[b]	10 cpm
Plastic scintillator	$^{12}C(n,2n)^{11}C$	>20	20.4 m	13 to 2700 g	88 cpm[b] at 85% efficiency (1700 g scint)	165 cpm (1700 g scint)
Mercury	$Hg(spall)^{149}Tb$	>600	4.1 h	up to 500 g	0.03 cpm[c]	0.1 cpm
Gold foils	$^{197}Au(spall)^{149}Tb$	>600	4.1 h	1-in. diam 0.5 g	2.7×10^{-6} cpm[c]	0.1 cpm
Aluminum	$^{27}Al(n,\alpha)^{24}Na$	>6	15.0 h	16.9 to 6600 g	101 cpm[b] 6600 g E_n = 14 MeV	111 cpm (16.9 g) 118 cpm (6600 g) NaI(Tl)
Aluminum	$^{27}Al(spall)^{22}Na$	>25	2.6 y	16.9 g	0.21 cpm[b]	67 cpm NaI(Tl)
Plastic scintillator	$^{12}C(spall)^{7}Be$	>25	53 d	16.9 g (1 in. high)	0.21 cpm[b]	67 cpm Na(Tl)

(a) Unit fluence rate ≡ 1 neutron $cm^{-2}s^{-1}$.

(b) At saturation and unit time.

(c) At saturation, zero decay time and zero bias.

Table XIX. Activation reactions commonly used in the determination of thermal neutron fluence rates at accelerators.

Reaction	Decay products	Half-life	Detector	Sensitivity (a)
$^{115}In(n,\gamma)^{116m}In$	β^- γ: 0.47 MeV (36%) 1.09 MeV (53%) 1.25 MeV (80%)	54.2 m	8" dia × 4" NaI γ spectrometer β-particle detector	Four foils 7.6 × 15.2 cm total mass 46 g, have a sensitivity of 300 cpm.
$^{197}Au(n,\gamma)^{198}Au$	β^- γ: 0.42 MeV (95%)	2.70 d	β-particle detector 8" dia × 4" NaI γ spectrometer	2.54-cm diam foil, mass 0.5 g, has a sensitivity of 1.8 cpm (Typical G-M counter background: 10 cpm). 5.08-cm-diam foil, mass 1.0 g, has a sensitivity of 13.4 cpm. [NaI(Tl) crystal background: 48 cpm.]
$^{23}Na(n,\gamma)^{24}Na$	β^- γ: 1.37 MeV (100%) 2.75 MeV (100%)	15.0 h	γ spectrometer	Used in form of Na_2CO_3 cylinder 4.5 cm diam × 2 cm high, mass 12 g Na. 3.0 cpm.

(a) Sensitivity at saturation and zero decay time for unit neutron fluence rate ≡ 1 neutron $cm^{-2}s^{-1}$.

Table XX. Types of activation threshold detectors.

Reaction	Sample type	Threshold (MeV)
^{32}S–^{32}P	Sulphur powder or pellets	3
^{27}Al–^{27}Mg	Aluminum discs or pellets	3
^{27}Al–^{24}Na	Aluminum discs or pellets	6
^{27}Al–^{22}Na	Aluminum discs or pellets	35
^{27}Al–^{18}F	Aluminum discs or pellets	35
^{19}F–^{18}F	Teflon cylinders	12
^{12}C–^{11}C	Polyethylene cylinders or plastic cylinders	20
^{12}C–^{7}Be	Polyethylene cylinders or plastic cylinders	35
Bi-fission	Fission chamber	50

Table XXI. Specifications of the CERN radioactive gas monitor.

Monitor volume	~ 1 m^3	
Gas flow rate	~ 16 $m^3 h^{-1}$	
Detectors (GM Tubes)	Berthold BZ/120A	Philips 18555
Sensitivity (per Bq/cm^3 ^{85}Kr)	1600 cps	~ 16 cps
Unshielded background rate	~ 7 cps	~ 0.5 cps
Concentration range (Bq/cm^3)	0.001–1	0.074–74
Calibration factor (total release per output pulse)	4.3 MBq/pulse	440 Bq/pulse

VIII. FIGURE CAPTIONS

Figure 1. A revised version of the "Livingston Plot," first prepared in 1961 (Livingston and Blewitt, 1961), in which the maximum particle energy achieved in the laboratory is shown, plotted against the date of attainment. The envelope to the curves for various accelerator types (dashed line) shows that for about every seven years an increase of a factor of ten in energy has been obtained. New technologies have thus far appeared when previous technologies appear to have saturated (after Panofsky, 1980).

Figure 2. Fraction of total energy, U, deposited by an EM cascade shower *vs* depth, integrated over all radii about the shower axis (Van Ginneken, 1974, after Bathow *et al.*, 1970).

Figure 3. Fraction of total energy, U, deposited beyond a cylindrical radius, R/X_M, as a function of radius for showers caused by 0.1–20 GeV electrons incident on various materials (after DeStaebler *et al.*, 1968).

Figure 4. Fluence-to-dose equivalent conversion coefficients for electrons and photons as functions of particle energy (after Alsmiller and Moran, 1967b; ICRP, 1973) and for thin-target bremsstrahlung (the quantity of bremsstrahlung is the number of "equivalent quanta;" see text) as a function of bremsstrahlung end-point energy, E_0 (after Tesch, 1966).

Figure 5. Photon absorbed dose rate from a typical beam absorber as a function of the angle, θ, from the beam direction, normalized to 1 kW of beam power and to a source-to-detector distance of 1 m (after Nelson *et al.*, 1966 and DeStaebler *et al.*, 1968).

Figure 6. Absorbed dose of electron-photon stray radiation at a distance of 1 m from an iron target at various orientation angles, ϕ, as a function of the angle of observation, θ. Target was struck by 5-GeV electron and data are normalized to 1 J incident beam energy (after Dinter and Tesch, 1977). For (a)-(d), the angle of observation θ increases in the clockwise direction and the detector is on the opposite side of the target from the point of beam incidence.

(a) Showing geometry and data for t = 0.2 cm (0.11 X_0). Histogram is a Monto-Carlo calculation.

(b) Same as (a) except for t = 1 cm (0.57 X_0).

(c) Same as previous except for t = 5 cm (2.84 X_0).

(d) Same as previous except for t = 10 cm (5.68 X_0).

For (e)-(h), θ is measured in same sense as ϕ; dips in curves occur when detector (TLD) is nearly in the target plane (i.e., $\theta \approx \phi$; see inset).

(e) t = 0.2 cm.

(f) t = 1 cm.

(g) t = 5 cm.

(h) t = 10 cm.

Figure 7. Absorbed dose rate near a 1-cm diameter tungsten target struck by 200 MeV electrons, as a function of angle, θ. Target thicknesses used: 2, 4 and 10 X_0 (from Fasso *et al.*, 1984).

Figure 8. The number of cascade neutrons per incident proton for each inelastic collision as a function of proton energy and mass number of the target (after Metropolis *et al.*, 1958a,b).

Figure 9. The number of evaporation neutrons produced per incident neutron or proton for each inelastic collision as a function of incident energy (after Metropolis *et al.*, 1958a,b).

Figure 10. Cascade and evaporation-neutron emission spectra from an aluminum target bombarded by 450 MeV, 660 MeV and 850 MeV protons.

Figure 11. Plot of neutron yields vs incident particle energy for several combinations of targets and ions. (1) Smith and Kruger (1951), $MnSO_4$, (2) Tai, Millburn, Kaplan and Moyer (1958), $MnSO_4$, (3) Allen, Nechaj, Sun and Jennings (1951), $^{32}S(n,p)^{32}P$, (4) Crandall, Millburn, and Schecter (1957), $MnSO_4$, (5) Wadman (1964) (40 and 80-MeV α^{++} on Ta), $^{58}Ni(n,p)^{58}Co$, and (6) Wadman (1964) (From Stephens and Miller, 1969.)

Figure 12. Experimental (points) and calculated (curves from FLUKA82) hadron fluences above different energy thresholds as functions of polar angle around a Cu target bombarded by 225-GeV protons. Data scaled as shown.

Figure 13. Experimental (*) and calculated histograms (FLUKA82) of energy absorption distributions for target depths, inside a cylindrical Al target bombarded by 200-GeV protons, plotted as functions of target radius. Data are scaled as shown for each target depth (after Stevenson *et al.*, 1986).

Figure 14. Yield of photoneutrons produced in electromagnetic cascades initiated by electrons incident on thick targets per unit beam power, as a function of incident energy (after Swanson, 1979b).

Figure 15. The energy spectra of neutrons and other hadrons in a volume of earth at the end of a concrete tunnel. The primary source is the cascade generated within an iron target bombarded by 500 GeV protons (after Gabriel and Santoro, 1971).

Figure 16. Unfolded fluence spectrum at 2 meters from beam line for four types of Tevatron run and one Main Ring run.

Figure 17. Cumulative fraction of absorbed dose and neutron fluence for the 800GeV spectrum of Fig. 15.

Figure 18. Neutron spectra measured by the Health Physics Group of the Lawrence Berkeley Laboratory in the mid-1960s (see text for the explanation of the designations PSB, RT, BEV and CR).

Figure 19. Neutron spectra measured at the 7-GeV proton synchrotron (Nimrod) of the Rutherford Laboratory using Bonner spheres (see text for the explanation of the designations PLA, P1, X2).

Figure 20. Neutron spectra measured at the Princeton-Pennsylvania 3-GeV proton synchrotron using Bonner spheres.

Figure 21. O'Brien neutron spectrum (O'Brien, 1968, 1971).

Figure 22. The energy spectrum of protons from the iron shield wall (approximately 3000 g cm^{-2} thick) of the Dubna Synchrocyclotron which separates the cyclotron room from the experimental area.

a. Energy spectrum from a "thin" shield with the spectrometer aligned as shown in inset A.

b. Energy spectrum from a "thick" shield with the spectrometer aligned as shown in inset B. (after Aleinikov *et al.*, 1975).

Figure 23. Range-energy curves for muons in various materials (after Nelson *et al.*, 1983).

Figure 24. Recommended curve of dose equivalent for muons. The arrows indicate the approximate value of 40 fSv m^2 and the energy limits of 100 MeV and 100 GeV (after Stevenson, 1983).

Figure 25. Integral muon flux density at 1 m, per unit electron beam power, vs fractional muon energy, E/E_0, for electrons incident on a thick iron target. Data are normalized to 1 kW electron beam power. After Nelson (1968) as adapted by Swanson (1979a).

Figure 26. Muon flux density at 0° and corresponding absorbed dose rate at 1 m from an unshielded iron target per kW of electron beam power, as a function of electron energy. (After Nelson (1968) as adapted

by Swanson (1979a).

Figure 27. Contributions to the fractional energy loss by muons due to radiative processes in iron, as a function of muon energy as obtained from Lohmann *et al.* (1985). The quantities b(E) are defined in the text (after Groom, 1986).

Figure 28. Synchrotron radiation angular distribution for slow and relativistic particles showing direction of polarization (after van Steenbergen, 1979).

Figure 29. Universal synchrotron radiation spectrum. The dimensionless quantity G_2, defined by Eq.(28b), gives the relative power as a function of photon energy (units of the characteristic energy, ε_c) (after Krinsky *et al.*, 1985).

Figure 30. Primary synchrotron radiation spectrum at three LEP energies (after Fasso *et al.*, 1984).

Figure 31. Calculated kerma per photon for RPL glass dosimeters (uppermost curve) as a function of photon energy, compared to the calculated dose to the same material shielded by 1.7 mm of vacuum, air, CH_2 or Al. Calculations using program EGS (after Yamaguchi, 1982 and Dinter *et al.*, 1982).

Figure 32. Isodoses measured in a section of the PETRA tunnel (smoothed) using RPL glass dosimeters (Dinter, 1985a). Center of ring is to the right. Beamline is shielded by 3 mm of Pb. Units are kGy $(A \cdot h)^{-1}$.

Figure 33. Absorbed dose near the PETRA vacuum tube as a function of beam energy. Points are measurements with RPL glass dosimeters and curves are EGS calculations (±1 S.D.).

Upper data: Nearest to unshielded vacuum tube;
Middle data: Shielded by 3 mm Pb;
Lower data: Ratio of above (after Dinter, 1985a).

Figure 34. The variation in dose equivalent rate with time as observed at the boundary of the Stanford Linear Accelerator Center. The dose equivalent rates due to both photons and neutrons are indicated by solid lines; natural background due to each component by dashed lines. Periods of intense accelerator operation are evident from the fluctuations in the neutron dose equivalent rate (after Busick, 1978).

Figure 35. Contours of equal photon (a) and neutron (b) dose equivalent at the CERN Laboratory site for the year 1974. The principal radiation sources are: Experimental Hall West (EHW; extracted-beam target locations shaded), Intersecting Storage Rings (ISR; 30 + 30 GeV protons), Proton Synchrotron (PS; 24–28 GeV protons) with Booster (PSB), Synchro-Cyclotron (SC; 600 MeV protons), and Calibration facility (RPC; gamma and neutron sources) (after Bonifas *et al.*, 1974).

Figure 36. A comparison of the radial variation of the low-energy neutron fluence (by diffusion; dashed line) and that of the high-energy fluence (solid line), at distances out to 500 meters from a high-energy accelerator (after Moyer, 1962).

Figure 37. Measurements performed around various accelerators. On the abscissa is the distance from the accelerator in meters; on the ordinate is the product of the measured neutron flux density and the square of the distance. In these coordinates, a $1/r^2$ variation is represented by a horizontal line.

(a) Measurements of fast-neutron flux density performed at the CERN 28-GeV Proton Synchrotron (Ollendorf, 1964).

(b) Measurements of fast-neutron flux density performed at the Dubna 10-GeV Proton Synchrophasotron (Komochkov, 1970; Lebedev *et al.*, 1965).

(c) Measurements of dose-equivalent rate performed at the Brookhaven 30-GeV Proton AGS (Distenfeld and Colvett, 1966).

(d) Measurements of the fast-neutron flux density performed at the CERN 600-MeV Proton Synchrocyclotron (Rindi and Baarli, 1963).

(e) Fast-neutron flux density measurements performed at the DESY 7.5-GeV Electron Synchrotron (Bathow *et al.*, 1967).

(f) Fast-neutron flux density measurements performed at the Rutherford Laboratory Proton Linear Accelerator for a proton beam of 50 MeV (Thomas *et al.*, 1962; Simpson and Laws, 1962).

(g) Measurements made at the 12-GeV Proton Synchrotron at KEK (Katoh, 1977).

Figure 38. The effective neutron absorption length in air as a function of the upper neutron energy cutoff assuming a 1/E differential energy spectrum (after Stevenson and Thomas, 1984).

Figure 39. A comparison of calculated and experimental values of the production cross-section of ^{54}Mn in an iron block irradiated by 1 and 3 GeV incident protons. The calculated values (histogram) and the experimental values (circles) are shown as a function of radial distance from the incident beam at those depths in the iron (after Armstrong and Alsmiller, 1968 and Shen, 1964).

Figure 40. The effiency of ^{7}LiF thermoluminencent dosimetry as a function of linear energy transfer. The solid and dashed curves show predictions based on 1-trap and 2-trap theory (Jahnert, 1972). Experimental points for protons of several energies and naturally occurring alpha particles due to Jahnert are indicated by open circles and squares respectively. Experimental points due to Thomas and Perez-Mendez (1980) for protons (O); α-particles (□); $^{6+}$C ions (); $^{8+}$O ions (□); $^{10+}$Ne ions (Δ) and $^{18+}$Ar ions (∇) are also shown.

Figure 41. Response functions for the high-energy neutron detectors used in the sixties and seventies by the LBL group [^{27}Al(n,α)^{24}Na; ^{12}C(n,2n)^{11}C; Bi fission; ^{32}S(n,p)^{32}P; ^{27}Al(n,spall)^{22}Na; ^{12}C(n,spall)^{7}Be; Hg → ^{149}Tb] (Gilbert *et al.*, 1968).

Figure 42. Excitation functions for the reactions ^{12}C → ^{11}C induced by neutrons, pions and protons. The arithmetic mean of the positive and negative pion cross-sections is shown as the pion curve (after Stevenson, 1984a).

Figure 43. Distribution of neutron moderation times for four types of rem counters (Dinter and Tesch, 1976): 30- and 45-cm spheres, ^{6}Li scintillator; Andersson-Braun (AB); and Leake counter.

Figure 44. The fission cross-sections of natural uranium, natural thorium, bismuth, gold and tantalum as a function of neutron or proton energy (from Patterson and Thomas, 1973). (• Hudis and Katcoff, 1969; O Kon'shin *et al.*, 1965; □ Wollenberg and Smith, 1963, 1973; × Brandt *et al.*, 1971).

Figure 45. The response of Bonner sphere detectors as a function of neutron energy for spheres of different size.

Figure 46. The response of a high pressure parallel plate recombination chamber as a function of quality factor Q. The curve shows the response predicted from Jaffe theory. The experimental points were reported by Sullivan and Baarli, 1963.

Figure 47. Daily rate of neutron dose equivalent taken at the 88-Inch Cyclotron monitoring station for the second half of 1976. The total dose equivalent for this period was 62 μSv (6.2 mrem), with an average daily dose equivalent of 340 nSv (34 μrem) to be compared with the national daily dose equivalent rate due to cosmic ray neutrons of 0.14–0.16 μSv (14–16 μrem) (after Thomas, 1979).

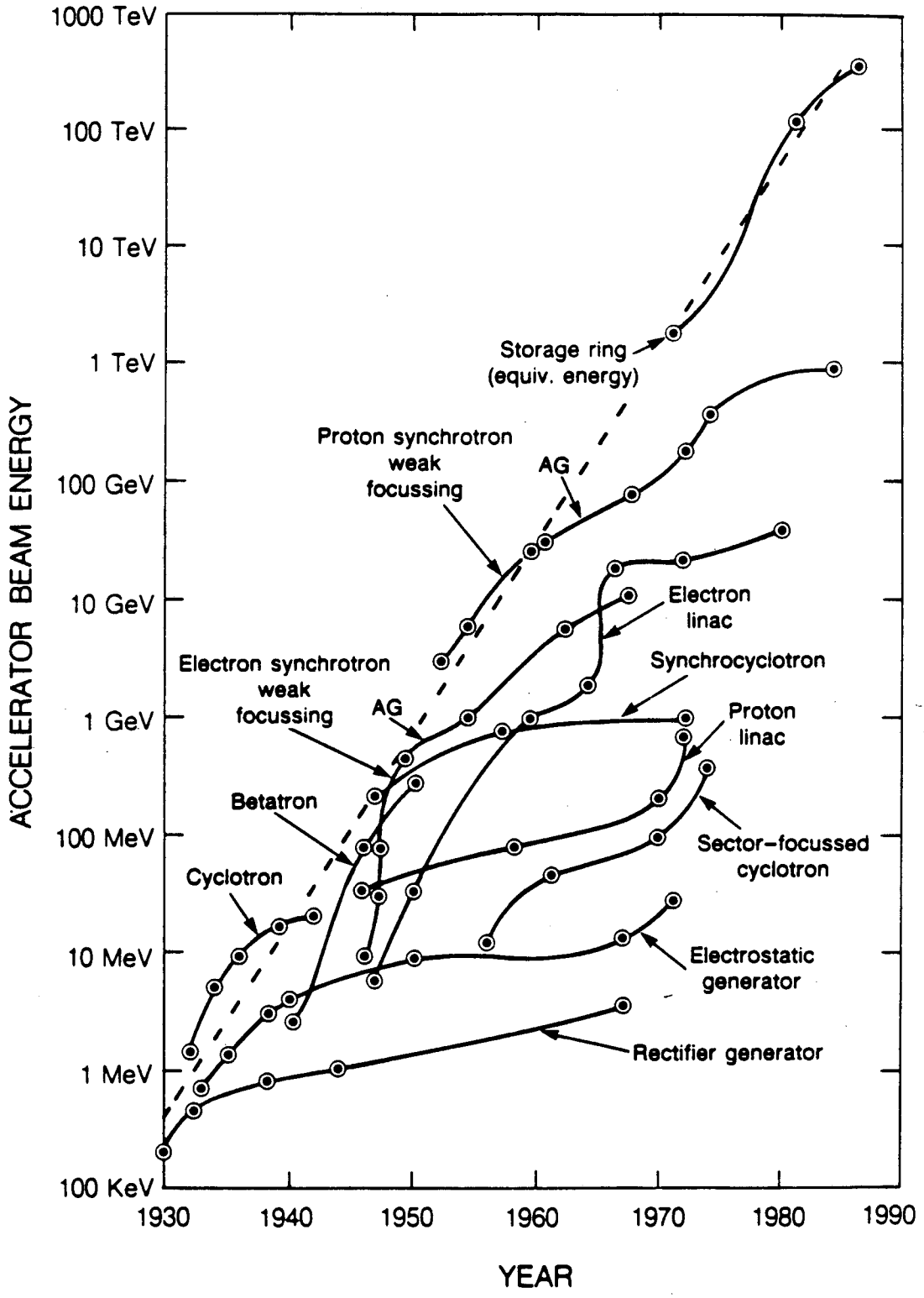

XBL 853-10145

Fig. 1
Thomas & Swanson

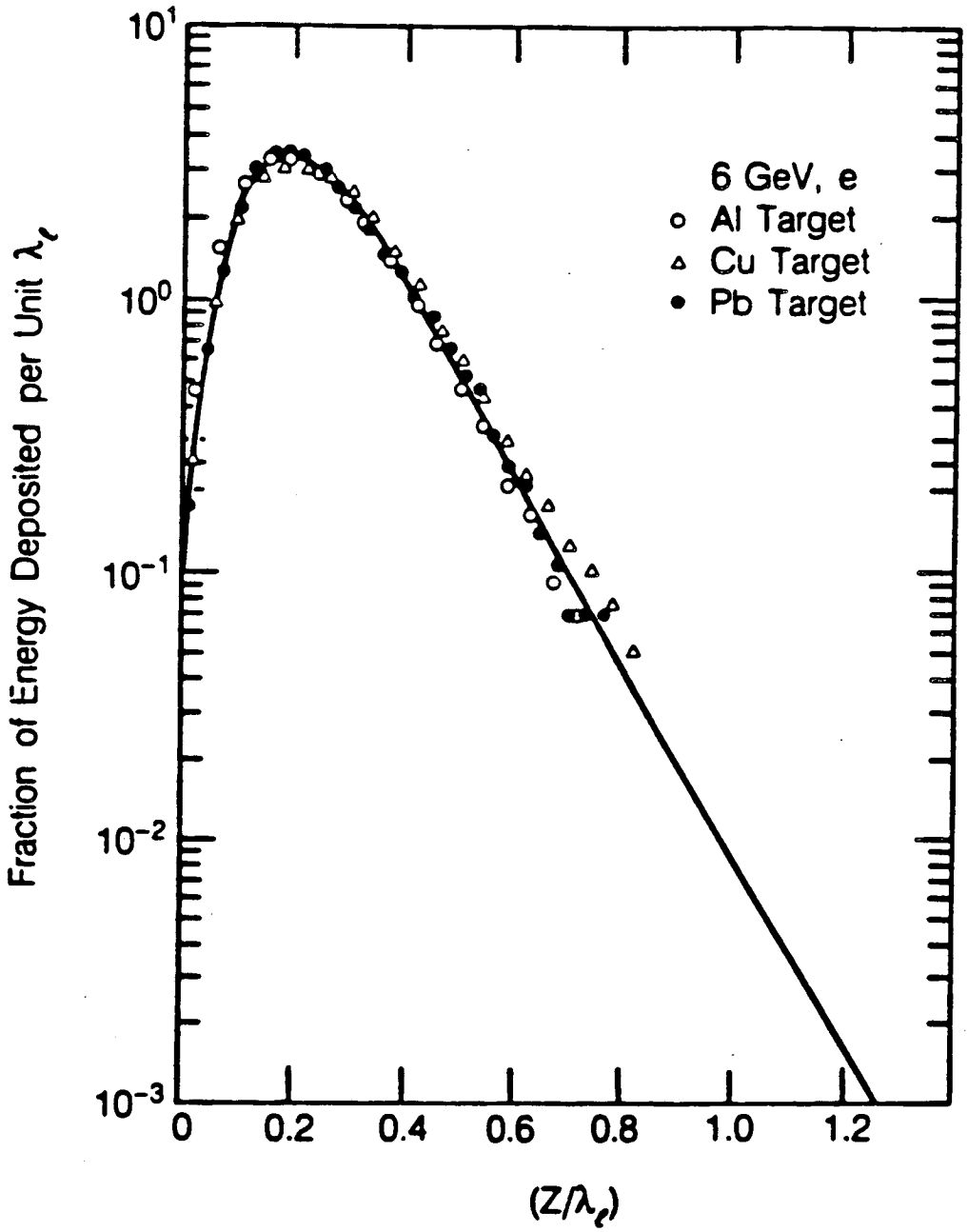

XBL 8610-9647

Fig. 2
Thomas & Swanson

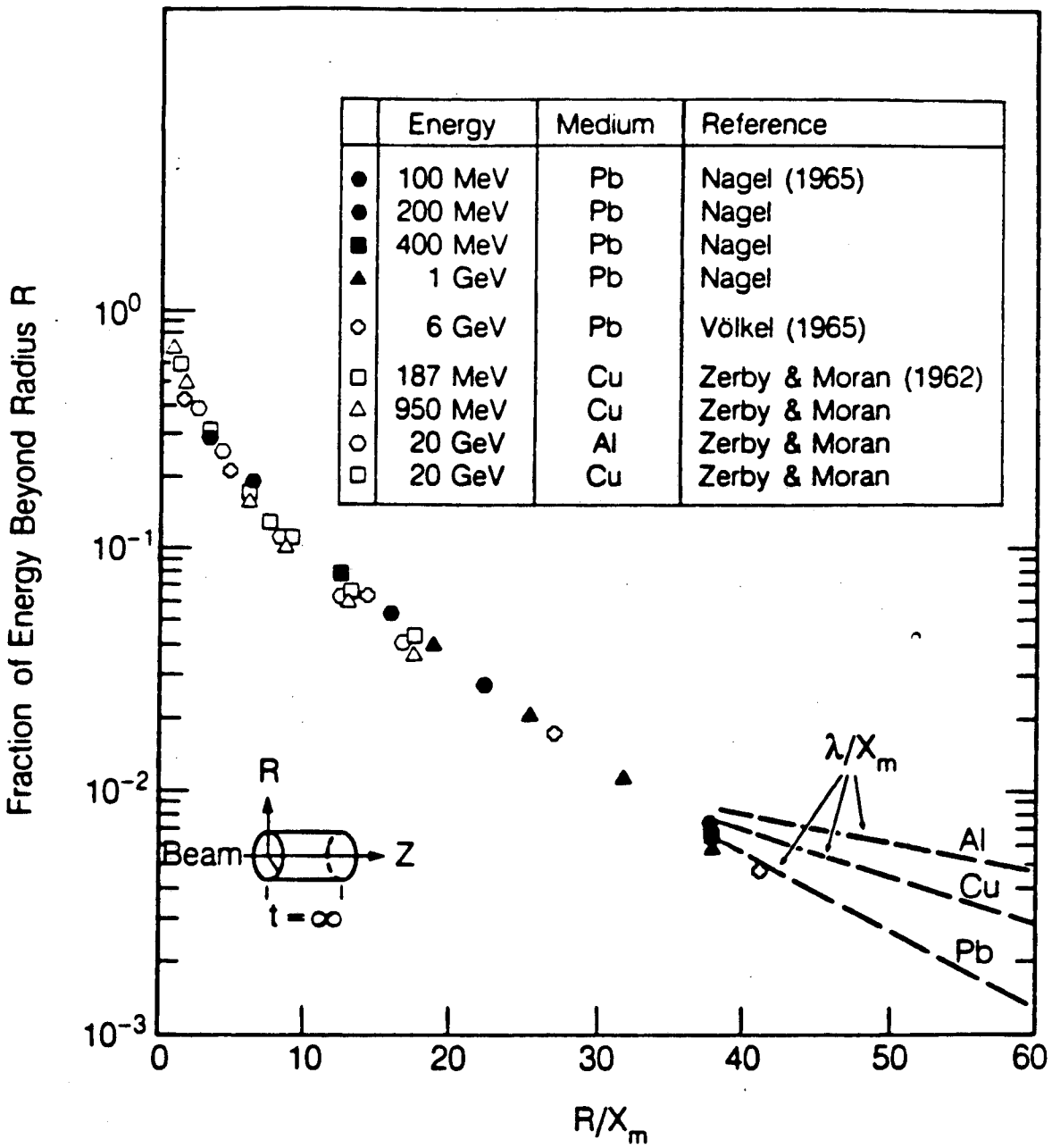

XBL 8610-9646

Fig. 3
Thomas & Swanson

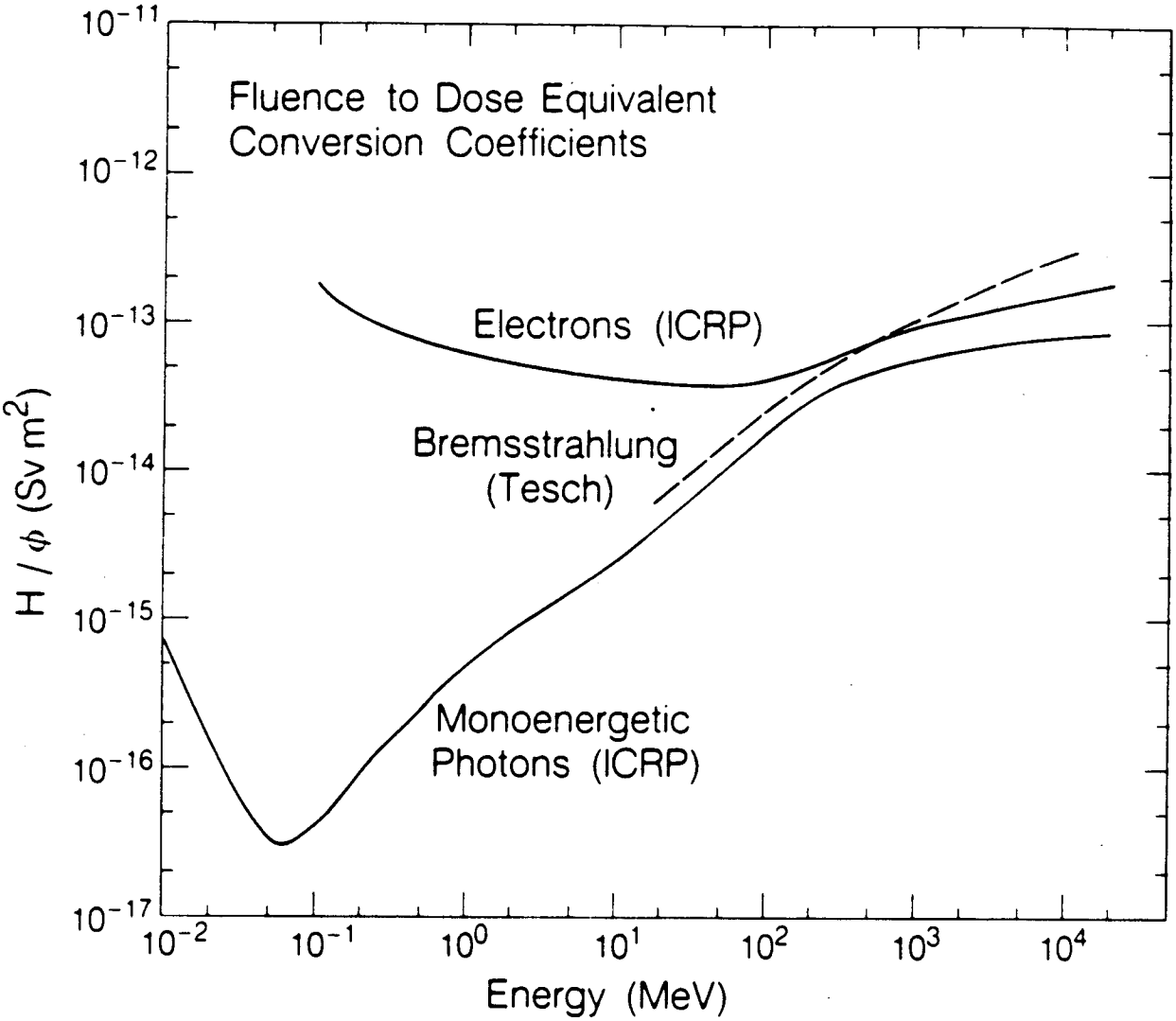

XBL 878-9776

Fig. 4
Thomas & Swanson

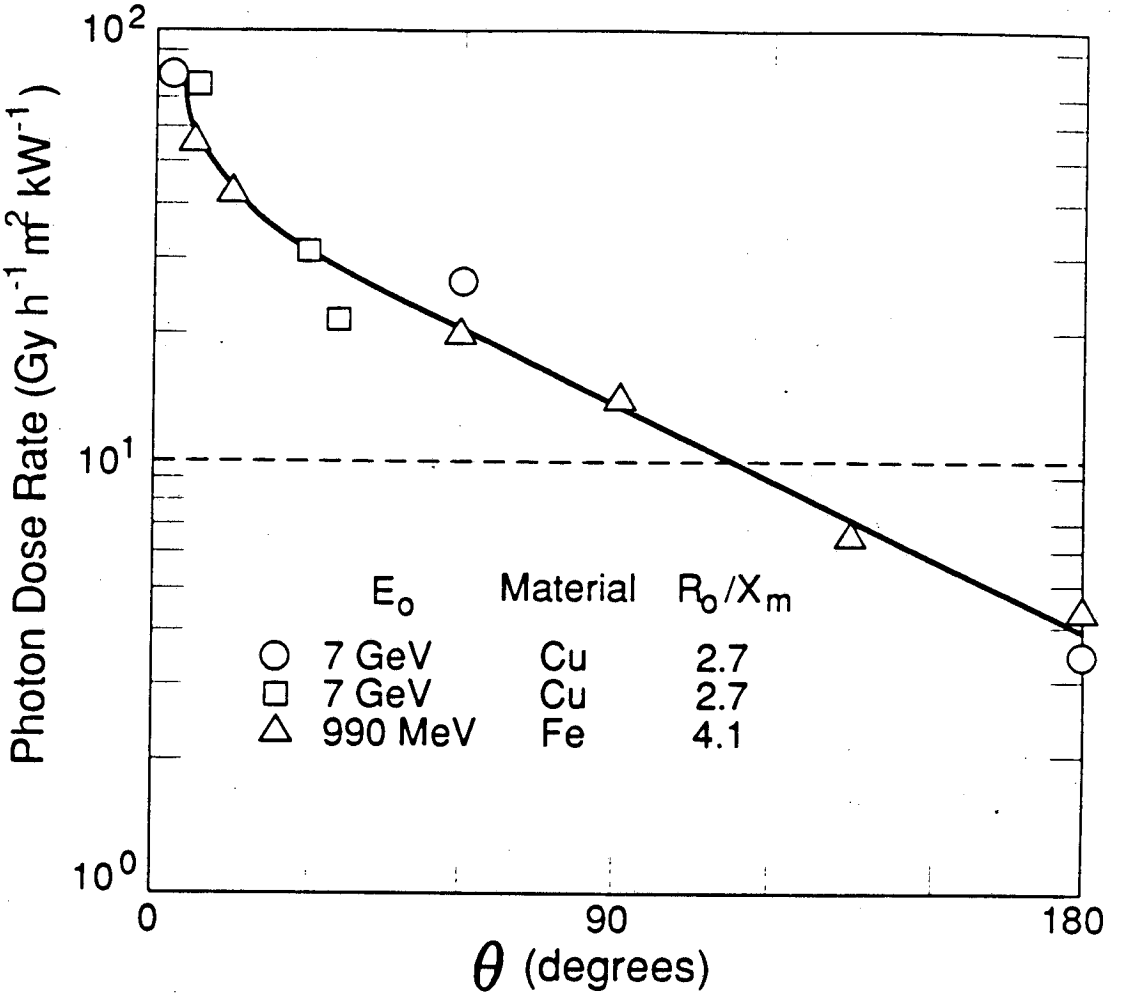

XBL 889-3443

Fig. 5
Thomas & Swanson

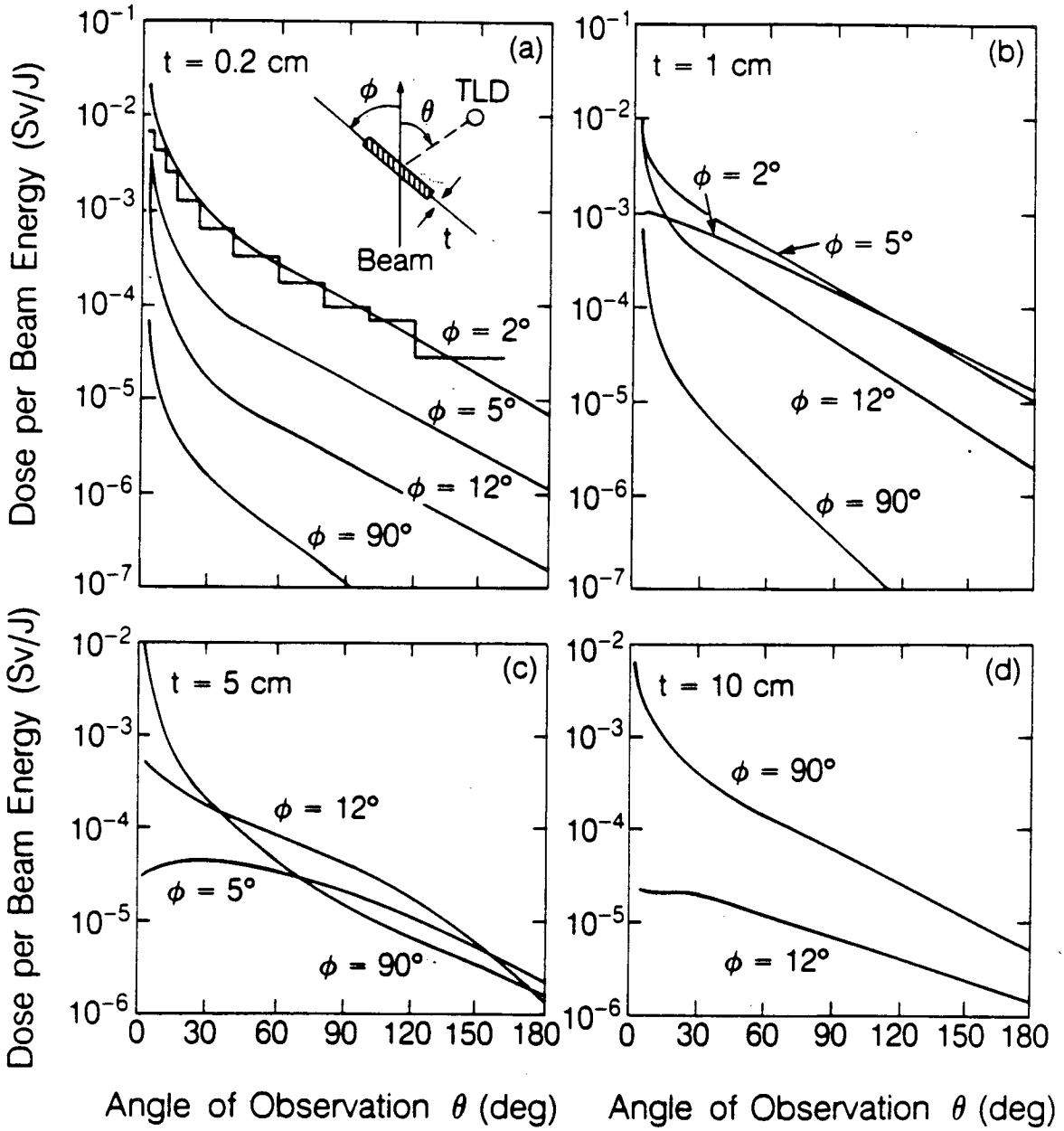

XBL 878-9774

Fig. 6 (a-d)
Thomas & Swanson

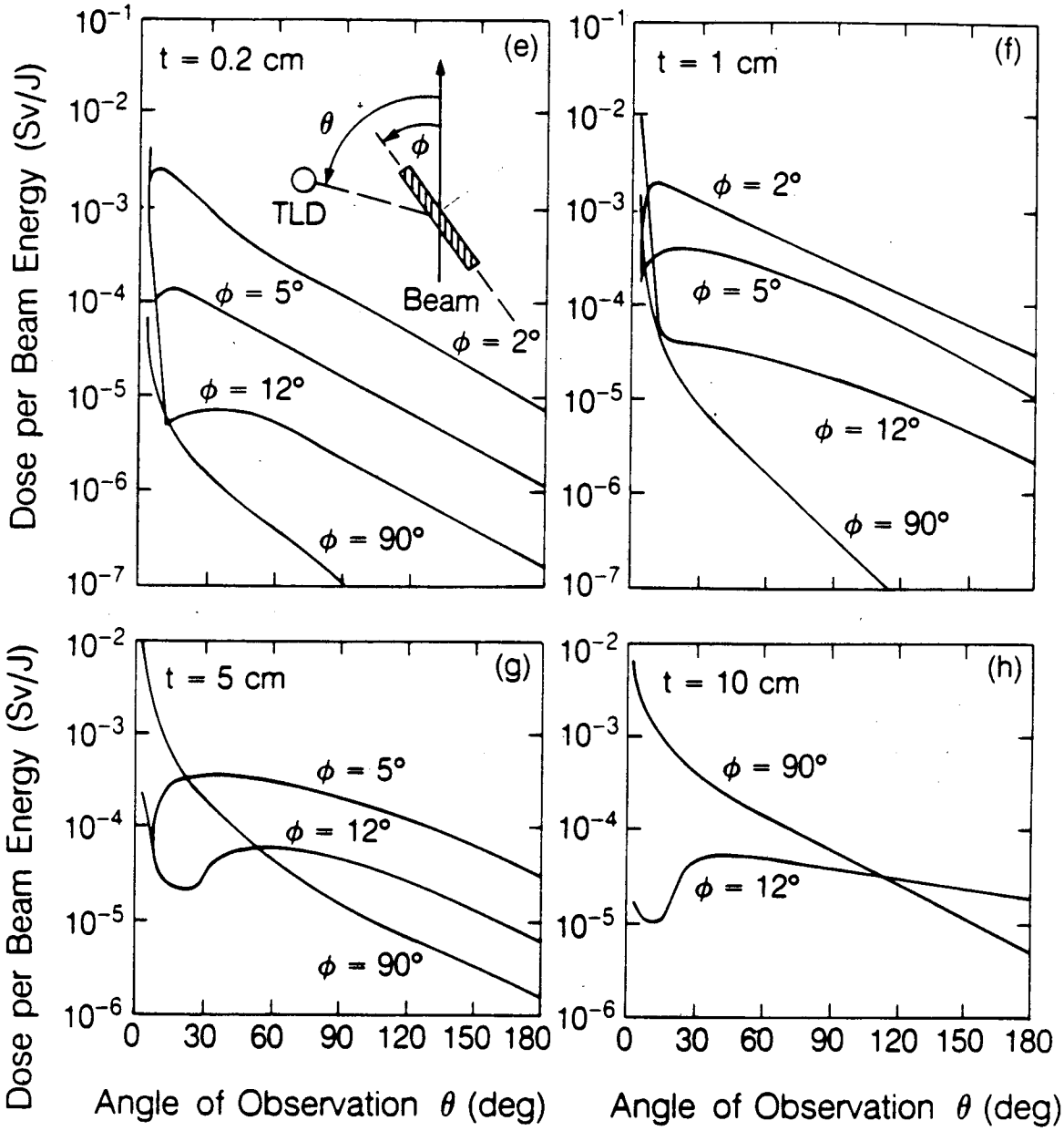

XBL 878-9775

Fig. 6 (e-h)
Thomas & Swanson

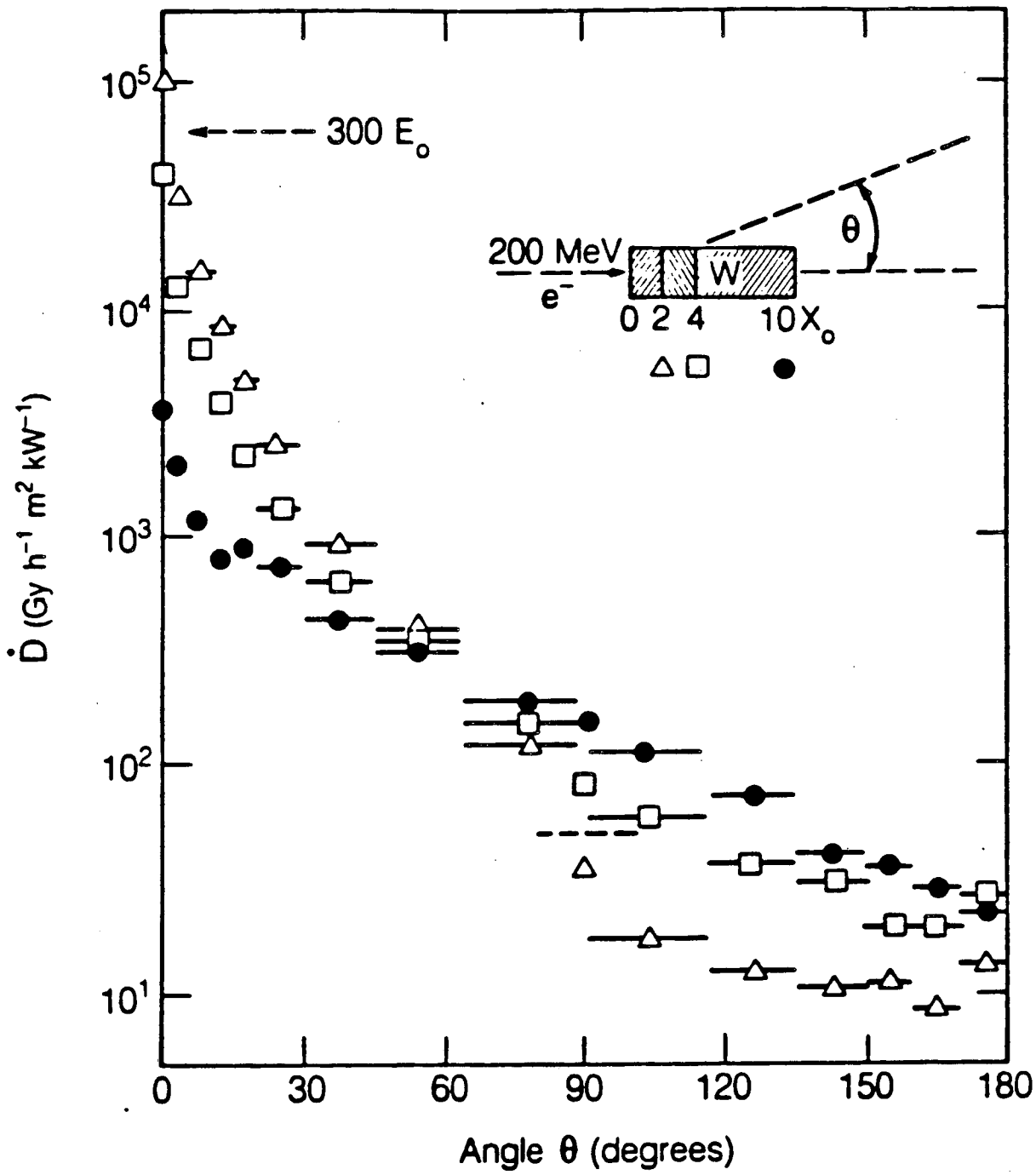

XBL 8610-9645

Fig. 7
Thomas & Swanson

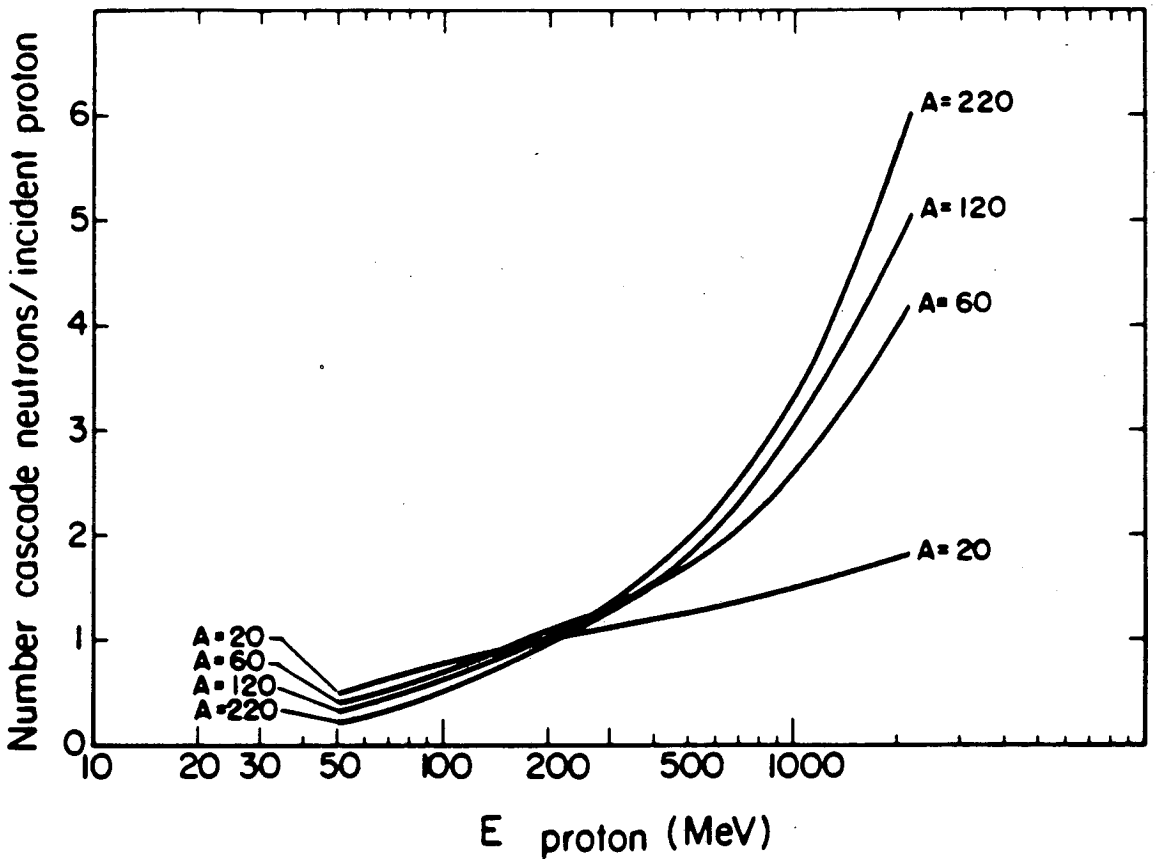

MU 28232

Fig. 8
Thomas & Swanson

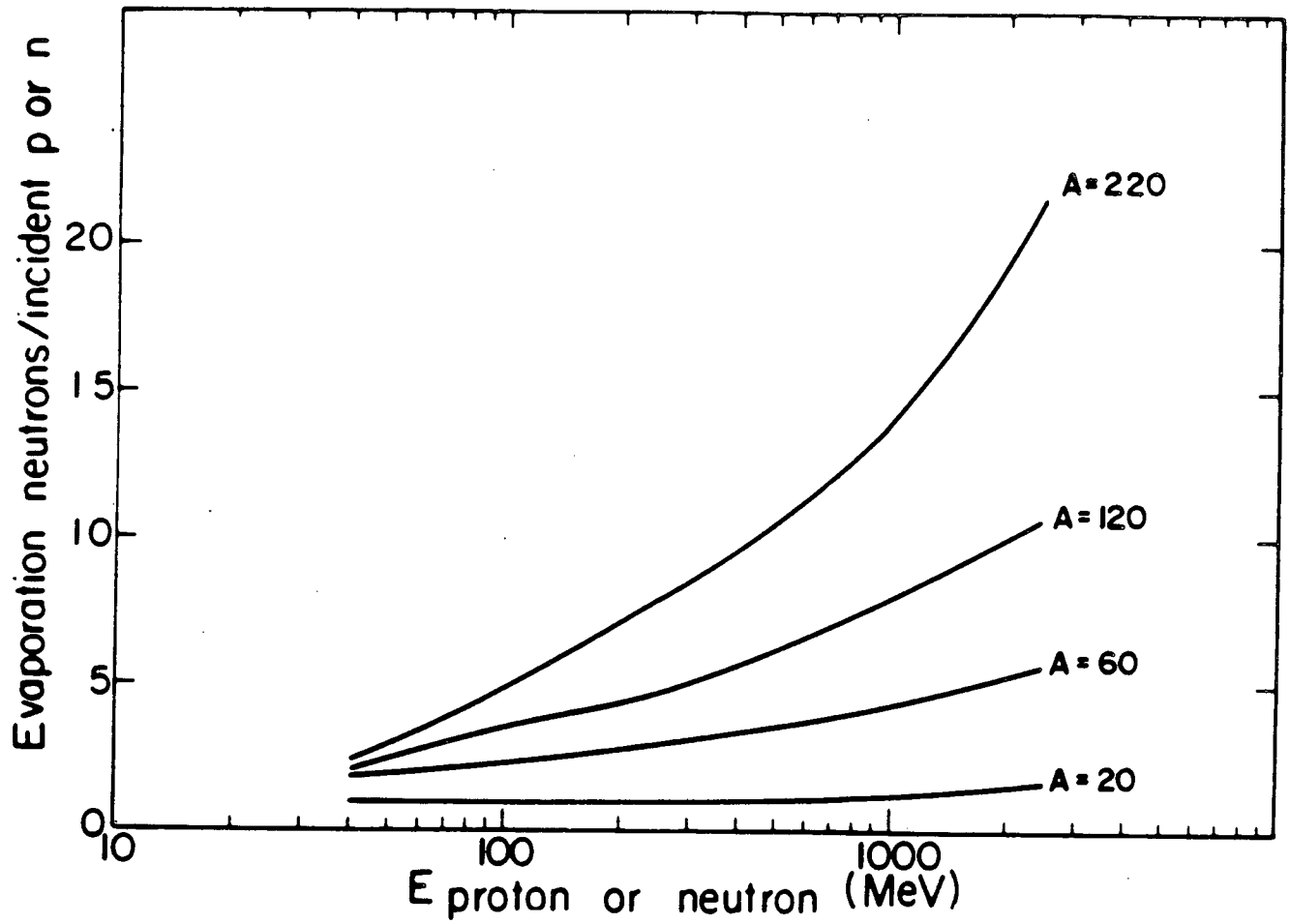

MU 28237

Fig. 9
Thomas & Swanson

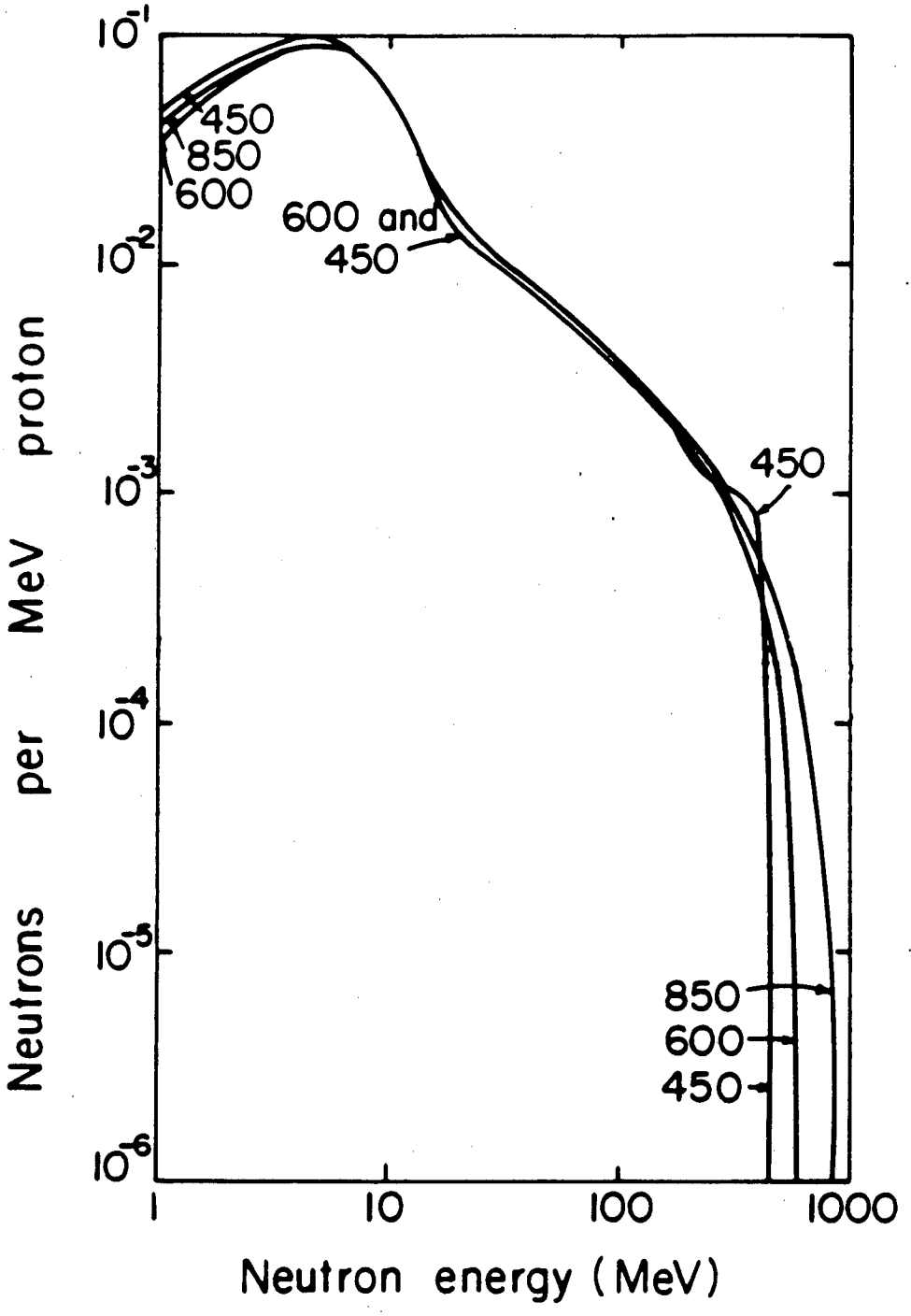

Fig. 10
Thomas & Swanson

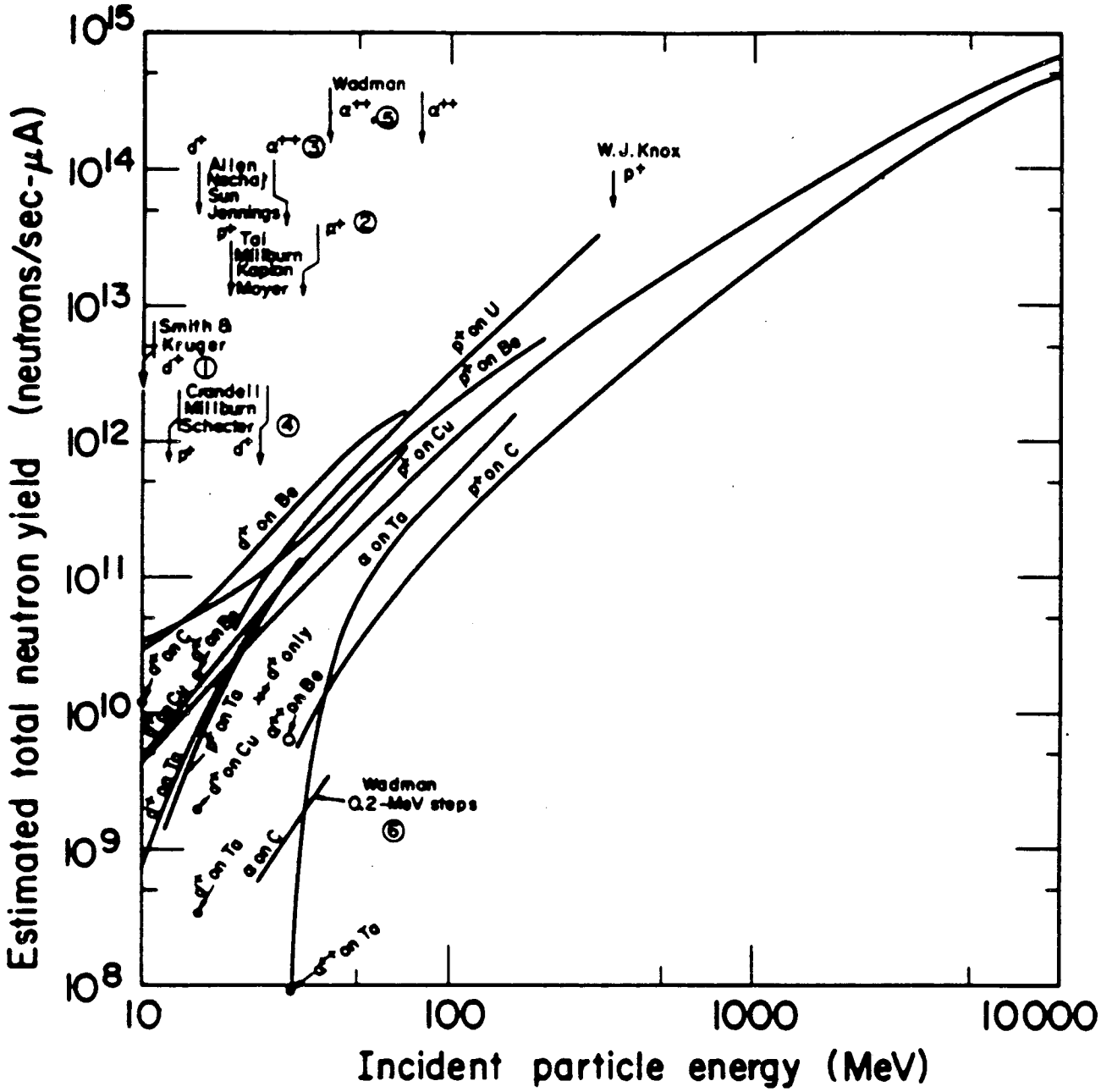

XBL6910-6059

Fig. 11
Thomas & Swanson

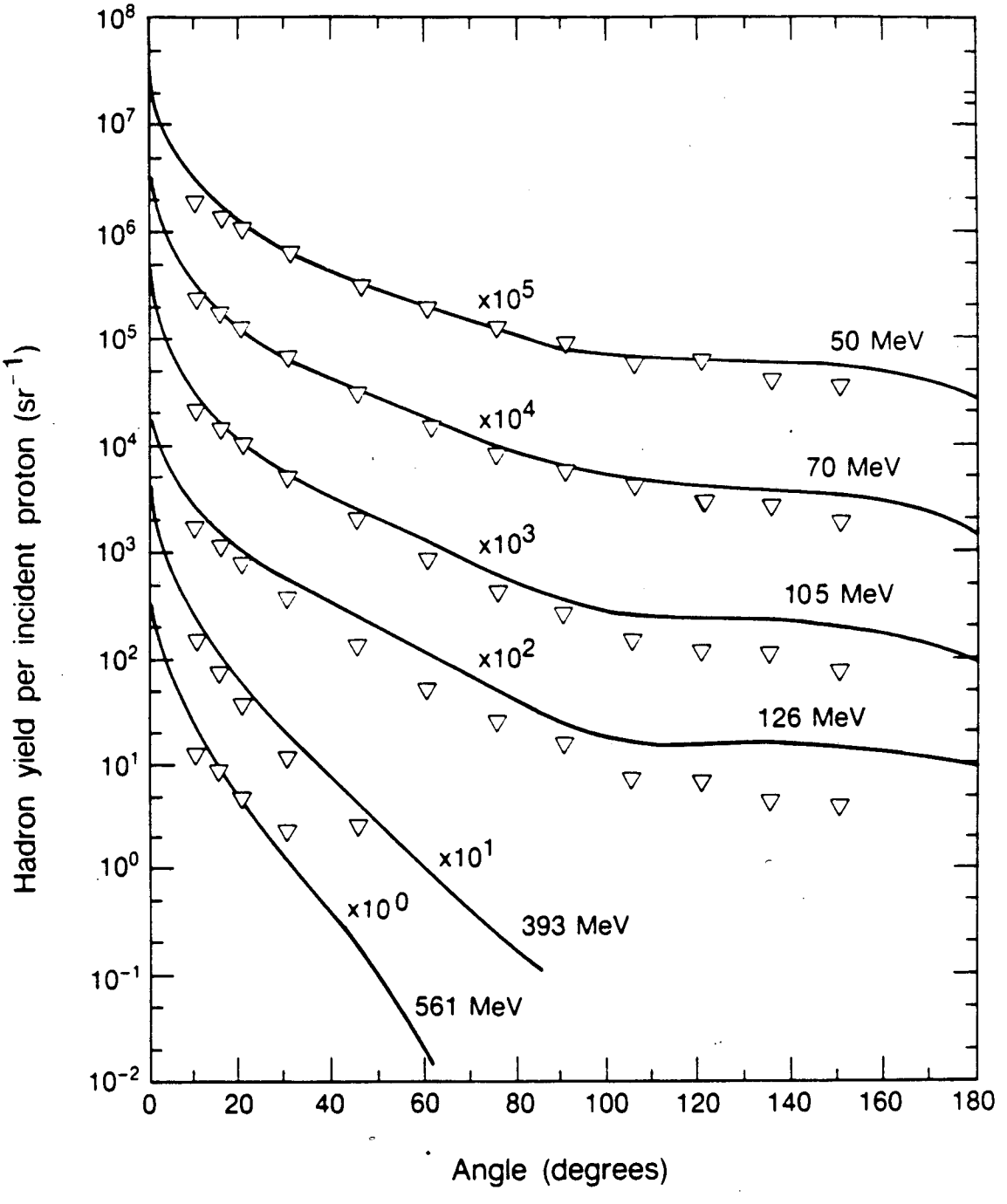

XBL 889-9725

Fig. 12
Thomas & Swanson

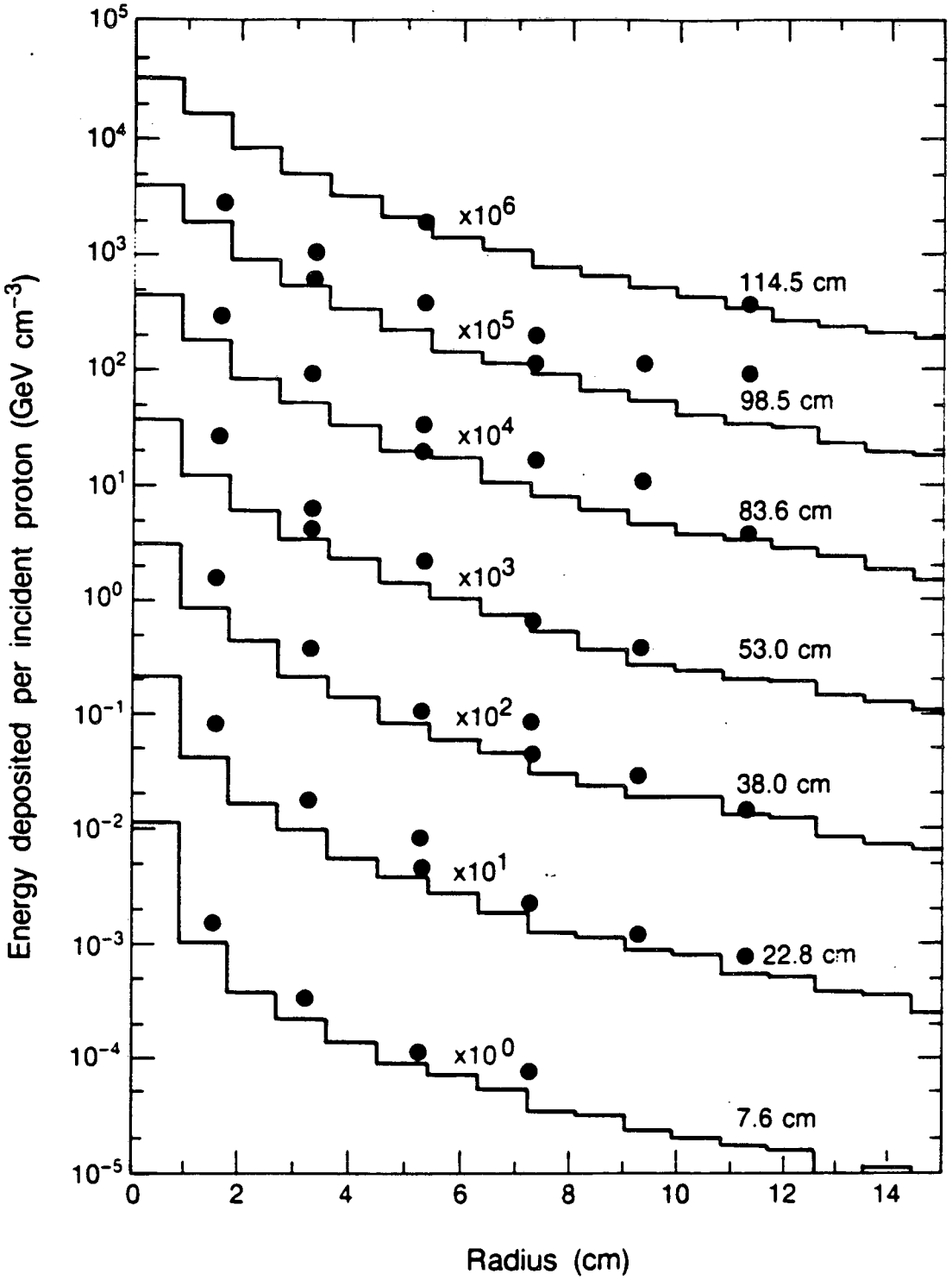

Fig. 13
Thomas & Swanson

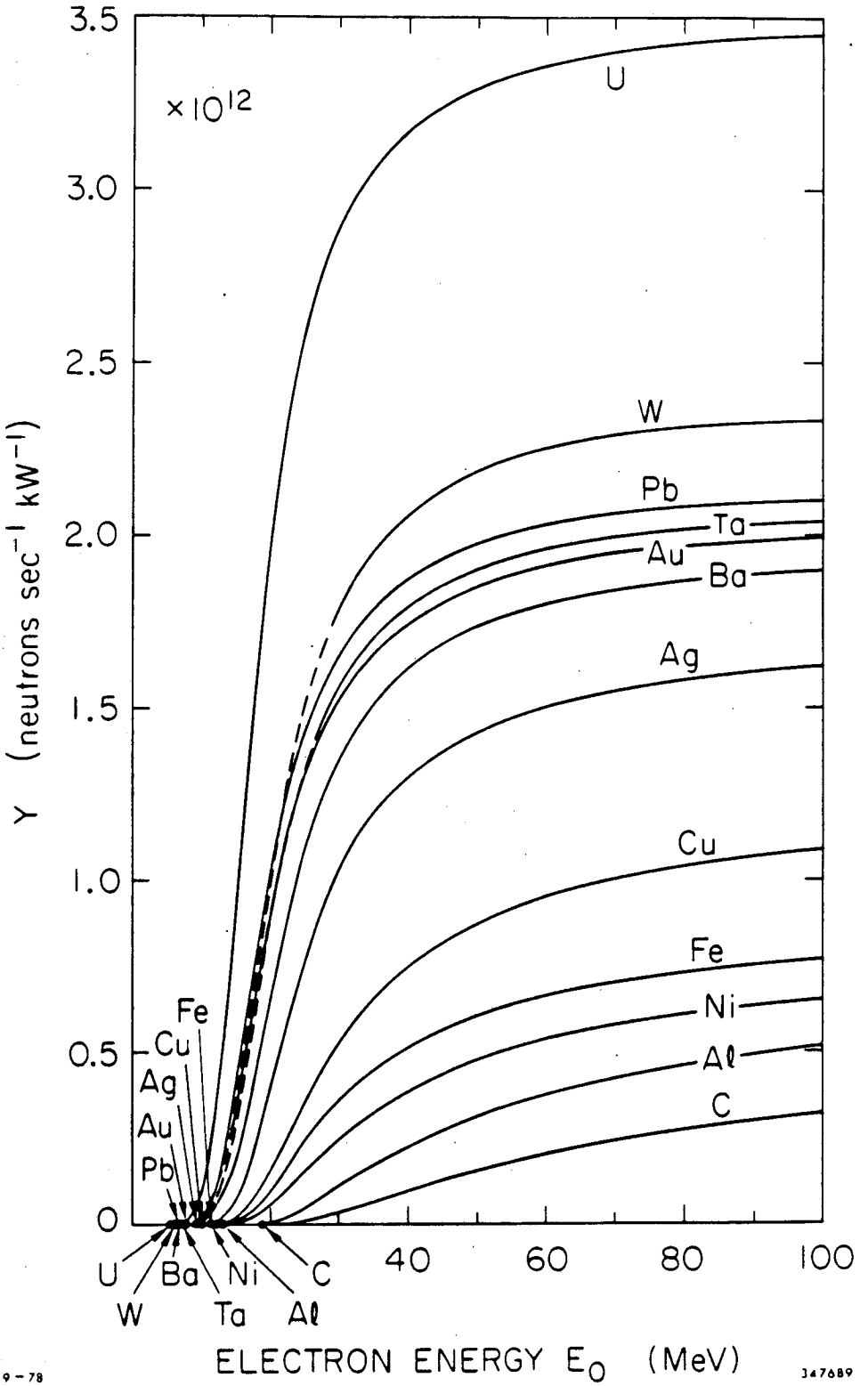

Fig. 14
Thomas & Swanson

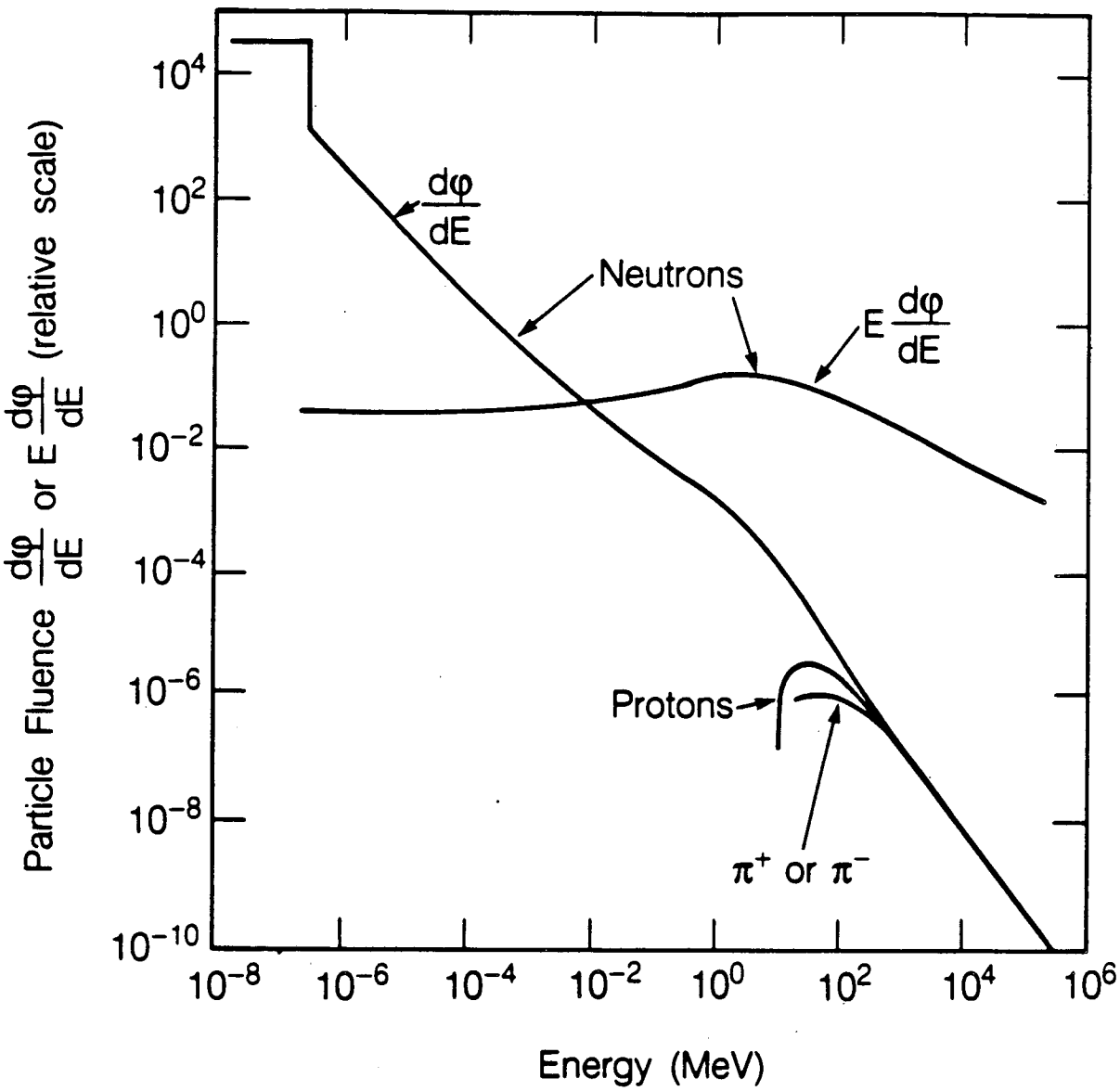

XBL 868-12020

Fig. 15
Thomas & Swanson

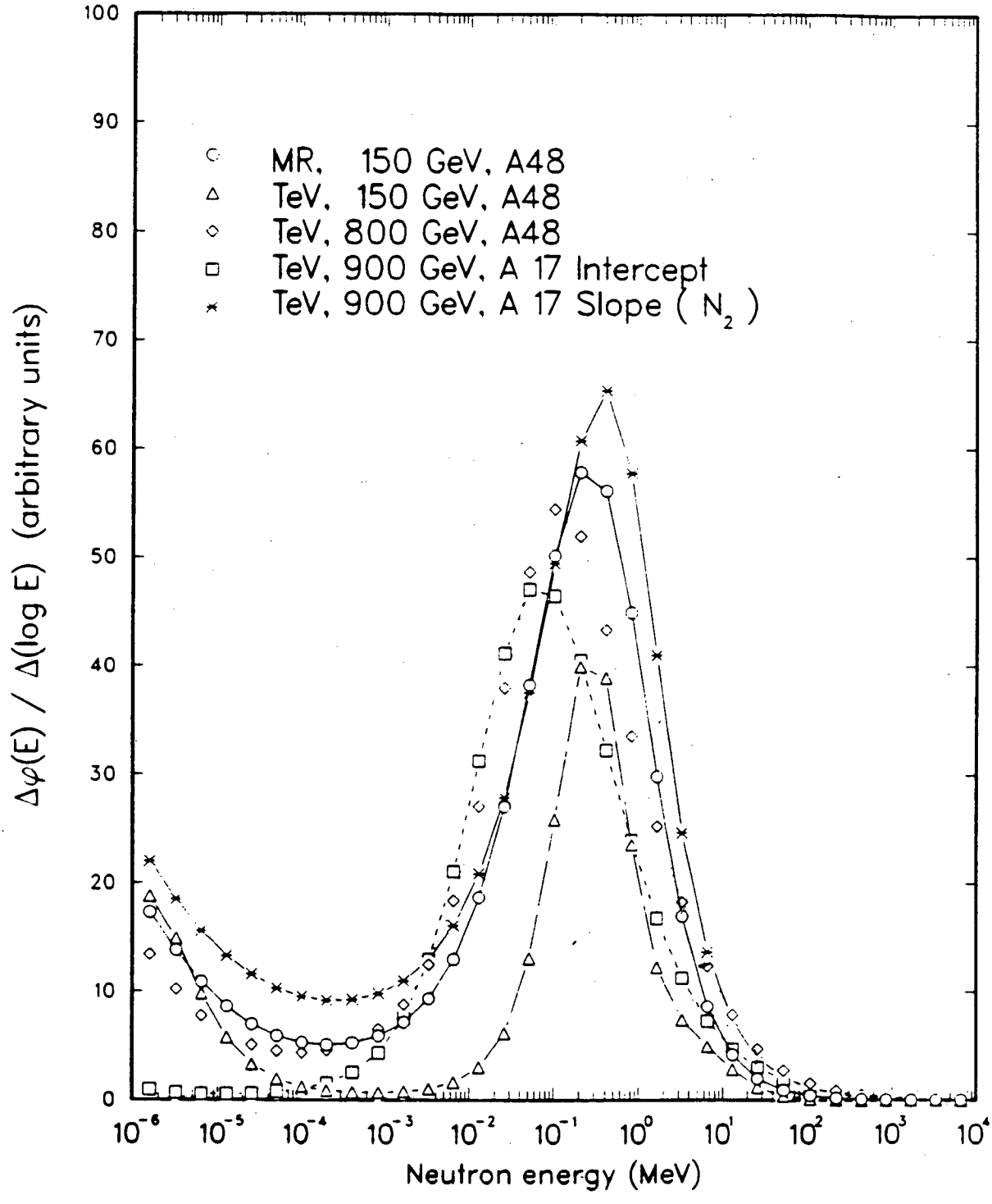

XBL 889-3442

Fig. 16
Thomas & Swanson

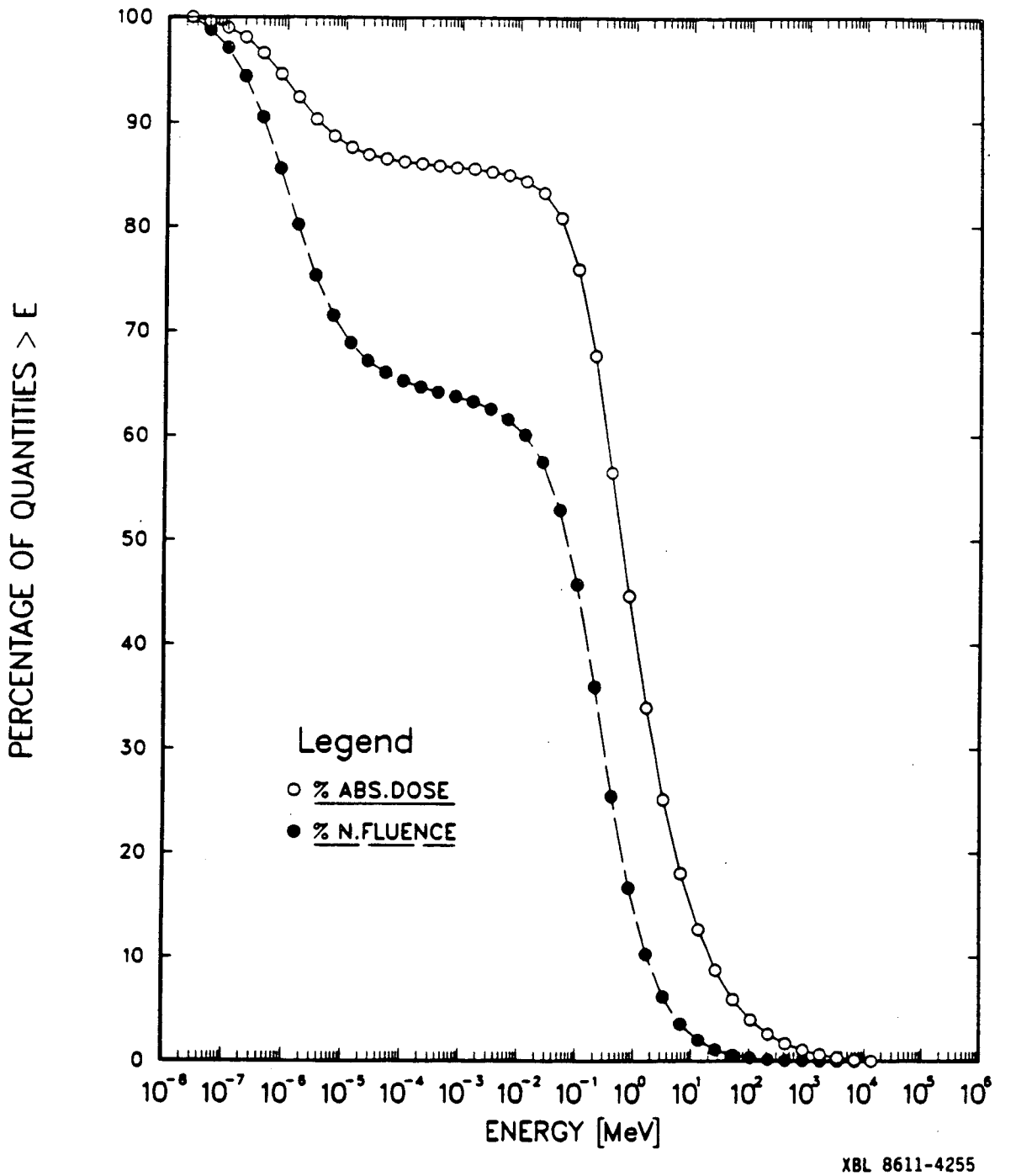

Fig. 17
Thomas & Swanson

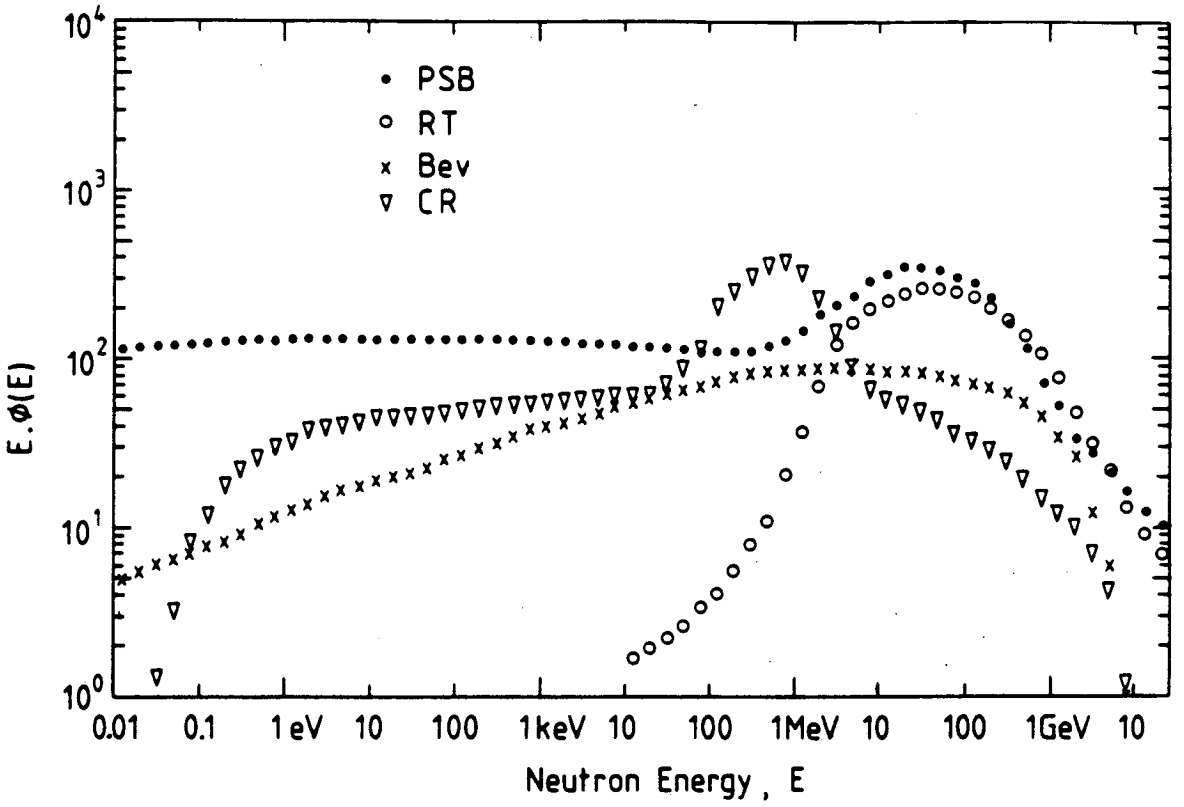

Fig. 1

XBL 8412-5057

Fig. 18
Thomas & Swanson

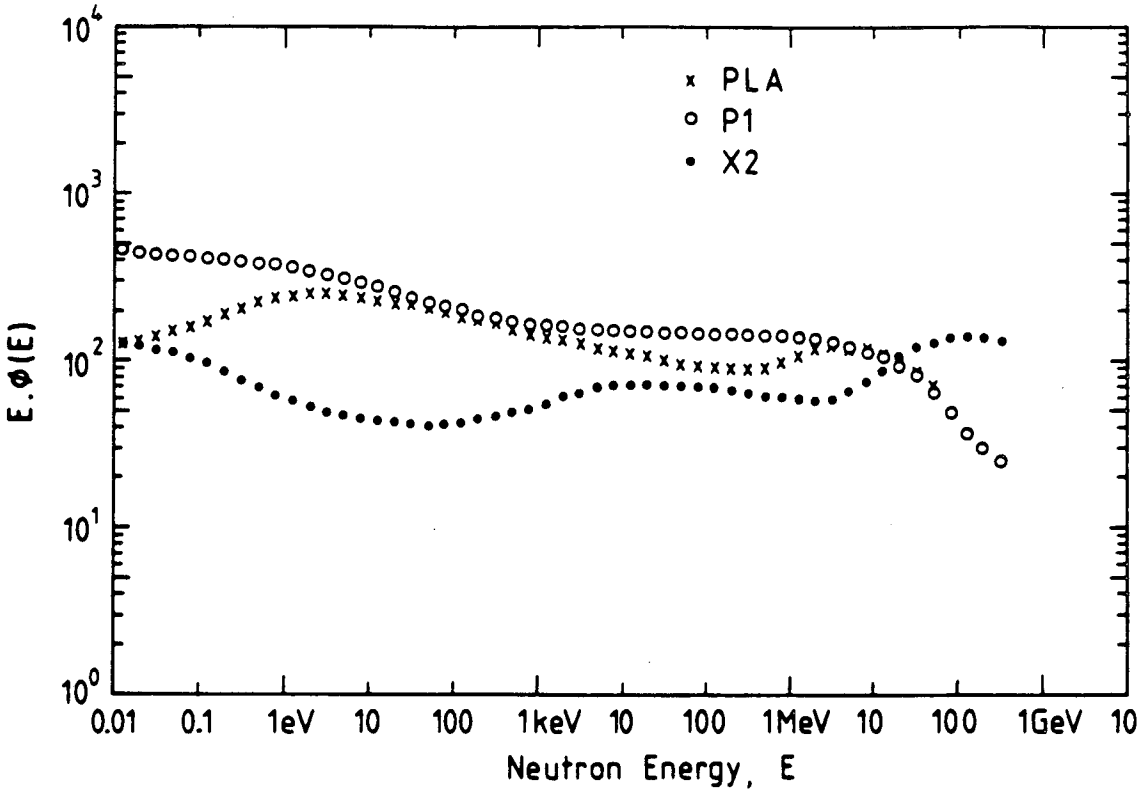

XBL 8412-5058

Fig. 19
Thomas & Swanson

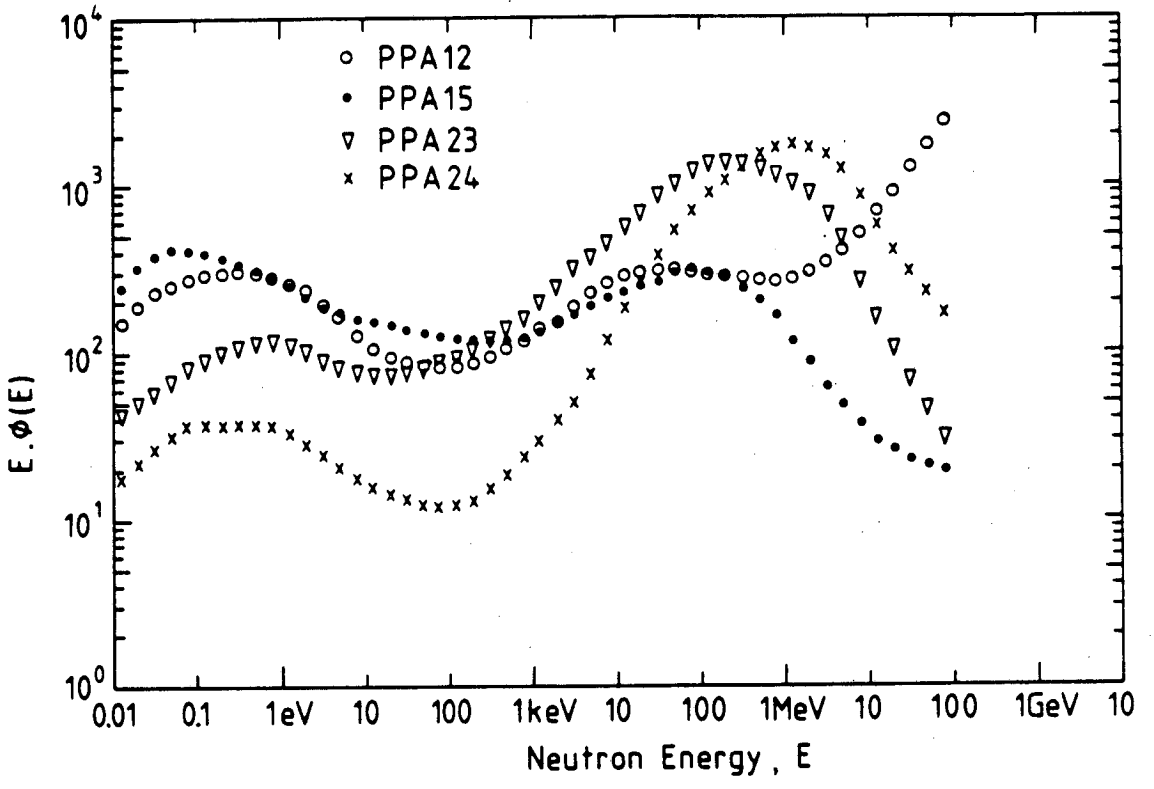

XBL 8412-5059

Fig. 20
Thomas & Swanson

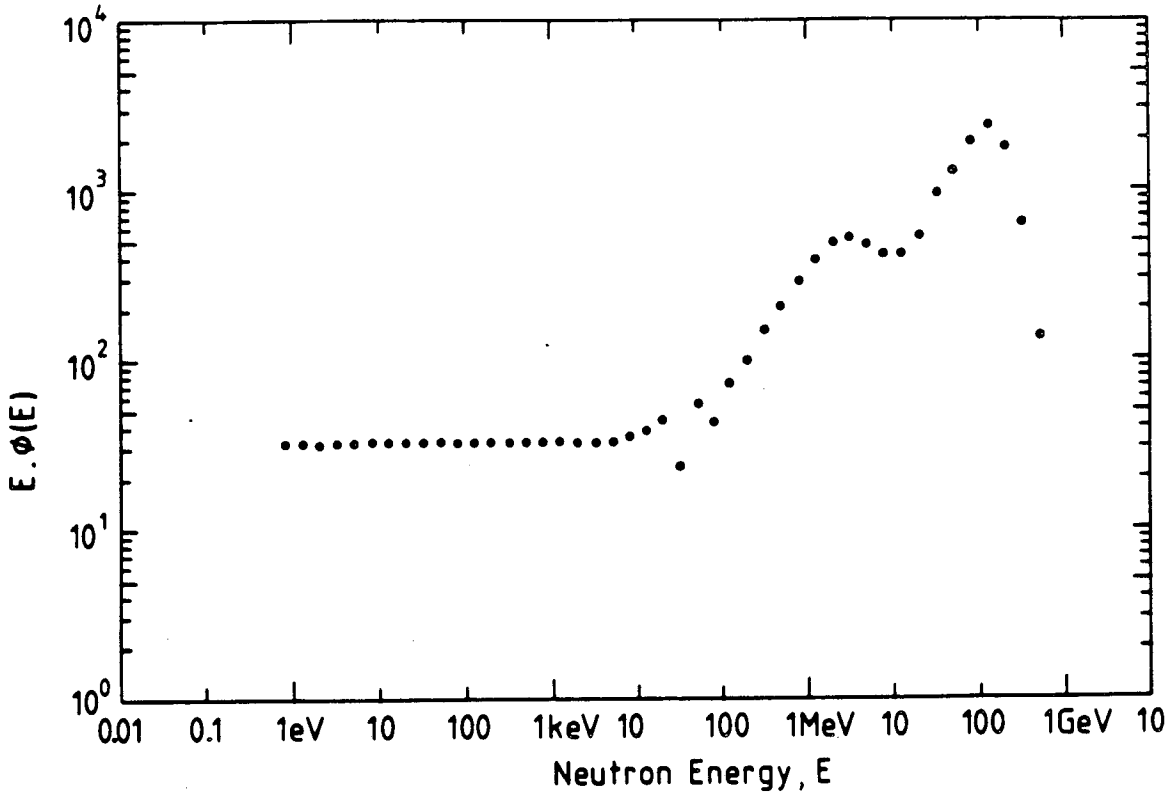

XBL 8412-5060

Fig. 21
Thomas & Swanson

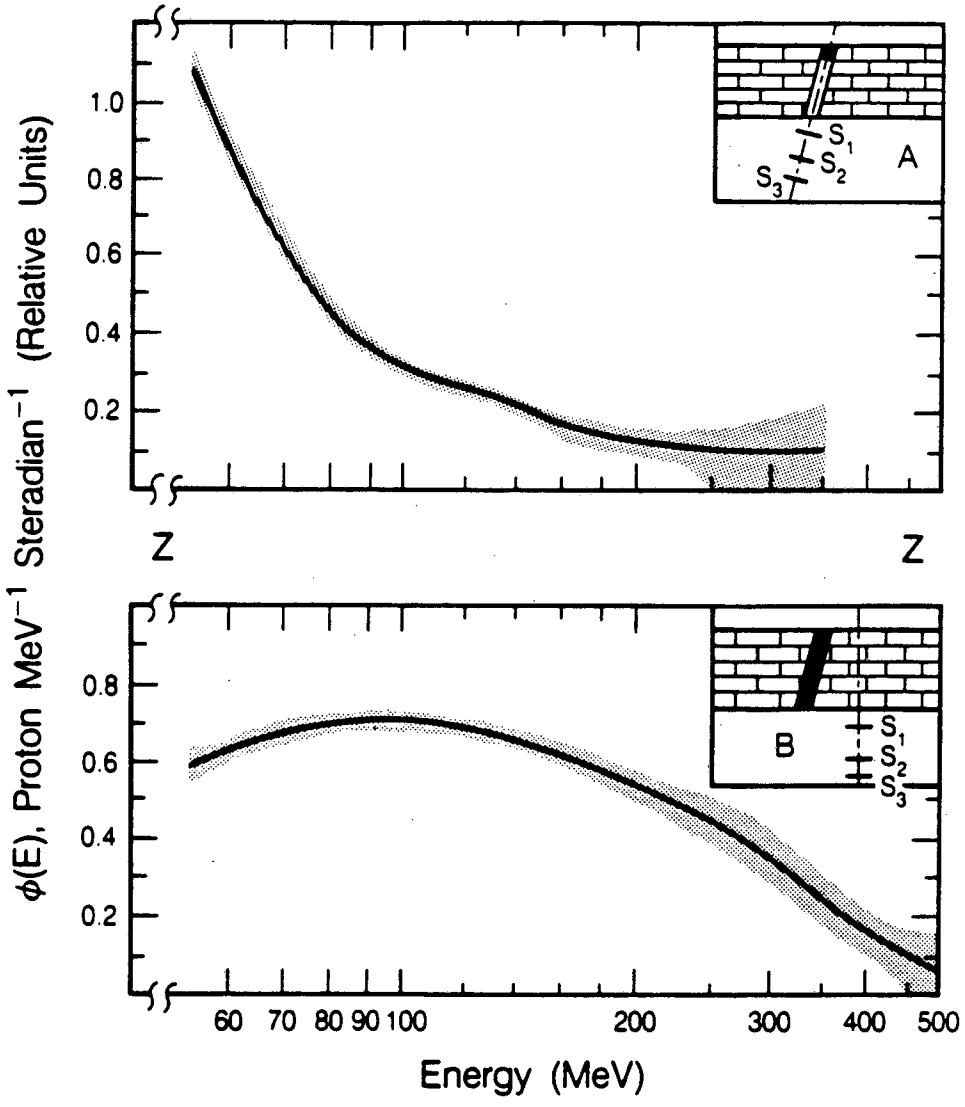

XBL 859-3856

Fig. 22
Thomas & Swanson

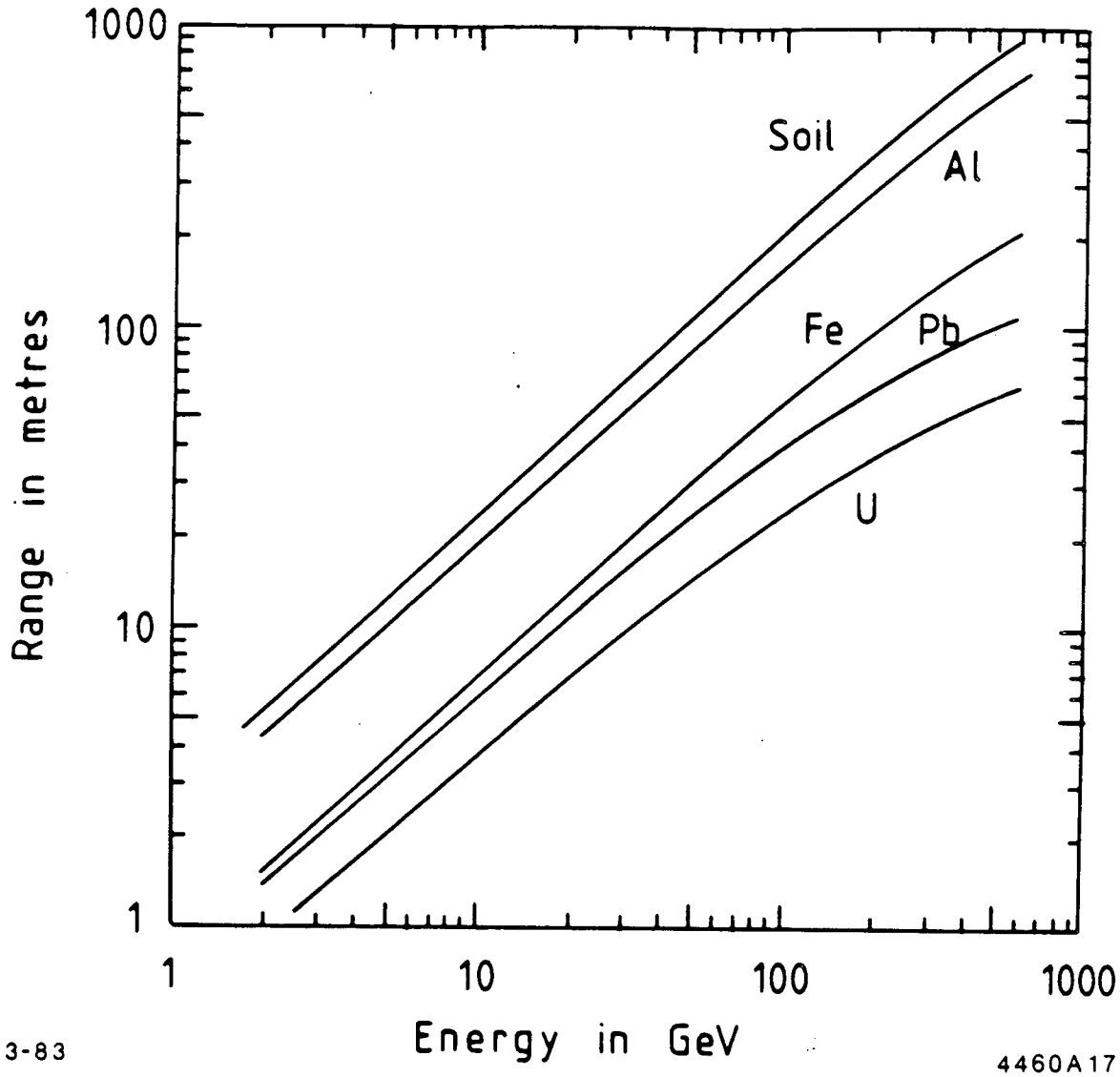

XBL 889-3444

Fig. 23
Thomas & Swanson

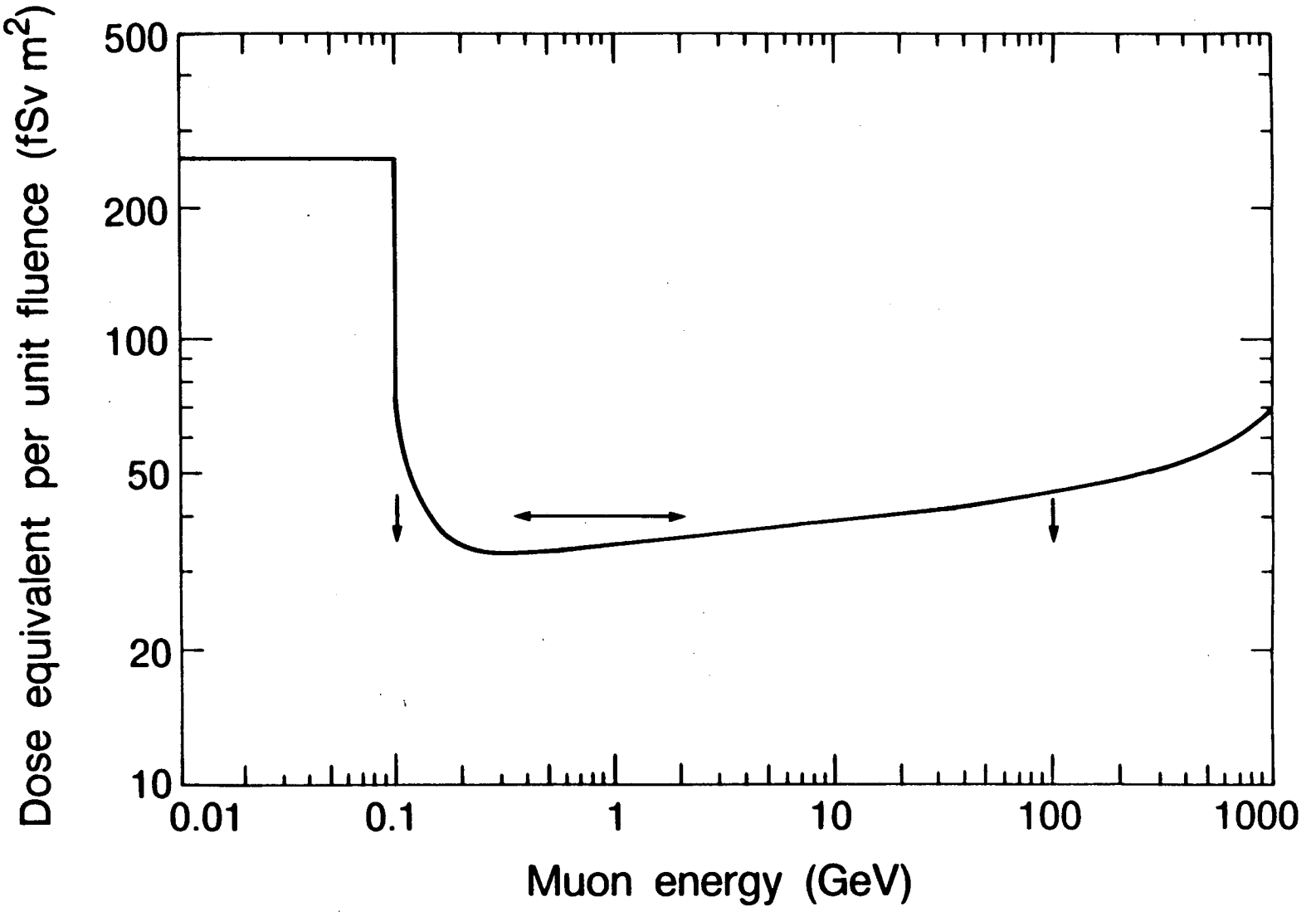

XBL 8611-9670A

Fig. 24
Thomas & Swanson

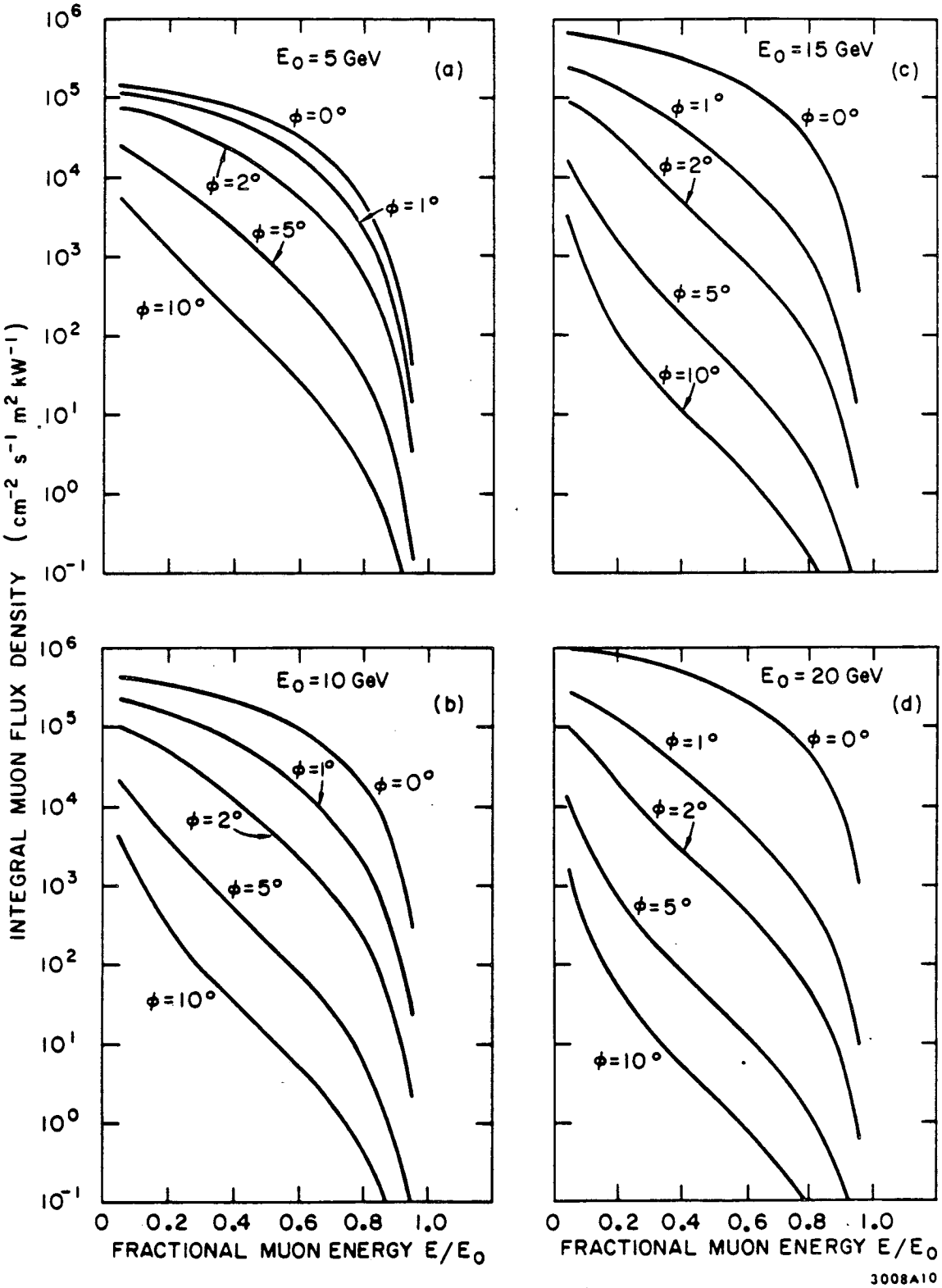

Fig. 25
Thomas & Swanson

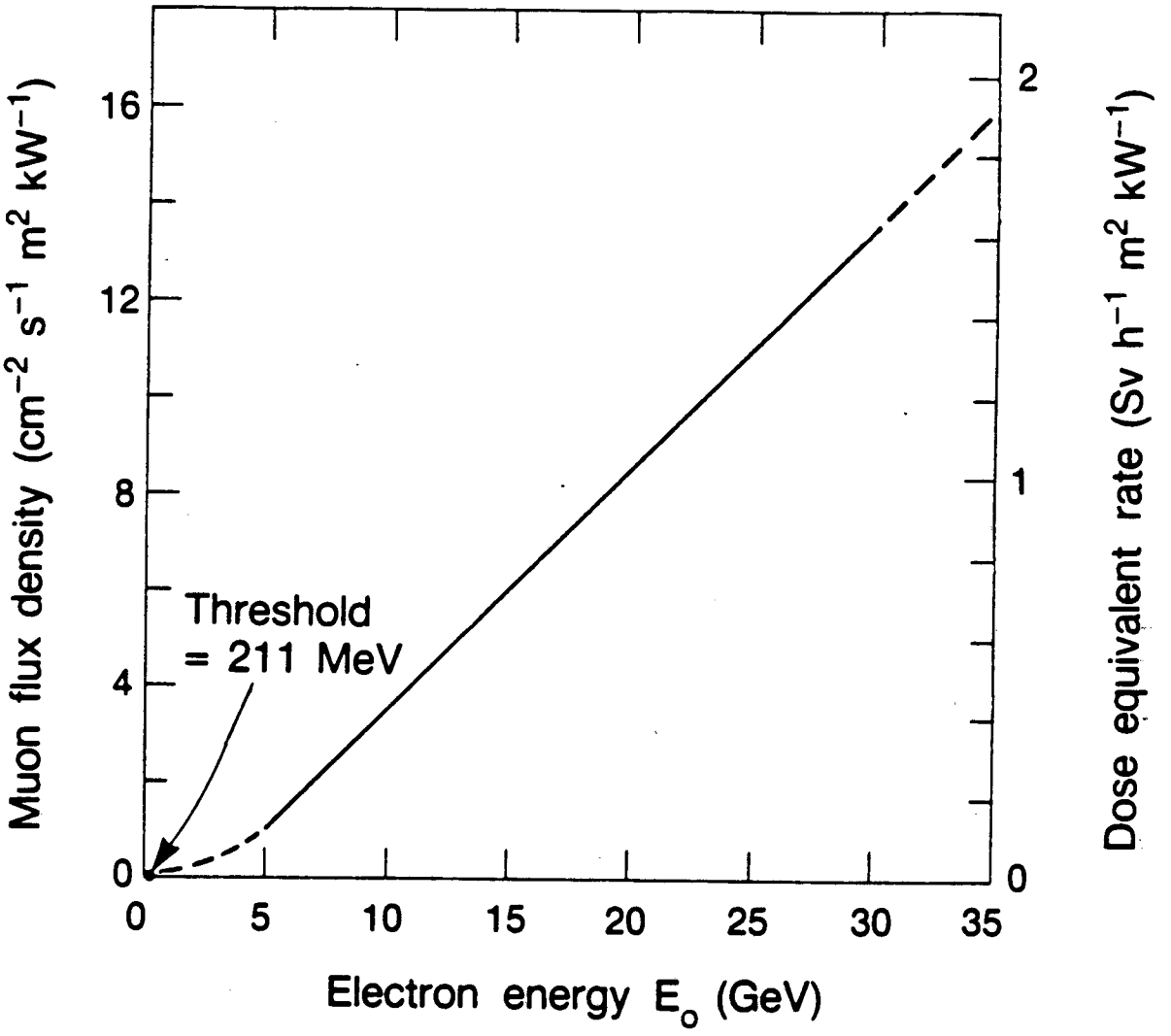

XBL 8710-5940

Fig. 26
Thomas & Swanson

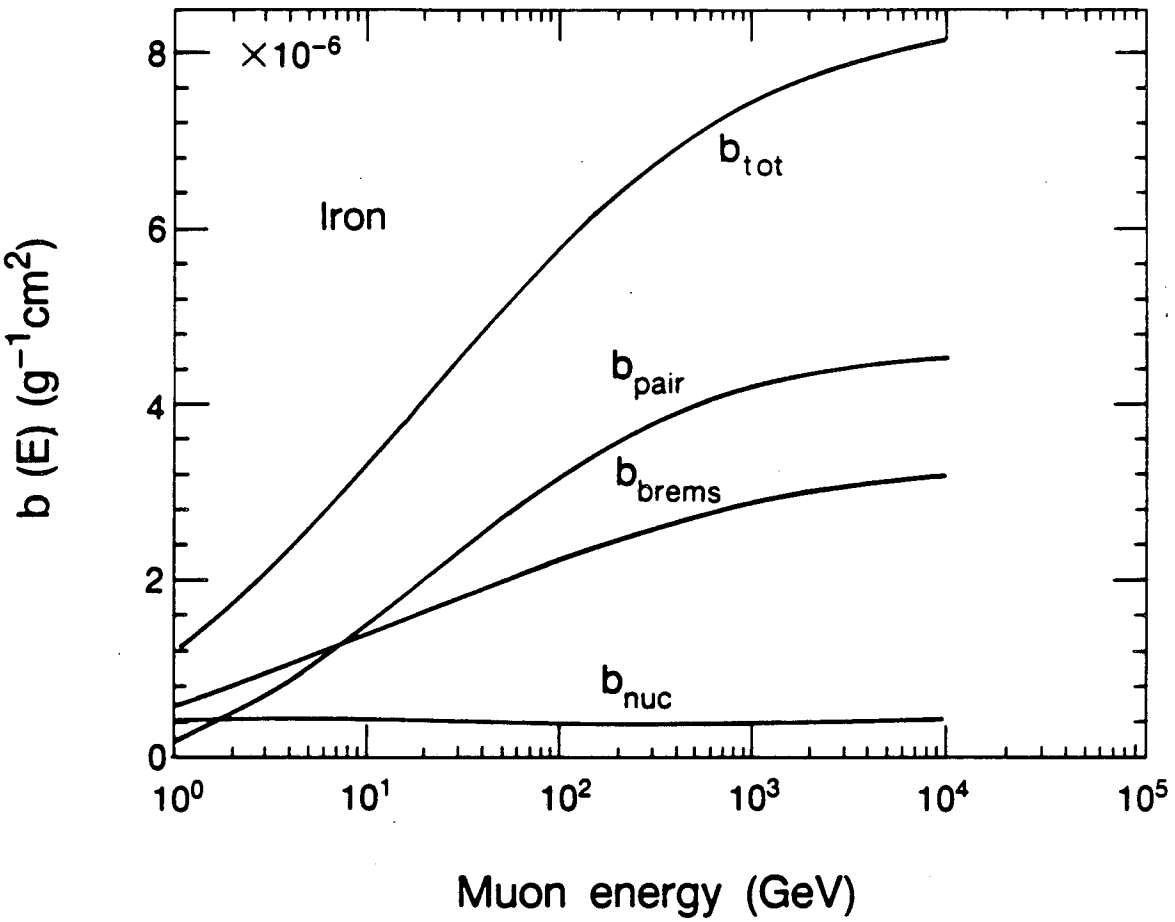

XBL 8710-5939

Fig. 27
Thomas & Swanson

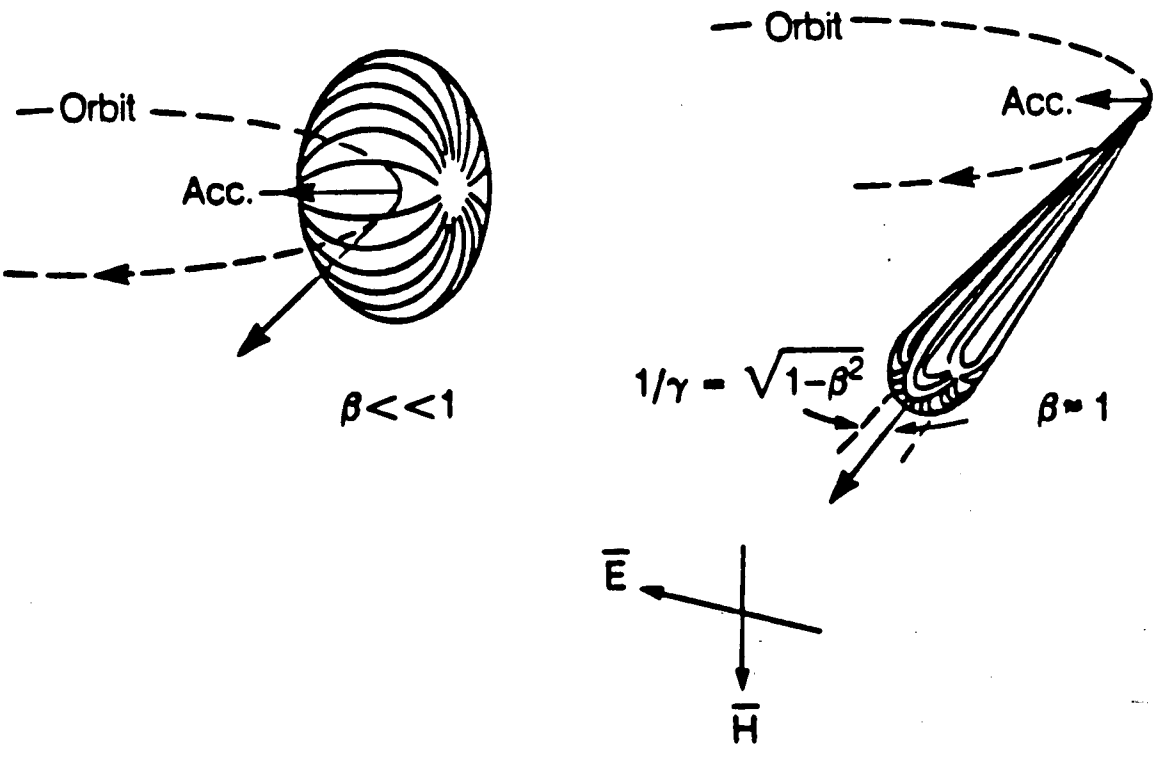

XBL 8611-9668

Fig. 28
Thomas & Swanson

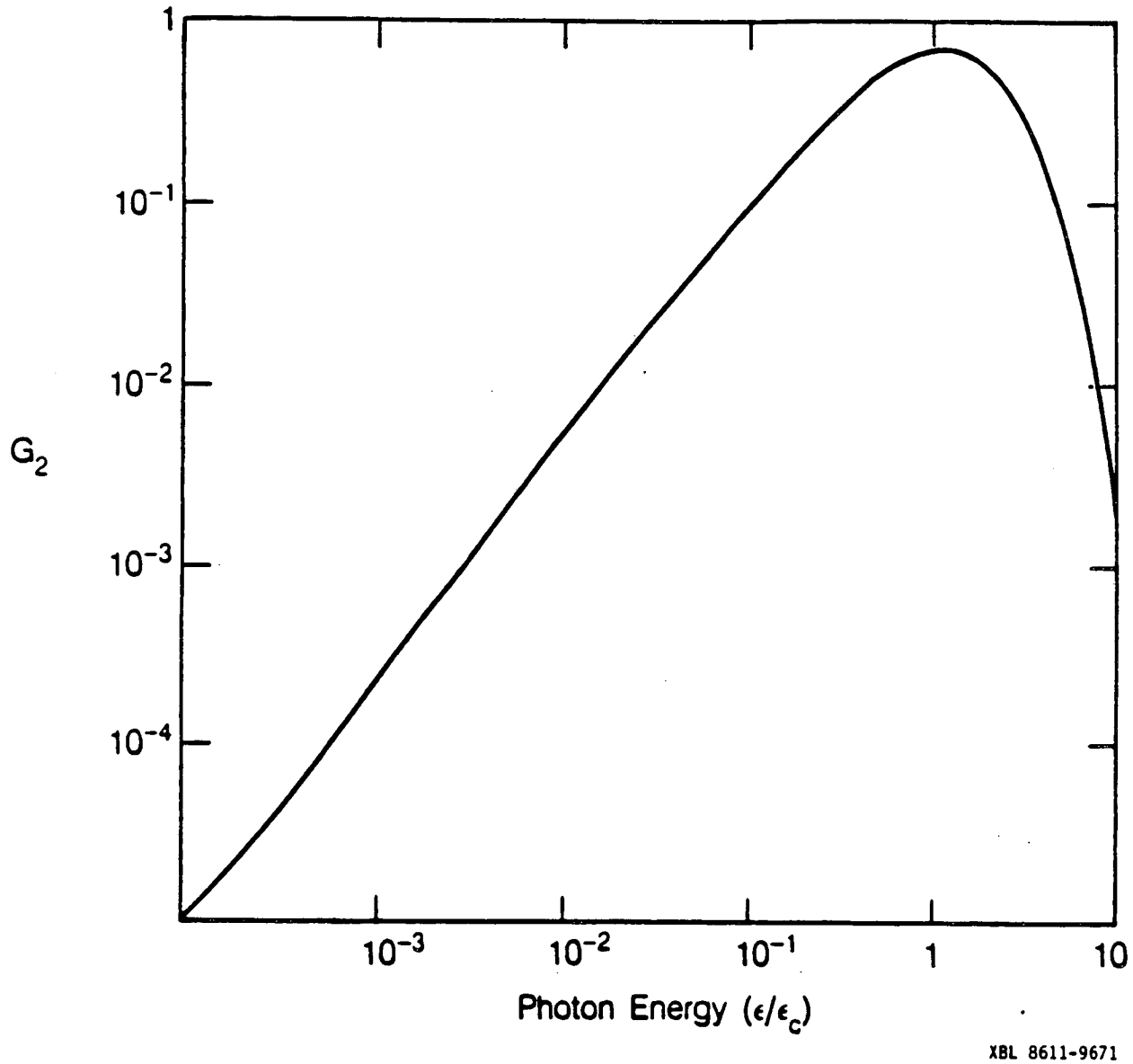

Fig. 29
Thomas & Swanson

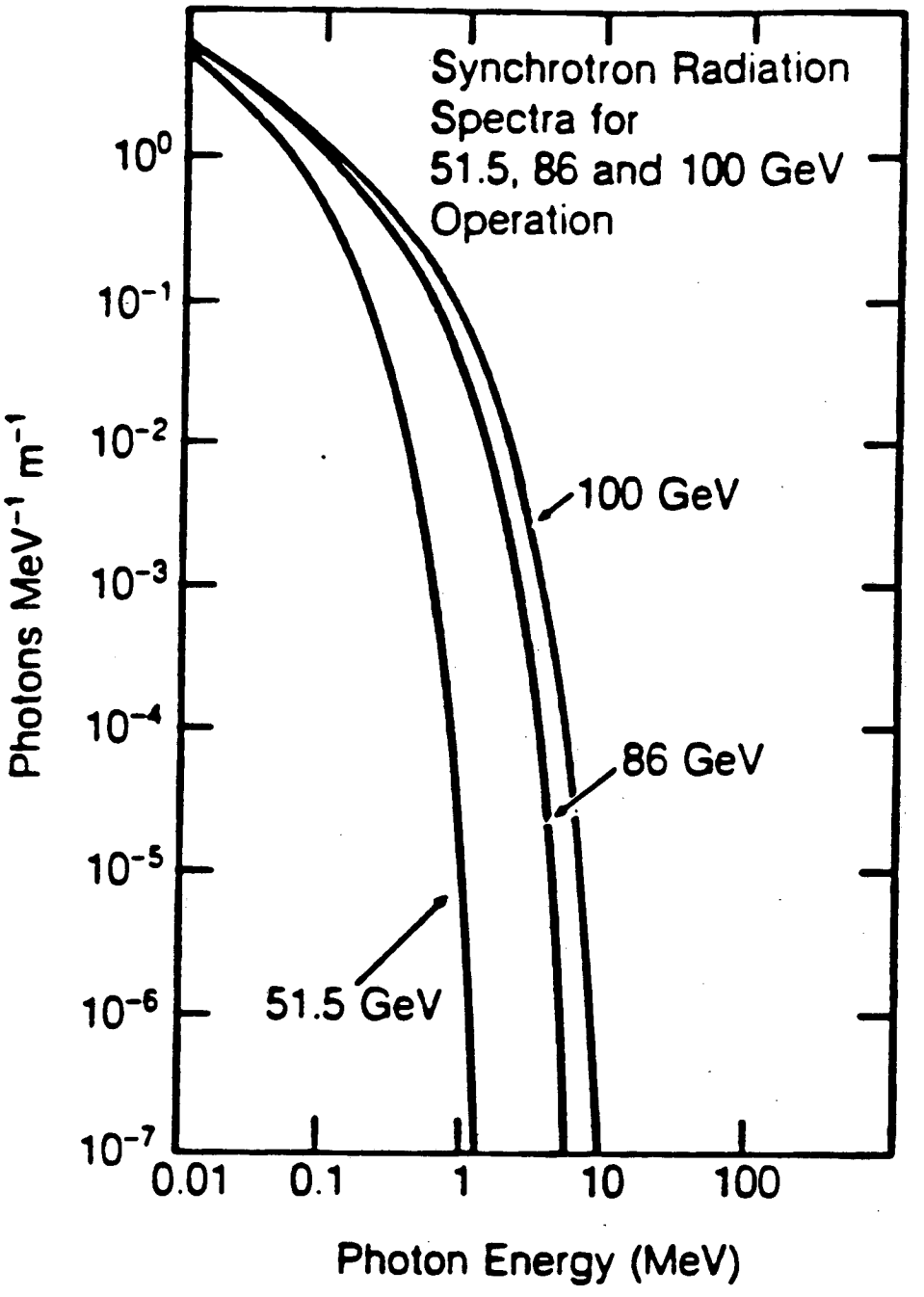

XBL 8610-9649

Fig. 30
Thomas & Swanson

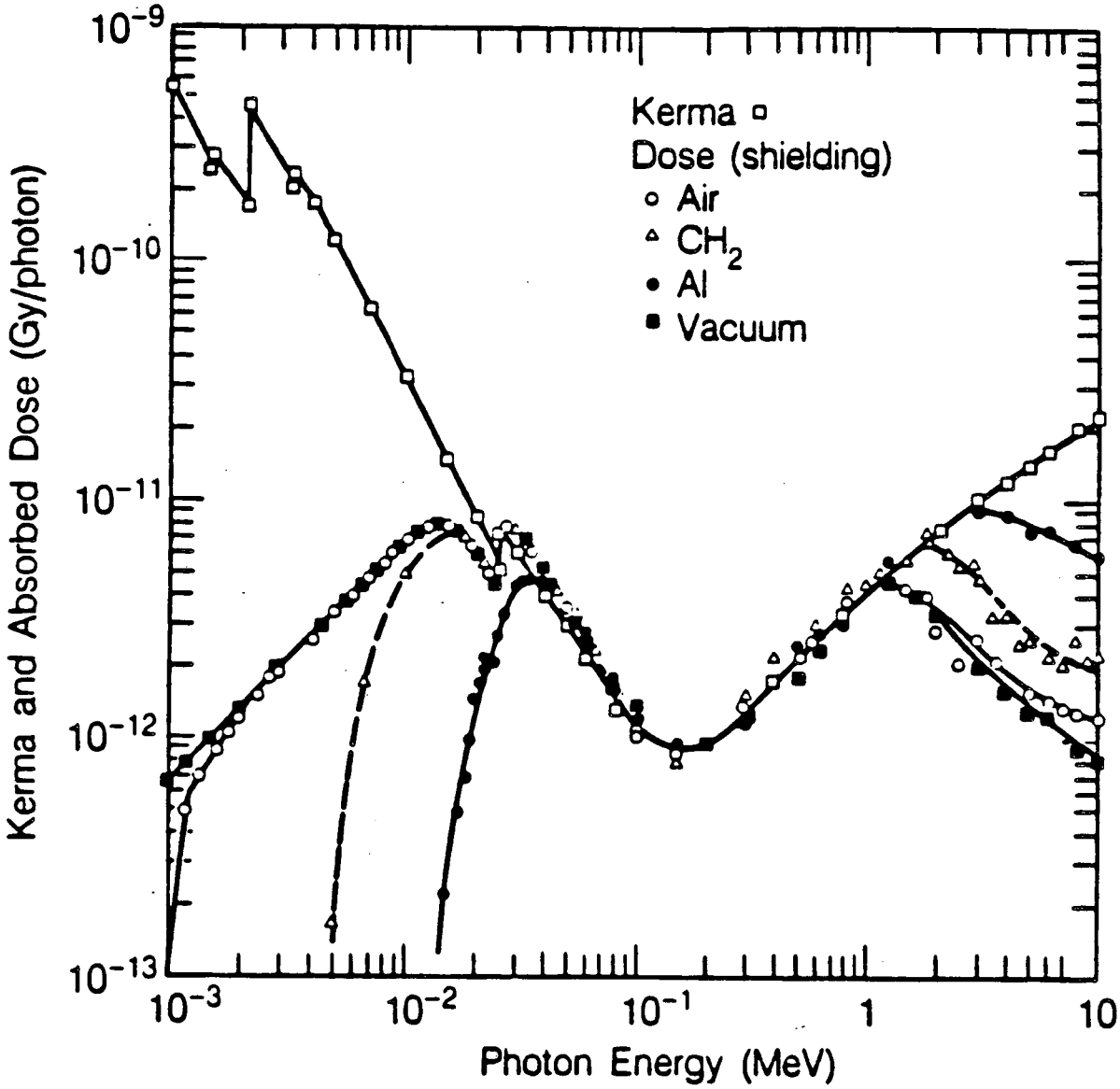

XBL 8611-9673

Fig. 31
Thomas & Swanson

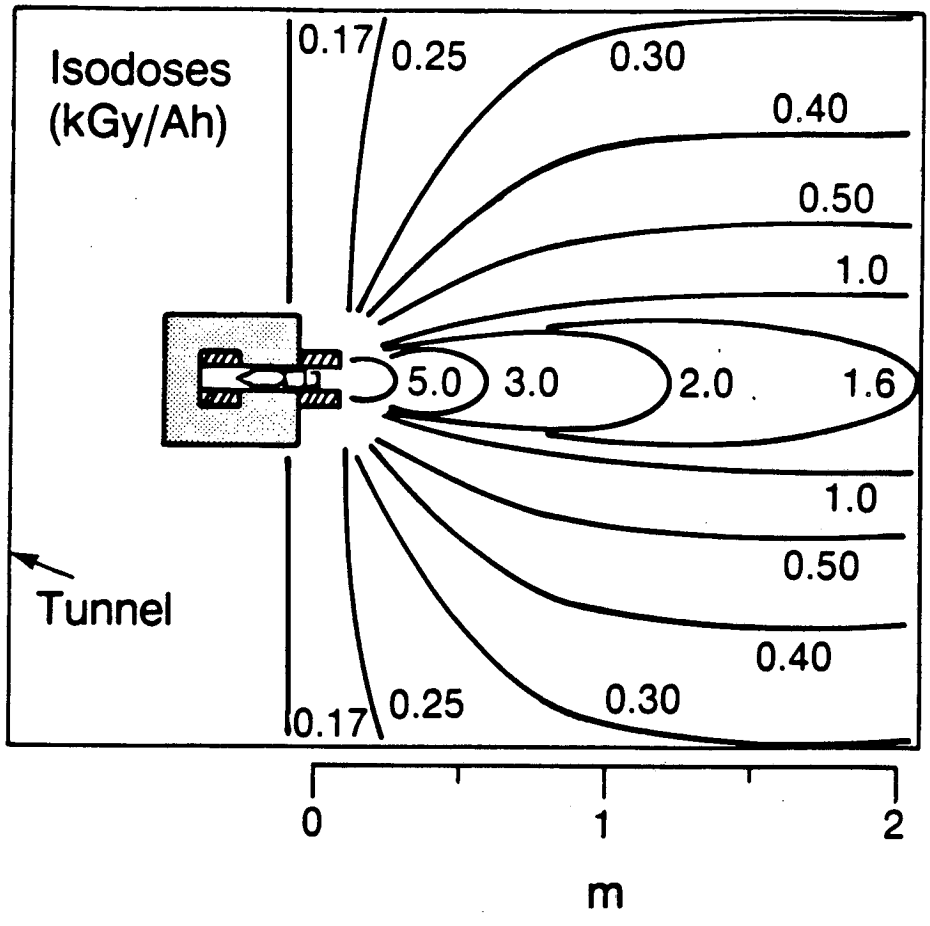

XBL 8710-5934

Fig. 32
Thomas & Swanson

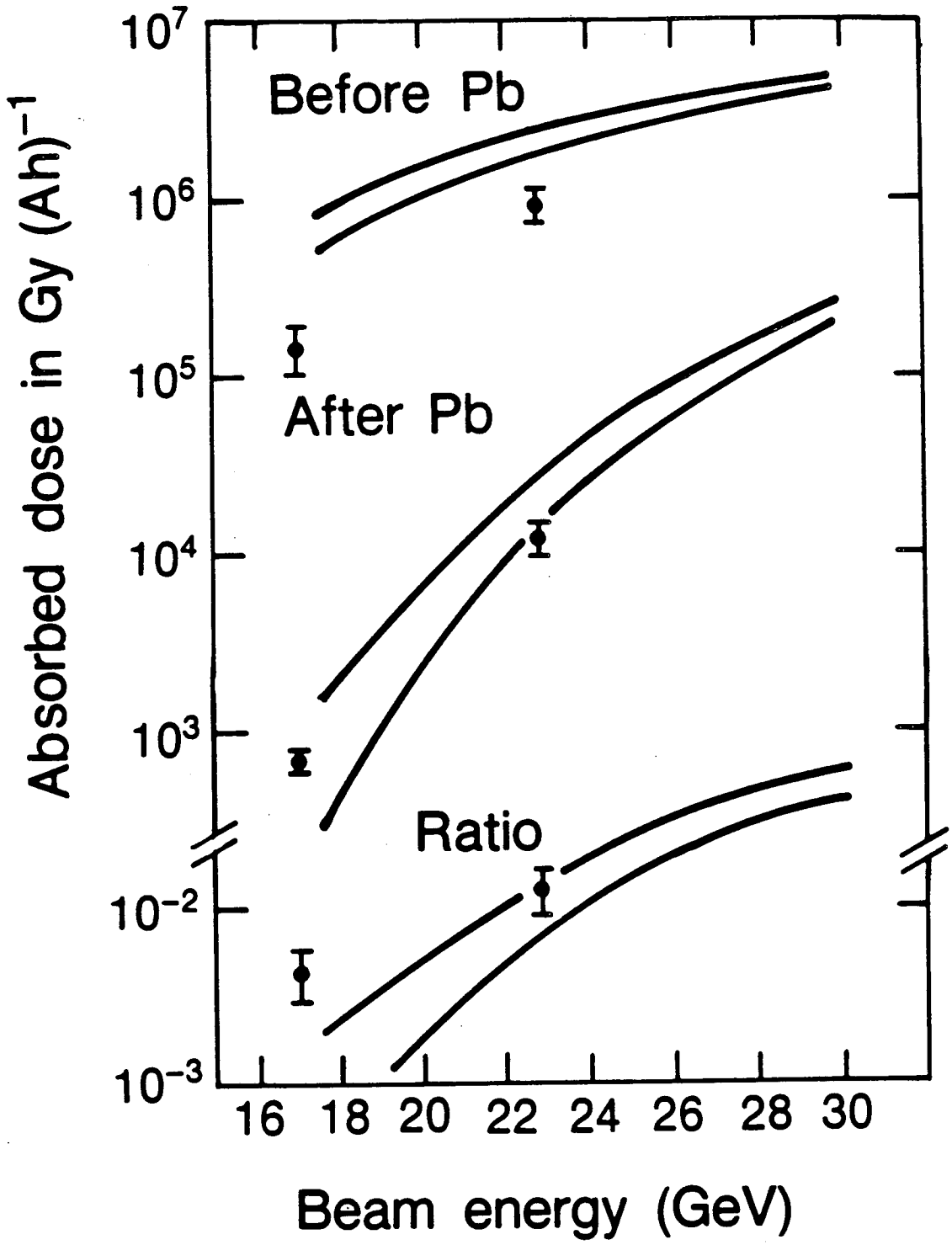

XBL 8611-9669

Fig. 33
Thomas & Swanson

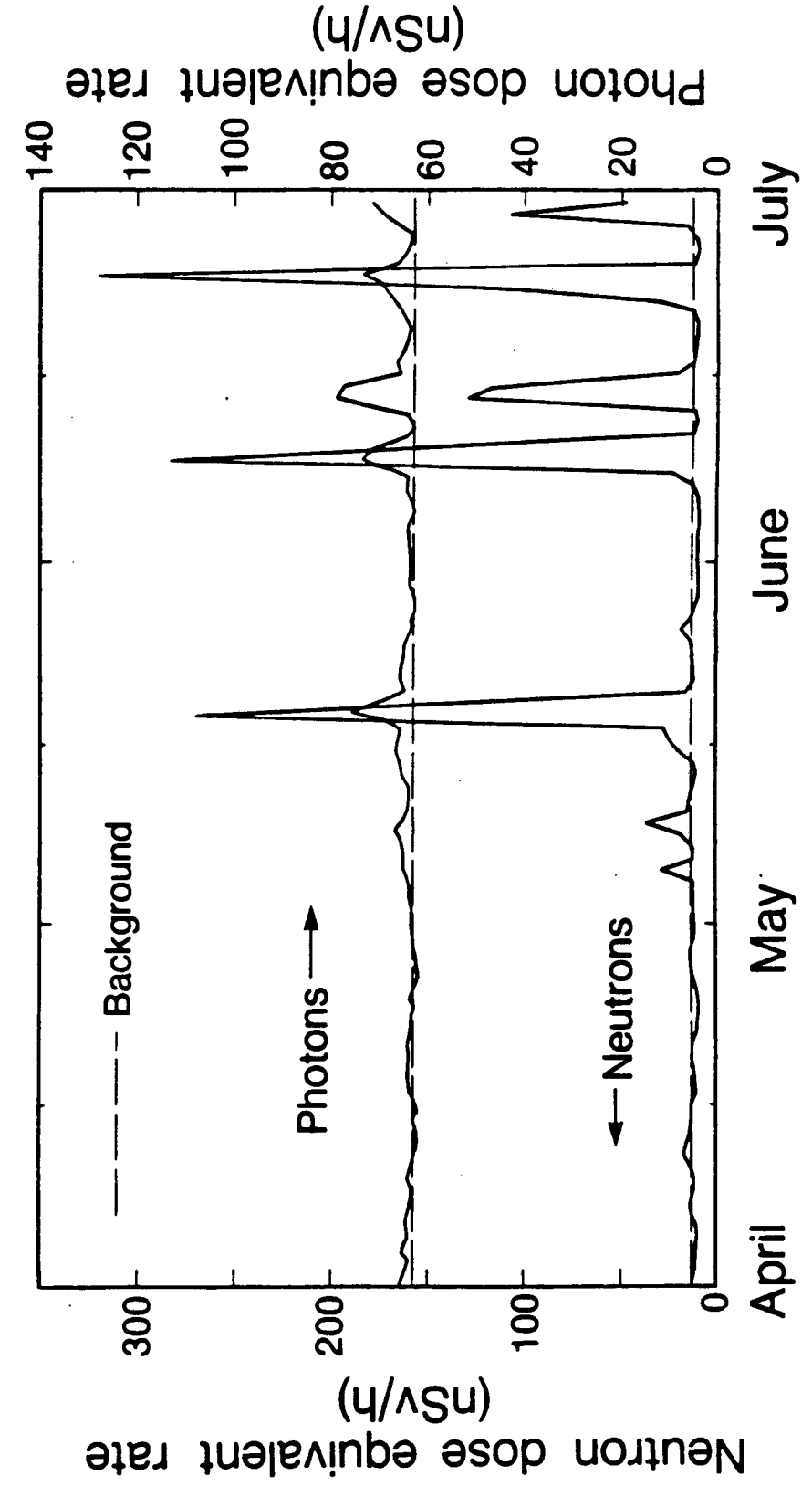

XBL 8710-5941

Fig. 34
Thomas & Swanson

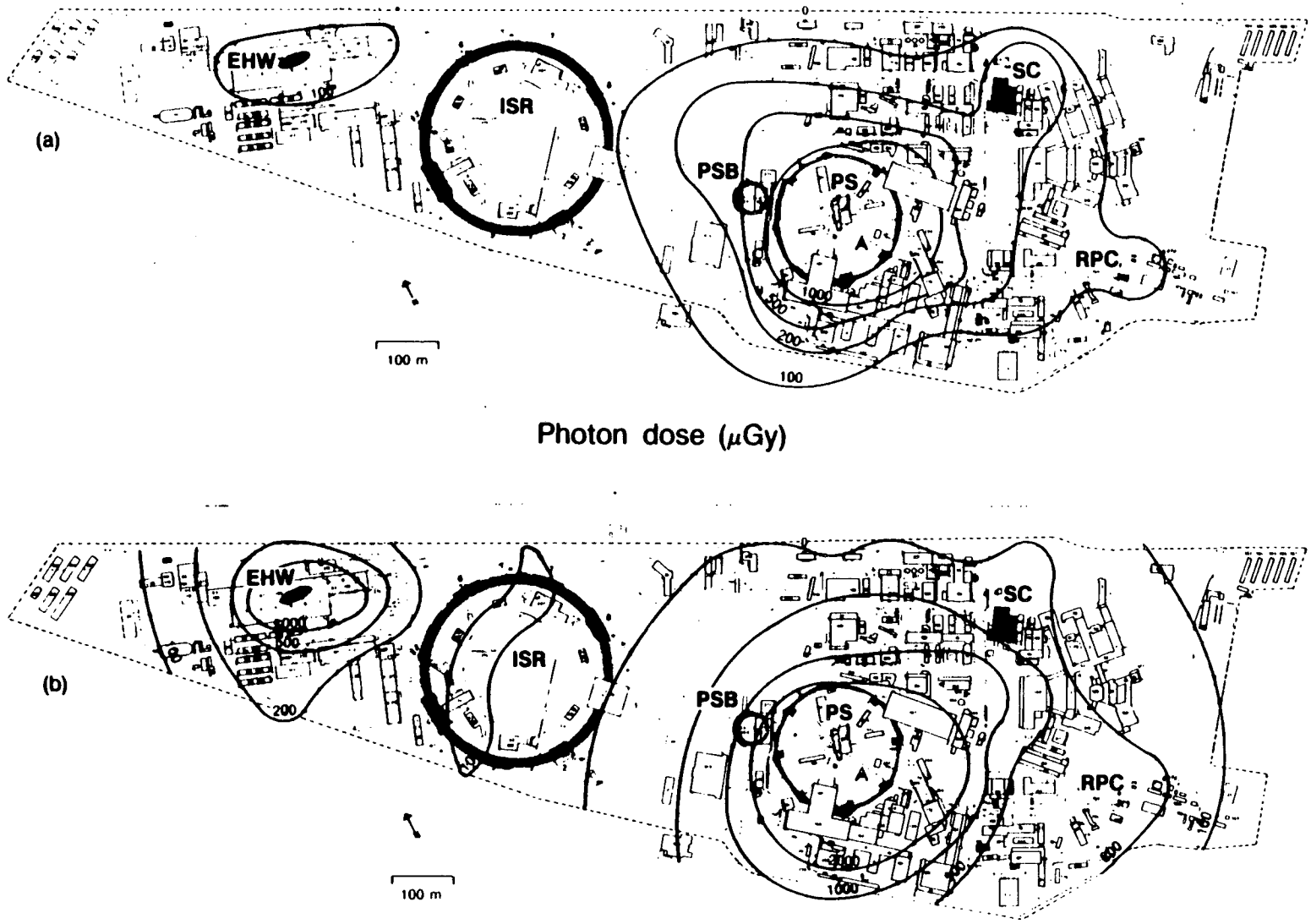

Fig. 35
Thomas & Swanson

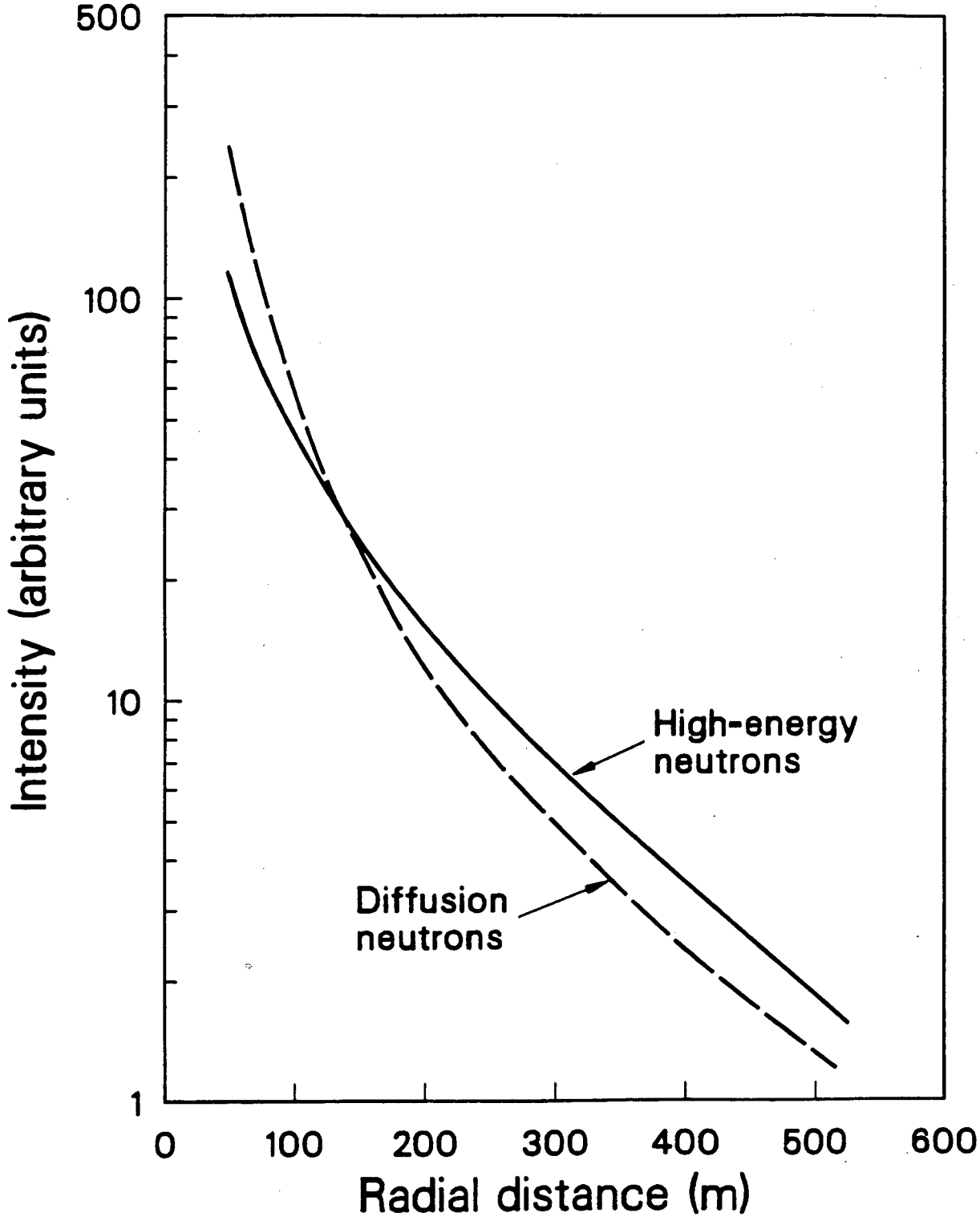

XCG 869-7359

Fig. 36
Thomas & Swanson

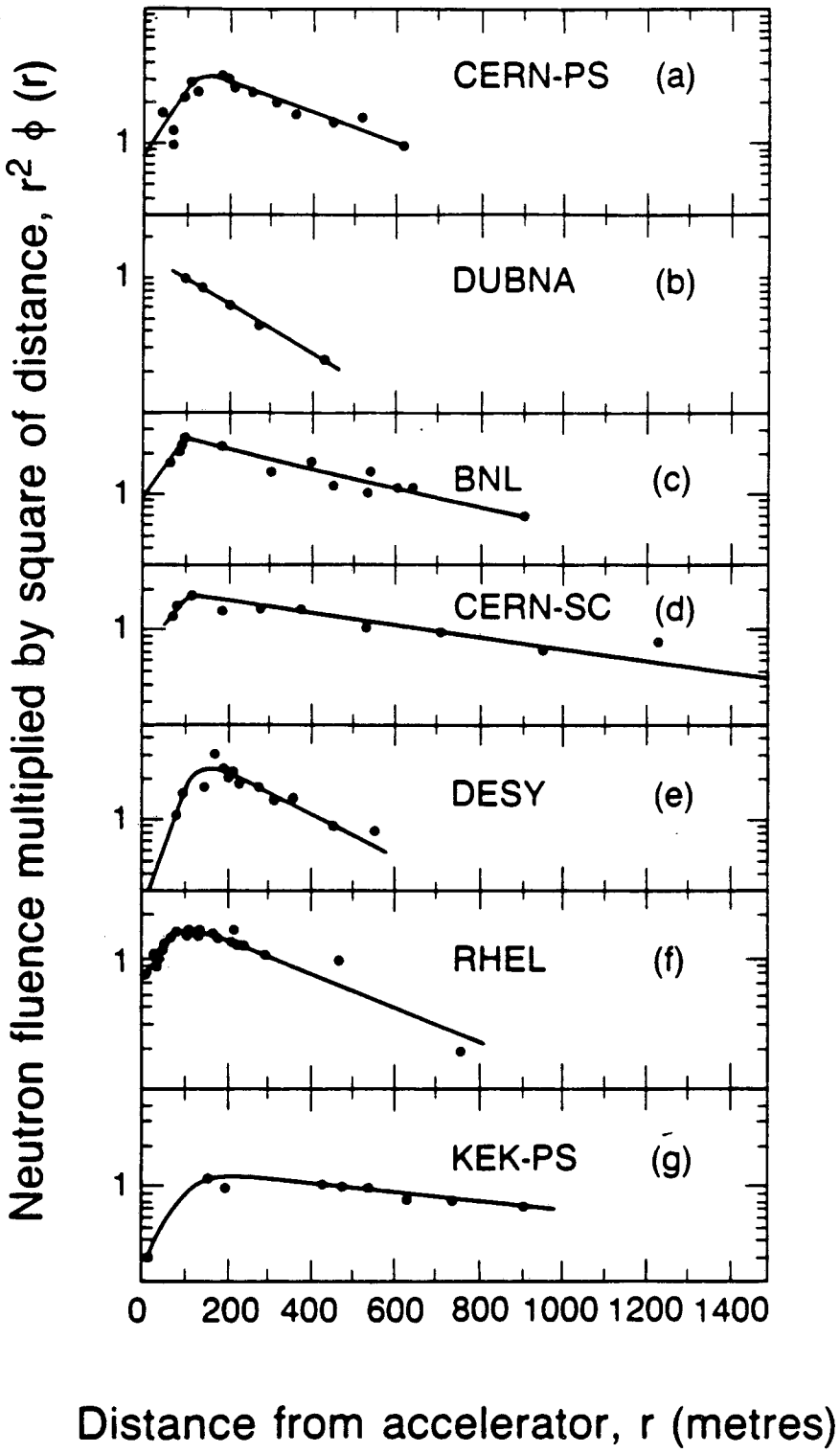

XBL 853-8051

Fig. 37
Thomas & Swanson

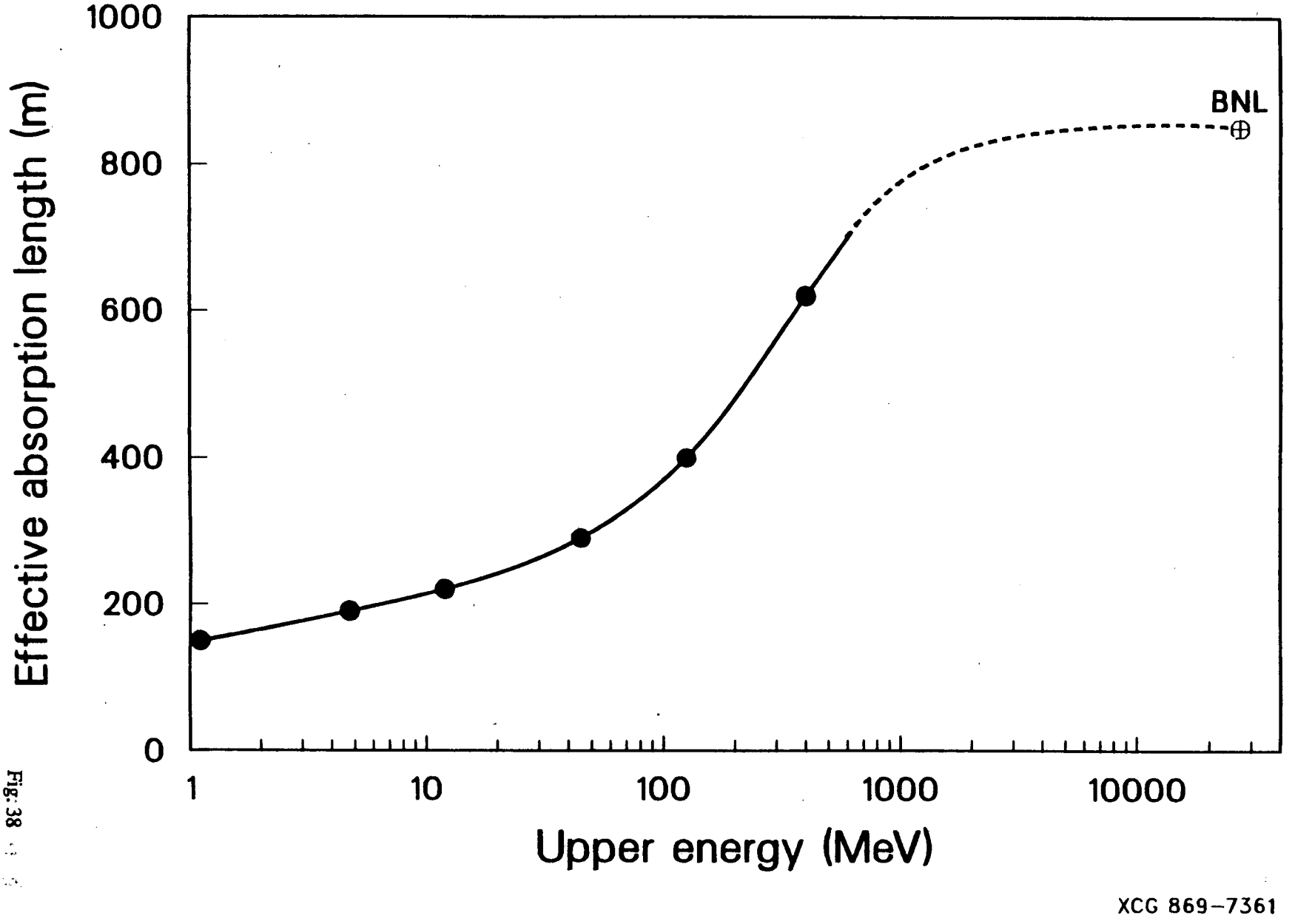

Fig. 38
Thomas & Swanson

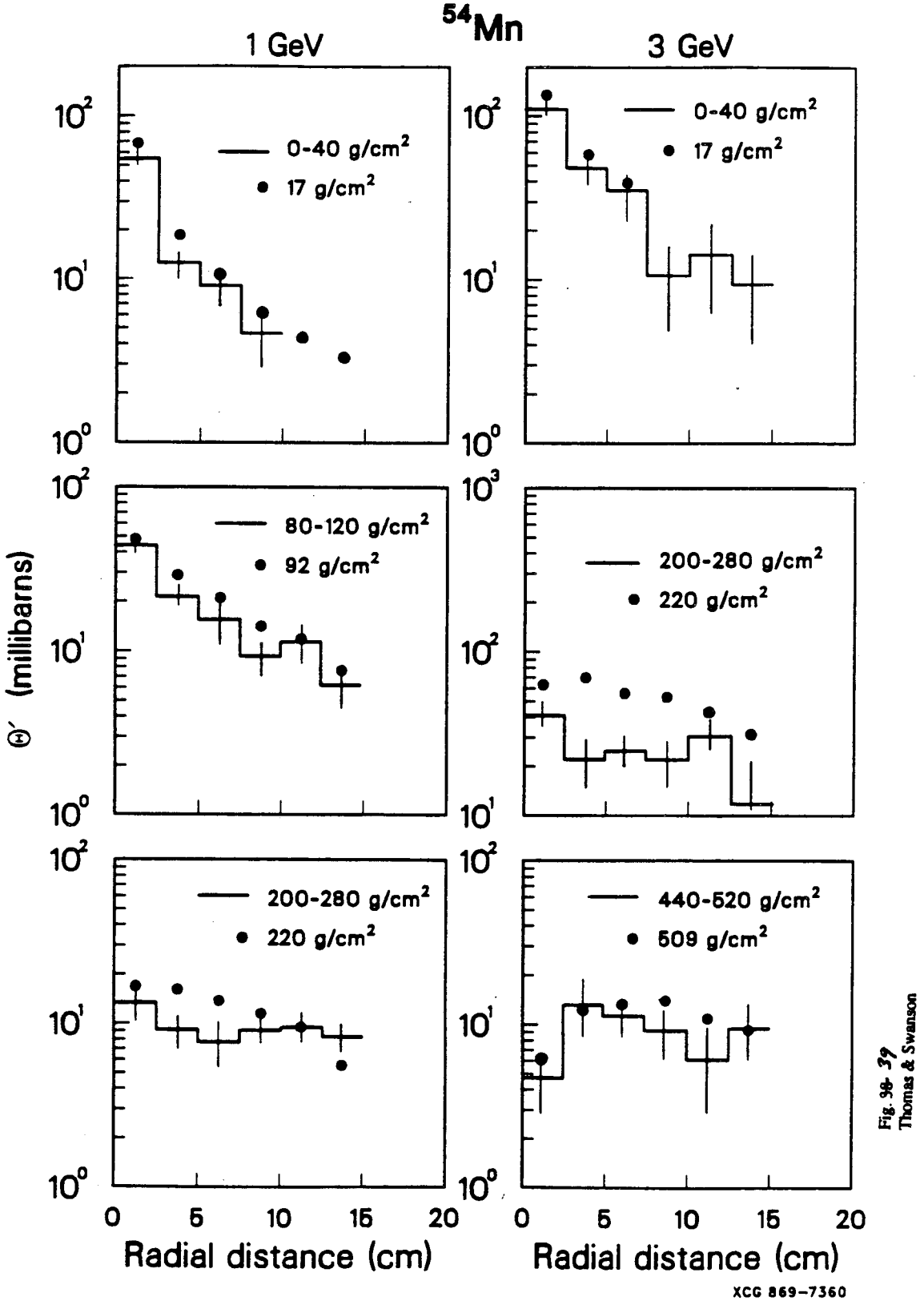

Fig. 39
Thomas & Swanson

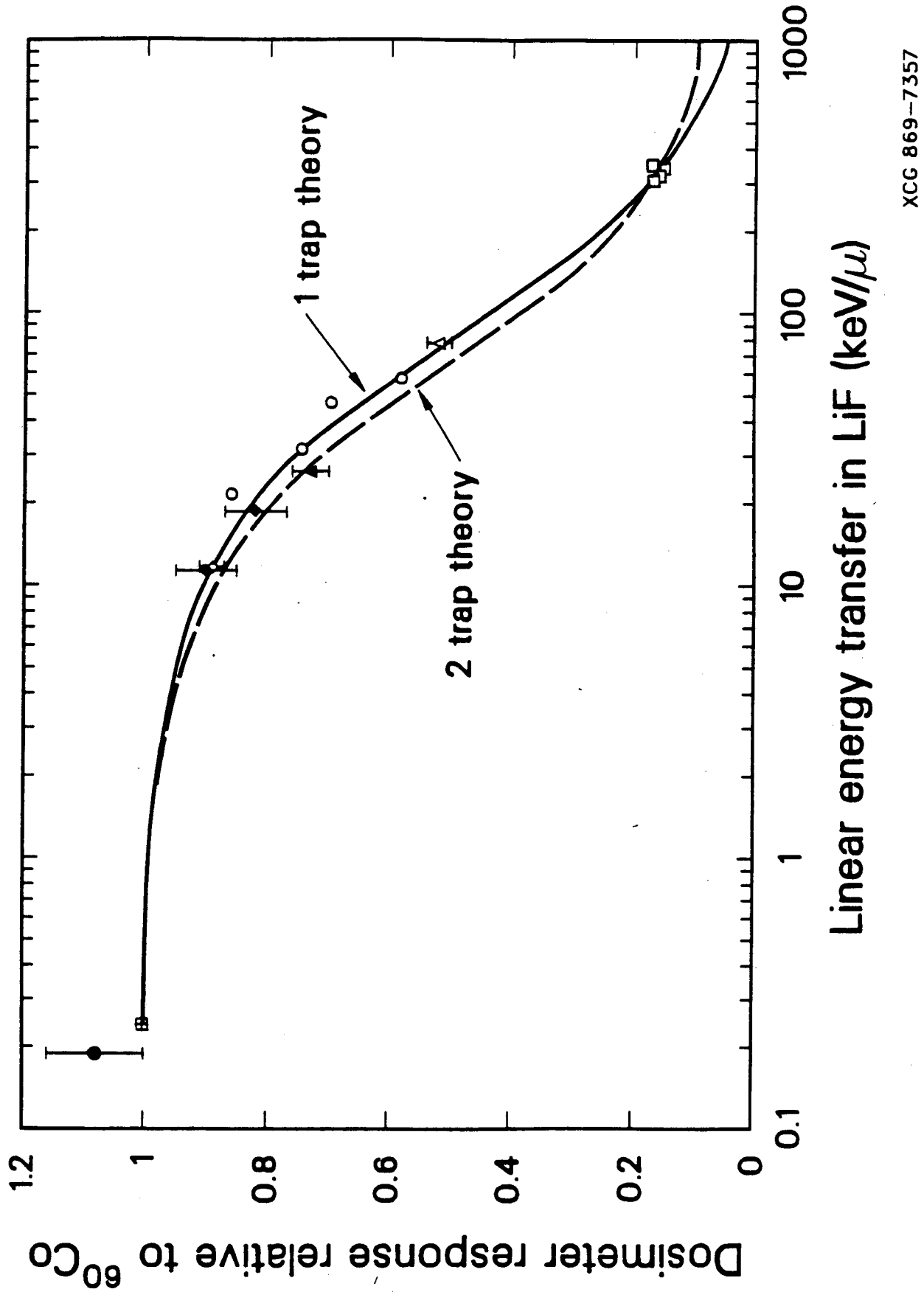

Fig. 40
Thomas & Swanson

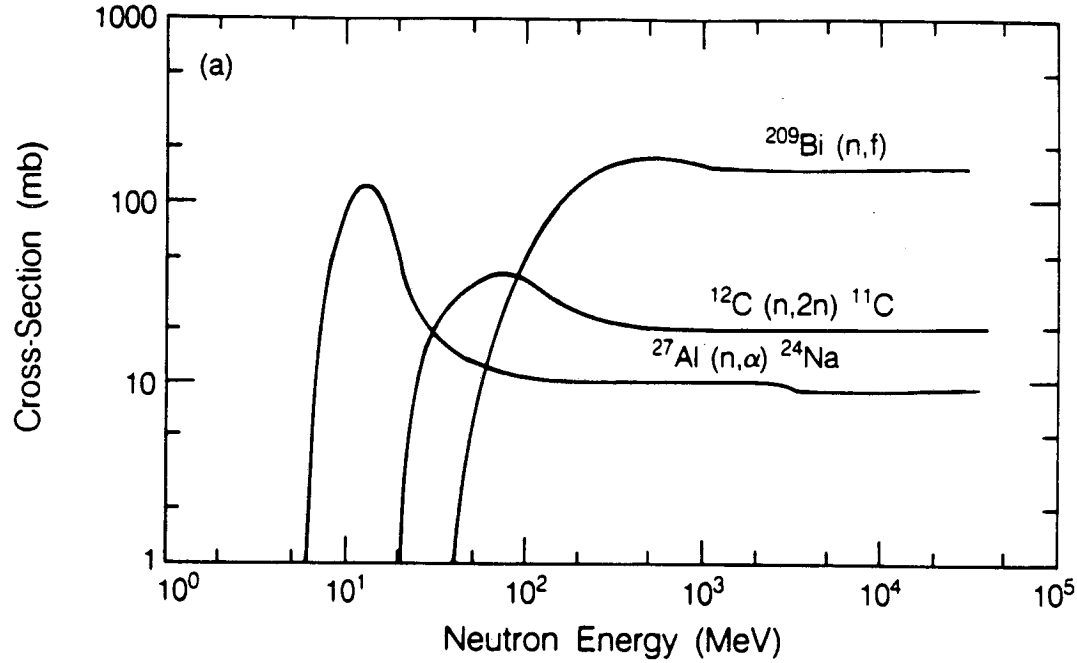

XBL 878-9777

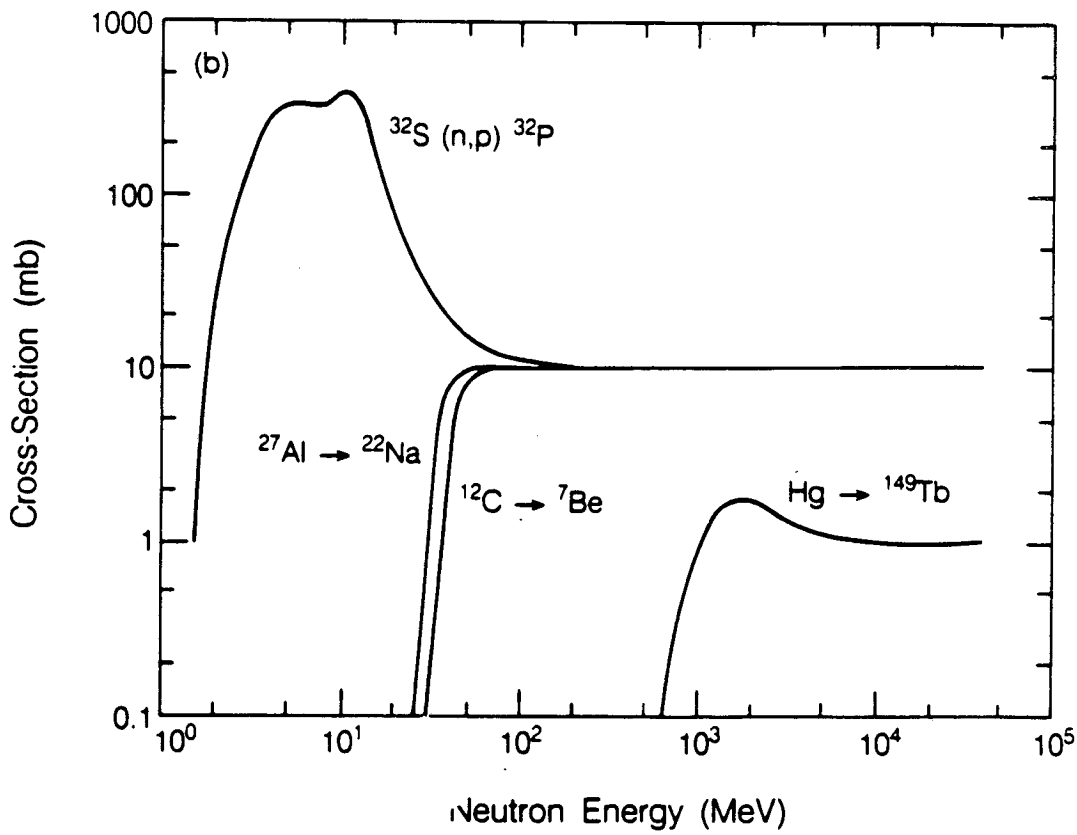

XBL 878-9778

Fig. 41
Thomas & Swanson

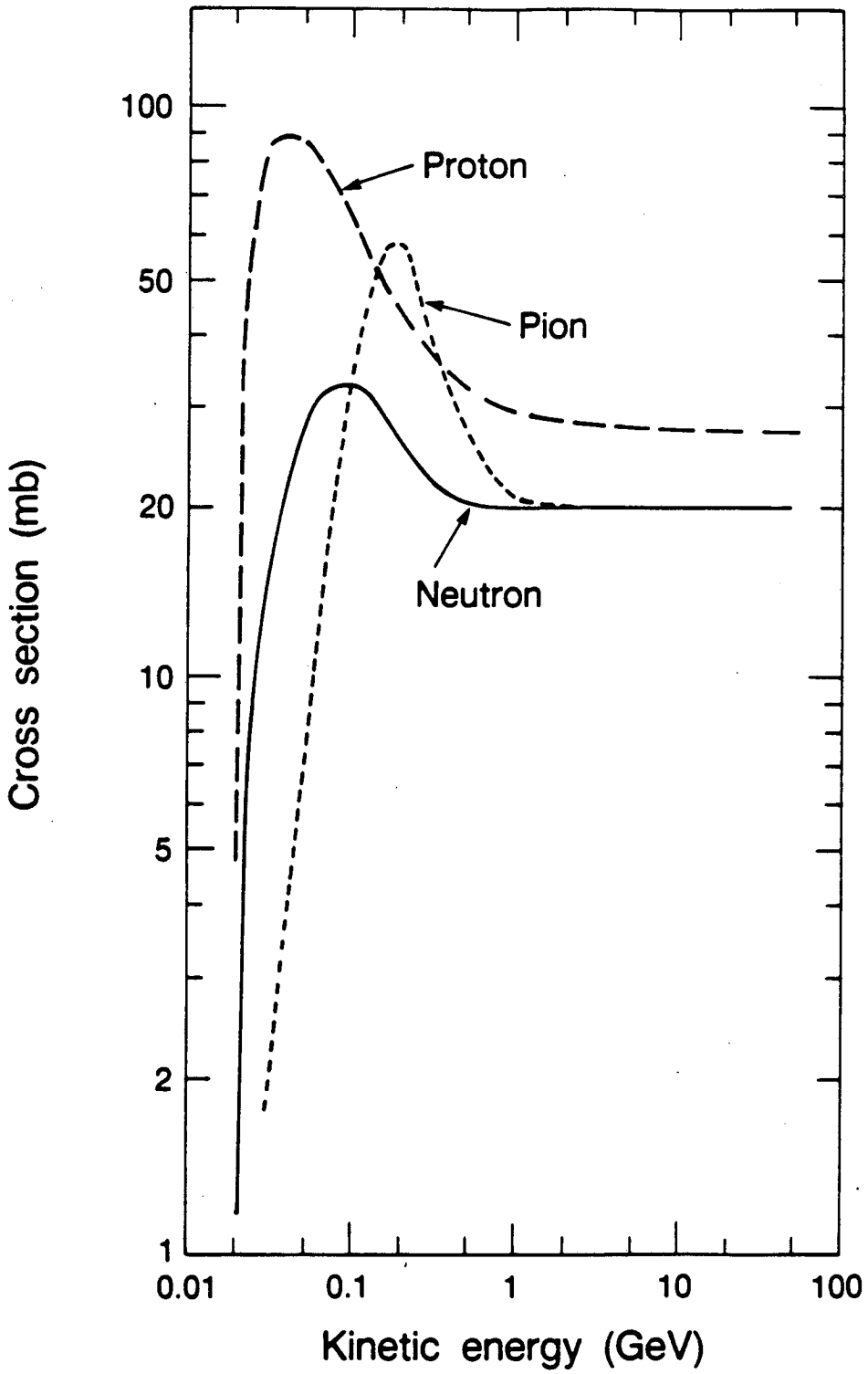

XBL 8710-5932

Fig. 42.
Thomas & Swanson

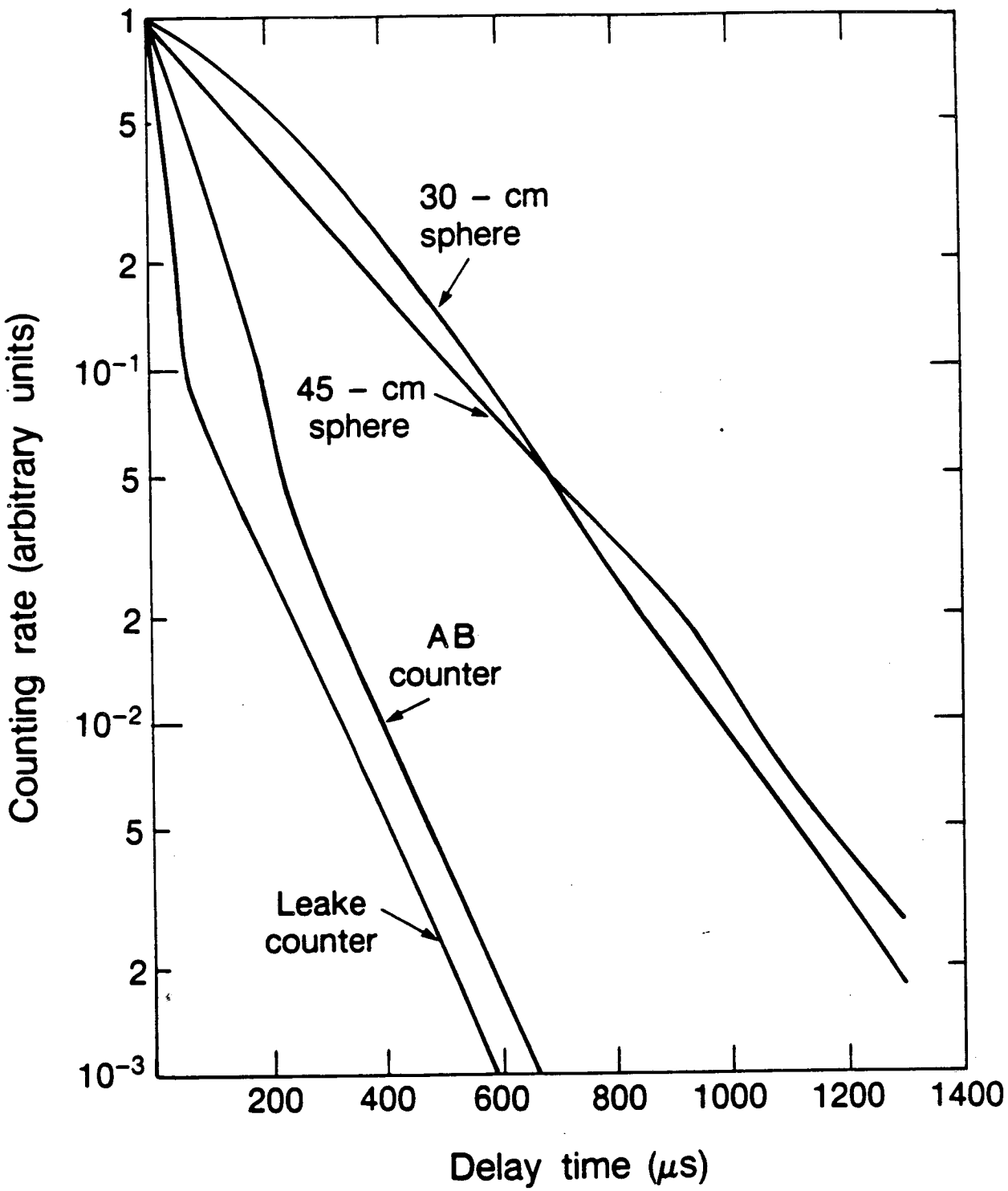

XBL 8711-5950

Fig. 43
Thomas & Swanson

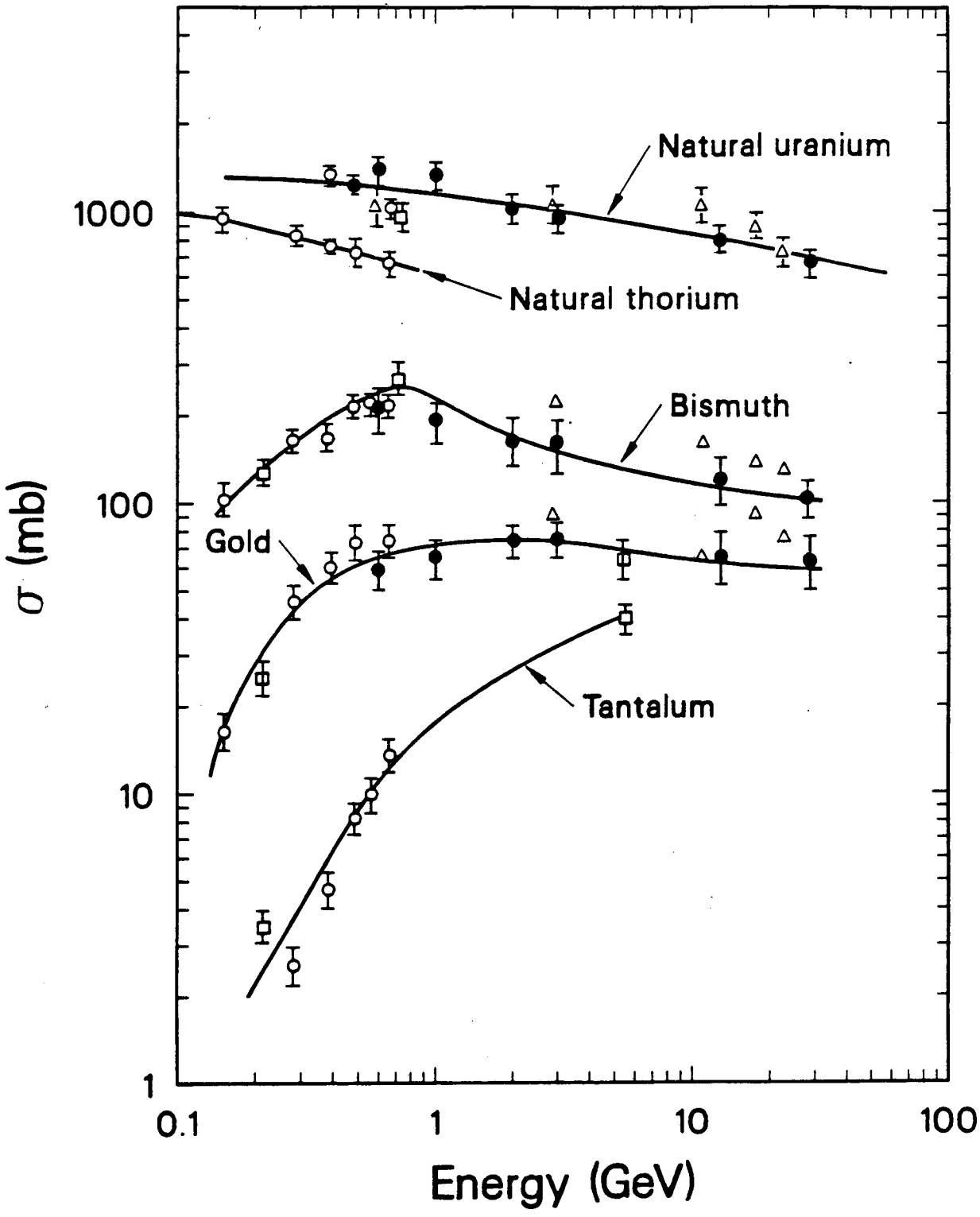

XCG 869-7362

Fig. 44
Thomas & Swanson

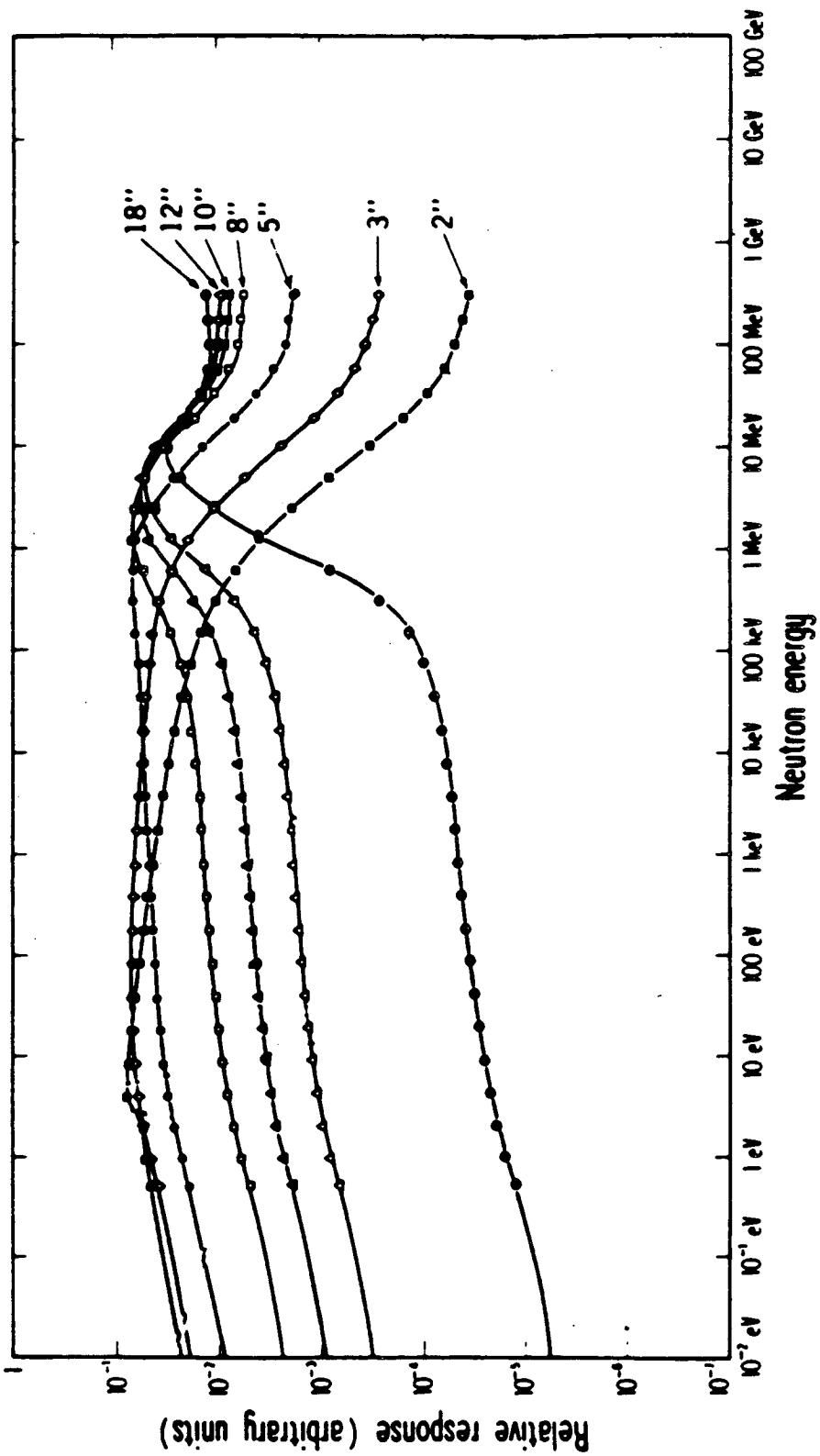

XBL 859-3784

Fig. 45
Thomas & Swanson

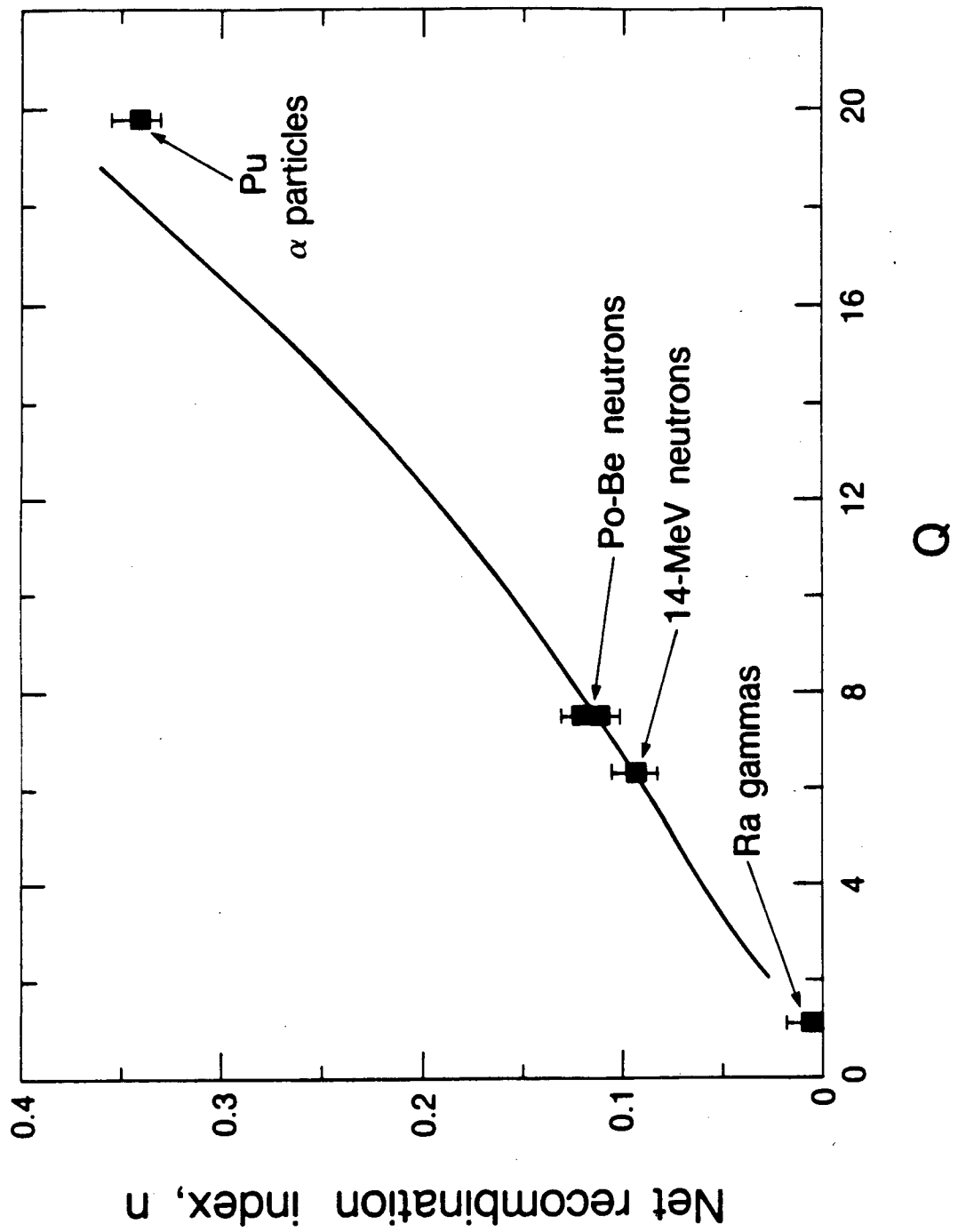

XBL 8710-5936

Fig. 46
Thomas & Swanson

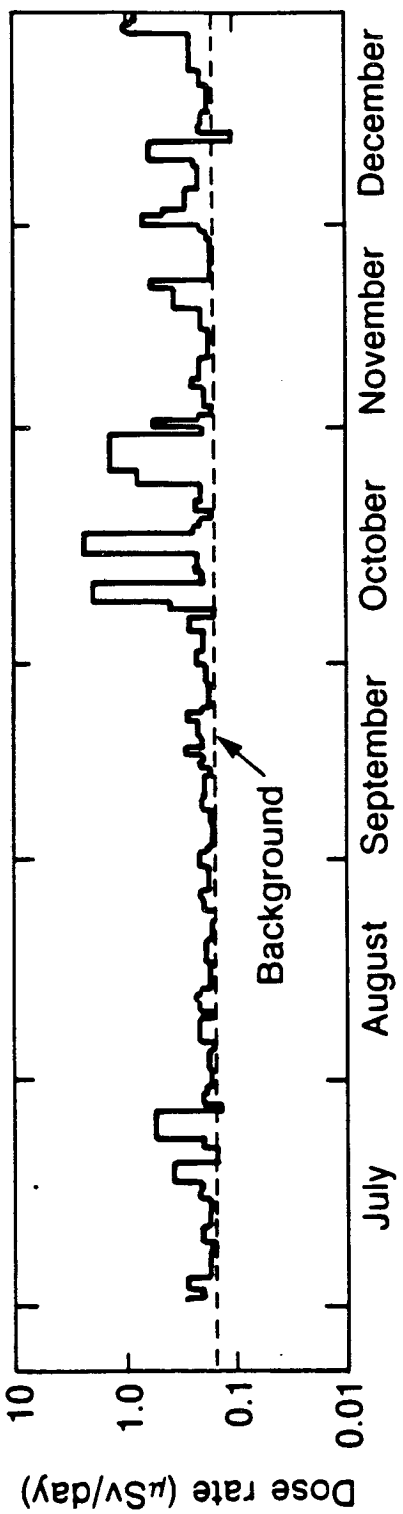

XBL 8710-5933

Fig. 47
Thomas & Swanson

LAWRENCE BERKELEY LABORATORY
TECHNICAL INFORMATION DEPARTMENT
1 CYCLOTRON ROAD
BERKELEY, CALIFORNIA 94720